

DNA Catenation along Native Budding Yeast  
Chromosomes

**Ainhoa Mariezcurrena Antón**

University College London

and

The Francis Crick Institute

PhD Supervisor: Frank Uhlmann

A thesis submitted for the degree of

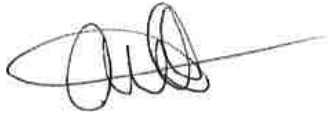
Doctor of Philosophy

University College London

September 2016

## Declaration

I Ainhoa Mariezcurrena Antón confirm that the work presented in this thesis is my own. Where information has been derived from other sources, I confirm that this has been indicated in the thesis.

A handwritten signature in black ink, consisting of several loops and a long horizontal stroke extending to the right.

## Acknowledgements

I would like to thank Frank for giving me the opportunity to work on such an interesting and challenging project, and for all the patience and understanding to let me (slowly) get familiar with the topic and methods. It has been a unique learning experience. Also, I would like to thank my thesis committee, Paul Bates, John Diffley and Julie Cooper, for helpful and encouraging discussions.

A big thank you to all the members of the Chromosome Segregation lab, present and past, for the scientific and non-scientific chats along the way. Celine, thank you for sharing your knowledge and technical tips, you have been a very important mentor. Yasu, Catarina and Sofia, thank you for guiding me through some terrible troubleshooting times and for making sure the morale was kept high! Thank you Molly and Rahul for being understanding and strict (respectively) bench neighbours; it sure has taught me how to work in a team! Of course this PhD would not have been the same (may even have not been completed) without our late trips to the Whippet, Seven Stars, Enterprise and the odd Day & Night. Thank you Simon, Steph, Graham, Dan, Chiara, Rahul, Marina, Fabien, Chris and Masashi for making sure there was some local London culture and gastronomy between all those southerners.

Thank you to the three strongest women I know: my grandmother, my mother and my sister. Elena, I am quite lucky to have you as such an unconditional friend. Not only has your scientific contribution been priceless (and I definitely apologize for making you spend so much time in the lab), but also your company has just been irreplaceable.

Last but not least, I would like to thank Vidhu for embarking on this intercontinental journey with me. It's been a bumpy road, but completely worth it.

Above all, this work is dedicated to my father. I am truly grateful for having had such an inspiring figure behind me, without his generosity and vision I would certainly not be where I am today.

## Abstract

Despite the discovery of the double helical structure of DNA in 1953 by Watson and Crick, there are still many aspects of DNA topology that are not well understood. DNA catenation arises as a consequence of replication and results in the physical interlinking between replicated sister chromatids. Catenanes must be resolved prior to chromosome segregation; failure to do so can result in chromosome segregation errors and consequent aneuploidy. Type II topoisomerases, a highly conserved and essential class of enzymes, are the main decatenases in the cell.

When and where catenation arises along authentic eukaryotic chromosomes, where it persists, and when and where it is resolved, is poorly understood. This is mainly due to the technical difficulties of visualizing intertwinings between linear DNA molecules. We describe here our attempt to study catenation of native budding yeast chromosomes by looping out segments of linear chromosomes as DNA circles.

We used site-specific recombination to excise chromosomal regions of 8 to 18 kb. The topoisomer pattern produced circular monomers that were accompanied by slower migrating bands whose behaviour is consistent with that of catenanes. They appear during DNA replication, and are resolved by topoisomerase II treatment *in vitro*. We find catenanes at replication termination regions and cohesin binding sites, where catenanes are expected to arise and persist, but not to a greater extent than elsewhere in the genome. We propose that once formed, catenanes distribute freely along chromosomes. Moreover, we provide evidence for precatenane formation, as DNA intertwinings between loop outs during replication elongation but before termination are detected. This approach allows us to provide previously inaccessible insight into the topology of eukaryotic chromosomes.

---

Keywords: catenation; topoisomerase II; topoisomers; Cre recombinase.

# Table of Contents

<b>Acknowledgements</b> .....	<b>3</b>
<b>Abstract</b> .....	<b>4</b>
<b>Table of Contents</b> .....	<b>5</b>
<b>Table of figures</b> .....	<b>8</b>
<b>Abbreviations</b> .....	<b>12</b>
<b>Chapter 1. Introduction</b> .....	<b>15</b>
<b>1.1 Historical perspective</b> .....	<b>15</b>
<b>1.2 DNA topology</b> .....	<b>18</b>
1.2.1 Measuring DNA topology: linking number, twist and writhe .....	19
1.2.2 Physiological topoisomers: supercoils, catenanes and knots.....	20
1.2.3 The physiological relevance of supercoiled genomes .....	22
<b>1.3 DNA topoisomerases</b> .....	<b>24</b>
1.3.1 Classification & Mechanisms of action .....	24
1.3.2 Roles of topoisomerases.....	30
1.3.3 Topoisomerases and replication .....	30
1.3.4 Topoisomerases and transcription-induced torsional stress .....	35
1.3.5 Topoisomerases and chromosome segregation .....	36
1.3.6 Topoisomerases and chromosome condensation.....	41
1.3.7 Topoisomerases as cellular toxins .....	43
<b>1.4 How does topo II act globally?</b> .....	<b>45</b>
<b>1.5 Regulation of topoisomerases</b> .....	<b>48</b>
1.5.1 Regulation of topo II .....	48
1.5.2 C-terminal domain (CTD) of type II topoisomerases .....	49
1.5.3 Sumoylation and phosphorylation .....	50
1.5.4 Protein-protein interactions .....	51
<b>1.6 Complexities in chromosome organization</b> .....	<b>52</b>
1.6.1 Topological domains .....	53
1.6.2 Chromosome size .....	55
1.6.3 Composition .....	56
<b>1.7 Open Questions</b> .....	<b>60</b>
<b>1.8 Aim and outline of this thesis</b> .....	<b>60</b>
<b>Chapter 2. Materials &amp; Methods</b> .....	<b>63</b>
<b>2.1 Yeast techniques</b> .....	<b>63</b>
2.1.1 Yeast strains .....	63
2.1.2 Yeast growth .....	64
2.1.3 Cell cycle arrests.....	65
2.1.4 Yeast Transformation.....	66
2.1.5 Mating and tetrad dissection .....	66
2.1.6 Spot Dilution assay .....	66
<b>2.1 General molecular biology methods</b> .....	<b>66</b>
2.1.1 Cloning.....	66
2.1.2 Protein analysis.....	71
2.1.3 DNA analysis .....	72
<b>2.2 Cell biology and Microscopy</b> .....	<b>78</b>
2.2.1 Flow cytometry .....	78

2.2.2	<i>URA3</i> -GFP cohesion assay .....	78
<b>Chapter 3.</b>	<b>Local DNA topology of budding yeast chromosomes.....</b>	<b>80</b>
<b>3.1</b>	<b>How to study chromosomal topology: site specific recombinases and integrases .....</b>	<b>80</b>
<b>3.2</b>	<b>Establishing a Loop Out system.....</b>	<b>82</b>
3.2.1	Construction of strains .....	82
<b>3.3</b>	<b>Technical optimization of the topological analysis of chromosomal loop outs .....</b>	<b>84</b>
3.3.1	Optimization of topological analysis through southern blotting.....	85
3.3.2	Optimization of Cre Recombination.....	88
<b>3.4</b>	<b>Validation of the loop out .....</b>	<b>89</b>
<b>3.5</b>	<b>Topology of a chromosomal region .....</b>	<b>90</b>
3.5.1	Determination of the topoisomer identity .....	92
3.5.2	G1-arrested diploids do not present catenated species .....	93
3.5.3	Effect of the spindle on a centromeric Loop out .....	94
<b>3.6</b>	<b>Chromosomal elements &amp; topology .....</b>	<b>95</b>
3.6.1	Topologies of replication origins and termination regions .....	96
3.6.2	Catenanes are not restricted to regions of cohesin enrichment .....	97
3.6.3	Catenanes are present at condensin-binding sites .....	98
<b>3.7</b>	<b>Topology of the loop out during the cell cycle .....</b>	<b>100</b>
3.7.1	Loop out of the efficient replication origin: ARS508 .....	100
3.7.2	Chromosome topology of a heterochromatic region .....	101
<b>3.8</b>	<b>Exploring the models for catenane formation .....</b>	<b>103</b>
3.8.1	Analysis of the ARS508 loop out in the absence of replication termination .....	103
3.8.2	The introduction of a replication fork barrier does not affect the levels of catenanes .....	104
3.8.3	Replication of the ARS loop out in the absence of functional topo II.....	106
<b>3.9</b>	<b>Unidirectional recombination.....</b>	<b>108</b>
3.9.1	Construction of a $\phi$ C31 integrase system .....	109
3.9.2	Telomeres .....	111
<b>Chapter 4.</b>	<b>Mapping active topoisomerases.....</b>	<b>115</b>
<b>4.1</b>	<b>Rationale .....</b>	<b>115</b>
<b>4.2</b>	<b>Establishing the conditions for the ChIP .....</b>	<b>117</b>
<b>4.3</b>	<b>Mapping active topoisomerases .....</b>	<b>118</b>
4.3.1	Etoposide-trapped topo II maps to replicating regions during S phase .....	118
4.3.2	Ectopic topo II associates with replicating regions during S phase .....	121
4.3.3	Topo I activity maps to narrow regions around early-firing origins during S phase.....	123
4.3.4	Topoisomerase association and activity are reduced during G2/M .....	125
<b>Chapter 5.</b>	<b>Catenation and sister chromatid cohesion .....</b>	<b>129</b>
<b>5.1</b>	<b><i>Paramecium Bursaria Chlorella Virus</i> topo II: an unregulated topo II.....</b>	<b>129</b>
<b>5.2</b>	<b>Sister chromatid cohesion .....</b>	<b>129</b>
<b>5.3</b>	<b>DNA damage in the presence of CV-topo II.....</b>	<b>131</b>
<b>5.4</b>	<b>Overexpression of CV topo II reduces the levels of catenated reporter plasmid in G2/M .....</b>	<b>132</b>
<b>Chapter 6.</b>	<b>Discussion.....</b>	<b>135</b>

<b>6.1 Local topologies of budding yeast chromosomes</b> .....	<b>135</b>
6.1.1 SMCs and catenation.....	140
6.1.2 Catenane formation during DNA replication.....	143
<b>6.2 Topo II activity across the genome</b> .....	<b>145</b>
6.2.1 Organization of chromosomes.....	147
<b>6.3 Catenation and SCC</b> .....	<b>148</b>
<b>6.4 Concluding remarks</b> .....	<b>149</b>
<b>Chapter 7. Appendix</b> .....	<b>152</b>
<b>7.1 Distribution and biochemistry of topoisomerases</b> .....	<b>152</b>
<b>7.2 SMC complexes</b> .....	<b>152</b>
<b>7.3 Construction of <i>loxP</i>/Cre loop out strains</b> .....	<b>153</b>
7.3.1 Introduction of <i>loxP</i> sites across the genome.....	153
7.3.2 Checking the <i>loxP</i> strains.....	154
<b>7.4 Construction of <i>attB</i>/φ31C</b> .....	<b>155</b>
7.4.1 Introduction of <i>attB</i> and <i>attP</i> sites across the genome.....	155
7.4.2 Checking the <i>attB</i> /φ31C strains.....	156
<b>7.5 Detection of loop outs</b> .....	<b>157</b>
<b>7.6 Prs-rDNA sequencing primers</b> .....	<b>158</b>
<b>Reference List</b> .....	<b>160</b>

## Table of figures

Figure 1-1. Primary and secondary structures of DNA.....	18
Figure 1-2. Topological relationships in a covalently closed DNA molecule.....	21
Figure 1-3. General reaction mechanism of topoisomerases.....	24
Figure 1-4. Topology modification by type I topoisomerases.....	26
Figure 1-5. Topology modification by type II topoisomerases.....	29
Figure 1-6. The termination model for DNA catenation.....	32
Figure 1-7. The precatenane model for DNA catenation.....	33
Figure 1-8. Penetrance of cohesin mutants is locus dependent in budding yeast..	38
Figure 1-9. Models for topo II topology simplification.....	46
Figure 2-1. Schematic representation of the vector containing the <i>loxP</i> cassette. .	67
Figure 2-2. Schematic representation of the RFB cassette vector.....	68
Figure 2-3. Schematic representation of the <i>attB-K.I URA3-attP</i> cassette vector...	69
Figure 2-4. Schematic representation of the P <sub>GAL1</sub> - $\Phi$ 31C construct.....	70
Figure 2-5 Schematic representation of the minichromosome <i>prs-rDNA</i> .....	71
Figure 2-6. PicoGreen standards.....	73
Figure 3-1. Site-specific recombination to study the local topology of chromosomal regions.....	81
Figure 3-2. Schematic of the loop out strain construction strategy.....	84
Figure 3-3. Optimization of genomic DNA extraction.....	85
Figure 3-4. kDNA decatenation assay to determine which steps in the genomic DNA preparation protocol might inhibit topo II activity.....	86
Figure 3-5. Probe optimization.....	87
Figure 3-6. Comparison between the two Cre constructs.....	89
Figure 3-7. Validation of the loop out.....	90
Figure 3-8. Topoisomer pattern of a 17 kb TER loop out in G2/M-arrested cells....	91
Figure 3-9. Identification of topoisomers produced after Cre-mediated recombination.....	92
Figure 3-10. Induction of the loop out in diploid cells arrested in G1 does not produce catenanes and/or unwanted recombination products.....	93
Figure 3-11. Loop out of CEN region in G2/M in the absence or presence of the mitotic spindle.....	95

Figure 3-12. Assessing the local topologies of an ARS and a TER loop outs. ....	96
Figure 3-13. Analysis of catenane accumulation and cohesin enrichment. ....	98
Figure 3-14. Correlation between DNA catenation and condensin enrichment. ....	99
Figure 3-15. Analysis of the ARS508 loop out during one cell cycle. ....	100
Figure 3-16. Loop out of the <i>HMR</i> locus and southern blot analysis of the resulting topoisomers. ....	102
Figure 3-17. Catenanes form during replication elongation.....	104
Figure 3-18. Introduction of an RFB sequence does not noticeably affect the levels of catenanes. ....	106
Figure 3-19. Replication of an ARS loop out in the <i>top2-4</i> cells at restrictive temperature gives rise to a high molecular weight replication intermediate. ....	107
Figure 3-20. Strategy for the construction of <i>attB/ attP</i> Loop out strains. ....	110
Figure 3-21. Unidirectional site-specific recombination system to study chromosomal topology.....	111
Figure 3-22. Analysis of a telomeric loop out.....	112
Figure 4-1. Etoposide sensitivities of the PDR mutant strains.....	116
Figure 4-2. Preliminary tests to determine the timing and concentration of etoposide.....	118
Figure 4-3. Association and activity of topo II during S phase along Chr. III.....	119
Figure 4-4. Analysis of genome-wide topo II peaks.....	121
Figure 4-5. Comparison between endogenous and ectopic topo II association and activity along budding yeast Chr. I during replication. ....	122
Figure 4-6. Correlation between ectopic and endogenous topo II.....	123
Figure 4-7. Comparison between association and activities of topo I and topo II during DNA replication. ....	124
Figure 4-8. Topoisomerase activities along Chr. III during nocodazole arrest. ....	126
Figure 5-1. Sister chromatid cohesion assay in the presence of an ectopic topo II.....	130
Figure 5-2. Effect of CV topo II overexpression on genome integrity. ....	131
Figure 5-3. CV topo II expression reduces minichromosome catenation in G2/M	133
Figure 6-1. Model for catenane formation and distribution along native budding yeast chromosomes.....	139
Figure 6-2. Future experiments to study catenane formation along native chromosomes.....	144

Figure 7-1. Eukaryal SMC complexes.....152

## List of tables

Table 1. List of strains used in this study .....	63
Table 2. List of cell cycle arrests used in this study.....	65
Table 3. Primers for integrating the RFB sequence in the genome .....	68
Table 4. Primers used to clone the <i>attP</i> -KanMX cassette .....	69
Table 5. List of primary antibodies used in this work. ....	72
Table 6. Characteristics of the <i>loxP</i> /Cre strains used in this study .....	83
Table 7. Characteristics of the <i>attB</i> /φ31C strains used in this study.....	109
Table 8. Classification of the major types of topoisomerases.....	152
Table 9. Primers for the construction of the <i>loxP</i> /Cre strains .....	153
Table 10. Primers for genotyping and sequencing of the <i>loxP</i> /Cre strains .....	154
Table 11. List of primers for the construction of the <i>attB</i> /φ31C strains .....	155
Table 12. List of primers used for genotyping and sequencing the <i>attB</i> /φ31C strains .....	156
Table 13. List of probes used in this study .....	157

## Abbreviations

A	Adenine
AA	Amino acid
ARS	Autonomously replicating sequence
ATP	Adenosine Triphosphate
BLM	Bloom syndrome ReQ1-like helicase
Bp	Base pair
BrdU	5'-Bromo-2'-deoxyuridine
BSA	Bovine serum albumin
C	Cytosine
CDS	Coding DNA sequence
CEN	Centromere
ChIP	Chromatin Immunoprecipitation
CTD	Carboxy-terminal domain
DNA	Deoxyribonucleic Acid
dNTP	Deoxynucleotide triphosphate
DSB	Double-stranded break
dsDNA	Double-stranded DNA
DTT	Dithiothreitol
DW	Distilled water
EM	Electron microscopy
FOA	5-Fluoorotic acid
FWD	Forward
G	Guanine
GFP	Green fluorescent protein
HMR	Hidden Mat Right (Mating Locus <i>S.cerevisiae</i> )
HU	Hydroxyurea
Kb	Kilobase(s)
kDNA	Kinetoplast DNA
Lk	Linking number
LO	Loop Out
OD	Optical density

P32	Phosphorus-32
PAGE	Polyacrylamide Gel Electrophoresis
PBS	phosphate-buffered saline
PCR	Polymerase Chain Reaction
PFGE	Pulsed-field gel electrophoresis
P <sub>GAL1</sub>	Galactose inducible promoter
P <sub>MET3</sub>	Methionine repressible promoter
PMSF	Phenylmethylsulfonyl fluoride
RFB	Replication Fork Barrier
rDNA	Ribosomal DNA
REV	Reverse
RNA	Ribonucleic Acid
Sc	Supercoil
SDS	Sodium dodecyl sulfate
SMC	Structural Maintenance of Chromosomes
SSC	Saline and Sodium Citrate
ssDNA	Single-stranded DNA
T	Thymidine
TBS	Tris-buffered saline
TCA	Trichloroacetic acid
TER	Termination region
Topo	Topoisomerase
Tw	Twist
Wr	Writhe
YNB	Yeast Nitrogen Base
YP	Yeast Peptone

# **Chapter 1**

## **Introduction**

## Chapter 1. Introduction

### 1.1 Historical perspective

The proposal of the double helix as the structure for the genetic information (Watson & Crick, 1953a) is arguably one of the highest scientific achievements of the 20<sup>th</sup> century. It was radically different to alternative structures proposed at the time, and its biological significance was questioned for decades after its publication, despite ample evidence that the structure was accurate (Franklin & Gosling, 1953) and that it existed in biological systems (Wilkins et al., 1953). Nowadays, the model almost seems common sense (Fig.1-1): DNA is composed of two helical chains coiled around the same axis, with the chains held together by hydrogen bonds between the purine and pyrimidine bases (adenine with thymidine, and guanine with cytosine; Watson & Crick, 1953a), Watson and Crick realized the implications of the double helical structure: because the two chains are intertwined, they would have to untwist if they were to separate, and at the chromosome scale, “*a considerable amount of uncoiling would be necessary; [...] although it is difficult to see how these processes occur without everything getting tangled up, we do not feel that this objection will be insuperable*” (Watson & Crick, 1953b). It is interesting to note that a year later, Delbrück proposed a solution to prevent the predicted entanglement problem resulting from unwinding the double helix, namely a ‘breakage and reunion model’, where a strand of the helix would be broken, the intact strand passed through the gap and the break resealed (Delbrück, 1954). Delbrück incorporated this idea into a complicated model for DNA replication that turned out to be incorrect; however, he inadvertently stumbled nature’s mechanism to deal with the topological challenges resulting from the double helical structure of DNA.

DNA topology as a field in its own right formally began with the discovery of supercoiled DNA in 1965 (Vinograd et al., 1965). At this time, the focus lay on understanding the process of ring formation in phage  $\lambda$  DNA: the complementary sequences at its single-stranded ends allowed their intramolecular joining to form rings (intermolecularly, they joined to form oligomers; Hershey et al., 1963; Wang, 2009). These DNA rings could be converted to covalently closed molecules in the presence of *E. coli* DNA ligase— a reaction product that went on to lead the way to

the confirmation that the helical periodicity of DNA, or the number of base pairs (bp) per helical turn, was  $\sim 10.5$ , and that it depended on temperature and counterions (Wang, 1969; Wang, 1979). Covalently closing DNA rings also enabled the measurement of the changes in DNA structure by other molecules, for example, how ethidium bromide untwists the DNA helix by approximately  $26^\circ$  (Wang, 1974a), or how the binding of *E. coli* RNA polymerases results in unwinding of  $\sim 1$  turn per bound polymerase (Saucier & Wang, 1972). These findings demonstrated that protein binding to DNA does not require any drastic change in the double helix, but that binding is usually stimulated by negative supercoiling, with examples including RNA polymerases (Botchan et al., 1973) and endonucleases (Wang, 1974b).

An important question at the time was why these  $\lambda$  DNA rings were so readily converted to their supercoiled form. As it turned out, serendipity led to one of the most important discoveries in the field: instead of supercoiled DNA, most of the DNA rings in the lysate of  $\lambda$  infected *E. coli* cells accidentally left on the bench instead of in the fridge were found to be relaxed (Wang, 2009). The enzyme responsible for removing supercoils (or relaxing DNA) was isolated and given the name of  $\omega$  protein ( $\omega$  for the angular velocity that was so heavily used for separating supercoiled DNA) (Wang, 1971; Wang, 2009). This enzyme was the first of a kind: it was found to transiently break DNA backbone bonds, alter the topology of its DNA substrate (i.e. interconvert topological isomers) and subsequently religate the break, as predicted by Delbrück; the first topoisomerase to be identified (Wang, 1971).

Topoisomerase biology quickly began to flourish. Apart from the aforementioned *E. coli*  $\omega$  protein, some of the early topoisomerases to be discovered were the mouse “nicking-closing” enzymes (Baase & Wang, 1974; Champoux & Dulbecco, 1972), prokaryotic gyrases (Gellert et al., 1976a; Liu & Wang, 1978) and the *int* gene product of bacteriophage  $\lambda$  (Kikuchi & Nash, 1979). Gyrase were different from the rest in that they required a cofactor (ATP) to catalyse their reaction, which resulted in, surprisingly, the introduction of negative supercoils into bacterial DNA (Gellert et al., 1976a). By the end of the decade it was already noted that these enzymes played vital roles in DNA metabolism, including replication (Champoux & Dulbecco, 1972; Wang, 1971), transcription (Wang, 1973), recombination (Kikuchi & Nash, 1979), chromosome condensation

(Baase & Wang, 1974), nucleosome assembly (Germond et al., 1979), and virus encapsidation (Bauer et al., 1977).

The 1980s brought a different subclass of topoisomerase, namely type II topoisomerases. With the exception of gyrases, the previously discovered enzymes belonged to the type I group, characterized by their ability to create (and religate) single-stranded breaks (SSB) in DNA. The Alberts group isolated and characterized the T4 DNA topoisomerase, different from the aforementioned in that it was capable of completely breaking the double helix in a reversible way, which, as it subsequently proved to be the case with gyrase, depended on ATP hydrolysis (Liu et al., 1980). As proposed in the original study, we now know that type II topoisomerases are widespread in nature, and are (as type I topoisomerases) of great importance for most genetic processes, including replication, transcription and recombination (Liu et al., 1980).

Since then, research on topoisomerases and DNA topology has branched out tremendously. Through X-ray crystallography and single molecule studies, we have built a very detailed picture of the mechanism of action of these enzymes. Cellular and genetic studies (DiNardo et al., 1984; Goto & Wang, 1982; Goto & Wang, 1984; Holm et al., 1985; Morham et al., 1996), on the other hand, have shown how topoisomerases act in their biological context, where they localize and how they are regulated to maintain the cellular topological homeostasis. Importantly, these enzymes have also been established as important targets for anticancer therapies, as well as antibiotics (Gellert et al., 1976b; Hsiang & Liu, 1985; Tewey et al., 1984).

Yet, despite all the findings accomplished since 1953 many questions remain open. Clear evidence for a model of the topology of the replicon, or unit of replication (Jacob et al., 1963; Schwartzman & Stasiak, 2003) is missing: how does topology change as replisomes progress and meet one another, to what extent do topoisomerases counteract those topological changes? Topoisomerases, through their effect on DNA topology, have roles in a myriad of nuclear functions. Indeed, it remains enigmatic how such small molecules acting locally can control global, genome-wide topology, what takes them to their site of action and ensures the completion of their crucial tasks at particular cell cycle stages, and how the cell can sense, if at all, topological changes in return.

## 1.2 DNA topology

DNA has evolved into a vehicle that transmits genetic information from mother to daughter cells, with its functional elegance reflected in its double helical structure. The genetic information encoded in DNA is usually considered a one-dimensional arrangement of bases; however, it is the three-dimensional configuration of DNA that directs how the information is accessed. The structure of DNA is typically characterized by two complementary polynucleotide chains multiply interwound, forming a double helix (Figure 1-1).

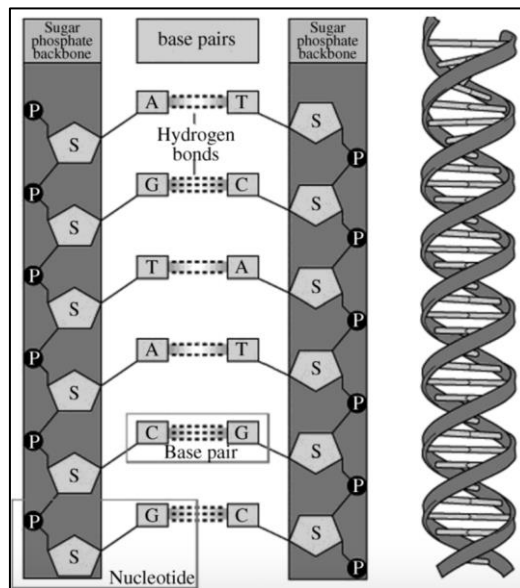


**Figure 1-1. Primary and secondary structures of DNA**

DNA is composed of repeated units of nucleotides (1 nt =  $\sim 3 \times 10^{-10}$  m), themselves formed by a phosphate group, a (2'-deoxyribose) pentose sugar and a base (A, C, G or T). Two chains (Watson and Crick) of nucleotide strands are intertwined around each other, where the phosphate and sugar groups make up the sides of the ladder, and the bases form the rungs (From Buck, 2009).

The prevailing conformation, the so-called B-DNA, is a right-handed helix with 10.5 bp per helical turn, and although locally the shape of DNA may differ from the B-DNA, the overall structure of a DNA molecule is accurately described by this conformation. The double-helical arrangement confers upon it structural stability; however, it also poses a challenge when separation of the strands is required. In addition to its double helical nature, DNA is compressed into the dense nuclear environment; consequently, three-dimensional relationships in the double helix are topological (Deweese et al., 2009).

Topology is a field of mathematics that describes relationships that are not altered by elastic deformation. Topological aspects of DNA come about by the fact that the two strands are interwound, and untangling them— which takes place during the majority of genetic processes— proves to be complicated. In the case of linear DNA in solution, untangling occurs readily due to the free rotation of the ends of the DNA molecule. However, linear DNA has hardly any physiological relevance: DNA found in living organisms has effectively no free ends, thus, restricting or forbidding its untangling (Clarke, 2009).

A DNA segment or molecule whose free end rotation is impossible is termed a topological domain, the most typical example being circular DNA, characteristic of bacterial, mitochondrial, chloroplast and some viral genomes. Eukaryotic genomes, despite being overall linear, putatively consist of DNA loops attached to protein complexes and/or nuclear matrices, each loop being a domain topologically equivalent to covalently closed circular DNA molecules (Mirkin, 2001).

### **1.2.1 Measuring DNA topology: linking number, twist and writhe**

The fundamental topological parameter of a topological domain is given by the linking number (Lk). Lk describes the number of times the Watson strand wraps around the Crick strand in a plane projection (Liu et al., 2009), and thus measures the linking between the two strands of DNA— the algebraic sum of all intersections. Lk is a topological property of closed systems and is independent of the geometry of the DNA (Bates & Maxwell, 2005). Thus, Lk is an integer with a constant value: it cannot be altered by local deformations of the DNA strands (i.e. it is a topological invariant; Buck, 2009). In other words, the basic strained state of a closed DNA molecule cannot be changed: any coiling in that DNA is “locked” into the system (Bates & Maxwell, 2005). Changes in Lk can only occur by creating a (transient) break in the DNA helix and rotating or passing the strands through each other.

Lk is described by two properties of DNA, namely twist (Tw) and writhe (Wr), the two geometric forms in which the topological state of DNA molecules can manifest. Tw is a measure of how the individual strands wind around one another (i.e. how tightly the helix is wrapped around its axis), and thus it indicates the helical pitch, or number of bp per complete revolution (Bates & Maxwell, 2005). The right-handed twist of the Watson-Crick helix is given a positive value by convention.

Wr is a property of the spatial course of the double helix, and it describes the coiling of the helical axis (i.e. how it is contorted in space; Buck, 2009). It is defined as the number of times the double helix crosses itself in a 2D projection. Tw and Wr are not topological invariants, and thus may change under deformations of the DNA helix (Buck, 2009). The relationship between these three parameters is given by:

$$Lk = Tw + Wr$$

This equation explains that any local changes in Tw are compensated by opposite variations in Wr, and vice versa (i.e. Tw and Wr can be interconverted), to keep Lk constant in a given topological domain.

### **1.2.2 Physiological topoisomers: supercoils, catenanes and knots**

For an N bp long circular DNA molecule:

$$Lk_0 = Tw_0 = \frac{N}{\gamma}$$

where  $\gamma$  describes the number of base pairs per helical turn. The above equation describes a relaxed DNA molecule, like the Watson-Crick structure, free of torsional stress, i.e. in the lowest free-energy state (Liu et al., 2009). For relaxed DNA molecules, e.g. a planar DNA circle,  $Wr=0$ , and the Lk is given by the number of double-helical turns around the circle (Bates & Maxwell, 2005). For example, a relaxed DNA molecule of 1050 bp should have an  $Lk_0 = 1050 \text{ bp} \div 10.5 \text{ bp/turn} = 100$  (under standard conditions, 0.2 M NaCl, pH 7, 37°C; Dewese et al., 2009).

Conversely, supercoiled molecules are characterized by  $Lk \neq Lk_0$ , with the difference being quantified by  $\Delta Lk$ . When  $\Delta Lk$  is negative, the corresponding DNA molecule is referred to as negatively supercoiled; if  $\Delta Lk$  is positive, the DNA is positively supercoiled. The former is underwound relative to a relaxed molecule, which can manifest as a relative untwisting of the helix, or an increase in the number of base pairs per turn. Conversely, positively supercoiled molecules are overwound, with a lower helical repeat than their relaxed counterpart. Supercoiling can manifest not only as changes in twist, but also in writhe, or the spatial course of the helical axis: underwound and overwound DNA molecules adopt higher order helical coiling (hence the name ‘supercoiling’; Figure 1-2a). The most prominent supercoiled configurations are plectonemic and solenoidal (Figure 1-2b).

Plectonemic or interwound DNA is characteristic of prokaryotes and is characterized by the winding of the DNA helix around another part of the same molecule (Adrian et al., 1990; Bates & Maxwell, 2005). Solenoidal (or toroidal) DNA forms as DNA wraps around the histone octamer in eukaryotic chromosomes (Davey et al., 2002).

To compare supercoiling between different molecules, it is useful to normalize  $\Delta Lk$  for DNA length:

$$\sigma = \frac{\Delta Lk}{Lk_0} = \frac{\Delta Lk \gamma}{N}$$

Thus,  $\sigma$  measures supercoiling density, and estimates the number of supercoils per helical turn. In living cells,  $\sigma$  varies from -0.02 to -0.09. Thus, following the previous example, a 1050 bp underwound by 6% ( $\sigma = -0.06$ ) would have 94 turns of the helix, instead of the 100 expected for its relaxed counterpart, and its  $\Delta Lk = -6$ . Supercoiling, which introduces torsional and bending deformations, is energetically unfavourable and, conversely, local relaxation favourable.

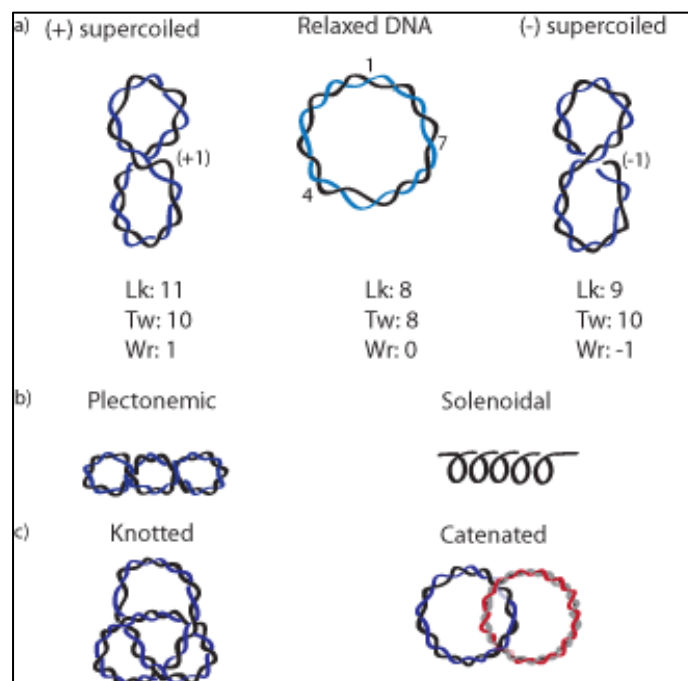


**Figure 1-2. Topological relationships in a covalently closed DNA molecule**

(a) (+) and (-) supercoiled molecules adopt higher order helical conformations with respect to relaxed DNA. (b) Supercoiling typically adopts a plectonemic or a solenoidal shape in the absence and presence of histones, respectively. (c) Knots and catenanes are topological invariants, and require breaks in the DNA for their resolution.

DNA molecules can adopt other conformations apart from supercoiling. Knots and catenanes (Figure 1-2c) are two examples of structures detected in living cells, where one or more DNA molecules become interlinked, respectively. Their formation is facilitated by the fact that the nuclear environment is crowded, and the organization of chromosomes as individual entities is challenging. Naturally occurring knots have been observed in DNA from bacteriophage capsids, probably arising from the joining of the single-stranded extensions at the ends of the phage DNA (Liu et al., 1981). Knots can also be generated *in vitro*, for example, through site-specific recombination by the integrase (Azaro & Landy, 2002) and the resolvase (Wasserman et al., 1985) families of recombinases. Catenanes, on the other hand, are much more common in nature than knots, and their presence has been reported in a multitude of biological systems (Bates & Maxwell, 2005; Farcas et al., 2011; Sundin & Varshavsky, 1981). They originate during replication and impede the segregation of DNA molecules during cell division (Sundin & Varshavsky, 1981; diNardo et al., 1984). Unlike supercoils (sc), which can be interconverted from twists to writhes, knots and catenanes are constrained as writhes. They are topological invariants: the number of crossings for a given knot or catenane can only be changed by breaking the DNA strands.

### **1.2.3 The physiological relevance of supercoiled genomes**

Topology is an important active player in genome functioning, and topological relationships affect virtually any aspect of DNA metabolism. First, supercoiling can reduce the overall volume occupied by a DNA molecule, as it triggers the formation of plectonemic superhelices with diameters of only a few times larger than that of DNA itself, and thus aids in the organization of genomes into small cellular/nuclear volumes (Holmes & Cozzarelli, 2000; Vologodskii & Cozzarelli, 1994). Moreover, as explained above, in any given topological domain, a change in  $T_w$  (secondary structure) is compensated by a change in  $W_r$  (overall shape). For example, unwinding of a stretch in a DNA molecule will be reflected by a change in global supercoiling— and vice versa— as long as both strands have no breaks. Thus, an immediate benefit of DNA supercoiling is that it could be used as a sensor of DNA integrity; the fact that supercoiling is required for replication

initiation could mean that replication can only start if both strands are intact, (Mirkin, 2001) in addition to facilitating duplex unwinding.

DNA processing is directed not only by specific nucleic acid sequences, but also by the energetics of DNA topology (Sissi & Palumbo, 2010). As mentioned previously, the genomes of most living organisms are negatively supercoiled, and this global underwinding conveys single-stranded character that enables the temporary unwinding that takes place during all major genetic processes (Bates & Maxwell, 2005). Thus, negative supercoiling supplies the energy for localized unwinding of the double helix, which, in turn, facilitates the access to polymerases and repair factors. Supercoiling may also assist the synapsis of distant sites of the chromosome (Embleton et al., 2004; Vologodskii and Cozzarelli, 1996) because high-order folding could put in contact chromosomal regions that would be otherwise far apart. Indeed, the importance of negative supercoiling for transcription, DNA replication and recombination has been demonstrated, mostly for prokaryotic systems. In eukaryotes supercoils accumulate in chromatin, constrained by the wrapping of DNA around nucleosomes (which provides the major mode of negative supercoiling in eukaryotic chromosomes; Schwartzman & Stasiak, 2003). Typically, DNA wrapping around a nucleosome leads to  $\Delta Lk = -1$ ; however, this decrease in Lk is dependent on the levels of histone acetylation, with highly acetylated histones (characteristic of euchromatin) being less able to sequester DNA and reducing the linking number only by  $\Delta Lk = -0.8$  (Norton et al., 1989; Osborne & Guarente, 1989). In line with this, DNA in silent chromatin/heterochromatin has been found to be more negatively supercoiled (Bi & Broach, 1997).

As well as affecting all major genetic processes, DNA topology can, in turn, be affected by these processes. Tracking systems that unwind DNA as they travel along the DNA seem to move linearly and do not change Lk (as this requires breaks in DNA), but compress supercoils into an increasingly shorter region (Bates & Maxwell, 2005). This results in progressively more overwinding ahead of the tracking system, which makes the unwinding of the helix more difficult, ultimately impeding DNA processes. Thus, in contrast to underwinding, positive supercoiling tends to inhibit DNA processes, because it opposes local melting of the double helix.

## 1.3 DNA topoisomerases

DNA topoisomerases are enzymes that modify DNA topology and regulate the topological state of cellular DNA; they evolved to deal with the topological challenges rooted in the double-helical structure of DNA (Wang, 2002). They comprise a ubiquitous family of enzymes whose mechanism of action encompasses characteristics of nucleases and ligases: they generate transient breaks, rearrange and religate their substrate DNA (Sissi & Palumbo, 2010). Topoisomerases are fundamental for the survival of all organisms and have crucial roles in DNA replication, transcription, chromosome condensation and segregation, and Holliday junction resolution; thus, deficiencies in their activities give rise to diseases linked to genome instability (Clarke, 2009).

### 1.3.1 Classification & Mechanisms of action

All topoisomerases share a basic reaction mechanism (Figure 1-3).

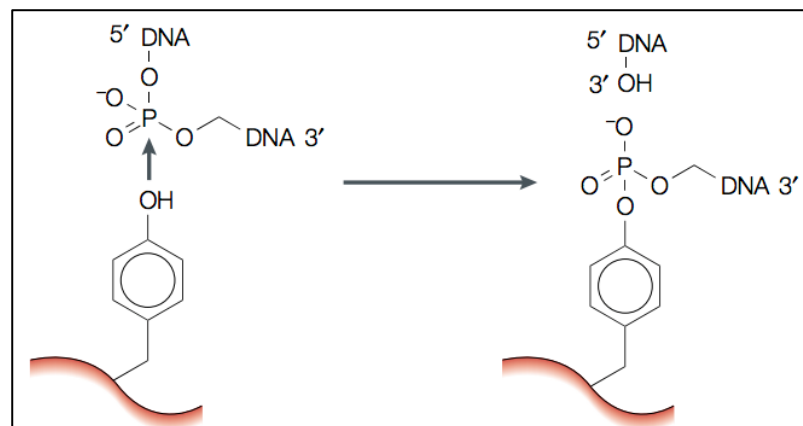


**Figure 1-3. General reaction mechanism of topoisomerases.**

During the topology-remodelling reactions of type IA and II topoisomerases, the active tyrosyl group of the enzyme establishes a covalent bond with the 5'-phosphoryl group of the DNA through a transesterification reaction that breaks the DNA backbone bond. In the case of type IB topoisomerases (not depicted), the tyrosyl group is linked to a 3'-phosphoryl group (from Wang, 2002; *with permission from Nature Publishing Group*).

They initiate DNA cleavage by nucleophilic attack by their active site tyrosyl residues on the phosphate of the DNA backbone (Champoux, 2001). Following a

transesterification reaction, a covalent phosphotyrosyl bond forms between topoisomerase and the newly created DNA end, and a hydroxy moiety is formed on the opposite end of the broken strand. The covalent bond maintains the energy of the sugar-phosphate backbone, and it also keeps genomic integrity during the reaction. After the topological transaction, ligation proceeds as the reverse of the cleavage event, i.e. by nucleophilic attack of the hydroxy moiety on the phosphotyrosyl bond, which breaks the protein-DNA bond and reforms the DNA backbone link, restoring a chemically identical structure to that of the initial substrate (Champoux, 2001).

Topoisomerases fall into two main groups, type I and type II. Type I enzymes make transient breaks on one strand of the DNA at a time, whereas type II enzymes act as dimers to temporarily break a pair of strands in the double helix (Wang, 2002).

#### **1.3.1.1 Type I topoisomerases**

Type I topoisomerases, denoted by odd roman numbers, e.g. topo I and topo III, are active in their monomeric form and do not require a high-energy cofactor. They are further divided into class IA or IB, depending on their mechanism of action and the polarity of the covalent linkage between DNA and enzyme.

Type IA topoisomerases bind a negatively supercoiled substrate, leading to the unwinding of a short stretch of DNA. They transiently break the single stranded region, and attach to the 5'-terminal phosphate of the DNA at the site of the break (Kim & Wang, 1992; Wang, 2002). Acting as a bridge that connects the newly generated DNA ends, they subsequently pass the opposite strand through the break (Figure 1-4a). As relaxation proceeds, and the substrate becomes less (-) supercoiled, the enzyme becomes progressively less proficient; thus, overwound or (+) supercoiled DNA is not a good substrate for this subclass of topoisomerases (Wang, 2002). In the presence of a nick or gap, type IA topoisomerases may also pass a double helical segment through a second helix, resulting in catenation/decatenation reactions (Tse & Wang, 1980). This subclass requires the presence of divalent metal ions for catalysis. Type IA topoisomerases have roles in recombination, including Holliday junction resolution (Harmon et al., 1999; Wallis et

al., 1989), recombinational DNA repair (Zhu et al., 2001) and the maintenance of genome stability (Watt & Hickson, 1994). In most species, topoisomerase III acts together with a 3'-5' helicase of the RecQ family, e.g. RecQ in *E. coli*, Sgs1 in *S. cerevisiae*, and BLM in human cells (Bachrati & Hickson, 2003; Bocquet et al., 2014; Duguet, 1997)— and the complex further associates with the major ssDNA binding factor in each species (Bachrati & Hickson, 2003; Cejka et al., 2012; Sharma et al., 2006) to putatively disentangle homologous recombination intermediates containing Holliday junctions.

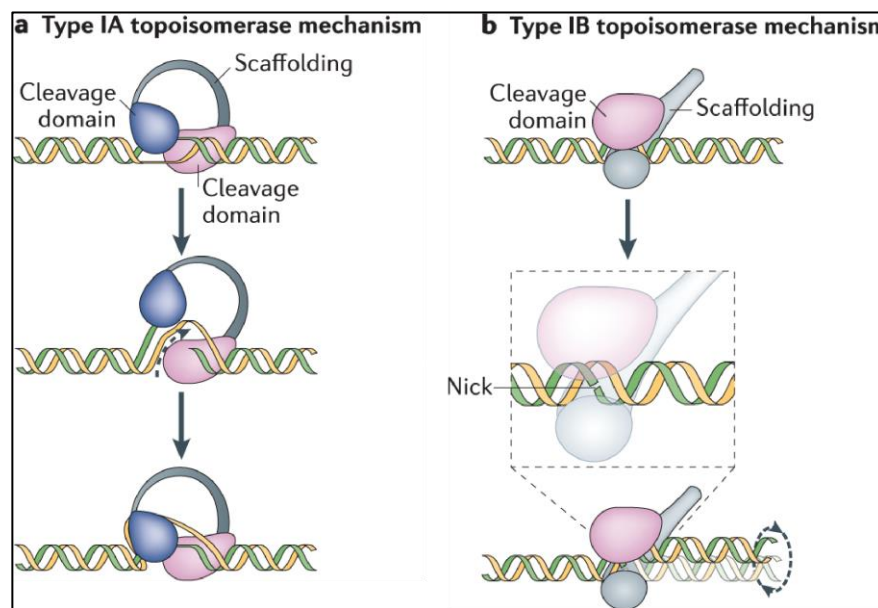


**Figure 1-4. Topology modification by type I topoisomerases**

(a) Type IA enzymes, like yeast topoisomerase III (*top3*), carry out a strand passage reaction of an intact strand through a transient single-strand break (SSB). (b) Type IB topoisomerases, e.g. yeast topoisomerase I (*top1*), act through a rotation mechanism around the induced SSB (From Vos et al. 2011; *with permission from Nature Publishing Group*).

The type IB subfamily includes most eukaryotic type I enzymes, and, as opposed to the bridging mechanism of the type IA enzymes, they probably act through DNA rotation. After cleaving one of the DNA strands, the type IB topoisomerase assumes a linkage to the 3' end (upstream) of the DNA: supercoils (sc) are relaxed by rotation of the free 5' end around the intact strand (Figure 1-4b; Koster et al., 2005; Krogh & Shuman, 2000). Because the interaction between the enzyme and the downstream region of the break is mostly ionic in nature, this region is able to rotate. Thus, the segments flanking the nick can turn around one

of the single bonds opposing the nick (Champoux, 2001). Type IB topoisomerases cleave one strand in a double-stranded DNA (dsDNA) region, and can relax both (-) and (+) sc. This subclass of enzymes has been reported to carry out catenation/decatenation reactions *in vitro*, as long as the DNA substrate contains nicks and/or gaps (Brown & Cozzarelli, 1981). However, the mechanism of this reaction remains unclear, and so does its biological significance since a linear dsDNA break intermediate (covalently attached to the enzyme on one end) would be expected to form during the reaction (Wang, 2002). Type IB enzymes do not require divalent metal ions for catalytic activity.

It is worth noting that the integrase (Int) family of site-specific recombinases (hereby referred to as tyrosine recombinases) uses a very similar mechanism to catalyze the formation and resolution of Holliday junctions (Krogh & Shuman, 2000). Tyrosine recombinases, including  $\lambda$  Int, Cre and Flp, share very little sequence homology to type IB topoisomerases; however, their catalytic domains are structurally very similar (Cheng et al., 1998). The main mechanistic difference is that the 5' hydroxyl formed by topo IB is rejoined to its original strand by a single topoisomerase molecule, whereas four recombinase molecules are required to rejoin the similarly created 5'-OH moiety to a 3' phosphate partner in a DNA strand of a distant region (Sherratt & Wigley, 1998).

### 1.3.1.2 Type II topoisomerases

Type II topoisomerases, which are designated by even roman numbers, e.g. topo II and topo IV, are active as multimers (homodimers, in the case of eukaryotic enzymes, and  $A_2B_2$  structure in prokaryotes) and require ATP and divalent metal ions for catalysis (Deweese et al., 2009; Wang, 1996). This subclass has two-fold symmetry, and the interface between the two halves consists of three gates, namely the N-, DNA-, and C-gates (Schoeffler & Berger, 2008; Yogo et al., 2012). The catalytic cycle of type II topoisomerases, the now well-accepted “two-gate mechanism” (Roca & Wang, 1994; Roca et al., 1996) has been extensively documented through biochemical and structural studies (Figure 1-5a). The strand passage reaction starts when the enzyme binds the G (gate) DNA segment at the DNA-gate (Deweese & Osheroff, 2009; Laponogov et al., 2013). Although binding does not seem to rely strictly on primary sequence, there is probably a preference

for certain tertiary structures, i.e. crossovers (Alonso-Sarduy et al., 2011; Roca et al., 1993; Watt & Hickson, 1994). On the other hand, DNA binding does not necessarily lead to strand passage (Roca et al., 1993). The N-terminal domains, closed by ATP binding, act like a clamp to capture a second DNA segment, T (transport; Bates & Maxwell, 2007; Laponogov et al., 2013). N-gate closure thus precedes DNA-gate opening (Martinez-Garcia et al., 2015), possibly acting as a safety mechanism to avoid futile cleavage cycles, and is followed by the transport of the T segment towards the DNA-gate. Here, a transient double strand break (DSB) is made on the G segment, maintaining a covalent bond between the newly formed 5'-ends and the enzyme's catalytic tyrosines on each side of the DNA gate. The scissile bonds on the double helix are staggered and positioned across the major groove from one another, with the cleaved DNA molecules containing 4 bp 5'-ssDNA cohesive ends attached to a protomer of topoisomerase II (Liu et al., 1983; Sander & Hsieh, 1983; Zechiedrich et al., 1989). ATP hydrolysis powers the passage of the T segment through the DSB in the G segment to leave by the C-gate (Bates & Maxwell, 2007), followed by the religation of the break and N-gate reopening to allow enzyme turnover (Martinez-Garcia et al., 2015; Schoeffler & Berger, 2008; Yogo et al., 2012). Abortive cycles have also been reported, as has ATP hydrolysis in the absence of strand passage (Lindsley & Wang, 1993). The biological relevance of these observations is unknown. Conversely, single molecule experiments have suggested that multiple T segments can be transported through a given DSB (Charvin et al., 2003; Smiley et al., 2007; Strick et al., 2000; Yogo et al., 2012), but how this apparent processivity is regulated, especially without dissociation of the G segment from the enzyme, is still to be clarified.

Type II topoisomerases are further divided into type IIA and IIB, ever since the discovery of the first type IIB enzyme in the archaeon *Sulfolobus shibatae* (Bergerat et al., 1997), and though both subclasses share a number of mechanistic features, there are clear structural differences between the two (Figure 1-5b). The IIA subclass includes the bacterial gyrase, which has a characteristic extended C-terminal domain that wraps ~140 bp of dsDNA around it (Lynn et al., 1986; Liu & Wang, 1978; Liu & Wang, 1981), and is thought to underlie the enzyme's preference for (+) supercoiled DNA as substrate (Kampranis et al., 1999) and its unique ability to introduce (-) sc in the bacterial chromosome (Gellert et al., 1976a; Kirkegaard & Wang, 1981; Kreuzer & Cozzarelli, 1980; Liu & Wang, 1978). As well

as gyrases, the type IIA subclass comprises most nonsupercoiling type II topoisomerases, such as the bacterial topo IV and the majority of eukaryotic topo II enzymes. The topoisomerase IIB subclass, of which topo VI is currently the only known example, is found in archaea, plants and a number of bacteria, protists and algae. Interestingly, Spo11, identified as a homologue of the DNA-binding subunit of topo VI, has been reported as an important factor during meiotic recombination in eukaryotes (Keeney et al., 1997).

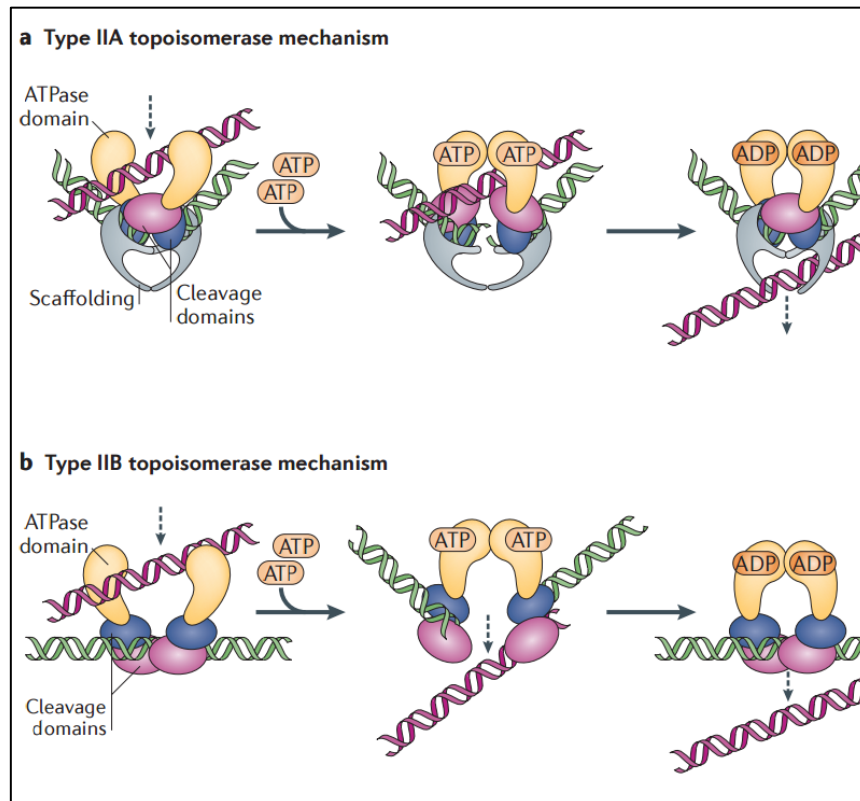


**Figure 1-5. Topology modification by type II topoisomerases.**

(a) Type IIA topoisomerases create a transient DSB and pass an intact duplex through it in an ATP-hydrolysis dependent manner. (b) Type IIB enzymes carry out a similar reaction, but differ from the type IIA subclass in their tertiary structure (From Vos et al., 2011; with permission from Nature Publishing Group).

### Topological changes by topoisomerases

Type I topoisomerases alter topology in steps of  $\Delta Lk = \pm 1$  (Wang, 1996): because they act on twists, they are only able to relax DNA or resolve interlinked ssDNA molecules (Champoux, 2001; Lopez et al., 2005). Decatenation and unknotting of intact duplexes requires type II enzymes, which can act on DNA writhes and change topology in steps of  $\Delta Lk = \pm 2$  (Liu et al., 1980). Following from

the first equation relating Lk,  $w_r$  and  $w_t$ , type II topoisomerases can also remove two supercoils (Deweese et al., 2009).

### 1.3.2 Roles of topoisomerases

All organisms whose genomes have been sequenced so far encode for at least one type I, and one type II topoisomerase. Under laboratory conditions, however, it has been shown that budding yeast cells can survive with just a copy of type II topoisomerase (i.e.  $\Delta top1$ ,  $\Delta top3$ ), although cells grow poorly (Walls et al., 1989). Multicellular organisms have more stringent topoisomerase requirements, especially during embryonic development. In mice, all six topoisomerases are indispensable to sustain life: knocking out topo I $\beta$  results in death between the 4- and 16-cell stage (Morham et al., 1996), topo II $\beta$  deletion allows embryonic development but leads to death at birth (Yang et al., 2000) and inactivating topo III $\alpha$  impedes proper implantation (Li & Wang, 1998). TopIII $\beta^{-/-}$  mice have a decreased lifespan and fertility problems (Kwan & Wang, 2001), and topo II $\alpha$  disruption leads to lethality, even in cultured cell lines (Wang, 2002).

The differential requirements of these topoisomerases imply that, although the enzymes perform similar reactions *in vitro*, their roles *in vivo* are not redundant. Therefore, the main DNA transactions in the cell, namely DNA replication, DNA transcription, chromosome segregation, chromosome condensation and recombination<sup>1</sup>, create topological challenges that require the specific action of a given topoisomerase.

### 1.3.3 Topoisomerases and replication

#### **Early stages of replication**

Topoisomerases play an important role in DNA replication: their regulation of the local topology around a replication origin can affect its firing. Examples include gyrase, which is required for activation of oriC in *E. coli* (Kornberg, 1984), topoisomerases I and II for activation of viral DNA origins in Simian virus 40 (Halmer et al., 1998), Epstein-Barr virus (Kawanishi, 1993) and Bovine papillomavirus (Hu et al., 2006), and topo I for *in vitro* DNA synthesis in budding

---

<sup>1</sup> The role of topoisomerases in recombination is beyond the scope of this thesis, and will not be further discussed.

yeast nuclear extracts (Mitkova et al., 2005). It has also been reported that origin recognition complex (ORC) binding to replication origins requires negative supercoiling in *Drosophila* (Remus et al., 2004), and that topo I is required for replication initiation close to the lamin B2 gene in human cells (Abdurashidova et al., 2007).

### **Late stages of replication**

The replication of topologically constrained DNA molecules leads to a number of topological problems (Postow et al., 1999). Perhaps most remarkably, as helicases at the replication fork unwind the parental strands to make them accessible to polymerases, the reduction in Lk caused by unwinding is compensated by formation of (+) sc—or overwinding— ahead of the fork (Champoux & Been, 1980; Postow et al., 2001), which must be dealt with by topoisomerases for replication to progress. In eukaryotes, both IB and IIA relax this torsional strain, with topo IB perhaps having a more significant role (Tuduri et al., 2014); in prokaryotes, gyrase is the main effector in removing these (+) sc (Zechiedrich et al., 1994). As forks travel from their origin, the unreplicated region becomes progressively smaller, with (+) sc eventually occupying a stretch of DNA that is not long enough for topoisomerases to act upon (Postow et al., 1999). How do cells then manage to complete replication and resolve the leftover topological problems? Two models have been postulated to explain how cells resolve DNA replication-induced topological challenges, namely the termination and the precatenane models.

### ***The termination model***

The termination model postulates that sister chromatid intertwinings originate at replication termination regions (Figure 1-6; Murray & Szostak, 1985; Sundin and Varshavsky, 1980). It provides an explanation of how DNA replication can be completed without immediate topoisomerase action (Fields-Berry & de Pamphilis, 1989; Spell & Holm, 1994). This model was proposed in the early 1980s and was supported by a number of experiments using the Simian virus 40 (SV40) replication model, which provided the first formal record that replication products appear as catenanes (Sundin & Varshavsky, 1980).

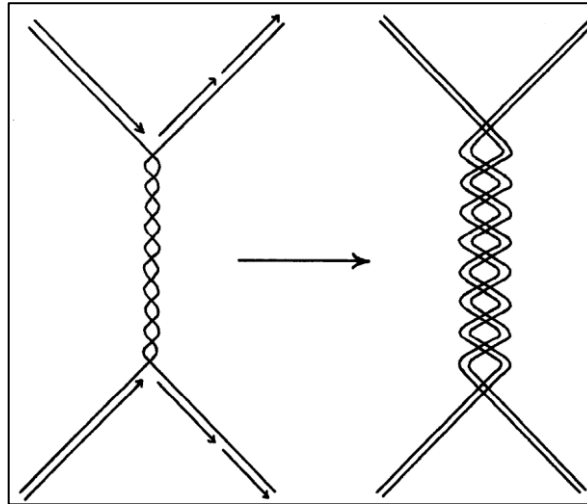


**Figure 1-6. The termination model for DNA catenation**

The termination model predicts that catenanes form at the regions of replication fork convergence. Topoisomerases cannot act on the (+) sc ahead of the forks in this region due to steric hindrance. To complete replication of the last few turns of the parental strands, replisomes must rotate, which leads to the intertwining of replicated DNA duplexes (From Murray & Szostak, 1985).

When converging replication forks are proximal, with approximately 200 nucleotides of unreplicated parental duplex in between them (Sundin & Varshavsky, 1981), they stall due to the accumulation of (+) sc in the region between the forks that cannot be removed due to steric exclusion of a swivelase (i.e. topoisomerase I and/or topoisomerase II). Catenation results from the unwinding and replication of this last DNA stretch: fork rotation converts each helical turn that gets replicated into a duplex intertwining (DiNardo et al., 1984). Both the virus (Sundin and Varshavsky, 1980) and early yeast studies using minichromosomes (DiNardo et al., 1984) found an average of 20-30 intertwinings after replication in the absence of a functional type II topoisomerase, indicating that the constraints imposed by replication forks may be similar in yeast and mammalian systems.

However, it has been recently reported that DNA synthesis does not significantly slow down upon fork convergence in *Xenopus* egg extracts, suggesting that leading strands simply pass each other before undergoing ligation to lagging strands (Dewar et al., 2015), as opposed to the fork stalling predicted by Sundin & Varshavsky. Moreover, the replisome dissociates after ligation (Dewar et al., 2015), unlike during the replication of the SV40 genome, where the helicase large T antigen is removed before unwinding of the last parental DNA stretch (Tack

& de Pamphilis, 1983). Similarly, genome-wide replication termination seems solely determined by origin position, timing and efficiency and does not correlate with pausing elements (McGuffee et al., 2013). Although higher temporal resolution might be required (e.g. to compare the replisome speed during the elongation and termination stages), this studies argues against major stalling events during termination, raises doubts on the presence of major topological constraints during this the last step of DNA replication.

### ***The precatenane model***

In contrast, the precatenane or elongation model postulates that, to counteract the supercoiling accumulated in the unreplicated region between the converging forks, some of the torsional stress can diffuse across the fork and take the form of intertwined replicated DNA behind the replication fork (Figure 1-7; Champoux & Been, 1980).

It assumes that, in order for (+) sc to be converted into precatenanes, replication forks must be able to rotate (Champoux & Been, 1980). Fork rotation would alleviate some of the stress ahead of the fork: while (+) sc can interfere with replisome progression, precatenanes do not oppose further helicase unwinding (Bermejo et al., 2008). However, precatenanes, which become catenanes after S phase is completed, need to be removed prior to chromosome segregation (Bermejo et al., 2008).

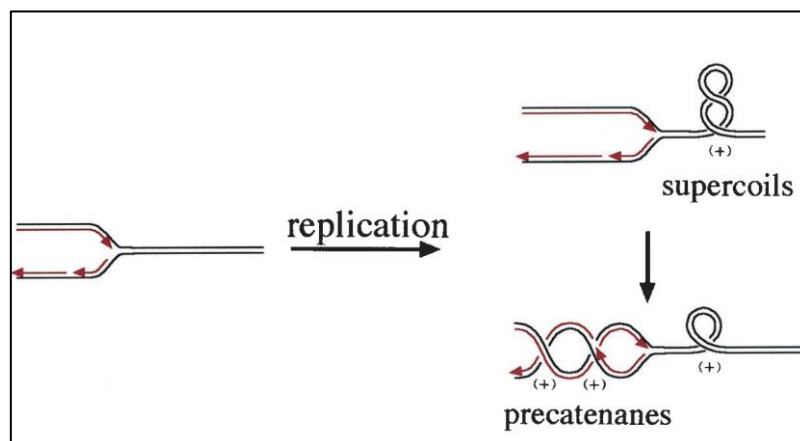


**Figure 1-7. The precatenane model for DNA catenation.**

Fork rotation during the elongation step of replication enables the transmission of (+) sc ahead of the fork into precatenanes at its wake (adapted from Postow et al., 2001).

In support of this model, replication of a plasmid *in vitro* using purified *E. coli* topoisomerases showed that unlinking occurred both in front of and behind the fork (Hiasa & Marians, 1994; Peng & Marians, 1993). Moreover, electron microscopy (EM) analysis of replication intermediates indicates that precatenanes do form as replication intermediates (Peter et al., 1998). *In vivo*, topological analyses of replicating molecules also support the precatenane model. In *E. coli*, replication intermediates of a plasmid with two opposing unidirectional ColE1 origins become knotted (maybe as a by-product of topo II activity on replication bubbles, rather than a biologically relevant structure during replication). Analysis of the knots through RecA coating and EM has provided further evidence for the precatenane model (Postow et al., 1999; Sogo et al., 1999). Moreover, partially replicated plasmids are more torsionally constrained in the absence of topo IV than in wildtype cells, suggesting that this enzyme is required during replication to remove precatenanes behind the replication fork (Cebrian et al., 2015). Further studies have obtained consistent results in *Xenopus* egg extracts, where it was shown that topo II acts behind the fork during replication (Lucas et al., 2001).

Despite these results, evidence for precatenane formation during replication elongation remains contested. The use of stalled replication forks is problematic because it may affect the behaviour and structure of the replication intermediates and create differences from actively replicating molecules, for example, due to continuing gyrase activity in the absence of replication fork progression (Postow et al., 1999; Schvartzman & Stasiak, 2003).

### **Replication fork rotation**

A key requirement for precatenane formation is that the replisome can freely rotate, but it is yet unclear whether this is the case: while rotation is simple to imagine if replisomes travel independent of one another (Breier et al., 2005; Reyes-Lamothe et al., 2008), it seems almost impossible if the replisomes remain associated as proposed by the fixed double-replisome model (Dingman, 1974; Falaschi, 2000; Levine et al., 1998). In fact, evidence from a number of systems suggests that replisomes are largely immobile (Cook, 1991; Jackson & Cook, 1986; Nakamura et al., 1986). In summary, how catenanes originate *in vivo* in eukaryotic cells remains an open question.

Replisome components could have an indirect role in modulating catenane levels through controlling the degree of fork rotation and thereby the diffusion of (+) sc to the region behind the fork, i.e. their conversion into precatenanes. For example, in *E. coli*, it has been observed that overexpression of the replisome clamp loader  $\gamma$  requires the action of topo IV during S phase (Espeli et al., 2003; Levine & Marians, 1998). In budding yeast, deletion of specific replisome-associated factors Tof1 (Timeless) and Csm3 (Tipin) leads to higher catenation levels in plasmid DNA, which can be interpreted to mean that these proteins usually prevent fork rotation (and thus precatenane formation; Schalbetter et al., 2015). However, the direct role of fork rotation in topology remains to be tested; Schalbetter and colleagues studied a genetic interaction between replisome components and topological outcomes but were unable to define the origin of the catenanes.

#### **1.3.4 Topoisomerases and transcription-induced torsional stress**

Transcription-induced topological challenges probably resemble those that arise during the elongation step of DNA replication. The transcriptional machinery, as the replication machinery, locally alters DNA topology producing (+) sc ahead of the elongating RNA polymerase (Pol I, II or III) and (-) sc in its wake (Liu & Wang, 1987; Mondal & Parvin, 2001).

If not dealt with, this accumulation of superhelical tension inhibits further transcription. Experimentally, this is supported by the fact that in the absence of topo I and topo II activities, transcription of *E. coli*  $\beta$ -galactosidase from a plasmid is repressed, suggesting that DNA topology can locally affect transcription (Caron et al., 1994; Gartenberg & Wang, 1992).

In bacterial systems, gyrase is probably the most important effector in removing transcription-induced (+) sc, while type IA topoisomerases relax the (-) sc (Nitiss, 1998; Wang, 2002; Drolet et al., 1995). The absence of topo IA in some prokaryotes, e.g. *Shigella flexneri*, is perhaps compensated for by the expression of topo IV (or other topoisomerases; Bhriain & Dorman, 1993; Kato et al., 1990).

In eukaryotes, the division of labour between the different topoisomerase enzymes is more elusive as studies often have contradictory results depending on the system used. In particular, the relative efficiencies of the different

topoisomerases in relaxing supercoils differ if the substrate is naked or chromatinized DNA (Salceda et al., 2006). In budding yeast, the presence of at least one topoisomerase (topo IB or topo IIA) is sufficient to support transcription (Kim & Wang, 1989a). The absence of both enzymes, however, inhibits RNA Pol I and Pol III (Brill et al., 1987; Schultz et al., 1992) and interferes with rDNA and polyA<sup>+</sup> RNA synthesis (Brill et al., 1987; Yamagishi & Nomura, 1988). This could be due to differences in processivity and/or translocation between RNA Pol I and Pol II (responsible for transcribing rRNA and mRNA, respectively) in the presence of torsional stress or due to differential localization of the template DNA in the nucleus (Matera, 1999; Misteli, 2001). Overall transcription is reduced by a global increase in (+) sc, as it occurs in double topoisomerase mutants (*top1Δ*, *top2-4 ts*) ectopically expressing bacterial type I topoisomerase that preferentially removes (-) sc (Gartenberg & Wang, 1992), suggesting that there is a threshold in torsional tension after which transcription and possibly other DNA processes are precluded (Joshi et al., 2010). On the other hand, closer inspection of how the inactivation of topoisomerases affects transcription revealed that the transcription of long (>3 kb) genes was precluded in topo II mutant cells (but not in topo I mutants; Joshi et al., 2012). Inactivation of topo II precluded Pol II elongation, rather than initiation, indicating that the overaccumulation of (+) sc as the transcriptional machinery travels along the chromosome is usually removed by topo II and not topo I (Joshi et al., 2012).

### **1.3.5 Topoisomerases and chromosome segregation**

Effective segregation of sister chromatids requires the removal of all interlinks between the two strands of DNA (Watson & Crick 1953). For relatively small genomes, like the *E. coli* chromosome ( $\sim 4.7 \times 10^6$  bp), this comes down to  $\sim 4.5 \times 10^5$  links per generation (Nolivos et al., 2016), for small eukaryotic genomes, like the budding yeast ( $1.25 \times 10^7$  bp), it would be in the order of  $1.2 \times 10^6$  links per generation, whereas for large mammalian genomes, e.g. human cell ( $3.3 \times 10^9$  bp), the task is more daunting, with over  $3.2 \times 10^8$  links requiring removal. Topoisomerases are very effective at performing this unlinking, considering the astounding efficiency in sister chromatid segregation, e.g. with only 1 in  $10^5$  mitotic

and 1 in  $10^4$  meiotic divisions experiencing loss of a chromosome in budding yeast (Murray & Szostak, 1985).

While most interlinks are removed before mitosis, and most probably ahead of the fork during DNA replication, an important proportion of the unlinking revolves around the removal of sister chromatid intertwinings. Being the main decatenase in the cell, the most obviously expected consequence of improper topo II activity is defective chromosome segregation, which is the case in bacteria (Wang et al., 2008) and eukaryotes, both during mitosis (diNardo et al., 1984; Holm et al., 1985; Holm et al., 1989; Uemura et al., 1987; Spell & Holm, 1994) and meiosis (Rose et al., 1990). Historically, the first phenotype characterized in fission yeast topo II mutants, namely the so-called *cut* (Cell Untimely Torn) phenotype, was described by cells attempting cytokinesis without the genome being segregated (Hirano et al., 1986; Uemura et al., 1987). In contrast to the *cut* phenotype, inactivation of topo II in mammalian cells can lead to a wide variety of phenotypes, each resulting from the specific time in the cell cycle when the enzyme is inhibited. This is probably due to the sheer size of mammalian chromosomes, which makes it easier to visualize changes in their morphologies. Topo II inactivation in metaphase blocks sister chromosome segregation; its inactivation in G2/M prevents segregation as well as chromosome resolution. In addition to these two phenotypes, mammalian cells in which topo II has been inactivated in G2 also fail to achieve chromosome individualization (Clarke et al., 2009).

### **DNA Catenation and Sister Chromatid Cohesion**

Sister chromatid cohesion (SCC) is integral for chromosome integrity, not only it is necessary for correct chromosome segregation in mitosis (Nasmyth, 2005), but it also seems to be required for DSB repair through homologous recombination (Ledesma & Aguilera, 2006). The current view is that the conserved cohesin complex tethers sister duplexes together by embracing them within its ring-shaped structure (Haering et al., 2008). The cohesin complex, formed by the Structural Maintenance of Chromosomes (SMC) proteins Smc1 and Smc3, the kleisin subunit Scc1 and Scc3 (Figure 7-1), mediates sister chromatid cohesion from S phase until the metaphase to anaphase transition, when the protease separase cleaves Scc1 (Uhlmann et al., 1999; Uhlmann et al., 2000). Two main lines of research support a major role of the cohesin complex in establishing and maintaining SCC: cohesin

mutants display increased distance between sister loci (Guacci et al., 1997; Michaelis et al., 1997), and cohesin binding to chromatin mirrors the SCC cycle (Michaelis et al., 1997), with non-cleavable cohesin preventing sister chromatid segregation (Uhlmann et al., 1999) and inducing cleavage of the cohesin complex early resulting in premature segregation (Uhlmann et al., 2000). However, it is becoming increasingly clear that other pathways contribute to SCC, especially considering the fact that the penetrance of the phenotype of cohesin mutants is locus dependent (Figure 1-9; Antoniaci & Skibbens, 2006; Ciosk et al., 2000; Diaz-Martinez et al., 2008; Guacci et al., 1997; Michaelis et al., 1997; Sullivan et al., 2004; Toth et al., 1999).

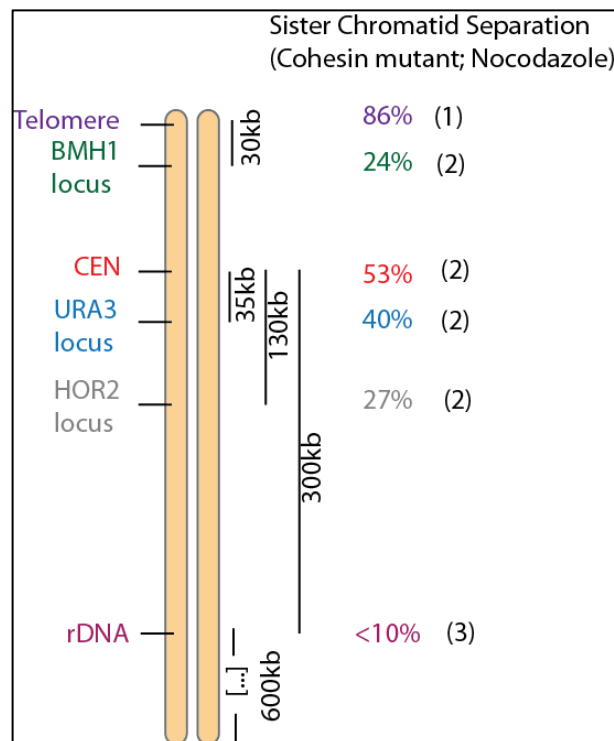


**Figure 1-8. Penetrance of cohesin mutants is locus dependent in budding yeast**

Tet and lac operators can be introduced into a given locus along budding yeast chromosomes, and SCC can be assessed using Tet- or lacR-GFP fusions. The absence of functional cohesin complexes affects SCC differently among the distinct loci studied so far. For example, SCC at the rDNA locus is hardly disturbed upon cohesin inactivation (only 10% of the cells show SCC defects), whereas telomeric SCC is almost completely dependent on an active cohesin complex (86% of the cells show premature sister chromatid separation; (1) Antoniaci & Skibbens, 2006; (2) Lam et al., 2006, (3) D'Amours et al., 2004).

In fact, the first formally proposed mechanism of SCC suggested that cohesion was provided by topological intertwinings (Tschumper & Carbon, 1983;

Murray & Szostak, 1985; Holm, 1994; Koshland & Hartwell, 1987; Spell & Holm, 1994). This idea was supported by studies that reported the presence of intertwinings before anaphase (Uemura & Yanagida, 1986; Holm et al., 1985). Because catenation occurs as a by-product of DNA replication (Sundin & Varshavsky, 1980), it physically couples replication to cohesion. In contrast, cohesin couples replication to SCC biochemically, and replication can proceed to completion in the absence of the cohesin complex (Diaz-Martinez et al., 2008). The levels of chromosomal DNA catenation are controlled by topo II and it has been proposed that this enzyme could reinforce cohesin-based SCC (Bachant et al., 2002). In fact, a number of studies suggest that both catenation and the cohesin complex are required for sister chromatid cohesion, and both need to be removed to achieve complete and correct segregation (Deehan-Kenney & Heald 2006; Diaz-Martinez et al., 2006; Toyoda & Yanagida, 2006). In budding yeast, it has been proposed that the contribution of sister chromatid intertwining towards cohesion also is locus-specific (Diaz-Martinez et al., 2008). Indeed, while the segregation of the majority of the genome is marked by cohesin removal, underscoring the role of the cohesin complex, the rDNA locus segregates later (Koshland & Guacci, 2000). Introducing an ectopic decatenase that cannot be subjected to endogenous regulation speeds up the rDNA segregation, suggesting that catenanes at least partly mediate cohesion at this locus (D'Ambrosio et al., 2008a). Moreover, topo II seems to play a role in modulating the levels of tension between sister kinetochores at mitosis (Porter & Farr, 2004): topo II inactivation in DT40 cells arrested in prometaphase due to cohesin depletion restores biorientation of chromosomes at the metaphase plate and deactivates the spindle assembly checkpoint (Vagnarelli et al., 2004). Similar observations have been reported in budding yeast (Dewar et al., 2004). Depletion of condensin has analogous effects after cohesin removal in *Drosophila* (i.e. cells progress through prometaphase; Coehlo et al., 2003), perhaps by interfering with topo II-mediated resolution of sister chromatids. These observations together suggest that the residual catenation could contribute to sister chromatid cohesion (Porter & Farr, 2004).

On the other hand, it was shown in budding yeast that  $\leq 5\%$  of a 14 kb minichromosome population is catenated prior to anaphase, which argues for a transient nature of intertwinings as well as their dispensability for SCC (Koshland & Hartwell, 1987). However, later studies have shown a size dependency effect on

the levels of detectable catenation in minichromosomes: while very small plasmids (i.e. <5 kb) are hardly detected as catenated topoisomers in wildtype cells (Ivanov & Nasmyth, 2007; Farcas et al., 2011), at least 20% of minichromosomes that are >20 kb are catenated in cells arrested in metaphase (Farcas et al., 2011; Charbin et al., 2014). Furthermore, it is known that minichromosomes are up to two orders of magnitude less efficiently segregated than endogenous chromosomes (Koshland & Hartwell, 1987), and it can be argued that the reduction in faithful segregation may be due to lower SCC levels in the absence of intertwinings.

In bacteria, the intertwining of sister DNA duplexes is, at least partly, responsible for chromatid cohesion (Wang et al., 2008). Topo IV inactivation inhibits locus separation; conversely, increasing the levels of the decatenase reduces cohesion substantially, suggesting that catenanes mediate sister chromatid cohesion in this system (Wang et al., 2008). Nevertheless, cohesion by physical DNA intertwining could be a peculiarity of systems where there is hardly any temporal separation between DNA replication and chromosome segregation, with strictly controlled, dedicated cohesion mechanisms playing a more prominent role in organisms with distinct S phase and mitosis. It would be interesting to find out the relative contribution of precatenation to sister chromatid cohesion in bacteria and archaea that experience clearly separated DNA replication and segregation (Wang et al., 2008).

The complete picture regarding the interplay between cohesin-mediated SCC and topo II-driven decatenation is far from being elucidated. Theoretically, using a protein structure to maintain SCC would facilitate efficient and simple chromatid segregation— the forces keeping the protein complex together are probably weaker than those holding a catenane, and alternative ways to disengage the complex would still be attainable. If intertwinings contribute towards SCC, decatenation should be controlled in time (ensuring complete removal of intertwinings by anaphase) and also in space, especially if catenanes are mobile along chromosomes (Bermejo et al., 2008). Up to very recently, it was very difficult to foresee how such temporal and spatial control could be achieved. On the other hand, it is becoming progressively more evident that topo II is subject to regulation (See section 1.5). Thus, it is plausible that proper SCC results from a balance between cohesin, catenation and possibly other mechanisms, and that their relative contributions vary across genomic loci.

### 1.3.6 Topoisomerases and chromosome condensation

Prior to sister chromatid segregation, cohesed sisters undergo condensation or protein-mediated packaging of the DNA (Hirano, 2010). Condensation is thought to be crucial for two processes, namely sister chromatid resolution and axial compaction, i.e. reduction of the length of chromosomal arms to prevent potential damage by cytokinesis (Hirano, 2000). Condensation, which is indispensable for accurate chromosome segregation, involves a highly coordinated folding of chromatin, yet is a poorly understood process at the molecular level (Cuvier & Hirano, 2003).

It is now well established that the evolutionarily conserved condensin complex determines mitotic chromosome architecture and stability through its role in chromosome condensation (Thadani et al., 2012). It is composed of the SMC ATPase subunits Smc2 and Smc4, as well as a kleisin subunit (CAP-H/Brn1 in budding yeast) and two HEAT-repeat subunits CAP-D2 and CAP-G (Ycs4 and Ycg1; Figure 7-1; Cuvier & Hirano, 2003; D'Ambrosio et al., 2008b). Interestingly, condensin purified from mitotic *Xenopus* extracts can introduce (+) sc on plasmid DNA in the presence of topo I *in vitro*, an activity that requires ATP hydrolysis and involves the wrapping of two oriented gyres of DNA around the complex (Bazzett-Jones et al., 2002; Cuvier & Hirano, 2003; Kimura & Hirano, 1997). In the presence of type II topoisomerase, purified Smc2/4 promotes knotting of supercoiled plasmid DNA (Stray & Lindsley, 2003), and this behaviour is also observed in the presence of an ATP hydrolysis defective Smc2/4 dimer (Stray et al., 2005). However, how this *in vitro* activity translates into the condensation process in the cell remains largely unknown (Cuvier & Hirano, 2003). *In vivo*, condensin has been found to promote chromosome recoiling during budding yeast anaphase, which in turn triggers sister chromatid separation (Renshaw et al., 2010).

Topo II, on the other hand, is also essential for chromosome condensation (Uemura et al., 1987), but again the mechanism through which it contributes to mitotic chromosome organization is unclear, with both structural and enzymatic roles having been suggested as important towards this means (Cuvier & Hirano, 2003). Strikingly, the failed chromosome segregation phenotypes of topo II (Uemura et al., 1987) and condensin (Bhalla et al., 2002; Saka et al., 1994; Strunnikov et al., 1995) mutants are very similar, which has pointed to the

hypothesis that chromosome condensation may drive topo II-mediated decatenation in mitosis (Hirano, 2000; Holmes & Cozzarelli, 2000). In *Xenopus* egg extracts, chromosome assembly after DNA replication takes place in two temporally distinct steps: first, topo II binds chromatin forming a topo II axis, followed by condensin-mediated compaction (Cuvier & Hirano, 2003).

In *E. coli*, the functional analogues of the SMCs are the Muk proteins, MukB, MukE and MukF (from the Japanese word for anucleate, *mukaku*). It has been established that both MukB and topo IV are required for efficient chromosome segregation (Hirano, 2010), and the interaction between the two complexes has been inferred from live-cell imaging (Nicolas et al., 2014) and shown *in vitro* (Hayama & Marians, 2010; Li et al., 2010). The C-terminal domain of ParC (Hayama & Marians, 2010), a region predicted to act as the geometry sensor of topo IV (Hirano, 2010; Corbett et al., 2005), interacts with the hinge of MukB (Hayama & Marians, 2010; Li et al., 2010). This interaction substantially stimulates topo IV-mediated relaxation, and, to a lesser extent, decatenation (Hayama & Marians, 2010; Li et al., 2010). However, why the interaction stimulates relaxation over decatenation, and what the influence of the whole MukBEF complex (rather than MukB-hinge or MukB alone) on topo IV function is, are still not understood.

How do these *in vitro* results translate into the cellular processes that drive condensation and segregation? The MukBEF complex normally associates with the origin region of the bacterial chromosome (Nicolas et al., 2014), presumably to position it, and is displaced from the termination region by MatP (Nolivos et al., 2016). One possibility is that MukBEF recruits topo IV through a physical interaction (Hayama & Marians, 2010) and directs its activity to decatenate different regions of the chromosome in a timely manner (Nolivos et al., 2016). Alternatively, MukBEF binding to DNA may alter its topology and make it a preferred substrate for topo IV catalysis (Zechiedrich et al., 1997). This hypothesis has also been proposed for eukaryotic condensin, from experiments using centromeric minichromosomes in the absence of topo II (Baxter et al., 2011; Baxter & Aragon, 2012), although whether this scenario represents the situation of native chromosomes in unchallenged cells is questionable.

In eukaryotes, it is yet unclear whether there is a physical interaction between condensin and topoisomerase II. Both the condensin complex and topo II colocalize to the axial region of mitotic chromosomes and cofractionate into the

chromosome scaffold (Farnshaw et al., 1985; Hirano, 2010; Maeshima & Laemmli, 2003). Genetic analyses suggest that there is a functional interaction (Coehlo et al., 2003); nevertheless, evidence for direct interaction is mostly lacking (Bhalla et al., 2002; Charbin et al., 2014; Lavoie et al., 2002), with the only exception reported in *Drosophila melanogaster* embryos (Bhat et al., 1996). In budding yeast, there is a statistically significant degree of colocalization, as determined by immunostaining on spread chromosomes and ChIP-on-chip (D'Ambrosio et al., 2008b), although these do not necessarily imply direct interaction.

Nevertheless, there seems to be an evolutionarily conserved functional interaction between condensins and type II topoisomerases that is of particular significance for mitotic chromosome organization and overall chromosome architecture.

### **1.3.7 Topoisomerases as cellular toxins**

Despite being essential enzymes, type II topoisomerases can be intrinsically dangerous due to their ability to create DSBs in the genome (Deweese & Osheroff, 2009). They form covalent bonds between their active site tyrosyl residues and DNA's terminal phosphates to maintain genome integrity; this DNA-protein intermediate is referred to as a cleavage complex (Champoux, 2001; Clarke, 2009). Cleavage complexes are transient intermediates in the enzyme's catalytic cycle, and are usually kept at low levels (and therefore are tolerated by the cell) because the cleavage-ligation equilibrium leans toward ligation (Wang, 1996). If their concentration is increased significantly, it results in the generation of permanent breaks, which ultimately induce illegitimate recombination and chromosomal aberrations (Fortune & Osheroff, 2000). In line with this, it is also established that high expression levels of wild type DNA topo II in budding yeast are known to be cytotoxic (Goto & Wang, 1984; Worland & Wang, 1989). This is possibly due to DSBs arising from DNA-tracking machineries colliding into topo II–DNA intermediate complexes, although other explanations, like aberrantly low levels of catenation that could result in insufficient sister chromatid cohesion, have not been ruled out.

To maintain genome integrity, covalently bound topo II–DNA cleavage complexes are usually short-lived (Fortune & Osheroff, 2000; McClendon &

Osheroff, 2007) and the reaction equilibrium typically favours ligation (McClendon & Osheroff, 2007; Schoeffler & Berger, 2008; Wang, 1998), with only 0.5-1% of the enzyme being part of such a complex in a reaction mixture (Deweese & Osheroff, 2009; Liu et al., 1983; Zechiedrich et al., 1989). Moreover, the relatively low abundance of single-stranded breaks— about 1/4-1/2 of the active complexes— suggests that there must be a high degree of coordination between the two active sites of the topoisomerase II dimer (Bromberg et al., 2003); once the first break is created, the second strand is usually cleaved ~20-fold faster (Mueller-Planitz & Herschlag, 2008).

The levels of topoisomerase II activity and cleavage complexes must be tightly regulated: too low levels may result in residual torsional stress and intertwining that will hinder chromosome segregation, too high levels may give rise to permanent DSBs (Bender & Osheroff, 2008; D'Arpa et al., 1980; McClendon & Osheroff, 2007; Pommier & Marchand, 2005; Wu & Liu, 1997). In mammalian cells, these DSBs are recognized and turn on signalling pathways involving Ataxia Telangiectasia Mutated (ATM), Ataxia Telangiectasia and Rad3-related protein (ATR) or DNA-dependent Protein Kinase (DNA-PK), eventually leading to extensive phosphorylation of histone H2AX (Rogakou et al., 1998) within a megabase of DNA around the DSBs (Rogakou et al., 1999). Eventually, genomic stability might be compromised, as the ensuing DNA damage might lead to mutations, chromosomal translocations, and, eventually, cell death (D'Arpa et al., 1980; Deweese & Osheroff, 2009; Kaufmann, 1998; McClendon & Osheroff, 2007). Similarly, type I topoisomerases can pose a threat to genome stability, when the enzyme fails to complete the reaction cycle and instead remains as a covalent DNA-protein intermediate, which constitutes a bulky DNA lesion that can interfere with DNA metabolism (Leppard & Champoux, 2005).

On the other hand, a number of pharmacological agents have been developed in the last few decades to exploit the genome-threatening property of topoisomerases. They are typically classified into two classes, namely catalytic inhibitors and poisons. Catalytic inhibitors decrease the overall activity of topoisomerases, while topoisomerase poisons alter the reaction equilibrium towards cleavage, thereby increasing the levels of cleavage complexes, which, as described above, can result in permanent strand breaks as DNA-tracking systems

collide with the covalently bound topoisomerase (D'Arpa et al., 1980; McClendon & Osheroff, 2007; Pommier et al., 1998).

Topoisomerase poisons are amongst the most widely prescribed anticancer drugs, with treatments against most types of cancer deemed curable by chemotherapy employing drugs against topo II (Baldwin & Osheroff, 2005; Dewese & Osheroff, 2009; Hande, 1998; Martincic & Hande, 2005). Interestingly, a number of these compounds are low-toxicity derivatives of natural products that have been used as folk remedies for centuries (Deweese & Osheroff, 2009). For example, etoposide is a synthetic analogue of Podophyllotoxin, from the mandrake plant (Hande, 1998). Topoisomerase-targeted drugs have also been used as powerful antibacterials, like the quinolone group (topo II poisons) and the coumarin family (gyrase inhibitors; Sissi & Palumbo, 2010).

#### **1.4 How does topo II act globally?**

DNA relaxation is an energetically favourable reaction. It can be carried out in the absence of ATP hydrolysis by type I topoisomerases. The fact that nonsupercoiling type II enzymes employ ATP hydrolysis seemed puzzling, until it was shown that the reaction carried out by these enzymes simplifies the topology of the products beyond the level of equilibrium, i.e. in the presence of ATP and topo II, a steady-state distribution narrower than the Boltzmann equilibrium distribution achieved by topo I is produced (consistent with the free energy associated with supercoiling; Rybenkov et al., 1997). Thus, at least locally, there is no thermodynamic mystery: the energy derived from ATP hydrolysis drives the reaction away from equilibrium. However, at a global scale, we still cannot explain how a small enzyme can alter the topology of the cell's genome (Stuchinskaya et al., 2009; Timsit, 2011), and ensure that, for example, all catenanes are resolved prior to anaphase. This is a particularly complex conundrum, considering that the complexity of a large DNA molecule is a global property of the assembly and is insufficiently described by local protein-DNA interactions (Sissi & Palumbo, 2010).

Despite the fact that topo II acts on a global scale, it has been suggested to cleave DNA at preferred sequences (Capranico & Binaschi, 1998); however, the consensus sequence is weak and prediction of scission sites is nearly impossible (Capranico & Binaschi, 1998; Dewese & Osheroff, 2009). This suggests that other

factors, possibly including local structure, accessibility, and/or flexibility determine cleavage (Velez-Cruz et al., 2005).

A number of models have been put forward to explain how global topology simplification occurs, and address the concept of a particular T segment being preferred over others in the strand passage reaction (Timsit, 2011). This would occur through either geometric or kinetic selection (Figure 1-10).

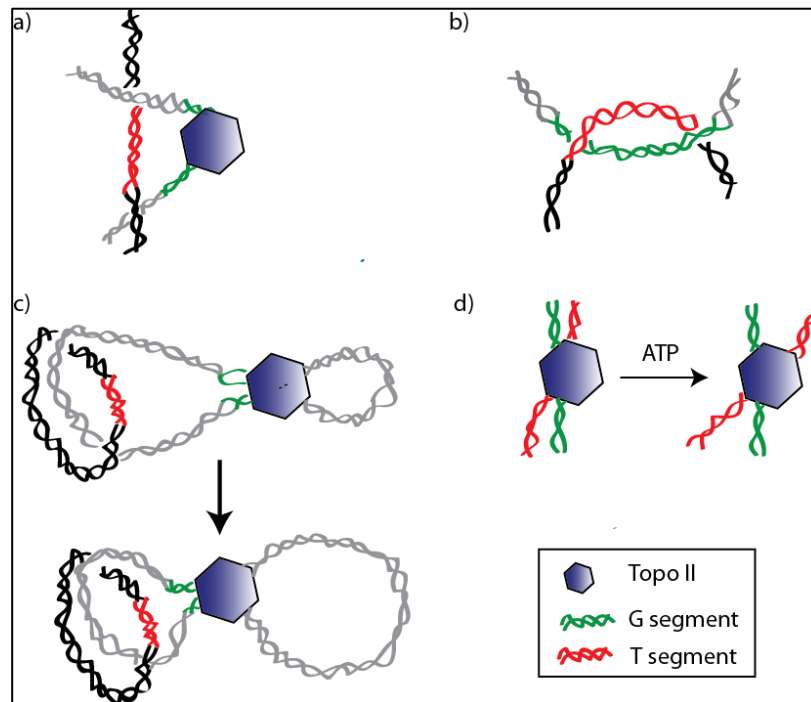


**Figure 1-9. Models for topo II topology simplification**

a) In the kinking model, topo II binding bends the G segment and repositions the enzyme with respect to other DNA regions, creating a preference over a particular T segment. b) According to the hooked juxtaposition model, the geometry of supercoils, catenanes and knots is favoured for recognition by topo II. c) Topo II creates a corral effect by tracking along a DNA stretch, progressively making this stretch shorter and facilitating the capture of a given T segment. d) Proofreading models propose that topo II initially traps a T segment, and an irreversible ATP-dependent step changes the enzyme-DNA conformation, which in turn favours T segment passage over loss. (Adapted from Bates & Maxwell, 2007)

Geometric models propose that the differential probability of the enzyme–T segment interaction comes from the local curvature of a given DNA segment. This curvature can be introduced by the enzyme, which by “kinking” the DNA creates a preferred orientation with respect to the global topology of DNA (Figure 1-10a; Vologodskii et al., 2001). Alternatively, geometric selection could come from the topoisomer curvature alone (rather than the DNA-enzyme complex), as in the

“hooked juxtaposition” model (Figure 1-10b; Buck & Zechiedrich, 2004). Type II topoisomerases preferentially associate with DNA crossovers or juxtapositions (Zechiedrich & Osheroff, 1990; Roca et al., 1993; Charvin et al., 2003; Charvin et al., 2005; Alonso-Sarduy et al., 2011), which can explain why the enzyme would preferably bind (+) sc, knotted and catenated DNA, (Stuchinskaya et al., 2009). Monte Carlo simulations (Vologodskii et al., 2001) and X-ray crystallography (Dong & Berger, 2007) studies support geometric models.

In contrast, kinetic tracking models propose that the enzyme recognizes a third site on DNA, tracks along it reducing the apparent DNA length, and eventually traps a T segment in a small loop (thus also called “corral effect”; Figure 1-10c; Rybenkov et al., 1997). The trapped segments are more likely to correspond to supercoiled knotted or catenated DNA, thereby explaining the eventual global topology simplification. While there is some experimental support for topo II binding to three sites on DNA (Trigueros et al., 2004), as kinetic tracking requires, circumstantial evidence argues against tracking, as the presence of protein roadblocks does not affect the topology simplification effect by topo II (Stuchinskaya et al., 2009). Finally, kinetic proofreading models have been put forward (Figure 1-10d; Yan et al., 1999; Yan et al., 2001) that postulate that the T segment preferences may be driven by geometric selection, but amplified through an irreversible ATP-dependent step. Experimentally, it has been shown that gyrase can capture and release the same T segment without passage (Bates et al., 1996; Kampranis et al., 1999). For decatenases, like yeast topo II, it has been reported that the rate of ATP hydrolysis can exceed the rate of the strand passage reaction (Lindsley & Wang, 1993), however, this does not directly show a proofreading effect.

Overall, there is no consensus to explain topo II topology simplification, and the models put forward so far cannot fully account for this effect. Understanding topology simplification will require more studies on the properties of different DNA crossovers, and how they differentially affect topo II-mediated recognition and processing.

## 1.5 Regulation of topoisomerases

Topology simplification is typically studied *in vitro*, often with the minimal set of components required for topoisomerase function. The main caveat is that these experiments largely exclude the potential effects of cellular components that may affect topo II-mediated topology simplification, through for example regulating the enzyme's subcellular localization and/or activity (i.e. processivity, reaction rate, etc.) or by altering the conformation of the DNA substrate.

Topoisomerases are abundant proteins in the cell, perhaps unsurprisingly, given the huge topological challenges that the cell has to overcome. There are many instances when topoisomerase action is necessary: every time a gene is transcribed, but most notably when catenanes need to be disentangled during mitosis. Several lines of evidence suggest that the activity of these enzymes is subject to regulation, activatory or inhibitory. One important example is the stimulation of topo I during the transcription pause-release cycle, whereby BRD4-mediated phosphorylation of the C-terminal domain (CTD) of paused RNAPII (which itself triggers release from the pause) enhances topo IB processivity to clear out (+) sc as the polymerase starts the elongation step (Baranello et al., 2016). Thus, key cell cycle events may fine-tune topoisomerase activities and/or localization to coordinate topological rearrangements required for DNA metabolism.

### 1.5.1 Regulation of topo II

Topoisomerase II is the main cellular decatenase, and, due to the potential problems that incomplete decatenation can lead to, one might naively assume its activity to be constitutive throughout the cell cycle and the genome. However, it is becoming progressively clear that many factors may affect topo II catalytic activity. First, the CTD of topo II is subject to post-translational modifications, with phosphorylation and sumoylation being the two most studied examples (Porter & Farr, 2004). Acetylation and ubiquitination of topo II have also been reported, but their effects on the enzyme's functions are more controversial. Moreover, an increasing number of factors seem to enhance the catalytic activity of topo II through protein-protein interactions. Understanding how the function of topo II is modulated will help elucidate how topological challenges come about in the cell, and whether there are mechanisms that sense them prior to their resolution.

### 1.5.2 C-terminal domain (CTD) of type II topoisomerases

Intriguingly, the domains that confer topo II catalytic activity are not sufficient for its localization to mitotic chromosomes (Linka et al., 2007); instead, it has been suggested that the non-conserved C-terminal domain (CTD) has a role in directing topo II to chromosomes (Lane et al., 2013). This region is a disordered and poorly conserved stretch of 200-300 amino acids (aa), dispensable for the topo II catalytic activity (Edgerton et al., 2016) and completely absent in the viral enzymes. Up to date, it has been refractory to crystallization, and studies on its function have not led to a uniform picture.

Budding yeast topo II CTD comprises a 250 aa region that has little homology with other eukaryotic type II topoisomerases. Deletion of most of the CTD (the most C-terminal 209 aa) has no noticeable effect on the enzyme's function *in vivo* or *in vitro* (Caron et al., 1994; Jensen et al., 1996). Leaky transcription of mutants lacking this fragment (i.e. driven by the repressed *GAL1* promoter, in the presence of glucose) complemented the lethality of the temperature sensitive allele *top2-4* at restrictive temperature, underscoring the fact that low levels of topo II are sufficient to attain viability. Interestingly, the adjacent approximately 40 aa are important for topo II's *in vivo* functions, but not its *in vitro* activities (Caron et al., 1994). One possibility is that this stretch is important for protein-protein interactions with other cellular entities, as evidenced by the reduced nuclear localization of some of truncated topo II proteins (Caron et al., 1994).

In higher eukaryotes, topo II's CTD has been implicated in the enzyme's dynamics on chromosomes (Lane et al., 2013; Linka et al., 2007). Deletion of the most C-terminal 31 aa of human topo II $\alpha$ —referred to as Chromatin Tether (ChT) domain because it binds DNA and histone H3 *in vitro*—precluded the stable interaction between the enzyme and chromosomes and affected mitotic chromosome formation and segregation (Lane et al., 2013). Fluorescence recovery after photobleaching (FRAP) analysis showed deletion of the ChT domain resulted in an increased mobility of the enzyme on chromosomes ( $t_{1/2}$  of 6.4 s versus 10.3 s for wildtype topo II $\alpha$ ; Lane et al., 2013). Given that the activity of topo II is excluded from nucleosome-rich regions *in vitro* (Galande and Muniyappa, 1997), ChT binding to histones could present a mechanism to help the enzyme position itself along the DNA (Lane et al., 2013).

### 1.5.3 Sumoylation and phosphorylation

Post-translational modification by SUMO (Small Ubiquitin-like MOdifier) is a major, highly conserved protein modification system with a wide impact on cellular functions. Vertebrates have three SUMO isoforms, all around 50% identical to the budding yeast single SUMO orthologue, Smt3 (Dasso, 2008). The SUMO conjugation process resembles that of ubiquitin, with three sequential enzymes (E1, E2 and E3), and it can be reversed by highly active SUMO proteases (Dasso, 2008). Budding yeast topo II modification by SUMO revealed a novel regulation mechanism on mitotic chromosomes (Takahashi et al., 2006), shown to also be the case in mammalian cells (Mao et al., 2000) and *Xenopus* egg extracts, where inability to properly sumoylate topo II in mitosis affects the enzyme's association with chromosomes and causes aberrant sister chromatid separation (Azuma et al., 2003).

Interfering with topo II sumoylation has been reported to hinder chromatid separation, ultimately inducing mitotic checkpoint arrests (Diaz-Martinez et al., 2006) or leading to anaphase bridging (Dawlaty et al., 2008). Because sumoylation has been suggested to control topo II localization to centromeres and the axis of mitotic chromosomes in vertebrates (Dawlaty et al., 2008; Ratner et al., 1996), it has been proposed that this post-translational modification may direct the enzyme to sites of residual catenation, as cells transition into anaphase (Diaz-Martinez et al., 2006). However, due to the inability to observe catenanes along eukaryotic chromosomes, this hypothesis has not been formally confirmed. In yeast, topo II-SUMO fusion proteins crosslink to centromeric DNA (Takahashi et al., 2006) and can accumulate in the nucleolus (Takahashi & Strunnikov 2008). In addition, topo II mutants that cannot be sumoylated (*top2-SM*) exhibit incomplete centromere compaction (Bachant et al., 2002). In line with these observations, Smt4 isopeptidase (which removes the Smt3/SUMO-1 posttranslational modification) is required to maintain chromatid cohesion in metaphase (in a cohesin-independent manner) at centromeres and centromere proximal regions but not at chromosome arms, as determined by separation of GFP-labelled lac operator arrays (Bachant et al., 2002).

More recently, sumoylation of budding yeast topo II CTD has been reported to be essential for the recruitment of Ipl1 (Aurora B) to inner centromeres,

independently of the Shugoshin-H2A pathway (Edgerton et al., 2016). This finding has been complemented with the observation that topo II CTD sumoylation triggers the formation of Haspin kinase–topo II complexes in *Xenopus* egg extracts, and Haspin–mediated phosphorylation of H3 in turn promotes Aurora B recruitment to centromeres (Yoshida et al., 2016). Together, these observations indicate that sumoylation of topo II is required for organization of mitotic chromosomes.

The topo II CTD also contains sites for cell-cycle dependent phosphorylation which putatively modulates the enzyme's activity and localization, e.g. phosphorylation of serine 1212 seems to relocalize topo II $\alpha$  from the arms to the centromeric region of mitotic chromosomes (Ishida et al., 2001; Porter & Farr, 2004). Moreover, *in vitro* experiments have shown that topo II can be phosphorylated by Aurora B, indicative of mitotic activity (Morrison et al., 2002). Protein Kinase C and casein Kinase II have been reported to phosphorylate topoisomerase II *in vitro* in *Drosophila* (Ackerman et al., 1988; deVore et al., 1992), human cells (Sahyoun et al., 1986), budding yeast (Cardenas et al., 1992) and the sponge *Geodia cydonium* (Rottmann et al., 1987), which, in turn, stimulates the enzyme's catalysis 2-3 fold through an increase in the enzyme's rate of ATP hydrolysis (Ackerman et al., 1988; DeVore et al., 1992). Additional lines of research are required to fully understand the relevance of topo II CTD phosphorylation and its putative effect on the enzyme's activity during mitosis.

#### **1.5.4 Protein-protein interactions**

A number of recent studies have identified a number of protein-protein interactions between topo II and different cellular factors that affect the enzyme's activity and/or stability. One such interaction is promoted by ATM, which interacts with and phosphorylates topo II $\alpha$  at Serine 1512 (S1512; Tamaichi et al., 2013). Interestingly, this phosphorylation seems important for regulating the enzyme's cellular levels, and S1512A mutants display higher protein stability (Tamaichi et al., 2013). Mitogen-Activated Protein (MAP) kinases have also been reported to interact with topo II; for example, phosphorylated Extracellular Signal-Regulated Kinase 2 (ERK2) binds to and stimulates topo II $\alpha$  catalytic activity *in vitro* and *in vivo* (Shapiro et al., 1999). Other than kinases, chromatin-binding proteins have also been reported to regulate topo II. For instance, the chromatin-associated

protein High Mobility Group Box1 (HMGB1, from the HMG-box protein family) enhances topo II $\alpha$ -mediated DNA cleavage, which in turn stimulates its catalytic activity (Stros et al., 2007). Similarly, the chromatin remodelling BRG1-Associated Factors (BAF) complex has been shown to interact with topo II $\alpha$ , which greatly stimulates the enzyme's activity on chromosomes (Dykhuisen et al., 2013).

Tumour suppressor proteins have been recently linked to type II topoisomerases. In mammalian cells, BRCA1 was found to interact with topo II $\alpha$  during S phase, and affects its ubiquitination (Lou et al., 2005). Strikingly, extracts from cells lacking BRCA1 were inefficient at kDNA decatenation *in vitro*. This activity could be rescued by reconstituting BRCA1 in these cells, suggesting a link between this tumour suppressor in regulating topo II-mediated decatenation (Lou et al., 2005). In line with these observations, it has been recently noted that *Drosophila* topo II interacts with Mus101/TopBP1 (a BRCA1 C-Terminus domain-containing protein), and abrogation of this interaction results in chromosome segregation defects (Chen et al., 2016).

Although the relevance of these interactions needs to be fully elucidated, a picture of complex regulatory networks to control DNA topology is starting to emerge.

## 1.6 Complexities in chromosome organization

A second caveat of topology simplification assays is that, for simplicity, they often use DNA substrates that are possibly different from the endogenous substrates. Thus, these assays could be overlooking aspects of DNA topology influenced by particular sequences (e.g. protein binding sites) that could in turn affect their recognition by topoisomerases.

Our understanding of chromosome topology is based on findings using exogenous plasmids or minichromosomes. Molecular cloning allowed the introduction of replicators (Struhl et al., 1979), telomeres (Szostak & Blackburn, 1982; Szostak, 1982) and centromeres (Clarke & Carbon, 1980; Stinchcomb et al., 1982) into DNA molecules in order to approach the structure and behaviour of natural chromosomes (Murray & Szostak, 1985). While the mechanisms of replication, organization and segregation may be similar for minichromosomes and

chromosomes, it has never been directly tested because detailed analysis of endogenous chromosome behaviour is technically very difficult. One noticeable difference is in stability: linear artificial chromosomes and circular centromeric plasmids are at least ~100-fold more prone to mitotic loss with respect to endogenous chromosomes, an effect that seems to be dependent on the length of the DNA molecule (Murray & Szostak, 1983; Murray & Szostak, 1985). Minichromosomes can probably be pictured as small, independent topological domains, and, in many aspects, their topological behaviour may not exactly emulate that of endogenous chromosomes. Differences in size (typically, 5-40kb in minichromosomes versus 230 kb for the smallest budding yeast chromosome (Chr. I), protein binding, DNA/chromosomal elements and nuclear localization might account for possible differences in their topological states between the two.

### **1.6.1 Topological domains**

Topological stresses generated by cellular machineries that track along DNA are probably confined to closed topological domains and physical barriers restrict their diffusion to other chromosomal regions (Postow et al., 2004).

This idea comes from the widespread view that eukaryotic chromosomes are intricately organised, starting with the wrapping of DNA into nucleosomes and 10 nm chromatin fibres (Kawamura et al., 2010). At larger scales, chromatin organisation is thought to involve chromatin-chromatin interactions, as well as chromatin tethering to nuclear membranes, possibly mediated by protein factors but still incompletely understood (Kawamura et al., 2010). Moreover, it has been suggested that entire chromosomes, or chromosomal elements— such as centromeres and telomeres— occupy specific positions in the nucleus, as evidenced by *in situ* hybridization and immunofluorescence (Chung et al., 1990; Ferguson & Ward 1992; Gartenberg & Wang, 1993). Electron microscopy has allowed the visualization of supercoiled loops ranging from 1-300 kb that protrude from the amorphous, globular mass in both eukaryotic and bacterial chromosomal preparations (Delius & Worcel, 1974; Paulson & Laemmli, 1977). Furthermore, a genome-wide study of helical tension in budding yeast using psoralen photobinding followed by hybridization of the crosslinked DNA to arrays concluded that different

chromosome compartments confined varying levels of torsional stress (Bermudez et al., 2010). Together, these results support a view of DNA arranged into topological domains, through attachment to chromosomal anchors.

Micromanipulation experiments have been used to determine which factors contribute to the stable and well-characterized elasticity of isolated native chromosomes (Marko, 2008). For example, applying a force of 500 pN to newt mitotic chromosomes extended them to double their native length; treatment with restriction nucleases completely dissolved these chromosomes, pointing at a network organization with approximately 15 kb stretches of chromatin strung between crosslinks (Poirier & Marko, 2002; Pope et al., 2006). Protease treatment, on the other hand, only partially decondenses mitotic chromosomes (Pope et al., 2006) and, while reducing chromosome stiffness, protease-treated chromosomes remain elastic. A role for RNA in stability has been discarded, since experiments using RNase showed no relaxation of mitotic chromosomes (Almagro et al., 2004). Alternatively, DNA entanglements (i.e. catenation and/or knotting) could be partially responsible for organizing chromosome architecture (Kawamura et al., 2010). Addition of recombinant topo II $\alpha$  reduces the native chromosome spring constant (i.e. stiffness) by 35% without detectably altering chromosome morphology, in a manner that depends on hydrolysable ATP and DNA cleavage by topo II (i.e. the effect is abolished in the presence of topoisomerase inhibitors). Because the same effect is not observed with topo I or topo III, it suggests that DNA intertwinings and knots, but not supercoils or hemicatenanes, contribute to mitotic chromosome mechanical stability (Kawamura et al., 2010). Moreover, the 35% decrease suggests that the densities of entanglements and of protein cross-linkers should be similar: if the former was much larger than the latter, spraying topo II on the chromosomes would almost entirely eliminate chromosome elasticity, whereas if the opposite was the case, topo II addition would have no significant effect on the spring constant (Kawamura et al., 2010).

The topo II strand passage reaction can also result in catenation and knot formation (i.e. entangling activities), which are thermodynamically favoured in tightly packed polymers (Arsuaga et al., 2002). Condensing mitotic chromosomes are rigidified through ATP dependent cross-linking (Gerlich et al., 2003), which in turn could stimulate topo II to add intrachromosomal links (Marko & Siggia, 1997). At the end of mitosis, the cross-linkers are removed from chromatin (e.g.

condensin), potentially offering a driving force for topo II towards its disentangling activities.

However, few methods are available to investigate intact nuclear architecture directly. Most of the aforementioned experiments disrupt the nuclear structures and thus may create artificial readouts. *In situ* hybridization, electron microscopy and psoralen binding, which depends not only on superhelical tension, but also nucleoprotein structure, must be interpreted with caution.

Conversely, recent evidence suggests that chromosomal ends may partly be able to rotate. Budding yeast cells whose only relaxation activity comes from ectopic expression of the bacterial topo I, which acts solely on (-) sc (*top1Δ, top2-4, pGDP E. coli topA*; Gartenberg & Wang, 1993) accumulate (+) sc ( $\Delta Lk = +4\%$  with respect to wild type), and their overall transcription is largely precluded (Salceda et al., 2006). Interestingly, there seems to be a positional dependence of transcriptional inhibition, as genes within ~100kb of a telomere are normally transcribed, whereas genes in more internal parts of the chromosome experience a reduction in transcript levels (Joshi et al., 2010). This effect is observed in all 32 telomeric regions and is independent of subtelomeric chromatin structure (i.e. it is observed in the presence and in the absence of the SIR complexes that organize heterochromatin-like structures at subtelomeric regions; Joshi et al., 2010). Thus, it seems that torsional stress can dissipate through chromosome ends, suggesting that even if telomeres are tethered and confined within a restricted volume (Hediger et al., 2002), they are still able to rotate, at least temporarily (Joshi et al., 2010). Moreover, the transcriptional stall seen in the chromosomes of these cells is gradual, arguing against the presence of barriers delimiting strict topological domains, and instead, suggestive of torsional stress slowly diffusing throughout the chromosome.

### **1.6.2 Chromosome size**

Experimental evidence from minichromosome studies suggests that the length of a DNA molecule affects its mitotic stability. For example, linear minichromosomes of 55 kb are lost in 1 in 100 mitoses (Murray & Szostak, 1983), whereas 100 kb minichromosomes increases the stability by a factor of five; linear minichromosomes of 15 kb or less seem to undertake random segregation at

mitosis and are much more frequently lost (Murray & Szostak, 1985). The idea that chromosome size affects its behaviour is not a new one: it was first suggested by Spell & Holm, when they analysed chromosome breakage by PFGE, and noticed that in the absence of functional topo II, small chromosome arms were hardly ever broken, whereas 1/3 of long chromosome arms, usually at a region centred around 200 kb from the centromere, exhibited breakage (Spell & Holm, 1994). Densitometry quantifications of the smear of breakage products showed that the longest chromosome arms exhibited 40% breakage, and that artificial circularization of chromosomes did not significantly increase it when compared to telocentric chromosomes of sufficient arm length (>320 kb; Spell and Holm, 1994). More recently, chromosome length has been reported to influence topological stress during replication, as topo I inactivation in budding yeast cells results in a late replication phenotype in longer, but not shorter, chromosomes (Kegel et al., 2011).

### **1.6.3 Composition**

Topoisomerases are highly conserved and necessary for genome functioning, replication and segregation in all organisms. However, it is less clear whether they act uniformly across the whole genome. Recent studies have suggested that chromosomes have specialized elements or regions with special topological properties and ensuing differential topoisomerase activity requirements.

#### **rDNA locus**

The budding yeast rDNA locus lies on the long arm of chromosome XII, and consists of a tandem array of 100-200 copies of a 9.1 kb repeat that contains the ribosomal genes. The rDNA array localizes to the nucleolus, where ribosomal rDNA is mainly synthesized, and it sequesters Cdc14, an essential phosphatase key in regulating mitotic exit (Visintin et al., 1999). This locus reaches full condensation in anaphase, later than the rest of the genome, in a manner that depends on the recruitment of condensin, which in turn promotes both rDNA sister chromatid resolution and subsequent hypercompaction (Guacci, et al., 1994; Sullivan et al., 2004; D'Amours et al., 2004; Machin et al., 2005; D'Ambrosio et al., 2008a).

Why this unique locus requires more than cohesin removal to achieve chromatid segregation seems to relate to the high levels of transcription occurring at this locus, because interfering with rDNA transcription abrogates the need for Cdc14 for rDNA segregation, and partially suppresses the locus segregation defects in condensin mutants (Tomson et al., 2006). Inactivation of condensin in metaphase (i.e. when all the genome except for the rDNA locus has been condensed) prevents correct nucleolar segregation; however, the defect can be rescued by ectopic expression of *Paramecium bursaria chlorella* virus (PBCV-1) topo II, but not endogenous yeast topo II (D'Ambrosio et al., 2008a). The 1061 aa long PBCV-1 topo II has been described as the minimal type II enzyme because it lacks the putatively regulatory C-terminal 260 aa (when compared to the budding yeast counterpart) but possesses the properties of eukaryotic topo II and has 45% amino acid identity to *Drosophila* and human topo II (Lavrukhin et al., 2000). Interestingly, overexpression of PBCV topo II in wildtype cells sped up rDNA segregation, which suggests that anaphase bridging and late segregation of this locus is due to persistent sister chromatid intertwinings, and that perhaps the regulation of decatenation of this locus could determine segregation timing and subsequently its positioning in the daughter nuclei (D'Ambrosio et al., 2008a; Gerlich et al., 2003). Altogether, these findings indicate that the rDNA locus might have different topological constraints than the majority of the genome, arising both from DNA replication and transcription machineries, implying that the roles of topoisomerases may be of particular significance at this locus.

### **Centromeres**

The centromere is the chromosomal locus that organizes the kinetochore, where spindle microtubules attach during cell division (Diaz-Ingelmo et al., 2015). Centromeres differ across eukaryotes: they are mostly confined long, epigenetically defined regions, with a few notable exceptions, like the budding yeast point centromere, which is formed by a short, 150-200 bp sequence (Bloom & Carbon, 1982). Topological analysis of budding yeast centromeres (inserted into minichromosomes) revealed that each centromere stabilizes a  $\Delta Lk = +0.6$  (Diaz-Ingelmo et al., 2015). This singular, positively supercoiled, topology, which is established through specialized centromeric nucleosomes (Furuyama & Henikoff,

2009), could be important for resisting spindle forces and/or during bipolar orientation at mitosis (Diaz-Ingelmo et al., 2015).

Several observations indicate that yeast centromeres (CEN) have specialized cohesion properties (Bachant et al., 2002), including the enrichment of cohesin complexes at these loci (Blat & Kleckner 1999), the fact that ectopic insertion of CEN sequences results in cohesin deposition at those places (Tanaka et al., 1999), and that removal of CEN sequences from minichromosomes affects their cohesion (Megee & Koshland, 1999). Strikingly, indirect immunofluorescence analysis shows that mammalian topo II (particularly the  $\alpha$  isoform) accumulates at centromeres from prometaphase until anaphase (Taagepera et al., 1993; Gorbsky, 1994; Rattner et al., 1996; Porter & Farr, 2004). Experiments using GFP-tagged topo II $\alpha$  have shown similar localization patterns, with the enzyme enriched at centromeres as well as along axial regions of metaphase chromosomes (Tavormina et al., 2002).

The high mobility of the enzyme in its association with chromosomes, i.e. the quick exchange between cytosolic and chromosome-bound topo II depends on catalytic activity, as it is inhibited in the presence of inhibitors that trap topo II as a closed clamp (Porter & Farr, 2004; Tavormina et al., 2002). Indeed, methods that detect catalytic activity instead of simply the presence of topo II by using poisons (e.g. Self Primed in situ labelling, SPRINS, and Differential Retention of Topoisomerase, DRT) have shown that “active” topo II accumulates at centromeres with a centromere/chromosome arm ratio of  $\sim 2.5$  in metaphase, and that this particular topo II accumulation depends on the heterochromatin structure of the centromeric region (Andersen et al., 2002; Agostinho et al., 2004; Porter & Farr, 2004). Molecular mapping using PFGE has also tracked etoposide-immobilized topo II-mediated DNA breaks near centromeres in human and chicken cells (Florida et al., 2000; Spence et al., 2002). The preferential activity of topo II at centromeres has also been detected using cleavage assays in *Drosophila* (Kas & Laemmli, 1992), as well as using microscopy in mouse cells treated with etoposide (Marchetti et al., 2001). The centromere-specific activity of topo II has not been well documented in the yeast systems, although there is some evidence that *S. pombe* topo II interacts with the outer centromere repeats (Murakami et al., 1992), and that *S. cerevisiae* sumoylation of topo II CTD triggers Aurora B recruitment to centromeres (Edgerton et al., 2016). Put together, these results suggest that the

centromeric region is a preferred substrate for topo II's catalytic activity during mitosis; however, it does seem like there is no role for topo II in kinetochore assembly and/or organization, as cells organize functional kinetochores irrespective of whether topo II is active or not (Porter & Farr, 2004). The most striking centromeric defect of topo II mutants is observed in cells where sumoylation is blocked: centromeric fibres acquire an abnormally elongated shape in budding yeast cells where the SUMO-machinery is compromised (Bachant et al., 2002). Similar lines of evidence have been reported in higher eukaryotes (Azuma et al., 2003, Mao et al., 2000), although sister chromatid cohesion dynamics is slightly different in this case. SUMO-modification of topo II has no detectable effect in topo II other than its relocalization to centromeres; however, whether the centromeric effect observed in these conditions is a direct consequence of topo II or other substrates (e.g. Pds5 is also a sumo-substrate; Stead et al., 2003), is yet to be clarified (Porter & Farr, 2004).

Thus, topo II seems to be preferentially associated with mitotic centromeres. However, for now how its activity at this locus is different from the rest of the genome is just speculation.

### **SMC5/6 binding regions**

Smc5/6 complex has been linked to catenanes and/or DNA replication-associated torsional stress. This poorly understood SMC complex is formed by Smc5/6 and the non-SMC Nse1-6 subunits (Fig. 7-1). Nse1 contains a RING finger domain, usually found in ubiquitin ligases, and Nse2 has SUMO ligase activity (Gallego-Paez et al., 2014). Smc5/6 has mostly been associated with homologous recombination-mediated repair of double-strand breaks, particularly due to epistasis with Rad51 (McDonald et al., 2004; De Piccoli et al., 2006). The complex associates with chromatin in interphase and largely comes off chromosomes during mitosis, a pattern reminiscent of cohesin (Gallego-Paez et al., 2014; Jeppsson et al., 2014). Outside its repair function, the role of Smc5/6 remains unclear. A number of studies have implicated the complex in chromosome organization, in particular in the resolution of DNA linkages arising from replication (Bermudez-Lopez et al., 2010), replisome progression and rotation (Kegel et al., 2011) and organization of repetitive chromosomal regions (Torres-Rosell et al., 2007). Interestingly, the number of Smc5/6 peaks increases substantially along

chromosome arms— correlating with cohesin-binding sites— when budding yeast cells undergo S phase in the absence of functional topo II, suggesting that this SMC complex might recognize catenation events (Kegel et al., 2011) In human cells, depletion of Smc5/6 retards S-phase progression and affects chromosomal structural integrity and topo II $\alpha$  mitotic localization, indicating that Smc5/6 might be important to organize chromosomes during or right after DNA replication (Gallego-Paez et al., 2014).

## 1.7 Open Questions

Topo II is inarguably required to decatenate chromosome intertwinings that result from DNA replication. However, there are many questions that remain unanswered. We still fail to understand the nature and “life cycle” of catenanes: how catenation arises and where along the chromosomes it originates is still to be clarified. Moreover, we know little about their distribution: are they stationary or mobile along chromosomes? Recent experiments have suggested that while most catenanes are resolved by topo II during or shortly after S phase, a small proportion of the intertwinings remains until mitosis (Charbin et al., 2014); further insights into how and why these interlinks are not immediately removed are required. Finally, we do not know what, if any, molecular mechanism coordinates decatenation through topo II’s timely activation in anaphase (Haering et al., 2008). Insights into the enzyme’s regulation will shed light into its ability to decatenate intertwinings at appropriate stages of the cell cycle. Future lines of research need to look into these questions in order to understand some of the most basic, conserved and intriguing aspects of cellular biology.

## 1.8 Aim and outline of this thesis

This project aims to tackle a number of unresolved questions regarding DNA catenation. Using budding yeast as a model organism, and taking advantage of its powerful genetics, we will try to clarify key aspects of chromosome topology and sister chromatid intertwinings.

The first part of the project investigates the local topologies of native budding yeast chromosomes. We will use site-specific recombination to loop out specific chromosomal regions and analyse their topologies. We will validate this system, and use it to convey previously unavailable information on (1) the distribution of catenanes along chromosomes and (2) their formation.

The second part of the project has a more protein-centric approach, and investigates when and where topoisomerases act along chromosomes. For this, we will perform ChIP-on-chip in the presence of topoisomerase poisons, which will enable us to map the active population of these enzymes.

We will then attempt to assess the contribution of catenation towards sister chromatid cohesion. We will use an ectopic topo II that does not respond to putative budding yeast regulation, and measure what effect its decatenating activity has on sister chromatid cohesion.

Finally, the results of this thesis will be discussed and put into perspective in the final chapter.

## **Chapter 2**

### **Materials and Methods**

## Chapter 2. Materials & Methods

### 2.1 Yeast techniques

#### 2.1.1 Yeast strains

The genotypes of the yeast strains (of the W303 background) used in this work are shown in Table1.

**Table 1. List of strains used in this study**

Strain No.	Genotype
CSL72	<i>MATa, ade2-1 can1-100 scc1-73::TRP1, ura3::3xURA3::tetO112 his3::HIS3::tetR-GFP P<sub>GAL1</sub>- SCC1 (R180D, R268D)-HA<sub>3</sub>::LEU2,</i>
CSL141	<i>MATa, ade2-1 trp1-1 can1-100 leu2-3, 112 his3-11,15 ura3-1 GAL psi+ (w303 wildtype)</i>
CSL1397	<i>MATa, ade2-1 trp1-1 can1-100 leu2-3,112 ura3-1 GAL psi+ TOP2-HA<sub>6</sub>::HIS3</i>
AM1	<i>MATa ade2-1 trp1-1 can1-100 his3-11,15 ura3-1, psi+ P<sub>GAL1</sub>-Cre::LEU2 loxP::ARS508:: loxP</i>
AM2	<i>MATa ade2-1 can1-100 leu2-3, 112 his3-11,15 ura3-1 GAL, psi+, CRE-EBD78::TRP1 loxP::ARS508:: loxP</i>
AM3	<i>MATa ade2-1 can1-100 his3-11,15 ura3-1 psi+ P<sub>GAL1</sub>-Cre::LEU2 loxP::ARS508:: loxP, top2-4::TRP1</i>
AM4	<i>MATa ade2-1 trp1-1 can1-100 his3-11, 15 psi+ P<sub>GAL1</sub>-Cre::LEU2 RFB::klURA3 loxP::ARS508::loxP</i>
AM5	<i>MATa ade2-1 trp1-1 can1-100 ura3-1 psi+ P<sub>GAL1</sub>-Cre::LEU2 P<sub>ADH1</sub>-hENT1-TK(1X)::HIS3 loxP::ARS508:: loxP</i>
AM6	<i>MATa ade2-1 trp1-1 can1-100 ura3-1 psi+ P<sub>GAL1</sub>-Cre::LEU2 loxP::TER501::loxP</i>
AM7	<i>MATa ade2-1 trp1-1 can1-100 ura3-1 psi+ P<sub>GAL1</sub>-Cre::LEU2 loxP::TER301::loxP</i>
AM8	<i>MATa ade2-1 trp1-1 can1-100 ura3-1 psi+ P<sub>GAL1</sub>-Cre::LEU2 loxP::TER301b::loxP</i>
AM9	<i>MATa ade2-1 trp1-1 can1-100 ura3-1 psi+ P<sub>GAL1</sub>-Cre::LEU2 loxP::TER404::loxP</i>
AM10	<i>MATa ade2-1 trp1-1 can1-100 ura3-1 psi+ P<sub>GAL1</sub>-Cre::LEU2 loxP::ARS702::loxP</i>
AM11	<i>MATa ade2-1 trp1-1 can1-100 ura3-1 psi+ P<sub>GAL1</sub>-Cre::LEU2 loxP::TER/CEN1004::loxP</i>
AM12	<i>MATa ade2-1 trp1-1 can1-100 ura3-1 psi+ P<sub>GAL1</sub>-Cre::LEU2 loxP::TER/CEN1004::loxP P<sub>MET3</sub>-CDC20::TRP1</i>
AM13	<i>MATa ade2-1 trp1-1 can1-100 ura3-1 psi+ P<sub>GAL1</sub>-Cre::LEU2 loxP::TER1004::loxP</i>
AM14	<i>MATa ade2-1 trp1-1 can1-100 ura3-1 psi+ P<sub>GAL1</sub>-Cre::LEU2 loxP::TER603::loxP</i>

AM15	<i>MATa ade2-1 trp1-1 can1-100 his3-11,15 psi+ P<sub>GAL1</sub>- PK<sub>3</sub>- ϕ31C::LEU2 attB::klURA3-ARS508-attP::KanMX</i>
AM16	<i>MATa ade2-1 trp1-1 can1-100 his3-11,15 psi+ + P<sub>GAL1</sub>- PK<sub>3</sub>- ϕ31C::LEU2 attB::klURA3-TER603-attP::KanMX</i>
AM17	<i>MATa ade2-1 trp1-1 can1-100 his3-11,15 psi+ P<sub>GAL1</sub>- PK<sub>3</sub>- ϕ31C::LEU2 attB::klURA3-TELO1R-attP::KanMX</i>
AM18	<i>MATa ade2-1 trp1-1 can1-100 his3-11,15 psi+ P<sub>GAL1</sub>- PK<sub>3</sub>- ϕ31C::LEU2 attB::klURA3- TER1004-attP::KanMX</i>
AM19	<i>MATa ade2-1 trp1-1 can1-100 his3-11,15 psi+ P<sub>GAL1</sub>- PK<sub>3</sub>- ϕ31C::LEU2 attB::klURA3-TER1417-attP::KanMX</i>
AM21	<i>MATa ade2-1 trp1-1 can1-100 his3-11,15 psi+ leu2-3,112::P<sub>GAL1</sub>-Cre- LEU2 RFB::klURA3 loxP::TER301::loxP</i>
AM22	<i>MATa MATa ade2-1 trp1-1 can1-100 ura3-1 psi+ P<sub>GAL1</sub>-Cre::LEU2 loxP::TER501::loxP</i>
AM24	<i>MATa RS::HMRE-a2a1-HMRI-TRP1-lacO256::RS P<sub>GAL1</sub>-R::LEU2 ade2::ADE2::lacR-GFP</i>
AM32	<i>MATa trp1-1 leu2-3,112 can1-100 psi+ ura3::3xURA3::tetO112 his3::HIS3::tetR-GFP P<sub>GAL1</sub>-CVTOP2-PK<sub>3</sub>::ADE2</i>
AM33	<i>MATa ade2-1 trp1-1 can1-100 psi+, ura3::URA3::tetO112 his3::HIS3::tetR-GFP P<sub>GAL1</sub>-TOP2-PK<sub>3</sub>::LEU2</i>
AM34	<i>MATa ade2-1 trp1-1 can1-100 GAL psi+ ura3::URA3::tetO112, his3::HIS3::tetR-GFP P<sub>TOP2</sub>-TOP2- PK<sub>3</sub>::LEU2</i>
AM35	<i>MATa ade2-1 trp1-1 can1-100 leu2-3,112 his3-11,15 psi MnC prsrDNA(URA3)</i>
AM36	<i>MATa trp1-1 can1-100 leu2-3,112 his3-11,15 psi+ MnC prsrDNA(URA3) P<sub>GAL1</sub>-CVTOP2-PK<sub>3</sub>::ADE2</i>
AM37	<i>MATa ade2-1 trp1-1 can1-100 ura3-1 psi+ TOP2-HA<sub>6</sub>::HIS3 P<sub>ADH1</sub>PDR1(DBD)-CYC8::LEU2</i>
AM38	<i>MATa ade2-1 trp1-1 can1-100 ura3-1 psi+ TOP2-HA<sub>6</sub>::HIS3 P<sub>ADH1</sub>PDR1(DBD)-CYC8::LEU2 ΔPDR5::KanMX</i>
AM41	<i>MATa ade2-1 trp1-1 can1-100 psi+ TOP2-HA<sub>6</sub>::HIS3 P<sub>ADH1</sub>PDR1(DBD)-CYC8::LEU2 ΔPDR5::KanMX ΔPDR3::URA3</i>
AM42	<i>MATa trp1-1 can1-100 psi+ TOP2-HA<sub>6</sub>::HIS3 P<sub>ADH1</sub>PDR1(DBD)- CYC8::LEU2 ΔPDR5::KanMX ΔPDR3::URA3 P<sub>GAL1</sub>-CVTOP2- PK<sub>3</sub>::ADE2</i>
AM43	<i>MATa ade2-1 can1-100 psi+ TOP2-HA<sub>6</sub>::HIS3 P<sub>ADH1</sub>PDR1(DBD)- CYC8::LEU2 ΔPDR5::KanMX ΔPDR3::URA3 TOP1- PK<sub>3</sub>::TRP1</i>
AM44	<i>MATa ade2-1 trp1-1 can1-100 psi+ his3-11,15 P<sub>ADH1</sub>PDR1(DBD)- Cyc8::LEU2 ΔPDR5::KanMX ΔPDR3::URA3</i>

### 2.1.2 Yeast growth

Cells were grown in YP (Yeast Peptone; 1.1% w/v yeast extract, 2.2% w/v bacto-peptone and 0.0055% w/v adenine) supplemented with 2% w/v glucose (YPD) or 2% raffinose/galactose (YPRaff/Gal). Cells carrying constructs of Cre

recombinase,  $\phi$ 31C integrase, *Saccharomyces cerevisiae* topo II (topo II) and *Paramecium bursaria chlorella virus* topo II (CV topo II) were grown in YPRaff, and expression of the respective proteins was induced upon addition of galactose (2% final).

Cells expressing Cdc20 under the control of the MET3 methionine repressible promoter were grown in YNB (Yeast Nitrogen Base; 0.8% w/v yeast nitrogen base) supplemented with CSM (Complete Supplement Mixture, Formedium) minus methionine and with 2% Raff/ Gal.

For the selection of transformants, YNB agar plates lacking the appropriate auxotrophic amino acid were used. In the case of selection of Kanamycin resistant colonies, cells were plated on YPD and replica-plated in YPD + geneticin G418 (50  $\mu$ g/ml). Sporulation was carried out on sporulation media (100 mM CH<sub>3</sub>COONa, 20 mM NaCl, 25 M KCl, 1.5 mM MgSO<sub>4</sub>, 1.5% w/v agar).

### 2.1.3 Cell cycle arrests

Cell cycle arrests used in this study are summarized in Table 2.

**Table 2. List of cell cycle arrests used in this study**

Arrest	From	Addition of	Construct
G1	Cycling cells	10 $\mu$ g/ml $\alpha$ factor	N/A
HU	G1 release	0.1 M HU	N/A
G2/M (-spindles)	G1 release or cycling	10 $\mu$ g/ml Nocodazole	N/A
G2/M (+spindles)	G1 release	Methionine	P <sub>MET3</sub> -Cdc20

Mid-log phase (OD<sub>600</sub>= 0.15) cells of the a-mating type were arrested in G1 upon addition of the pheromone  $\alpha$  factor (1:1000 of a 5 mg/ml stock in MeOH, added twice; O'Reilly et al., 2012). Unless G1 arrest was terminal, cells were released by washing the  $\alpha$  factor with at least seven times the volume of the culture. S-phase arrest was achieved by G1 release into YPD/ Raff containing 0.1 M hydroxyurea (HU; Sigma). G2/M arrest was induced upon addition of 10  $\mu$ g/ml Nocodazole (Sigma). Cells carrying the construct P<sub>MET3</sub>-Cdc20 were arrested in G2/M by G1-release into rich medium (YPRaff/Gal).

#### **2.1.4 Yeast Transformation**

Cells were transformed using the standard LiAc procedure. Briefly, ~10 OD<sub>600</sub> units of mid-log phase were spun down (3 krpm 4°C 5 min), washed with water and pelleted again (6 krpm RT 2 min). Pellets were washed in 1x TEL (10 mM Tris-HCl pH 7.5, 0.1 mM EDTA, 100 mM LiAc). 50µl of cells were added to 8 µl of DNA (~1 µg) +2 µl 10 mg/ml ssDNA, and mixed with 300 µl TELP (1x TEL 40% PEG 3350) by vortexing. Cells were incubated at 25°C for 2-4 h, and heatshocked at 42°C for 15 min, after which they were washed with 1 M Sorbitol and plated on the appropriate selective plates.

#### **2.1.5 Mating and tetrad dissection**

*MATa* and *MATα* strains were mated by mixing onto YPD plates and incubating overnight at RT. Diploids were selected upon restreaking onto double selection plates, replated onto sporulation plates and incubated for 5-7 days. Asci were treated with 1 M Sorbitol containing lyticase for 10 min at 30°C, after which tetrads were dissected onto YPD plates using the MSM400 Dissection Microscope (Singer Instruments). Plates were replica-plated onto the appropriate auxotrophic plates to enable selection of the correct genotype.

#### **2.1.6 Spot Dilution assay**

Logarithmically growing cells were diluted to OD<sub>600</sub> =0.3, and 10-fold serial dilutions were spotted onto YPD plates with or without etoposide. Plates were incubated for 2 days at 30°C and photographed.

### **2.1 General molecular biology methods**

#### **2.1.1 Cloning**

Cloning was carried out using the In-Fusion® HD cloning kit (Clontech) according to the manufacturer's instructions. The respective vector and insert sequences were amplified using CloneAmp HiFi premix (Clontech) in a thermal cycler under the following conditions: initial denaturation of 98°C 2 min, followed by 35 cycles of 98°C 10 sec, 55°C 10 sec, 72°C 10 sec/kb, and a final step of 72°C 2

min. Reaction products were separated on a 1% agarose gel in 1x TAE (40 mM Tris pH 7.5, 20 mM CH<sub>3</sub>COOH, 1 mM EDTA) and purified using the NucleoSpin® Gel and PCR Clean-up (Macherey-Nagel) kit according to the manufacturer's manual.

### 2.1.1.1 Plasmids used for strain construction

#### **LoxP cassette vector**

Evt'I+II, containing the *loxP* -*Kluyveromyces lactis* (K. I.) *URA3-loxP* cassette was obtained from T. Kuilmann. Removal of the *CYC8* terminator was achieved by cutting the vector with *NotI* and *BglIII* (New England Biolabs, NEB), treatment with Klenow (NEB) for 10 min at 37°C and ligation with T4 ligase (NEB) overnight at 16°C. Diagnostic restriction digest and sequencing were used to confirm the final construct “*loxP* cassette vector” (Fig 2-1).

This plasmid was used as template for PCR to introduce the *loxP* -*K. I. URA3-loxP* cassette in *S. cerevisiae* cells. The primers used for this PCR had an overhang of 50-70 nt homologous to the genomic locus of interest followed by a short sequence that annealed to the vector (FWD primer 5'-...CCGTTGAGTCACTGTCGA-3'; REV primer 5'-... CCATACTTCTTCGGACAT-3').

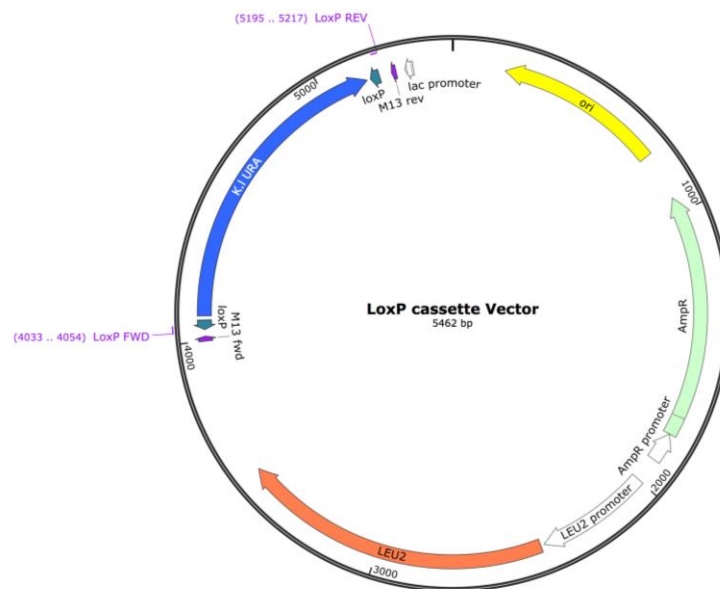


**Figure 2-1. Schematic representation of the vector containing the *loxP* cassette.**

The *loxP* cassette (*loxP* -*K. I. URA3-loxP*) was amplified by PCR from this vector, with primers annealing immediately upstream and downstream (indicated in purple) of the *loxP* sequences.

### RFB plasmid

We amplified the replication fork barrier (RFB) sequence element (130 bp) from *S. cerevisiae* genomic DNA and cloned it into a plasmid containing the *K. I. URA3* gene using the In-Fusion® HD cloning kit (Figure 2-2). For integration into the genome, we amplified the *K. I. URA3*-RFB cassette with the primers shown in Table 3. Integration was confirmed by genotyping and sequencing PCRs.

**Table 3. Primers for integrating the RFB sequence in the genome**

Locus	FWD primer/ REV primer
ARS50 8	aatttcagaaatattgcttacatcaaacgaaatagtaagcgtaaaccatataatccgctcgatcgtgattctgg ggctattcttttataccgcaaaagactataaaaatgatacatatcgttgaaacggtgaaagagaagggct
TER30 1	cacgtagcaggtccagagtaatcctgatgttctattaccgatctaggatcccaaaagatcgctcgatcgtg gtcaagaacaaagaaagaaaagtacaagtgtaaacatttctaacatcttttcggttttatgcggtgaaaga gaagggct

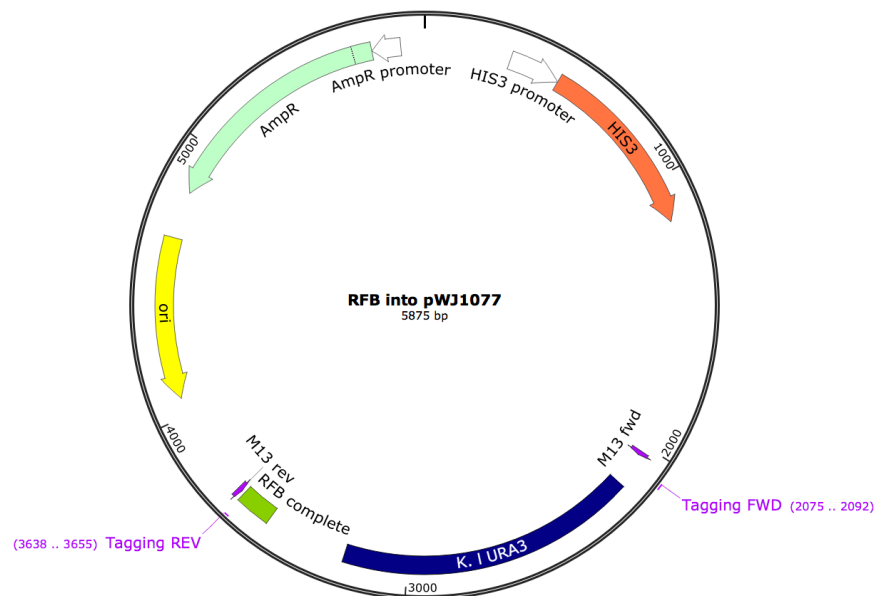


**Figure 2-2. Schematic representation of the RFB cassette vector**

This vector contains the RFB sequence from the rDNA repeats for amplification and integration of the RFB-*K. I. URA3* cassette into the chromosome.

### *AttB* and *attP* cassette vectors

For the unidirectional  $\phi$ 31C system, the *attB*-*K. I. URA3*-*attP* cassette was ordered from and synthesized by geneART © and cloned into the *LoxP* cassette vector backbone using the In-Fusion® HD cloning kit (Fig. 2-3). The primers used

for this PCR had an overhang of 50-70 nt homologous to the genomic locus of interest followed by a short sequenced that annealed to the vector (FWD primer 5'-GAATTCCGTTGAGTCACTGTCG...3', REV primer 5'-GAGGCCTCCAATGCAGGTGG...3').

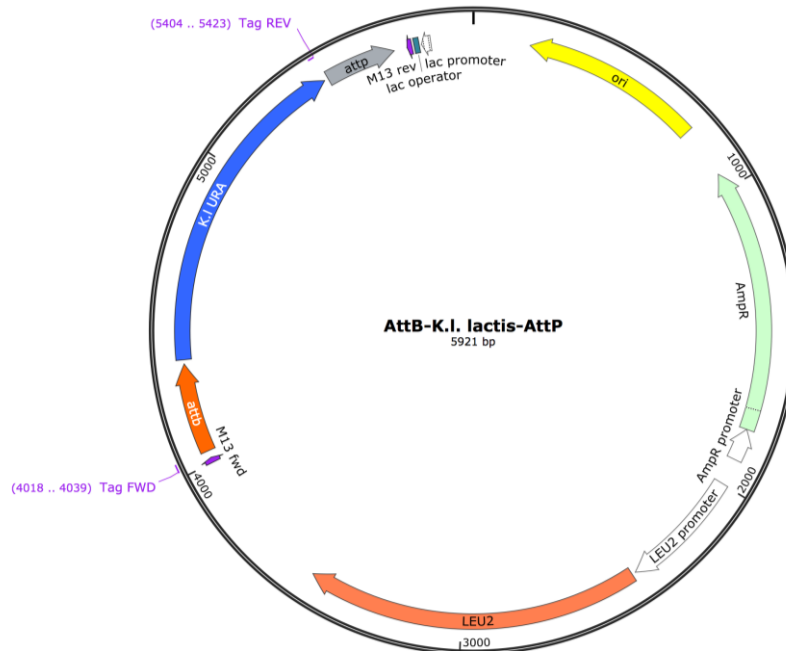


**Figure 2-3. Schematic representation of the *attB-K.I. URA3-attP* cassette vector.**

We also constructed a vector containing *attP*-KanMX, by PCR amplification of the vector pFA6-KanMX4 and the *attP* insert (from *attB-K.I. URA3-attP*) using the primers and In-Fusion® HD cloning kit (See Table 4).

**Table 4. Primers used to clone the *attP*-KanMX cassette**

	Primers	Size (bp)
Vector	gccagcgacatggaggc ttaaccggggatccgtcg	3890
AttP	ggatccccgggtaagcagcgactagtagtactgacgg ctccatgtcgctggccattccatacttcttcggacattg	292

### ΦC31 vector

The coding sequence of ΦC31 Integrase (codon-optimized for *S. cerevisiae* expression, ordered from and synthesized by GeneART®) was cloned using the

In-Fusion® HD cloning kit into p1064, a centromeric plasmid containing the *LEU2* marker and the galactose inducible GAL1 promoter (Figure 2-4).

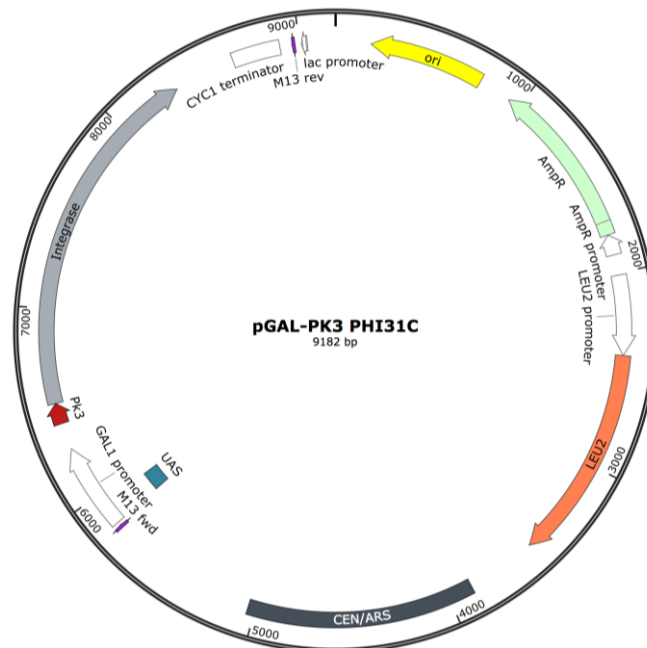


**Figure 2-4. Schematic representation of the P<sub>GAL1</sub>-Φ31C construct**

PK<sub>3</sub>-P<sub>GAL1</sub>-Φ31C was obtained by replacing the Cre ORF in p1064 by the Φ31C ORF (ordered from GeneART®). GAL1 promoter, Φ31C and plasmid elements are indicated.

### Prs-rDNA vector

As a reporter plasmid for assessing the catenation levels in the CV topo II strains, a centromeric plasmid containing an rDNA repeat was constructed using In-Fusion® HD cloning kit. Briefly, the centromeric vector prs316 was linearized with Sall (NEB) for 2 h at 37°C, and the 9.1 kb rDNA repeat was amplified from *S. cerevisiae* genomic DNA using primers (FWD) 5'-TATCGATACCGTCGACCTCATGTTTGCCGCTCTGATG-3' and (REV) 5'-CCCCCTCGAGGTCGACCCAAGAAAGATGTAAGAGACAAGTG-3'. Fragments were fused with the In-Fusion® HD cloning kit, and the final construct was isolated, confirmed (Section 7.6) and amplified in *E. coli* (Figure 2-5).

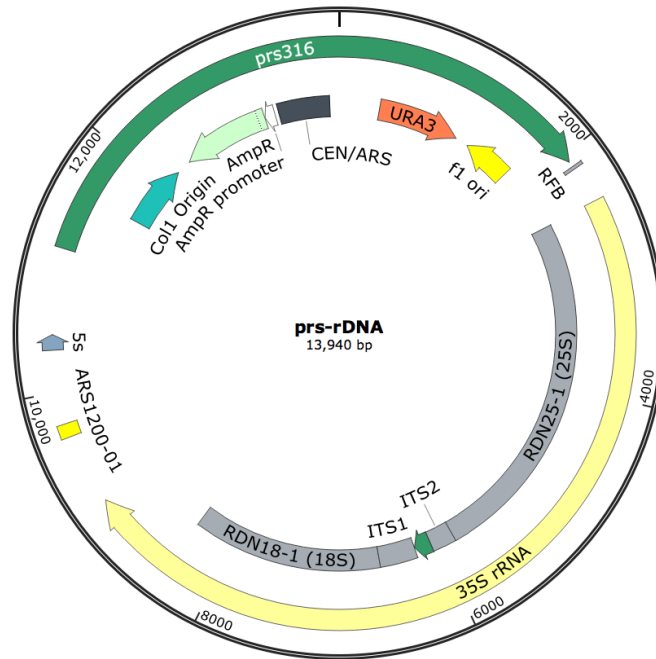


**Figure 2-5 Schematic representation of the minichromosome prs-rDNA**

An rDNA repeat was cloned into prs316, a centromeric 4.9 kb plasmid. The difference rDNA elements (RFB, 5S, ARS1200 and 35S), as well as the prs316 backbone are shown.

## 2.1.2 Protein analysis

### 2.1.2.1 TCA

2 OD<sub>600</sub> units of mid-log phase cells were spun down at (3 krpm 4°C 5 min) and pellets were resuspended in 1 ml 20% TCA. Pellets were washed with 1 ml Tris-Base and resuspended in 2x SDS loading buffer containing 0.2 M DTT. Glass beads were added and cells were broken using a fast-prep at 4°C. Cell debris was discarded and samples were boiled at 95°C and spun down.

### SDS-polyacrylamide gel electrophoresis (PAGE) and western blotting

10 µg of TCA extracts (estimated by Bradford analysis) were loaded on a 4-12% Bis-Tris or 3-8% Tris-Acetate precast gel (Thermo Fisher) and run according to the manufacturer's instructions. Proteins were then transferred to a nitrocellulose membrane using the TE 70 PWR semi-dry transfer unit (GE Healthcare) at 25 V 90 mA for 3 h. Membranes were then rinsed in PBS and blocked in 5% Milk PBS 0.2% Tween.

### 2.1.2.2 Antibodies

**Table 5. List of primary antibodies used in this work.**

Antibody	Source	Dilution
Mouse Anti-V5 (Pk)	Serotec (MCA1360)	1:5000
Mouse anti-HA (12CA5)	Cell services CRUK	1:5000
Rabbit Anti-Rad53	Abcam	1:1000
Mouse anti-Myc (9E10)	Cell services CRUK	1:2000
Mouse anti-Tubulin (TAT-1)	Cell services, CRUK	1:5000
Mouse anti-Cre	Millipore	1:1000
Mouse anti-BrdU	MBL	1:1000

As secondary antibodies, we used the HRP anti-mouse (sheep; 926-32280) and HRP anti-rabbit (sheep; NA934), purchased from Amersham and used at a 1:15000 dilution.

### 2.1.3 DNA analysis

#### 2.1.3.1 Genomic DNA preparation for Southern Blotting

10-15 OD<sub>600</sub> units of mid-log phase cells were spun down (3 krpm 4°C 5 min), and pellets were resuspended in 50% EtOH, and kept on ice. Samples were pelleted and washed with 1 M Sorbitol, 0.1 M EDTA. Cells were spheroblashed in 1 M Sorbitol, 0.1 M EDTA, 0.05 mg/ml zymolyase 100T (MP Biomedicals) and 8 µl/ml β-Mercaptoethanol for 45 min at 37°C. Spheroblasts were pelleted and incubated in 0.5 ml 50 mM Tris-HCl pH 7.5, 10 mM EDTA 1% SDS for 30 min at 65°C. 0.2 ml 5 M KAc was added, and samples were incubated on ice for 1 h. Samples were spun down (14 krpm 4°C 10 min) and supernatant was transferred to a new tube, left on ice for 1 h and spun down again. Supernatants were again collected in a fresh tube, added 1 ml EtOH 100% and left for 10 min at RT. Samples were spun down (14 krpm RT 3 min), and pellets were subsequently washed with 70% EtOH and air-dried. 0.3 ml TE buffer containing 1 mg/ml RNase A was added and samples were incubated for 1 h at 37°C. Ethanol precipitation (using 200 mM NaCl) was performed, and pellets were washed with 70% EtOH and air-dried, before resuspending in 0.1 ml TE buffer.

### 2.1.3.2 Quantification of DNA concentration

To determine the DNA concentration in the genomic DNA samples, PicoGreen® dsDNA quantitation assay (Invitrogen) was performed using the manufacturer's instructions. Briefly, 1 µl of DNA sample was mixed with 199 µl PicoGreen reagent 1:200 diluted in TE buffer on a 96-well plate. After a 5 min incubation at RT, the sample fluorescence was measured using a microplate reader (wavelengths: excitation ~480 nm, emission~520 nm). Sample concentration was calculated from a standards curve obtained using serial dilutions of a DNA sample of known concentration (commercial genomic DNA from *S. cerevisiae*, Amsbio; Figure 2-4)

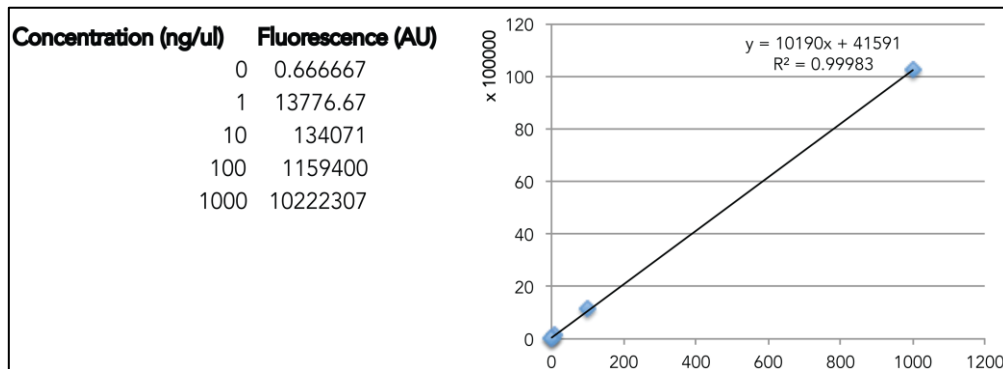


**Figure 2-6. PicoGreen standards**

Commercial budding yeast DNA (Amsbio) was serially diluted (1 ng to 1 µg, 1:10 dilution factor) and mixed with the PicoGreen solution. Sample fluorescence was measured and standards calculated averaging the values from three technical replicates.

### 2.1.3.3 In vitro assays

#### 2.1.3.3.1 kDNA

0.2 µg of catenated kinetoplast DNA (kDNA; Topogen) was treated with topo II (topo II purified from *S. cerevisiae* –gifted by C. Bouchoux- or human topo II $\alpha$ , Topogen) in 50 mM Tris-HCl, pH 8.0, 120 mM KCl, 10 mM MgCl<sub>2</sub>. 0.5 mM ATP, 0.5 mM DTT for 30 min at 37°C. Reactions were run in 1% agarose in 1x TAE buffer.

#### 2.1.3.3.2 Enzymatic Treatments

Restriction digest of ~1 µg of genomic DNA with NEB enzymes was set up in 20 µl reactions for 2 h at 37°C. Nicking reaction was carried out with Nt.Bpu10I (Thermo Fisher) in R buffer (10 mM Tris-HCl pH 8.5, 10 mM MgCl<sub>2</sub>, 100 mM KCl, 0.1 mg/mL BSA) for 30 min at 37°C. Topoisomerase II treatment of 1 µg of genomic DNA was performed in 50 mM Tris-HCl pH 8.0, 120 mM KCl, 10 mM MgCl<sub>2</sub>, 0.5 mM DTT, supplemented with 0.5 mM ATP using human topoisomerase IIα (Topogen) in a 20 µl final volume for 1h at 37°C.

Topoisomerase IV (*E. coli*, Topogen) treatment was carried out as for topo II, but in 40 mM Tris-HCl pH7.5, 6 mM MgCl<sub>2</sub>, 10 mM DTT, 100 mM C<sub>5</sub>H<sub>8</sub>KNO<sub>4</sub>, 50 µg BSA/ml and 40 µM ATP. Topoisomerase I (*E. coli*; NEB) treatment was performed as for topo II, but in 50 mM CH<sub>3</sub>COOK, 20 mM Tris-CH<sub>3</sub>COOH, 10 mM Mg(CH<sub>3</sub>COOH)<sub>2</sub>, 100 µg/ml BSA.

#### 2.1.3.4 1D Gel Electrophoresis

~1 µg of genomic DNA was loaded on a 0.5% 1x TAE agarose gel and run for 12-24 h at 1.5 V/cm on a B3 Self Recirculation System (Thermo Fisher) at RT. Gels were subsequently stained with 1:1000 GelRed™ (Biotium Inc.) in 1x TAE buffer for 1 h, and a picture was taken to assess the migration of the genomic bands and efficiency of digests.

#### 2.1.3.5 Capillary transfer

Gels were depurinated with 0.125 M HCl for 15 min, rinsed with water and incubated with denaturing solution (0.5 M NaOH, 1.5 M NaCl) shaking at RT for 30 min. They were rinsed with water and incubated with neutralizing solution (0.5 M Tris-HCl pH 7.5, 1.5 M NaCl) for 20 min, followed by a 5 min incubation in 20x SSC (0.3 M NaCl, 0.3 M Na<sub>3</sub>C<sub>6</sub>H<sub>5</sub>O<sub>7</sub> pH 7.0). DNA was transferred to N<sup>+</sup> Hybond nitrocellulose membrane (GE Healthcare) through capillary action using absorbent paper to soak 20x SSC through the gel and the membrane for 16 h. DNA was crosslinked to the membranes using the Stratalinker 1800 UV (120000µJ).

### 2.1.3.6 Southern blotting

Membranes were prehybridized with QuickHyb Hybridization Solution (Agilent) for 1 h at 68°C. Labelled probes were generated using the Prime-It II Random Primer Labeling Kit (Agilent), following the manufacturer's instructions. 50ng of template DNA in 23  $\mu$ l volume were mixed with 10  $\mu$ l random oligonucleotide primers, and boiled at 95°C for 5 min. 10  $\mu$ l of 5x \*dATP primer buffer (0.1 mM dCTP, 0.1 mM dGTP, 0.1 mM dTTP), 5  $\mu$ l [ $\alpha$ -<sup>32</sup>P] dATP at 3000 Ci/mmol, Perkin Elmer) and 1  $\mu$ l Exo(-)Klenow enzyme (5 U/ $\mu$ l) were added to the DNA and incubated for 30 min at 37°C. The reaction was interrupted upon addition of 2  $\mu$ l of stop mix (0.5 M EDTA), and purified using Illustra Microspin G50 column (GE Healthcare). Freshly prepared probes were then added to the membranes. Hybridization was allowed for 4 h at 68°C. Membranes were then washed twice in 2x SSC 0.1% SDS for 15 min at RT, and twice in 0.5x SSC 0.1% SDS, rinsed briefly in 50 mM Tris-HCl pH 7.5 and exposed overnight using Phosphor screen and cassette (Amersham biosciences), prior to scanning on Typhoon 9400 Imager.

### 2.1.3.7 Pulsed-field gel electrophoresis (PFGE)

20 OD<sub>600</sub> units of mid-log phase cells were spun down (3 krpm 4°C 3 min). Pellets were washed twice in 1 ml SP1 buffer (50 mM citrate/phosphate pH 5.6, 40 mM EDTA, 1.2 M Sorbitol), and spheroblasted with 0.6 mg/ml zymolyase-100T at 37°C for 40 min. Spheroblasts were spun down and resuspended in low melting point agarose in TSE (10 mM Tris-HCl pH 7.5, 0.9 M Sorbitol, 45 mM EDTA) to a final concentration of 10<sup>8</sup> cells in 100  $\mu$ l per plug (estimated using a haemocytometer). Plugs were solidified at 4°C for 10 min and transferred to 12 ml tubes, where they were covered with 3 ml 0.25 M EDTA, 50 mM Tris-HCl pH 7.5, 1% SDS and incubated at 55°C for 90 min. The solution was replaced with 0.5 M EDTA, 10 mM Tris-HCl pH 9.5, 1% lauryl sarcosine, 1 mg/ml proteinase K, and plugs were incubated at 55°C for 48 h. Plugs were then washed twice with T10xE (10 mM EDTA, 10 mM Tris-HCl pH 7.5) and incubated with T10xE with 0.04 mg/ml PMSF at 55°C for 1 h, after which they were washed twice with T10xE.

Running was performed in a 1% agarose gel (PFGE-grade, Bio-Rad) in 0.5x TBE (44.5 mM Tris-HCl pH 7.5, 44.5 mM Boric Acid, 1 mM EDTA) with the following conditions: 60-120 sec switch time, 120 angle, 6 V/cm, 14°C for 24 h. The

gel was subsequently stained with 1x Gel Red for 1 h and destained in distilled water overnight, before imaging, capillary transfer and southern blotting, as described previously.

#### **2.1.3.8 Quick genomic prep for PCR**

Genotyping PCRs were performed on DNA extracted using the following protocol. A toothpick of cells was resuspended in 0.1 ml lysis Buffer (0.2 M LiAc, 1% SDS) and incubated at 70°C for 10 min. 0.3 ml 100% EtOH was added, and the sample was centrifuged for 3 min at 14 krpm. Pellets were washed with 70% EtOH, dried and resuspended in 50 µl EB. 1 µl was used as template for genotyping PCR.

#### **2.1.3.9 Genotyping PCR**

1 µl quick genomic prep was added to the following reaction: 6 µl Q solution, 3 µl 10x PCR buffer, 0.5 µl dNTP mixture (25 µM each dNTP), 0.5 µl 10 µM Forward primer, 0.5 µl 10 µM Reverse primer, 0.5 µl 5 mM MgCl<sub>2</sub>, 17.5 µl DW and 0.5 µl Taq polymerase (NEB), and incubated in a thermal cycler under the following conditions: initial denaturation of 96°C 2 min, followed by 35 cycles of 96°C 15 sec, 50-55°C 20 sec, 72°C 2 min, and a final step of 72°C 5 min. Reaction products were separated on a 1% agarose gel in 1x TAE. 5 µl of PCR reaction were treated with 2 µl ExoSAP-IT (Affymetrix), and incubated at 37°C for 15 min, followed by 15 min incubation at 80°C. 3 µl was used as template for PCR Sequencing reaction.

#### **2.1.3.10 Chromatin Immunoprecipitation (ChIP)-on-chip analysis**

40 OD<sub>600</sub> units of mid-log phase cells were collected. For TOP2-HA<sub>6</sub>, CVTOP2-PK<sub>3</sub> and TOP1-PK<sub>3</sub> analysis, cells were crosslinked with formaldehyde (FA; 1.8% final) for 30 min at RT, added glycine (0.125 M final) and incubated for 5 min at RT. Etoposide- and Camptothecin-treated cells (0.5 mg/ml and 0.1 mg/ml, respectively, for 60 min) were not treated with FA. For BrdU incorporation, cells were added 200 µg/ml 20 min before release from G1 arrest and released into YPRaff/Gal containing 0.1 M HU and 200 µg/ml BrdU. Cells were added 0.5 M EDTA 0.1% NaN<sub>3</sub> and kept on ice for 10 min, followed by 3 washes in 0.1 M EDTA 10 mM Tris-HCl pH 7.5 0.1% NaN<sub>3</sub>.

Cells were washed 2x with ice-cold 1x Tris-buffered saline (TBS), and resuspended in lysis buffer (50 mM HEPES-KOH pH 7.5, 140 mM NaCl, 1 mM EDTA, 1% Triton X-100, 0.1% Na-deoxycholate, 1 mM PMSF 1x Complete Protein Inhibitors), added 1.2 ml glass beads and broken in the cell breaker (Multi-beads shocker Yasui Kikai; 14 cycles 30 sec on 30 sec off 2500 rpm). Samples were then sonicated (20 cycles, 30 sec on 30 sec off). Cell debris was discarded after spinning (15 krpm 4°C 5min) and cell extracts were incubated with antibody (anti-PK or -HA)-coupled Dynabeads<sup>®</sup> Protein A (Thermo Fisher) for 4 h at 4°C. Anti-BrdU antibody-coupled Dynabeads were prepared using the Dynabeads<sup>®</sup> antibody coupling kit (Thermo Fisher) according to the manufacturer's instructions. After the incubation, beads were washed twice in each of the following: lysis buffer, lysis buffer containing 200mM NaCl and wash buffer (10 mM Tris-HCl pH 8.0, 250 mM LiCl, 0.5% NP-40, 0.5% Na-deoxycholate, 1 mM EDTA), and once in TE pH 8.0 DNA was eluted upon incubating the beads with elution buffer (50 mM Tris pH 8.0, 1% SDS, 10 mM EDTA) at 65°C for 15 min, and crosslinking was reversed upon addition of 95  $\mu$ l (input samples) and 120  $\mu$ l (IP samples) TE 0.1% SDS and incubation at 65°C overnight. Samples were treated with Proteinase K (37°C, 2 h), purified using the Qiagen PCR purification kit, treated with RNase A (37°C, 1 h) and cleaned up by PCI extraction and NaCl/ethanol precipitation. Library preparation and amplification were carried out using the Sigma<sup>®</sup> GenomePlex<sup>®</sup> WGA kit. 7  $\mu$ g of DNA were fragmented with human apurinic/aprimidinic (AP) endonuclease (APE1) in APE1 buffer containing 8 units (U) UDG/reaction. Samples were then labelled with Biotin-11-dXTP by rTdT (60 U/reaction), and added Oligo B2 (0.05 mM), Eukaryotic Hybridization controls, herring sperm DNA (0.1 mg/ml), SSPE (6.25X), Triton-X (0.005%). Mixtures were boiled for 10 min, cooled on iced and used to hybridize GeneChip *S. cerevisiae* Tiling 1.0R arrays for 16 h at 42°C. Chips were processed with the GeneChip<sup>®</sup> fluidics station 450 and scanned using the GeneChip<sup>®</sup> 3000 7G scanner. Analysis was carried out using the R package *Ringo*.

## 2.2 Cell biology and Microscopy

### 2.2.1 Flow cytometry

1 ml of culture ( $OD_{600} \geq 0.15$ ) was spun down and resuspended in 1 ml 70% EtOH. After at least 2 h, cells were spun down, resuspended in 50 mM Tris-HCl pH 7.5 containing 0.1 mg/ml RNase A, and incubated at 37°C for at least 2 h. Cells were then pelleted, resuspended in 0.4 ml FACS buffer (200 mM Tris-HCl pH 7.5, 211 mM NaCl, 78 mM  $MgCl_2$ , 50  $\mu$ g/ml propidium iodide) and sonicated for 5 sec. 100  $\mu$ l cells were transferred to 500  $\mu$ l 50 mM Tris-HCl pH 7.5, vortexed and processed using the Becton Dickinson FACSCalibur with settings in linear mode (FSC threshold: 52, detector: E01, amplifier: 1.4; SCC: detector: 400, amplifier: 1; FL2 detector: 750, amplifier: 7). Data analysis and plots were done using FlowJo V.10.1.

### 2.2.2 URA3-GFP cohesion assay

2 ml of mid-log phase cells ( $OD_{600} \geq 0.15$ ) arrested in G2/M (nocodazole). 1ml culture was spun down (3 krpm 4°C 2 min), resuspended in 1 ml ice-cold 100% EtOH and sonicated for 5 sec. 30  $\mu$ l melted 1% agarose was loaded onto a slide and a second slide was pressed on top, to flatten the agarose. Once solidified, 5  $\mu$ l of cells was added onto the agarose layer and covered with a coverslip. 100 cells were scored for the presence of one or two *URA3*-GFP dots, using a Zeiss Axioplan2 microscope.

## **Chapter 3**

# **Local DNA topologies of Budding Yeast Chromosomes**

## **Chapter 3. Local DNA topology of budding yeast chromosomes**

The aim of this part of the project was to construct a system that would enable the investigation of local topologies, in particular catenation events, along native *S. cerevisiae* chromosomes.

### **3.1 How to study chromosomal topology: site specific recombinases and integrases**

Investigating the topology of linear eukaryotic chromosomes poses a technical challenge. Topological information is only retained in topologically closed systems, and while in living cells protein factors might act as topological barriers, isolation of nucleic acids would ultimately render long linear molecules topologically unconstrained. Only circular prokaryotic chromosomes and plasmids retain the topological relationships established *in vivo*, which is probably the reason why they have been the preferred substrates for topology assays. Moreover, eukaryotic chromosomes are usually orders of magnitude longer than their prokaryotic counterparts, making them even more challenging to study. Nevertheless, directly understanding the different topologies that occur in eukaryotic chromosomes would enhance our understanding of chromosome organization through replication, transcription, repair and segregation, and it seems that extrapolating from plasmid observations has its limitations.

Site-specific recombination could provide a powerful tool to study chromosome topology, by induction of a recombination reaction that results in excision of a covalently closed circle or “loop out”. This experimental set-up would require three elements, namely, an inducible recombinase (e.g. expressed under the control of an inducible promoter), and two recombinase target sites in tandem orientation, placed in the chromosome surrounding a region of interest to be excised (Figure 3-1).

A system like the aforementioned would provide a relatively simple tool to study the topology of different genomic loci, with their particular chromosomal elements, and would not necessarily lose substantial topological information

because recombination would be triggered after the locus of interest has undergone topological changes in the context of the whole chromosomes.

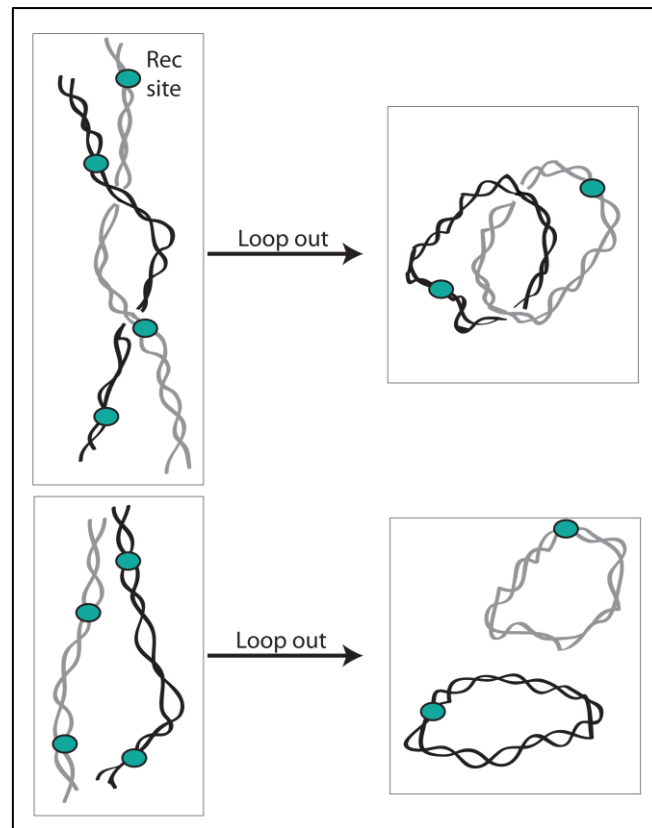


**Figure 3-1. Site-specific recombination to study the local topology of chromosomal regions.**

Two recombinase target sites (Rec site) are first inserted in the chromosome. Following replication, the sister chromatids may be catenated (upper panel) or not (lower panel). Induction of site-specific recombination, or loop out, would produce two interlinked circles or two free monomers, respectively. The reaction would also leave a recombinase target site in the remaining (linear) chromosome (not shown).

In order to study chromosome topology, we decided to use the *Cre/loxP* system, because it has been well characterized and previously used in budding yeast. The Cre protein of phage P1 is a member of the large tyrosine recombinase family (see Section 1.3.1), which also comprises the  $\lambda$  Int protein and the yeast Flp recombinase (Grainge & Jayaram, 1999). Their active site motif contains an RHR triad and a tyrosine nucleophile, similarly to the RKRH motif from type IB topoisomerases, and they perform a recombination reaction that involves formation and resolution of a Holliday junction by a tetramer of the recombinase (Grainge &

Jayaram, 1999). Tyrosine recombinases act on a pair of identical recombination sites, and thus their reaction can be bidirectional.

We will use Cre recombinase-mediated excision of chromosomal loci surrounded by *loxP* sites, hereby referred to as “loop out”. Similar loop out approaches have been previously taken with R recombinase (Chang et al., 2005; Gartenberg et al., 1993; Raghuraman et al., 1997) and Flp recombinase (Bi and Broach, 1997), although these were performed to study heterochromatin establishment. These previous loop out sizes were small (2-7 kb) and possibly their size precluded the maintenance of certain topologies. Based on previous minichromosome experiments showing a correlation between DNA molecule size and catenane accumulation (Charbin et al., 2014), we reasoned that loop out sizes between 7.5-18 kb would offer a good trade-off between efficient recombination and retention of meaningful topologic information.

## **3.2 Establishing a Loop Out system**

### **3.2.1 Construction of strains**

A number of regions of interest were identified for loop out, pertaining to what we divided into three groups of chromosomal features: replication, SMC complexes and sequence elements (although in most cases, there is an overlap between at least two groups). Replicon loop outs contained either an efficient replication origin or a replication fork merge zone, where replication is expected to terminate with relatively high frequency (based on genome-wide analysis of Okazaki fragments from McGuffee et al., 2013). This first group was designed with the purpose of testing the termination model for catenation (introduced in Section 1.3.3). SMC loop outs were designed to investigate topological differences between regions of cohesin and/or condensin enrichment and regions where these complexes are not substantially detected. Cohesin and condensin binding sites were identified by ChIP-on-chip analysis of Scc1 (Ocampo-Hafalla et al., 2007) and of Brn1 (D'Ambrosio et al., 2008b), respectively. Finally, the sequence element loop outs contained endogenous sequences that have unique features in terms of chromosome replication and/or organization, such as centromeres and ribosomal/tRNA genes. A list of the strains, the positions of their respective *loxP* sites, and predicted loop out sizes, is shown in Table 6.

**Table 6. Characteristics of the *loxP*/Cre strains used in this study**

Locus (Chromosome no.)	Element	Efficiency	Upstream <i>loxP</i>	Downstream <i>loxP</i>	LO (bp)
TER501 (V)	TER, CH, CN	-0.499	69508	86765	17257
ARS508 (V)	ARS, CH, CN, tRNA	0.919	84667	102414	17747
TER301 (III)	TER, CH	-0.404	48222	66258	18036
TER301b (III)	TER, CH,	-0.404	54930	66258	11328
TER603 (VI)	TER, CN	-0.642	176871	184501	7630
TER701 (VII)	TER	-0.453	859733	870128	10395
TER404 (IV)	TER, CH, CN, ribosomal gene	-0.580	489031	500957	11926
TER1004 (X)	TER, CEN, CHBS	-0.504	425102	436770	11668

TER: termination region; ARS: autonomous replication sequence; CEN: centromere; CH: cohesin binding site; CN: condensing binding site; LO: loop out. Efficiency is an estimate of the proportion of a cell population that fires a given replication origin (Efficiency: from 0 to 1; McGuffee et al., 2013), or experiences fork convergence at a given termination region (Efficiency: from -1 to 0; McGuffee et al., 2013).

All loop out loci contain at least one essential gene (according to the *Saccharomyces* Genome Database [www.yeastgenome.org](http://www.yeastgenome.org)) between the *loxP* sites in order to counterselect for spontaneous recombinants prior to Cre induction. Strain construction consisted of five steps: (1) integration of the cassette upstream, (2) excision of *K. lactis URA3-loxP* through *URA3* counterselection on 5-Fluorotic Acid (5-FOA) plates, (3) integration of the cassette downstream, (4) excision of *K. lactis URA3-loxP* on 5-FOA plates (Figure 3-2) and (5) introduction of the recombinase Cre. Genotyping PCR and sequencing were used to confirm that each step occurred successfully. Lists of tagging and sequencing primers are provided in the appendix (Section 7.3, Tables 9 & 10).

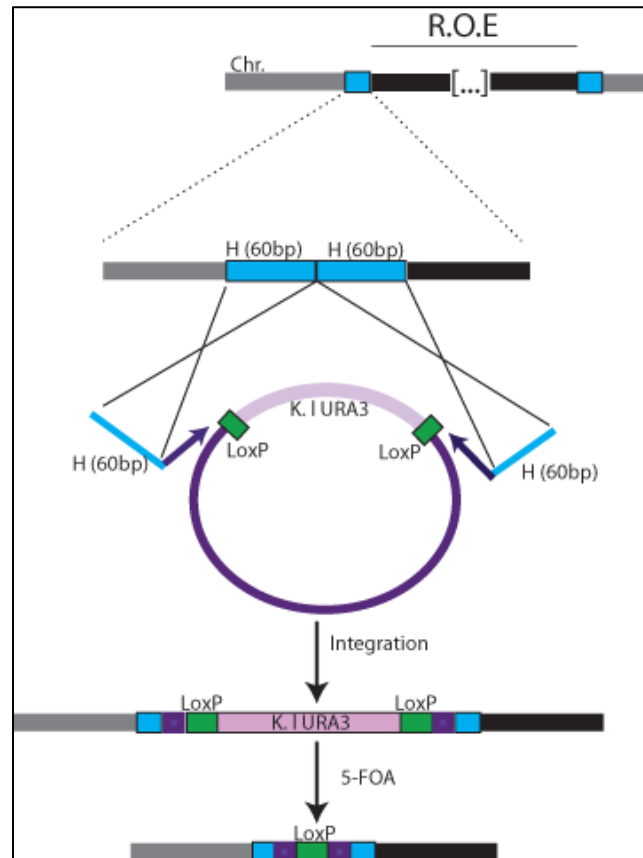


**Figure 3-2. Schematic of the loop out strain construction strategy**

To target *loxP*-*K. lactis* *URA3*-*loxP* cassettes to the genomic site of interest, the cassette was amplified using integration primers that contain 60 bp of homologous sequence (H) to the regions flanking the target site and transformed into WT cells. Positive transformants were grown on 5-Fluoroorotic acid (5-FOA) plates, to select for *URA3*-*loxP* excision events that yielded a single *loxP* in the chromosome. The same procedure was used to integrate a second *loxP* at a downstream genomic location (not depicted). PCR and sequencing confirmed the integrations of *loxP* sites. R.O.E: Region of excision; Chr: chromosome; K.I: *Kluyveromyces lactis*.

### 3.3 Technical optimization of the topological analysis of chromosomal loop outs

Initial experiments revealed that topological analysis of looped out chromosomal regions is more difficult than studying minichromosomes. Separation from the rest of the genomic DNA and detection with specific probes are simpler in the case of minichromosomes, probably because of their putative topological independence from the genome and the fact that they carry unique sequences, like the bacterial ampicillin resistance gene.

### 3.3.1 Optimization of topological analysis through southern blotting

Trial runs were performed to determine the right conditions to resolve the different loop out topoisomers, testing the length of the electrophoretic run and the voltage (not shown). To obtain high quality genomic DNA samples, we also tried a number of precipitation steps (Figure 3-3). This was driven by the observation that the migration of some of the samples was probably affected by salt and/or protein contaminants (not shown), and we therefore looked for additional DNA purification steps that could improve the quality of the samples. Using a strain where the predicted TER501 was surrounded by two *loxP* sites, we arrested cells in G2/M by adding the microtubule depolymerizing drug nocodazole, and induced Cre expression from the *GAL1* promoter by adding galactose. We collected samples every 30 min for 2 hr, and extracted genomic DNA as described in Section 2.1.3.1. The last timepoint (120 min) was divided into six samples: one was left as a control and the rest (a-e) were further purified through five different procedures (Figure 3-3a).

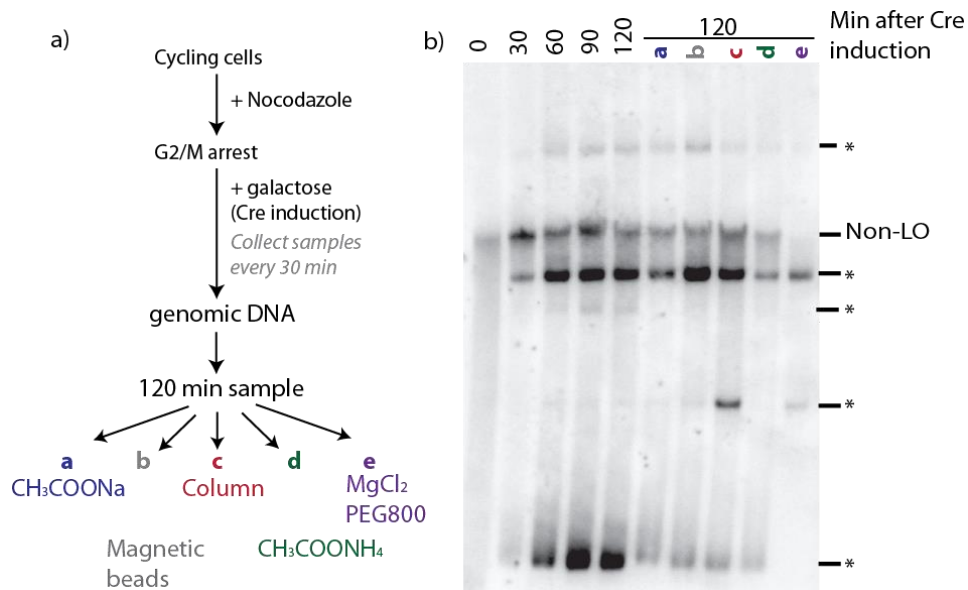


**Figure 3-3. Optimization of genomic DNA extraction.**

Cells were arrested in G2/M, Cre expression was induced and samples were collected every 30 min for DNA isolation. a) The 120 min timepoint was split into 6 samples, 5 of which were further processed as follows: (a) CH<sub>3</sub>COONa/ethanol precipitation, (b) magnetic beads clean up (chemagic SEQ Pure20, Perkin Elmer), (c) column based purification (Microcon YM10, Millipore) (d) CH<sub>3</sub>COONH<sub>4</sub>/isopropanol precipitation (e) 4% (w/v) PEG 8000/30 mM MgCl<sub>2</sub>. b) Southern blot analysis of the aforementioned samples. \*: looped out species, Non-LO: non-looped out.

However, it seemed like these extra steps led to loss of some species (Figure 3-3 lanes a-e, bottom band), and in some cases, to the artefactual enrichment of others (Figure 3-3 lane c). Thus, we did not include these purification steps in our protocol.

In addition, we noticed that some of the enzymatic treatments were not robust (i.e. not removing their expected substrates), particularly treatment with topo II to ascertain the identity of catenated topoisomers. To identify the enzymatic inhibitors, we performed kinetoplast DNA (kDNA) decatenation reactions in the presence of some potential contaminants that could have been carried over from the genomic DNA preparations (Figure 3-4). In this assay, we use kDNA from the trypanosome *Crithidia fasciculata* (Topogen), which is formed by a network of catenated 2.5 kb circular DNA molecules. During electrophoresis, catenated kDNA remains in the well of the gel, whereas decatenated circles are able to enter the gel and migrate through the agarose.

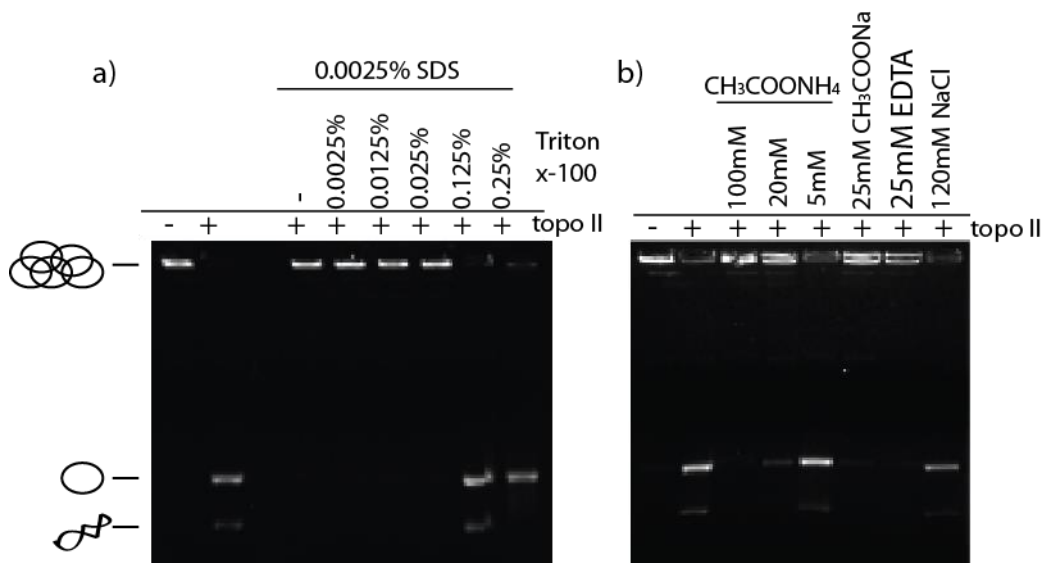


**Figure 3-4. kDNA decatenation assay to determine which steps in the genomic DNA preparation protocol might inhibit topo II activity**

The ability of topo II to decatenate kDNA in the presence of various reagents used for the genomic DNA preparation was assessed. (a) SDS had an inhibitory effect that could be ameliorated by addition of Triton X-100. (b) Acetate and EDTA also had an inhibitory effect on topo II activity.

Both acetate and SDS inhibit topo II activity, but this effect can be overcome by using NaCl (instead of CH<sub>3</sub>COONa or CH<sub>3</sub>COONH<sub>4</sub>) in the precipitation steps of DNA), and triton, which neutralizes the effect of SDS.

Finally, to detect the different loop out molecules, we designed a number of probes that aligned to unique genomic regions (as determined by single hits upon BLAST analysis with default parameters; Altschul et al., 1990). Preliminary experiments were conducted to determine the sensitivity and stringency of the probes, and showed that some probes hybridized non-specifically (Figure 3-5). To select appropriate probe for each loop out, we arrested cells in G2/M (nocodazole), induced Cre expression and collected samples for DNA isolation after 90 min. We either ran the sample untreated, or treated it with restriction enzymes. Restriction digest would allow us to easily distinguish between excised loop outs and non-recombined chromosomal regions, by producing two differently sized bands. Figure 3.5 shows a representative example of this procedure: before recombination, the 17.8 kb region around the predicted termination site TER501 is detected as a 2.9 kb band after BglII digest or as an 8.5 kb band following BamHI treatment. Conversely, after recombination these digests would yield bands of 5.8 kb and 13.2 kb, respectively (Figure 3-5a).

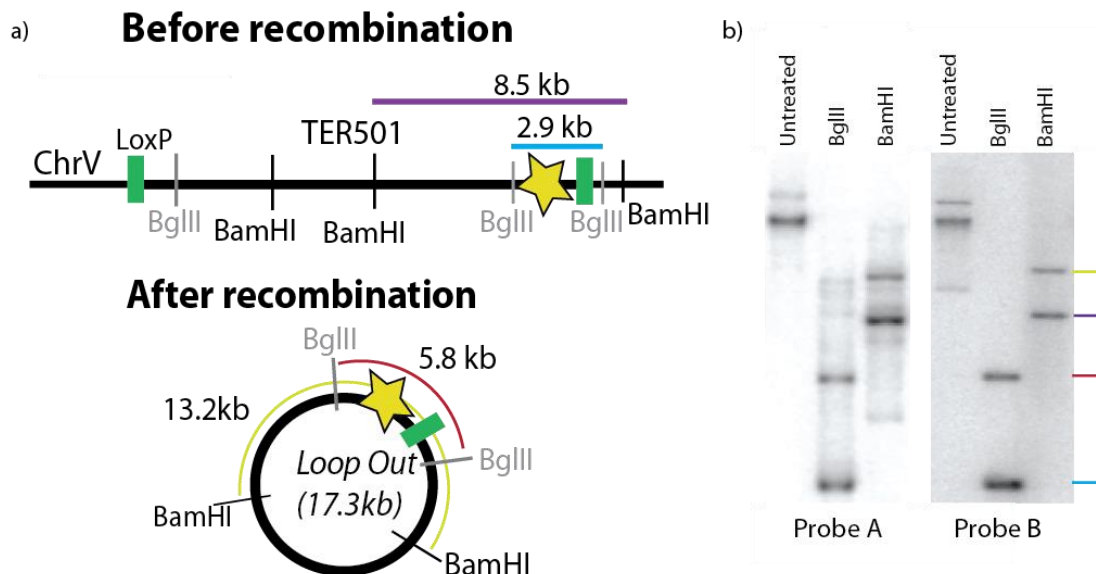


**Figure 3-5. Probe optimization**

For each loop out region, a number of probes were designed and tested using genomic DNA samples taken 90 min after Cre induction. For this particular termination region, TER501, DNA was run untreated, digested with BglII or with BamHI. (a) Schematic representation of the expected band sizes after the respective digests before and after recombination. (b) A number of probes were used for hybridization, and those that showed less non-specificity were selected for further experiments. For this particular region, probe B was chosen. TER: termination region; Chr: chromosome.

Figure 3-5b shows two different probes we tested to detect this region, with both Probe A and B detecting the expected bands, but A also detecting additional bands. Closer analysis, by BLAST alignments of smaller regions within the probe sequence, confirmed additional hits of this probe against genomic loci other than the region in the TER501 loop out, explaining the unexpected bands.

### **3.3.2 Optimization of Cre Recombination**

A potential drawback of our system is that recombination by Cre might not be efficient enough to allow the detection of infrequent topoisomers. It is effectively the local concentration of recombinogenic sequences that determines how efficient the recombination reaction will be (Burgess & Kleckner, 1999). In addition, a number of factors can affect site-specific recombinases like Cre, including (1) distance between target sites: reaction rate decreases with increasing distance, (2) accessibility of target sites: reaction rate decreases if the chromatin target is repressed, and (3) recombinase copy number: reaction rate increases with increasing copy number (M. Gartenberg, personal communication).

We also used two different versions of Cre recombinase. First, we tried Cre recombinase fused to the human oestrogen-binding domain (EBD), which is constitutively expressed from the strong TDH3 promoter ( $P_{TDH3}$ ), sequestered by heat-shock proteins (HSP) and inactive. It is released from HSP following  $\beta$ -estradiol addition ready to be relocated to the nucleus (Verzijlbergen et al., 2009). This system would enable a fast and synchronous loop out. However, recombination levels were not very high, because modification of Cre renders the enzyme less robust (M. Gartenberg, personal communication), and excision could sometimes be detected in the absence of  $\beta$ -estradiol. Therefore, we turned to unmodified Cre driven by the inducible galactose promoter ( $P_{GAL1}$ ). Although recombination does take longer, it is more efficient (Figure 3-6) and less leaky (not shown). As Figure 3-6b shows, expression of  $P_{TDH3}$ -Cre-EBD is higher than  $P_{GAL1}$ -Cre. In terms of activity, however, we observed more efficient recombination by the unmodified Cre (Figure 3-6c). Quantification of the looped out species showed that excision by Cre was around 3 times more efficient than Cre-EBD (with 40% and

15% of the DNA corresponding to excised DNA molecules, respectively; Figure 3-6d).

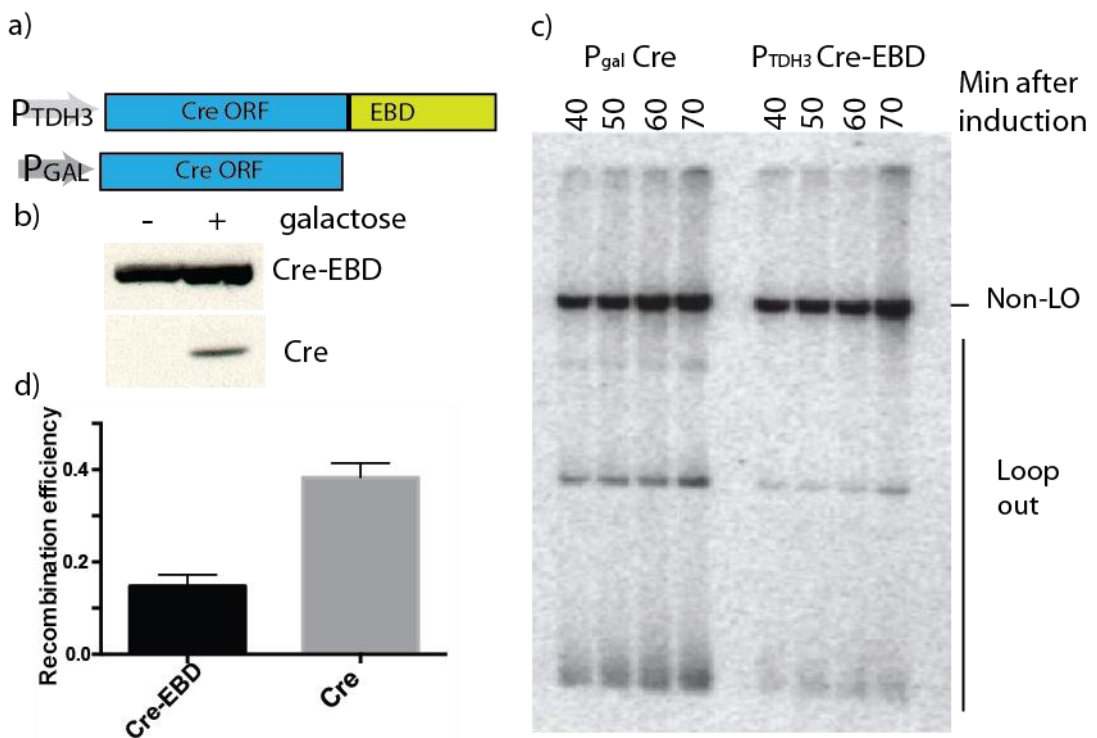


**Figure 3-6. Comparison between the two Cre constructs.**

A region centred at a predicted replication termination region (TER) in Chr. III was looped out either using  $P_{GAL1}$ -Cre or constitutively expressed  $P_{TDH3}$ -CreEBD. a) Schematic representation of the two different Cre constructs. b) Western blot showing the expression of the two constructs after 1 h in medium without galactose. c) Southern blot showing recombination triggered by the two Cre versions,  $P_{GAL1}$ -Cre and  $P_{TDH3}$ -Cre-EBD, which were induced by addition of galactose or  $\beta$ -estradiol, respectively. d) Quantification of excised DNA molecules. Recombination by Cre-EBD is not as efficient as unmodified Cre.

### 3.4 Validation of the loop out

Once optimized, we set out to determine the loop out kinetics by Cre. For this, we used a strain where a 17 kb region centred around the predicted TER501 region in chromosome V was surrounded by two *loxP* sites. We arrested cells in G2/M by nocodazole addition, induced Cre expression and collected samples for DNA isolation every 30 min. Loop out was confirmed by restriction digest (Figure 3-7), genotyping PCR and sequencing (not shown).

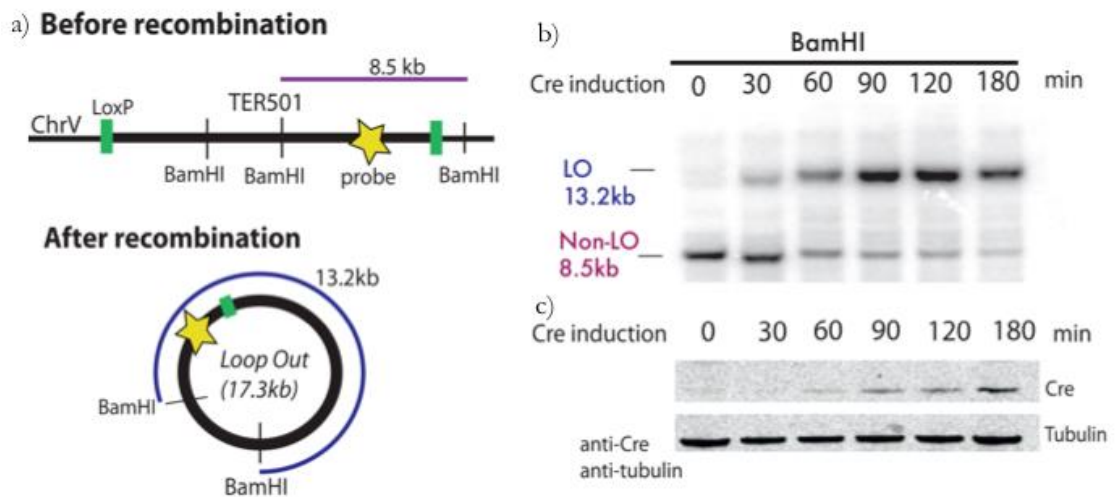


**Figure 3-7. Validation of the loop out.**

Cre-mediated recombination of a 17kb chromosomal region centered around TER501 was investigated in G2/M arrested cells (nocodazole). Cre was induced upon addition of galactose and samples taken every 30 min. (a) Schematic showing the expected sizes of looped out and non-looped out bands after BamHI digestion. (b) Southern blot of time-course samples treated with BamHI (upper panel). (c) Western blot showing Cre levels during the time-course.

We estimated the proportion of cells that had undergone recombination by quantifying the two bands after digest using the Typhoon 9400 Imager and ImageJ. Loop out efficiency reached 70-75% 120 min after Cre induction. Recombination usually plateaued around 90 min, with no marked increase in loop out levels after this time point. Smaller loop outs (<12 kb) had similar recombination kinetics but showed slightly higher efficiencies, of around 80-85% (not shown).

### 3.5 Topology of a chromosomal region

We then set out to investigate the pattern of topoisomers. We used the samples from the previous experiment, but instead of digesting them with BamHI, we ran them untreated (Figure 3-8). Before Cre induction, the single band observed corresponds to the unrecombined, or non-looped out (Non-LO) DNA. This band persists throughout the time-course because Cre-mediated recombination does not reach completion. From 60' onwards, we see the accumulation of 4 additional bands.

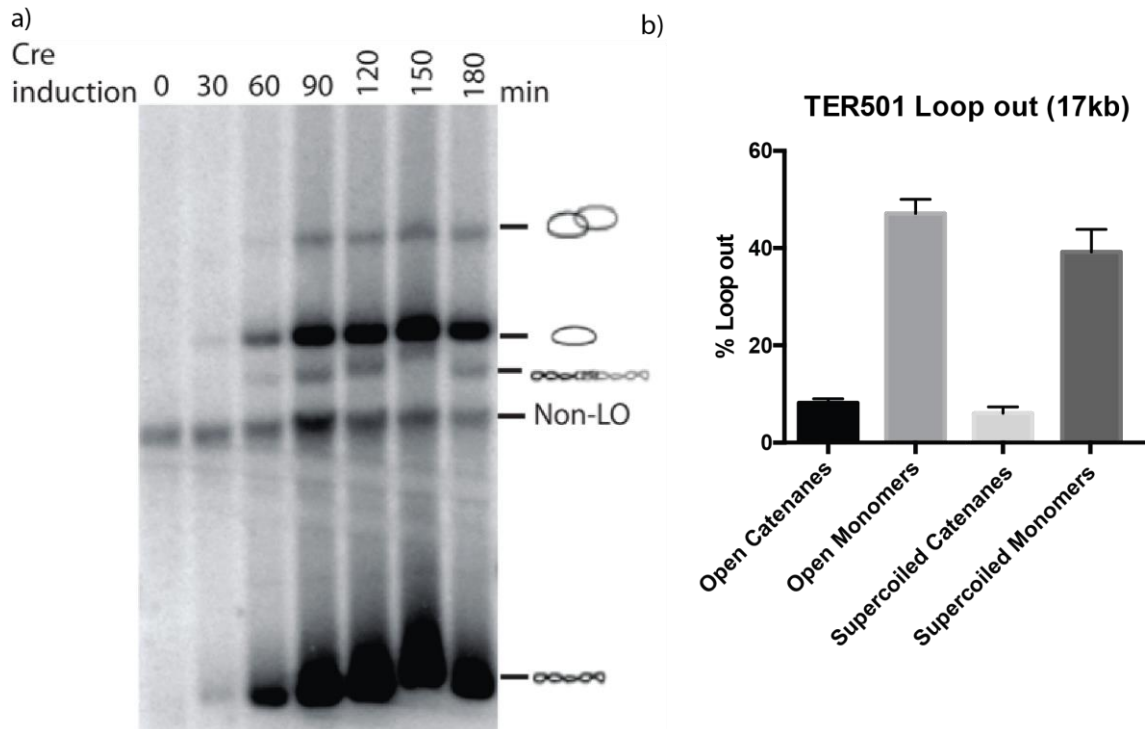


**Figure 3-8. Topoisomer pattern of a 17 kb TER loop out in G2/M-arrested cells.**

a) Time-course of Cre-mediated looping out of a chromosomal region in nocodazole-arrested cells. The identity of the bands was extrapolated from minichromosome studies, and is indicated to the right of the gel. From top to bottom: open catenanes, open monomers, supercoiled catenanes, non-looped out, and supercoiled monomers. b) Quantification of the different topoisomers. Non-LO: non-looped out.

.Extrapolating from minichromosome experiments (Charbin et al., 2014), we propose that the two most abundant topoisomers correspond to the monomeric loop outs (open/nicked for the slower-migrating band, and supercoiled for the faster-migrating one), and that the two less abundant species might correspond to the catenated forms of the loop out (the slower migrating band representing the open/nicked catenanes, and the faster migrating band representing the supercoiled catenanes). Cellular genomic DNA bound by histones would expectedly appear negatively supercoiled once deproteinised. However, during the DNA isolation process nicking often happens, which is the likely reason why we detect the open/nicked conformations of the loop out. The bands that might correspond to catenanes constitute about 15% of the looped out species, whereas about 85% of the loop out is present as monomeric species.

### 3.5.1 Determination of the topoisomer identity

To confirm the identity of the bands observed, we took two approaches (Figure 3-9). We first performed the loop out in different cell cycle stages with the underlying reasoning that catenane bands would only appear after DNA replication. Secondly, we performed *in vitro* treatments with a number of enzymes that alter DNA topology.

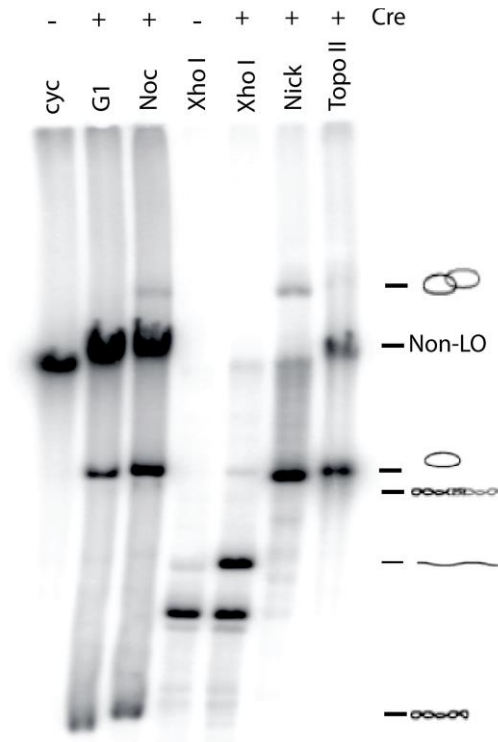


**Figure 3-9. Identification of topoisomers produced after Cre-mediated recombination.**

Cell cycle synchronization (lanes 1-3) and enzymatic treatments of the recovered DNA (lanes 4-7) help identify the topoisomers. Lane 1: genomic DNA before recombination; Lane 2: loop out induced in G1-arrested cells; Lane 3: Loop out in nocodazole-arrested cells. Lane 4: genomic DNA before Cre induction (sample 1) treated with XhoI. Sample 3 was treated with XhoI (lane 5), to reveal the linear form of the loop out, with nicking enzyme (lane 6) to reveal open topoisomers, and with human topo II $\alpha$  (lane 7) that removes catenanes and relaxes supercoils.

As predicted from the minichromosome pattern, the less abundant topoisomers accumulate only after DNA replication, and are removed by topo II treatment *in vitro*, consistent with what would be expected from catenated species. Thus, with this experiment, we confirm that using our site-specific recombination system, we can detect catenanes in a TER region in G2/M-arrested cells.

### 3.5.2 G1-arrested diploids do not present catenated species

An important question at this point is whether the topoisomer pattern we observe is a reflection of the local chromosomal topology, or rather an artefact of our recombination system. One possibility could be that after recombination of a non-catenated region after S phase, which would produce two monomeric loop outs, endogenous topo II mediates their catenation. To test this, we created a diploid strain that can be arrested in G1 (*MATa/MATa*). We first obtained *MAT $\alpha$*  haploids of our *loxP::TER501::loxP* strain, mated it to the original *MATa* strain, and performed a second mating type switch in the *MAT $\alpha$*  locus in the heterozygous diploid. We reasoned that in the scenario where this strain is arrested in G1 there should be no catenanes (since DNA replication has not occurred yet), but there would still be two monomeric loop outs that could be catenated by topo II (Figure 3-10a).

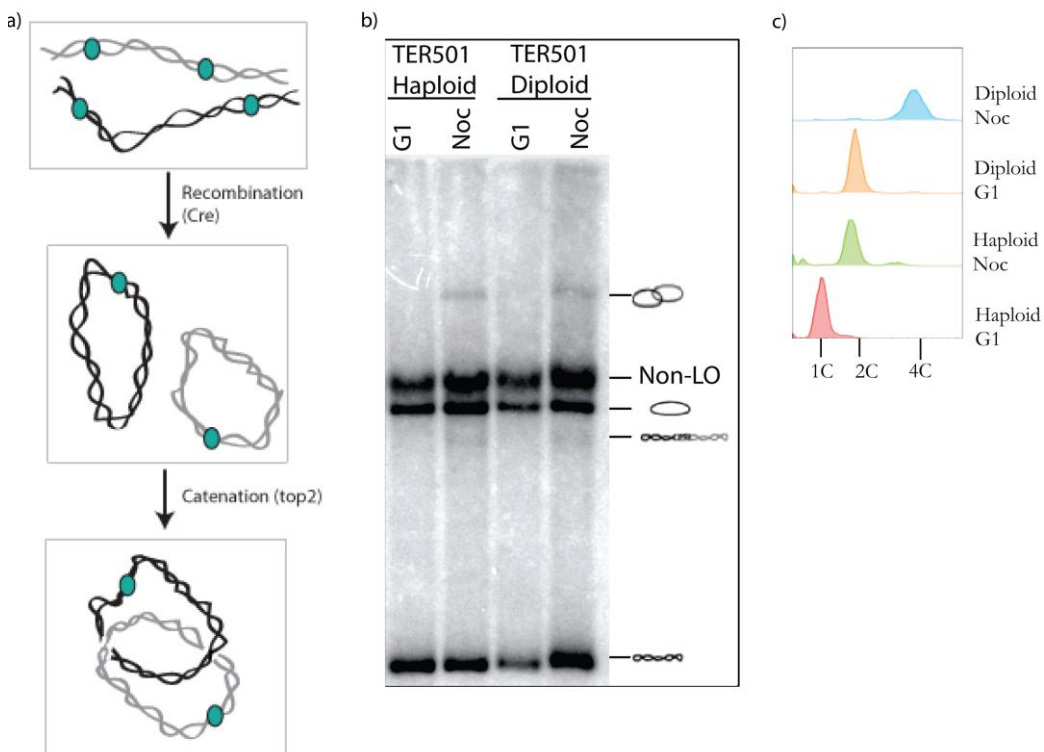


**Figure 3-10. Induction of the loop out in diploid cells arrested in G1 does not produce catenanes and/or unwanted recombination products**

a) Scheme showing how catenanes could be generated by topo II that do not reflect the topology of the local chromosome b) Southern blot comparing the loop outs performed in haploid and diploid strains in G1 and G2/M (nocodazole) arrests. c) FACS showing the arrests in which the respective loop outs were induced.

When we performed the topological analysis of the diploids, we could see that, as in the case of the haploid, diploids only present catenanes after S phase (Figure 3-10b & c). The lack of catenated species in the G1-arrested cells suggests that the topoisomer distribution we observed is not an artefact of our method, but rather a representation of the actual topology of the chromosomal region.

### **3.5.3 Effect of the spindle on a centromeric Loop out**

Spindle forces affect the topology of minichromosomes; namely, in the presence of a spindle, the population of catenated centromeric minichromosomes is markedly reduced, compared to a similar arrest in the absence of mitotic spindle forces (Farcas et al., 2011; Charbin et al., 2014). It has been proposed that the tension exerted by the spindle stimulates topo II-mediated decatenation (Figure 3-11a). On authentic chromosomes, the spindle effect is expected only around the centromere, which is known to undergo pre-anaphase breathing (Ocampo-Hafalla et al., 2007).

We constructed a strain in which the centromeric region of Chr. X (CEN10) was surrounded by two *loxP* sites, and observed that catenanes were readily detectable following loop out in nocodazole-arrested cells (Figure 3-11b). To assess the impact of the spindle on these catenanes, we first arrested cells in metaphase by depletion of the Anaphase Promoting Complex (APC) activator Cdc20, and split the culture into two. One half was treated with nocodazole, which depolymerizes the mitotic spindle, whereas the other half was mock-treated, maintaining its spindle. Figure 3-11c shows that in the absence of the spindle, the catenated species are readily visible. In contrast, the presence of the spindle leads to a great reduction in these species: quantification revealed a significant (~3-fold) decrease in the population of open catenanes (Figure 3-11d). The low number of catenanes observed is probably due to the low recombination efficiency (possibly as a result of growing the cells in minimal medium to prior to depleting Cdc20). Recombination efficiencies in this experiment (3 biological replicates) reached about 25%. However, the proportion of catenanes are consistent with previous experiments (Figure 3-8): around 15% of the LO species are catenated ( $0.25 \times 0.15 = 3.75\%$  catenanes in nocodazole-arrested cells). Therefore, like in the case of centromeric minichromosomes, spindle forces cause a reduction in the

catenated loop out population, probably by stimulating topo II-mediated decatenation of this chromosomal region.

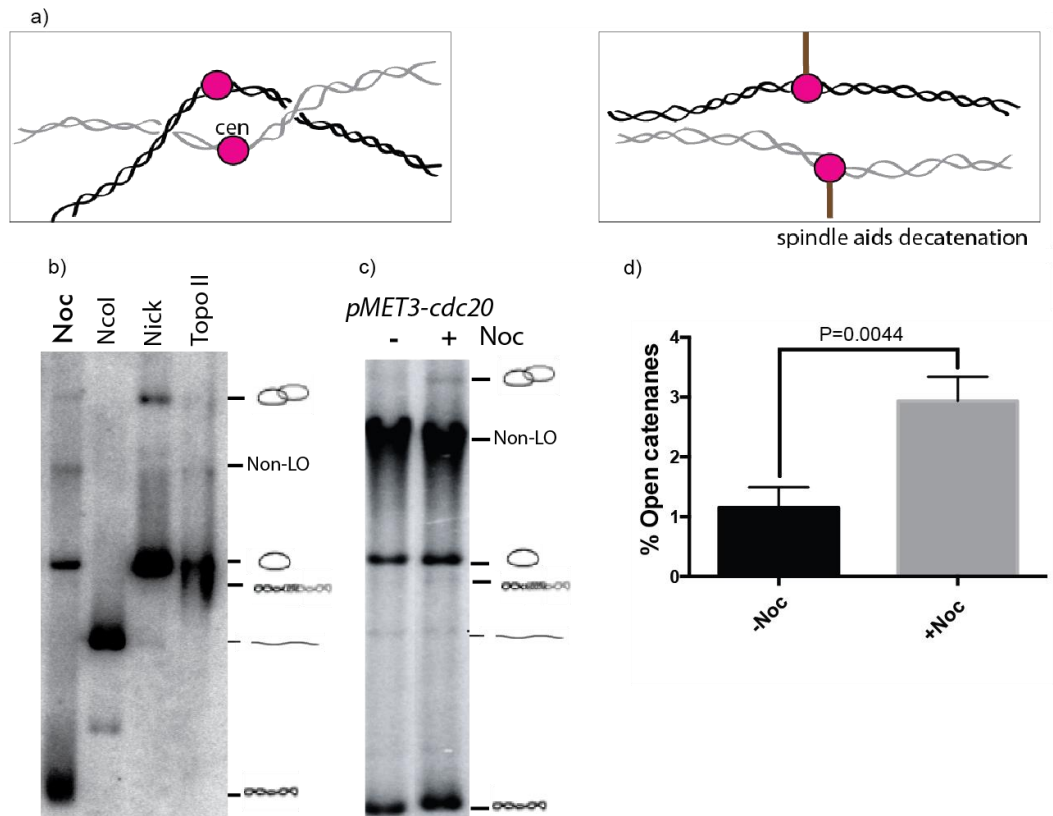


**Figure 3-11. Loop out of CEN region in G2/M in the absence or presence of the mitotic spindle**

a) Schematic representation depicting the effect that spindle forces have on centromeric catenanes, putatively stimulating topo II-mediated decatenation at this region. Centromeres are represented by pink circles. b) Southern blot of a centromeric loop out (CEN10) in G2/M arrested cells, and the respective *in vitro* treatments to confirm the identities of the topoisomers. c) Effect of the mitotic spindle on the topoisomer distribution of a centromeric loop out: cells arrested in G2/M with the spindle present exhibit a reduction in the catenated species (left lane) compared to cells arrested in the same cell cycle stage in the absence of spindles (right lane). d) Quantification of the open catenane population from (c).

### 3.6 Chromosomal elements & topology

Together, the experiments described so far suggested that our loop out method is able to capture the local topologies of native budding yeast chromosomes. So far, we have detected catenated loop outs of a predicted TER site in G2/M arrested cells. We then turned to our research questions. We first

decided to study the distribution of DNA catenation: where do we find catenanes along chromosomes?

### 3.6.1 Topologies of replication origins and termination regions

According to the termination model, catenanes will form at replication termination regions (TER) as replisomes converge. In contrast, stable catenanes would not be generated at or near replication origins (ARS) if replisome rotation during elongation is limited or prohibited. If catenanes were not able to translocate along chromosomes, we would expect to find them around TER but not ARS regions (Figure 3-12a).

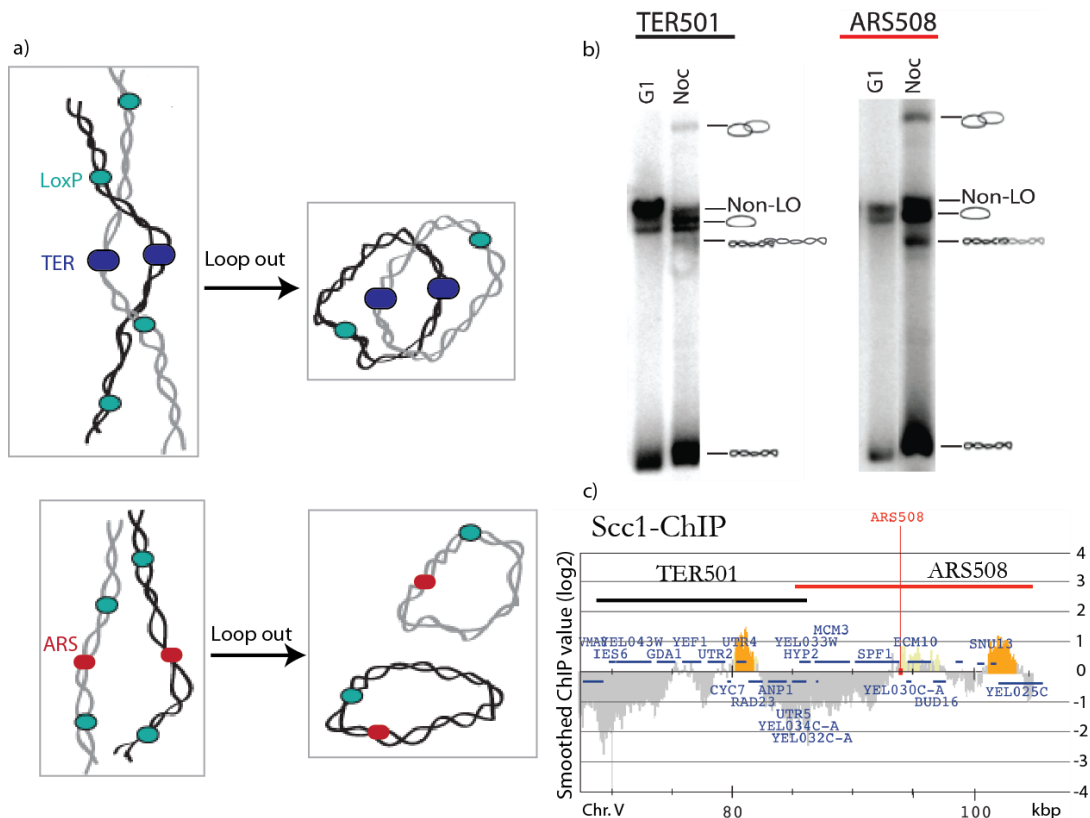


**Figure 3-12. Assessing the local topologies of an ARS and a TER loop outs.**

a) Schematic representation of the expected topologies, according to the termination model, of TER (top) and ARS (bottom) regions after S phase. b) Southern blotting of TER and ARS loop outs (left and right, respectively) from G1 and G2/M (nocodazole) arrested cells. c) Scc1 ChIP-on-chip experiment showing the association of the cohesin complex with the TER and ARS loop outs (Ocampo-Hafalla et al, 2007).

To test this, we decided to loop out replicated regions encompassing a termination site or a replication origin and compare the resulting topoisomers

(Figure 3-12b). Against our expectations, catenanes were detectable at both TER501 and ARS508 after DNA replication, and at similar levels (around 12-15% of the loop out species; not shown). This shows that catenanes are not restricted to regions of replication termination. Our result could be explained by two alternatives: (1) catenanes form at termination regions but get distributed to other regions, or (2) precatenane formation gives rise to intertwinings throughout the chromosome.

### **3.6.2 Catenanes are not restricted to regions of cohesin enrichment**

The cohesin complex has been proposed to protect intertwinings from topo II-mediated decatenation (Haering et al., 2008; Farcas et al., 2011; Charbin et al., 2014). These observations suggest that catenanes might be indeed maintained at cohesin binding sites, where presumably sister chromatids are prevented from separating. In fact, in our experiment comparing the TER and ARS topologies, we noticed that both loop out regions present substantial Scc1 association (Figure 3-12c); thus, the association of the cohesin complex could explain the presence of catenanes in these regions.

We set out to compare the topologies between TER loci where cohesin association is enriched with loci where cohesin is absent or markedly reduced. We took advantage of previously generated Scc1 ChIP-on-chip maps (Ocampo-Hafalla et al., 2007), and designed a number of strains where a TER with or without cohesin enrichment would be looped out.

As Figure 3-13 shows, catenanes were detectable at TER regions where the cohesin complex is enriched, but not to a greater extent than at TER regions where cohesin association was markedly reduced (12% of the loop out species are catenanes at TER301, compared with 11% at TER603). We note that there is a small Scc1 peak along TER603, and thus we cannot completely discard the possibility that, locally, cohesin is required to maintain catenanes. Nevertheless, the relative enrichment of cohesin on chromatin does not correlate with the levels of catenanes found on these two TER loop outs. Although this does not indicate whether the presence of catenanes depends on an active cohesin complex, it does suggest that intertwinings are not restricted to cohesin-enriched sites.

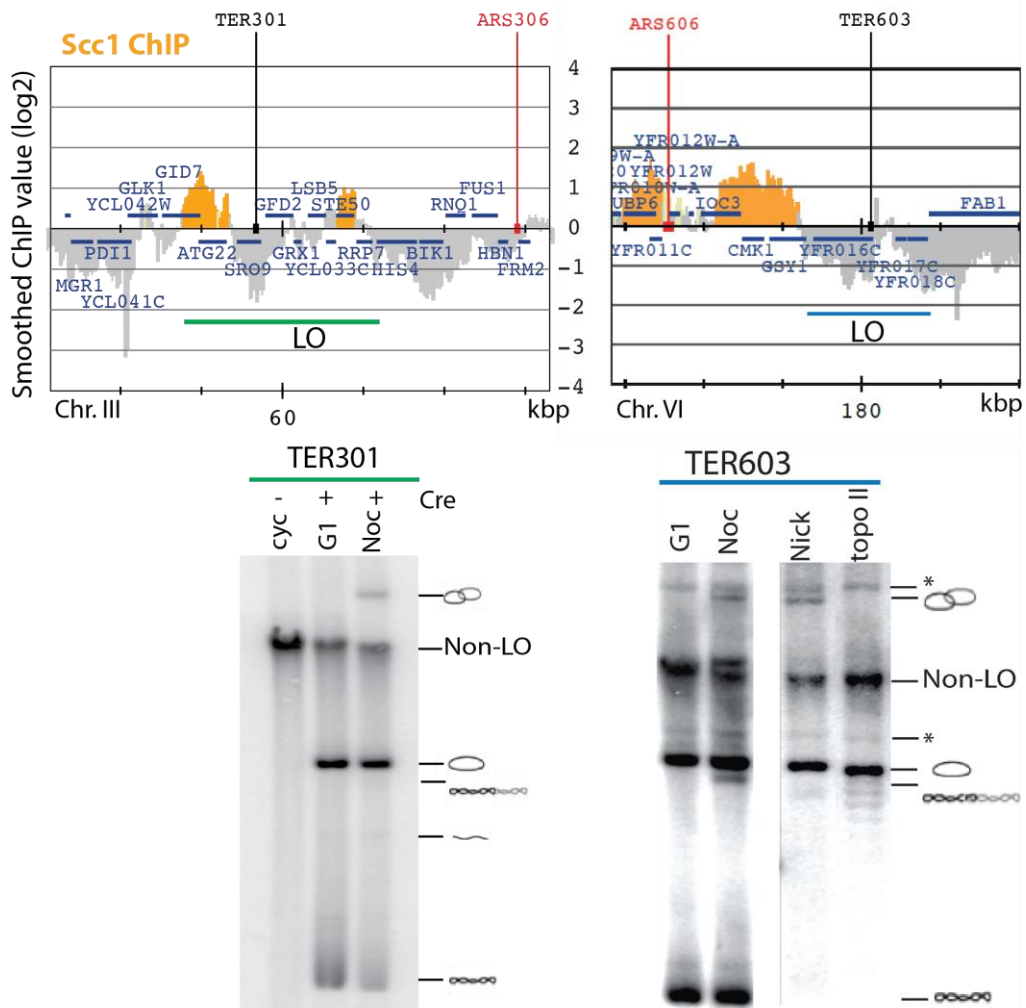


**Figure 3-13. Analysis of catenane accumulation and cohesin enrichment.**

Scc1 association is enriched around the TER301 region (top left). Loop of this region in G2/M presents some catenated topoisomers (bottom left). Conversely, the TER603 region does show substantial Scc1 association (top right). Topological analysis of this looped out region shows catenated species, nevertheless.

### 3.6.3 Catenanes are present at condensin-binding sites

In contrast to the cohesin complex, the condensin complex has been proposed to stimulate topo II-mediated decatenation (Baxter et al., 2011; Charbin et al., 2014). We therefore decided to compare the topologies between condensin-enriched and condensin-free TER regions. Using Brn1 ChIP-on-chip data (D'Ambrosio et al., 2008b), we designed a number of strains where a TER with or without condensin enrichment would be looped out.

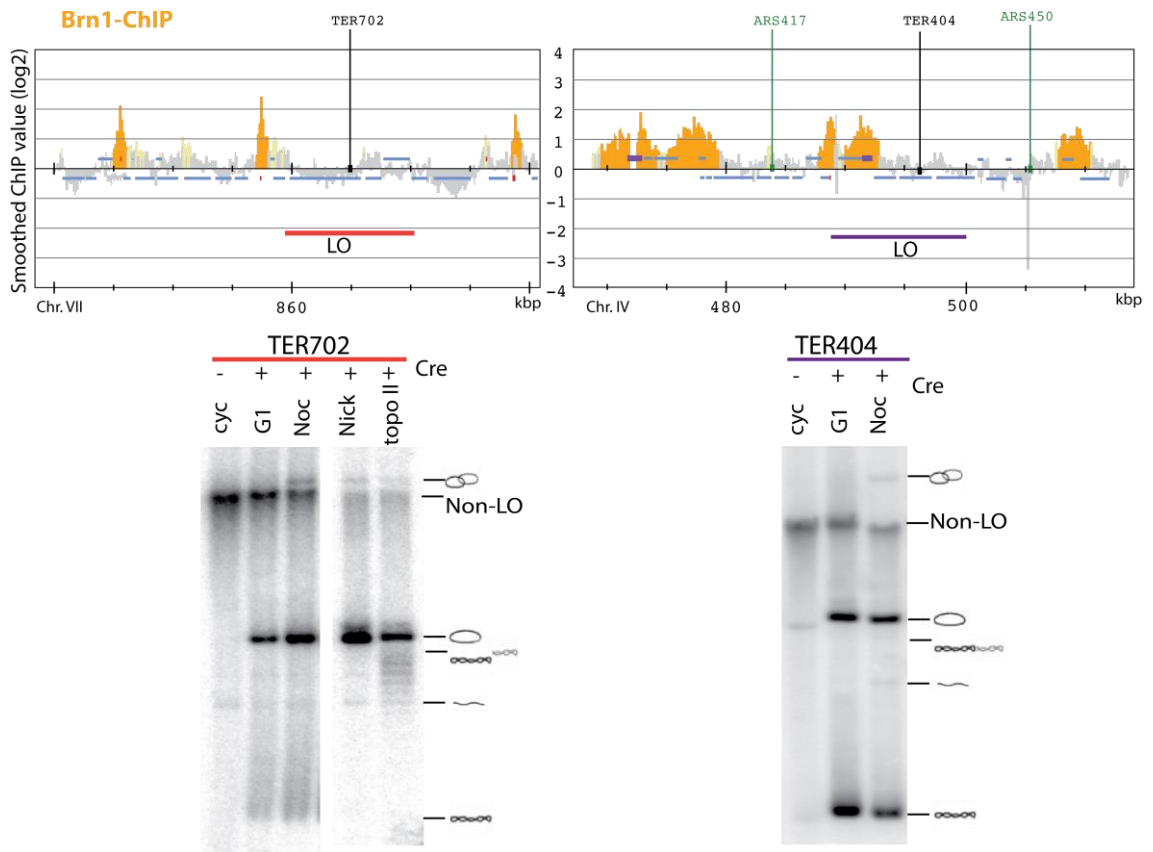


**Figure 3-14. Correlation between DNA catenation and condensin enrichment.**

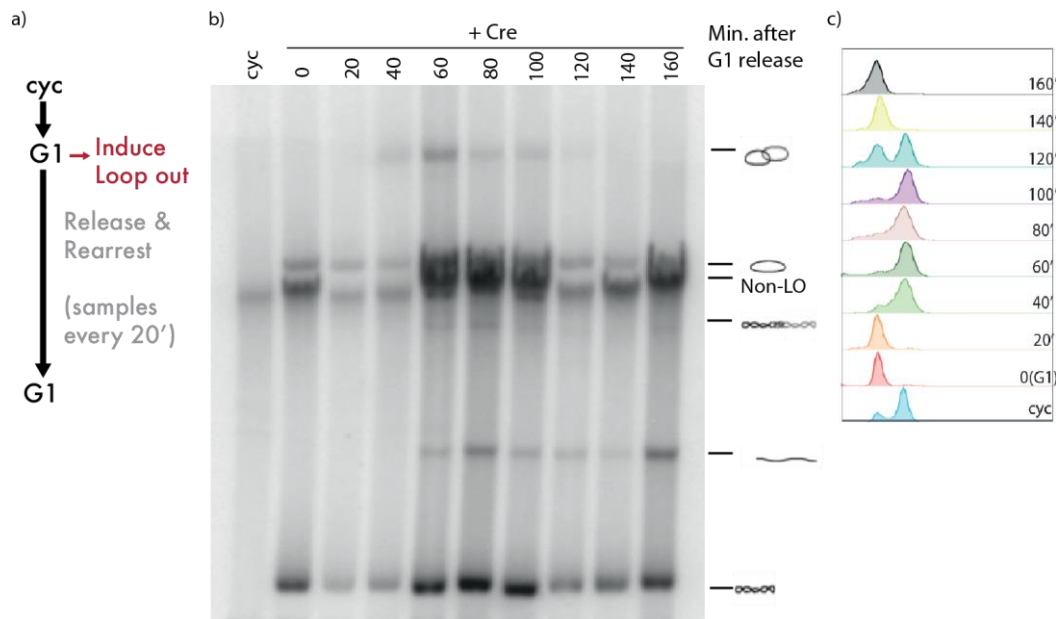
Brn1 ChIP-on-chip analysis (D'Ambrosio et al., 2008b) and southern blotting shows that in G2/M catenanes are present in chromosomal regions with reduced (left) as well as in substantial condensin enrichment (right).

Figure 3-15 shows that in both cases, i.e regions of marked condensin enrichment and regions of reduced condensin association, catenanes are present in G2/M (nocodazole) arrested cells. Quantification of these samples indicated that the proportion of the loop out corresponding to catenated species was 10% for TER702 and 15% for TER404 (not shown). We note the presence of some condensin enrichment at the TER703 loop out and thus we cannot conclusively compare between condensin-binding and condensin-free regions. However, the similar accumulation of catenanes in both loop out regions suggests that DNA catenation (or at least its maintenance during a nocodazole arrest) is not restricted to regions where condensin is not markedly accumulated, nor it is excluded from condensin-enriched loci.

### 3.7 Topology of the loop out during the cell cycle

#### 3.7.1 Loop out of the efficient replication origin: ARS508

We next turned to topological analysis of a looped out chromosomal segment during cell cycle progression. Only loop outs encompassing a replication origin can be used for this purpose because they can sustain DNA replication after loop out. We first arrested cells in G1 and induced Cre for 90 min. We then released the cells to pass through a synchronous cell cycle and collected aliquots for DNA isolation for topological analysis every 20 min (Figure 3-15a). Figure 3-15b & c show that in G1, only the monomeric forms of the loop out accumulate; as cells go through S phase, the catenated species appear, which are then lost as cells rearrest in G1.



**Figure 3-15. Analysis of the ARS508 loop out during one cell cycle.**

a) Experimental scheme: exponentially growing cells were arrested in G1; 1.5 h into the arrest, Cre activity (and loop out) was induced. 1.5 h later, cells were released into the cell cycle, and time points for DNA preparation taken every 20 min. b) Southern blot showing the topology of the loop out within one cell cycle. c) FACS showing cell cycle progression during the experiment.

Quantification of the bands indicated that loop out levels reached 60-65%; catenanes reached their maximum levels, 17% of the loop out species, 60 min after G1 release (not shown). In contrast, a similar experiment using a 21 kb centromeric minichromosome presented a maximum of 31% of the topoisomers as catenanes,

also 60 min after G1 release (not shown). The slight discrepancy in maximum catenane levels might be explained by the different sizes of the substrates (loop out is 17 kb; minichromosome is 21 kb), and/or in differential firing efficiencies of the replication origins contained within the two DNAs. Nevertheless, in both cases the catenated fraction of the DNAs slowly decreased after 60 min, and was completely absent by the 120 min time point, when cells were rearrested in G1.

This experiment emulates studies using minichromosomes in that it follows the topology of a DNA molecule outside the chromosomal context. The fact that we detect catenated loop out molecules as DNA replication occurs, and that this species is no longer detectable upon mitotic exit suggests that our recombination-based method indeed captures the physiological topology of eukaryotic chromosomes.

### **3.7.2 Chromosome topology of a heterochromatic region**

The experiments presented above have examined the topology of chromosomal regions with similar 'open' chromatin structure. Open chromatin could allow the translocation or distribution of catenanes along different chromosomal regions. Thus, we decided to investigate the topology of a region with different chromatin structure, namely the *HMR* locus. This locus assembles hypoacetylated histones (which have been reported to have a distinct supercoiling configuration; Bi & Broach, 1997) and is transcriptionally repressed (Cheng et al., 2005). We used a strain that contains a LacO array adjacent to the *HMR* locus, with both these elements surrounded by R target sites, and a copy of the R recombinase under the control of a galactose inducible promoter (gifted by M. Gartenberg; Figure 3-16a). *Zygosaccharomyces rouxii* R recombinase, like Cre, belongs to the tyrosine recombinase family. There are two origins in this loop out region, ARS317 and ARS318, which fire later and are less efficient than the previously studied ARS508 (according to the OriDB database, [cerevisiae.oridb.org](http://cerevisiae.oridb.org)).

We first monitored the topoisomer distribution of the *HMR* loop out during the course of one cell cycle. Topological analysis of this region shows that catenated topoisomers appear later than in the case of ARS508 (Figure 3-16c), consistently with the relative timing of firing of their respective origins. Moreover,

the reduced accumulation of catenated species (10% of the total loop out at 60 min, not shown) could reflect the relative inefficiencies of ARS317 and ARS318. As aforementioned, when cells undergo chromosome segregation and return to G1, the catenated species disappear, most probably due to topo II action.

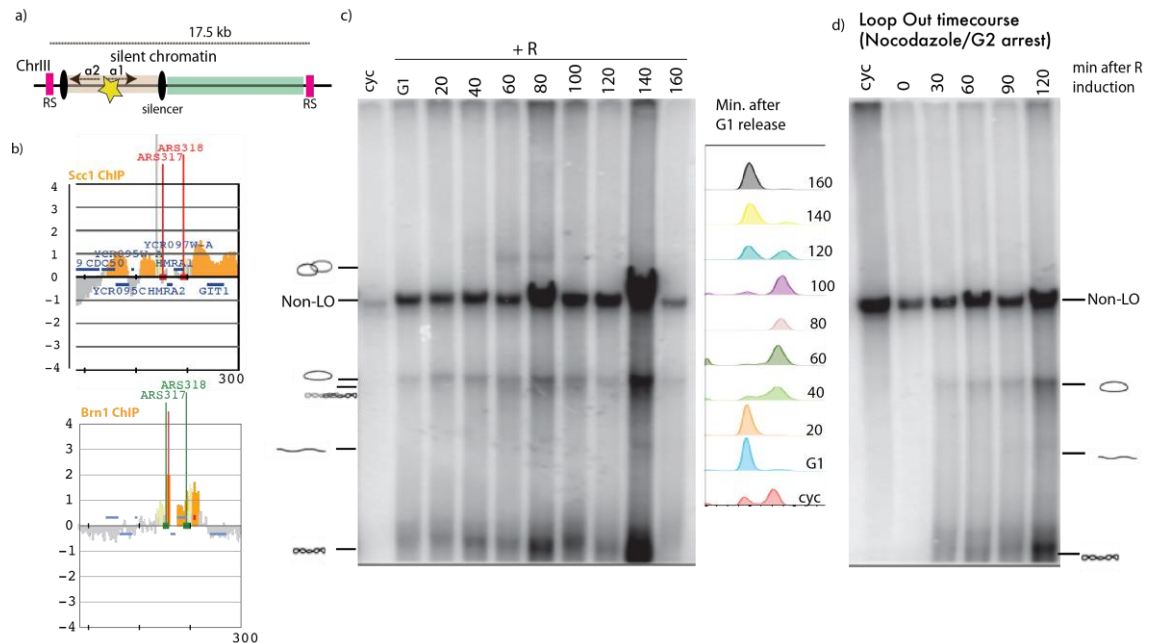


**Figure 3-16. Loop out of the *HMR* locus and southern blot analysis of the resulting topoisomers.**

a) Schematic of the *HMR* loop out: two silencers (shown in black) flank the heterochromatin-like region (shown in brown). The loop out also encompasses a LacO array (green bar). b) Cohesin (top) and condensin localization (bottom) to the *HMR* locus; y-axis shows the Smoothed ChIP value ( $\log_2$ ), x-axis shows a 30 kb region of Chr. III centered around the *HMR* locus. c) Topology of the *HMR* loop out during the cell cycle. R activity was induced in G1-arrested cells, and upon release into the cell cycle, samples were taken every 20 min for DNA isolation and topological analyses. d) Time-course showing R-mediated loop out of the *HMR* during a G2/M arrest.

Interestingly, in a G2/M *HMR* loop outs do not appear as catenated species (Figure 3-16d). This could reflect the fact that recombination of heterochromatin-like regions is less efficient (M. Gartenberg, personal comm.). However, it is probably not sufficient to explain why catenanes are not detectable in the 120 min time point, where the proportion of looped out species almost matches previous levels of recombination by Cre (58% recombination at 120 min, not shown). Similarly, time points 90 and 120 min in Figure 3-16c show comparable levels of

recombination as time point 60 Figure 3-16b, where we detect 55% recombination and catenated species are visible. An alternative (and biological) explanation would be that topo II has removed most intertwinings at this locus, and that catenanes from nearby regions might not redistribute into the *HMR* region due to local chromatin elements that act like topological barriers (Chang et al., 2005).

### 3.8 Exploring the models for catenane formation

Our second research aim regarding the local topologies of native budding yeast chromosomes was to investigate whether, in addition to catenane formation at replication termination, precatenane formation during elongation is prevalent.

#### 3.8.1 Analysis of the ARS508 loop out in the absence of replication termination

In order to test whether precatenanes form during replication elongation, we decided to carry out our loop out experiment in a scenario where replication is ongoing but has not terminated yet. For this, we decided to release the cells from a G1 arrest into low concentrations of hydroxyurea (HU), which would markedly reduce the speed of the replisomes without causing severe stalling. Cre was induced 30 min into the arrest, to allow early origin firing and replication of the loop out region. We also added bromodeoxyuridine (BrdU) to the cells, to analyse replication progression by ChIP-on-chip analysis of incorporated BrdU.

After 90 minutes in HU, the loop out (LO) region around ARS508 has replicated, but no major termination events between the forks arising from this replication origin and the forks from neighbouring origins could be detected, as judged by the BrdU peaks (IP/input), that had not merged (Figure 3-17, left panel). Under these conditions, topological analysis of the loop out revealed that the catenated species had already formed (Figure 3-17, right panel). This result supports idea that catenanes already form during ongoing DNA replication and before termination of DNA synthesis, consistent with the prediction of the precatenane model for DNA catenation.

One potential caveat of this experiment is that termination events could be artificially triggered in the loop out. This would be the case if recombination

occurred before the replisome had passed through the *loxP* sites, which would cause the convergence of the two incoming replication forks within the excised loop out. However, this is unlikely, because analysis of BrdU incorporation shows that replication of the loop out region has already occurred 60 min into the HU arrest (not shown), which corresponds to 30 min post-Cre induction, when loop out is just beginning to be detectable (See Section 3.5). Nevertheless, further experiments are required to exclude the possibility of replication termination occurring within the loop out.

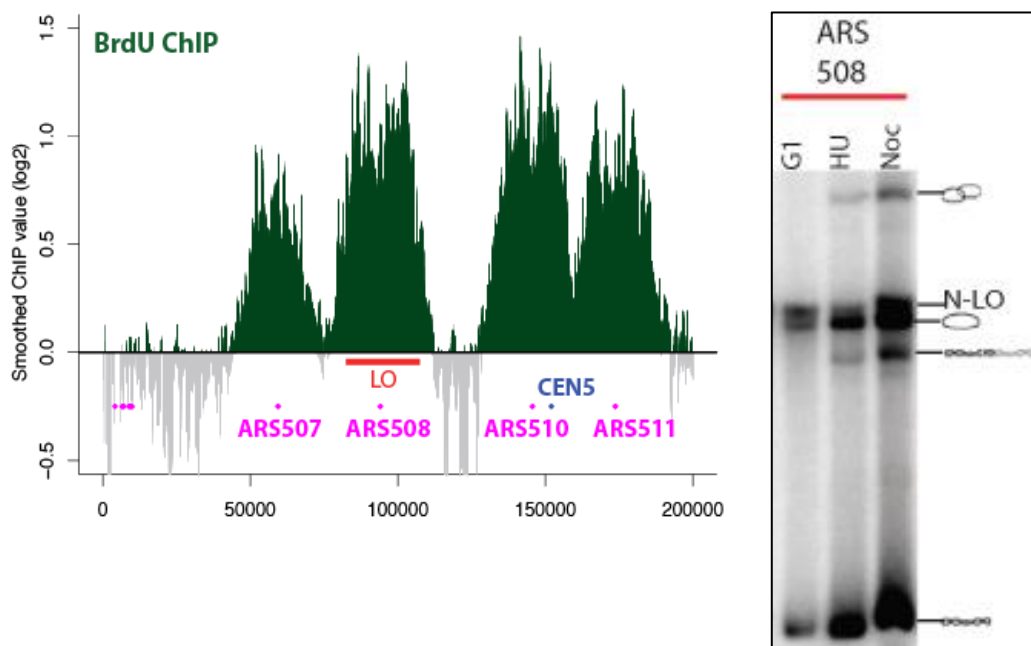


**Figure 3-17. Catenanes form during replication elongation**

At low levels of HU (0.1 M), replisomes progress slowly. BrdU ChIP-on-chip analysis (left) shows the incorporation of BrdU 90 min after release from G1 into HU and 60 minutes after Cre induction. Looping out of a region encompassing ARS508 that is already replicated but that does not present major replication termination events shows that the catenane band is present in HU (right panel, middle lane). For comparison, a G2/M (nocodazole) sample is shown (right panel, right lane).

### **3.8.2 The introduction of a replication fork barrier does not affect the levels of catenanes**

Replication termination is stochastic in budding yeast. The sites of fork convergence are largely determined by origin position and firing timing (McGuffee

et al., 2013). Thus the TER regions we have studied so far have low efficiencies of termination, i.e. they are sites of replisome convergence in a proportion of the cells within a population. There is one notable exception to stochastic termination, namely the replication fork barrier (RFB) of the rDNA locus. The RFB sequence constitutes a polar fork barrier, allowing the progression of the fork in the direction of 35S transcription, but not the opposite (Kobayashi et al., 2001). This sequence can act as a replication barrier when placed ectopically, i.e. at loci other than the rDNA locus (Cebrian et al., 2014).

We reasoned that integrating the RFB into our loop outs would create or reinforce termination events in ARS and TER loop outs, respectively. To determine the contribution of precatenation and catenation at termination towards total levels of intertwinings, we would compare the proportion of catenane species of a loop out that has an ARS only, with that of ARS+RFB. As a control, we could place the RFB in a TER loop out. This would increase the termination events in the predicted TER vicinity. For example, an estimated 40% of the cell population experiences termination in that the predicted TER301 (McGuffee et al, 2013), which would be expected to be close to 100% after RFB introduction. However, it would not markedly increase the total number of termination events in the whole 17 kb loop out (since the replication origins around TER301 are very efficient and the majority of the forks are expected to meet in this region). Thus, catenanes forming at termination sites would not increase noticeably between TER301 and TER301+RFB.

We integrated the RFB sequence next to ARS508 or to the predicted TER301 region in the loop out strains (at coordinates V: 96700 and III: 58771, respectively; Figure 2-2; 3-18a). As expected, we did not detect striking differences when we compared the pattern and relative abundances of topoisomers between TER301 and TER301+RFB, neither in G2/M nor in S (in our conditions, 90 min after release into 0.1 M HU, most cells had already replicated this region; 3-18b &c). Quantification indicated that in all cases, the catenated species corresponded to around 10% of the loop out species. This is probably because, as mentioned before, introducing the RFB sequence is not expected to markedly increase the number of termination events in the loop out region. Figure 3-18c shows that the ARS508+RFB did not noticeably show an increased proportion of catenanes with respect to ARS508 in G2/M (with 9% of the loop out species corresponding to

catenanes in the case of ARS508, and 11% in the case of ARS+RFB, not shown). This could be either because (1) catenanes formed at termination events have distributed evenly throughout the chromosome, or (2) termination events do not generate more intertwinings that would otherwise form during elongation. Considering the results we obtained in the previous experiment, we favour the second explanation: a number of intertwinings form per kb replicated, and whether that is during elongation or termination does not make a substantial difference.

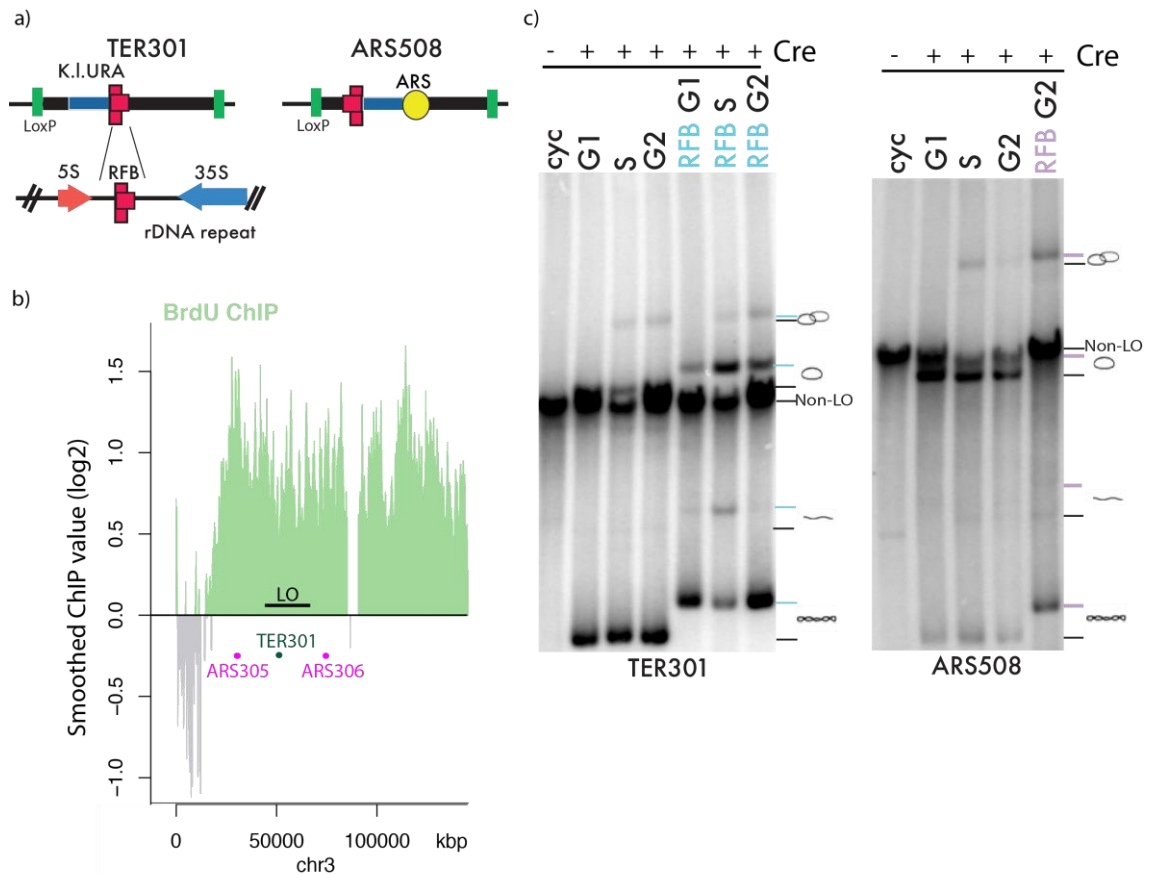


**Figure 3-18. Introduction of an RFB sequence does not noticeably affect the levels of catenanes.**

a) Schematic showing how the RFB was introduced in our loop out strains TER301 and ARS508. b) BrdU enrichment at the TER301 region during the HU arrest. c) Southern comparing the topologies of the loop outs with and without TER. Note that the +RFB loop outs are slightly larger than their –RFB counterparts due to the additional insertion of the K.I. *URA3* marker.

### 3.8.3 Replication of the ARS loop out in the absence of functional topo II

What are the topological consequences of the lack of topo II activity during replication of chromosomes? To gain insight into this question, we crossed our

ARS508 loop out strain with a temperature sensitive *top2-4* allele. We induced the loop out in G1 arrested cells (1.5 h into the arrest, for 1.5 h) and split the culture into three: one third of the cells was released into the cell cycle at the restrictive temperature (sample 1), another third was released at the permissive temperature but switched to the 37°C 60 min after release (after S phase, sample 2), and the remaining cells were released and maintained at 25°C (sample 3; Figure 3-19a).

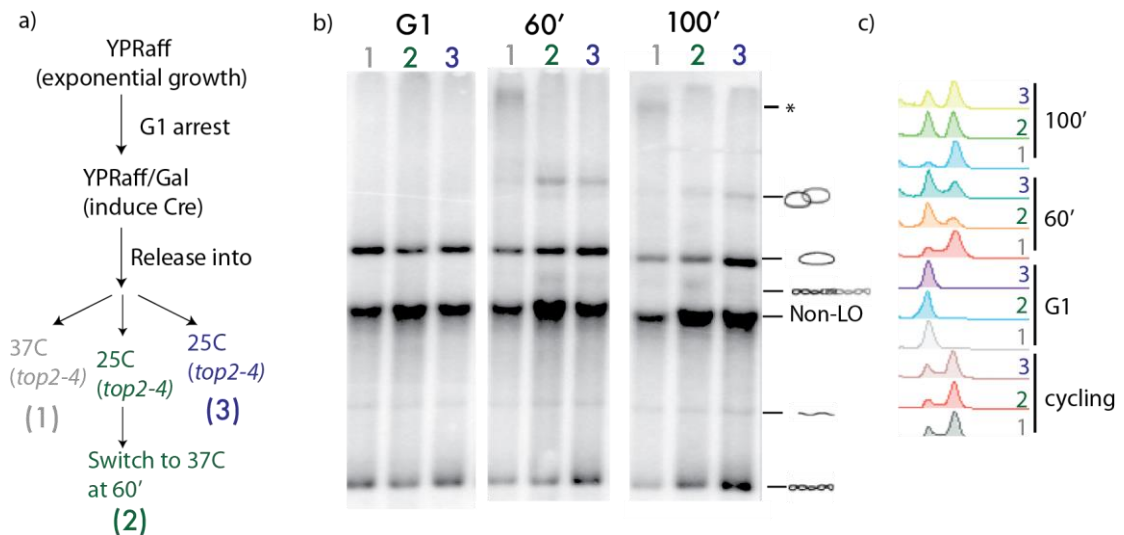


**Figure 3-19. Replication of an ARS loop out in the *top2-4* cells at restrictive temperature gives rise to a high molecular weight replication intermediate.**

a) Experimental design. The region around ARS508 was looped out during a G1 arrest and its topology analysed during interphase in the absence or presence of functional topo II. b) Southern blot showing the loop out topology in G1, S phase and G2 for the three experimental conditions. c) FACS showing cell cycle progression during the assay.

Loop out occurred with similar efficiency in the three cases (Figure 3-19b, around 45-50% in G1), manifest from the monomeric forms of the excised region. However, the topology of the loop out during replication markedly differed in conditions where topo II was inactive (sample 1) or active (samples 2 & 3; Figure 3-19b & c). Whereas in the latter case, we detected the supercoiled and open catenanes, as seen in previous experiments, the presence of catalytically dead topo II through S phase resulted in the accumulation of a slower migrating species appearing as a smear. This probably represents a heterogeneous population of replication intermediates, perhaps containing branched structures that hinder their migration through the agarose gel.

Budding yeast cells can undergo DNA replication in the absence of topo II without major problems, but reporter plasmids become highly catenated, and cells fail to segregate their chromosomes (Baxter & Diffley, 2008). Topo II catalytic mutants are slightly different: DNA replication proceeds with overall normal kinetics, but cells fail to complete DNA replication termination, with reporter plasmids being highly catenated and containing gaps or exposed 3' strands (Baxter & Diffley, 2008). Thus, the final stages of replication are compromised in this mutant, which is probably what we observe when the loop out undergoes DNA replication in the *top2-4* background at restrictive temperature. Ideally, we would make use of a *top2* allele that can result in the effective and conditional depletion of the protein to confirm that in the absence of topo II, the proportion of loop outs that undergo replication become catenated.

### 3.9 Unidirectional recombination

A potential problem associated with our *loxP*/Cre system is that recombination is bidirectional. This can theoretically allow several recombination events per cell that could allow the recombination of the loop out back into the chromosome and/or the fusion between two excised loop outs. In practice, this is unlikely for two reasons: (1) Cre prefers intramolecular over intermolecular recombination reactions (van Duyne, 2015), and (2) *in vitro* treatment with topo II would not remove fusions between two excised loop outs (but it does remove the putative loop out catenanes). Nevertheless, to discard the possibility of additional recombination events, we turned to a unidirectional recombination system.

In contrast to tyrosine recombinases, the large serine recombinase family carries out a unidirectional integration reaction with no competing reverse reaction (Sclimenti et al., 2001). The most thoroughly-studied member of this family, the *Streptomyces* phage  $\phi$ C31 integrase, needs no cofactors to perform efficient recombination between its *attB* and *attP* sites, and produces hybrid sites, *attL* and *attR* (Thorpe et al., 2000). This recombinase exhibits strict site selectivity: *in vitro* and in heterologous hosts, it only catalyses *attB/P* recombination. It has been shown to work in fly (Groth et al., 2004), mouse (Belteki et al., 2003), zebrafish (Lister, 2010) and human genomes (Groth et al., 2000). While serine recombinases

have the obvious advantage of unidirectionality, they have not been so well characterized in our model organism of choice (Xu & Brown, 2016).

### 3.9.1 Construction of a $\phi$ C31 integrase system

We first constructed strains containing the *attB* and *attP* sites around TER regions of interest (Table 7; supplementary 7.4). The strategy was similar to the *loxP* strain construction, with the slight modification that we left the selective markers in the chromosome for simplicity (Figure 3-20).

**Table 7. Characteristics of the *attB*/ $\phi$ C31 strains used in this study**

Locus (Chr. no.)	Element	Efficiency	AttB	AttP	LO (bp) (+ <i>K.I URA3</i> )
Telo R (I)	TELO, ARS, CN		311	12888	14277
ARS508 (V)	ARS, CH, CN	0.919	84680	96593	13613
TER1417 (XIV)	TER,	-0.427	420890	429872	8982
TER603 (VI)	TER, CN	-0.642	176871	184501	9267
TER1004b (X)	TER, CEN, CH, CN	-0.504	432667	438403	7235

TER: termination region; ARS: autonomous replication sequence; CEN: centromere; CH: cohesin binding site; CN: condensing binding site; efficiency is an estimate of the proportion of a cell population that fires a given replication origin (Efficiency: from 0 to 1; McGuffee et al., 2013), or experiences fork convergence at a given termination region (Efficiency: from -1 to 0; McGuffee et al., 2013).

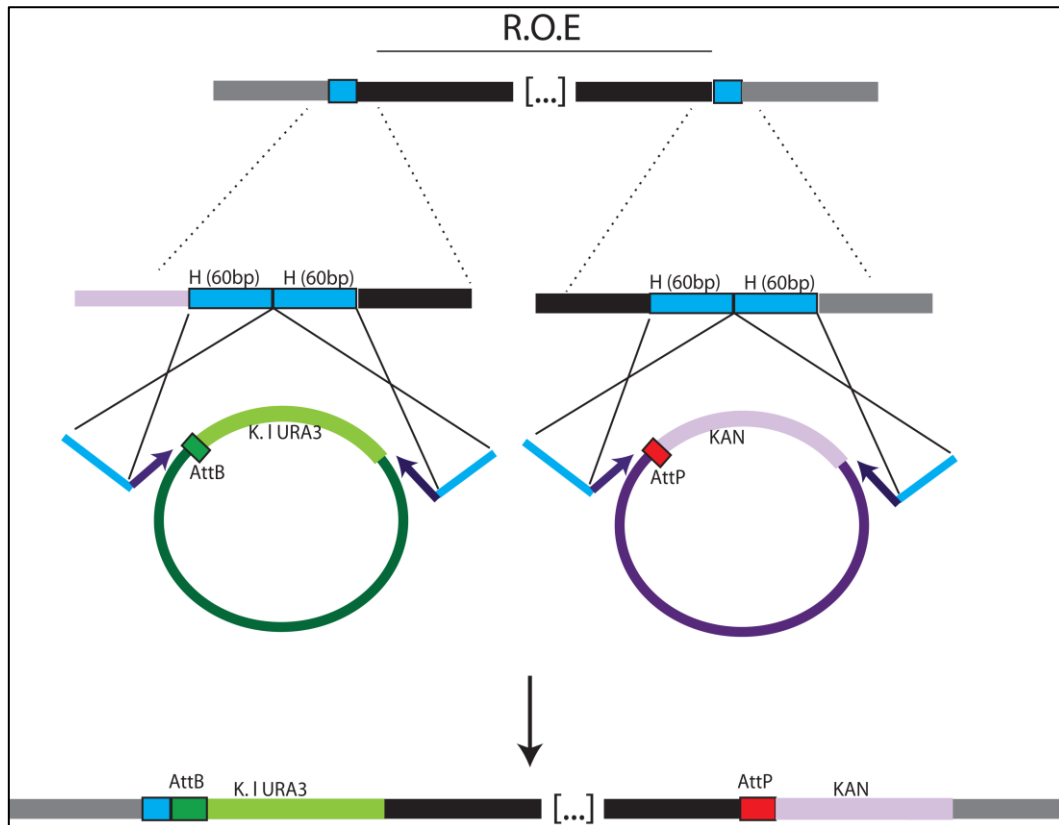


**Figure 3-20. Strategy for the construction of *attB/attP* Loop out strains.**

The *attB*-*K.I URA3* cassette was integrated in the genome, upstream of the region of excision (ROE), and positive integrants were identified by genotyping PCR and sequencing. Subsequently, the *attP*-*KanMX* cassette was inserted downstream of the ROE, and positive colonies were confirmed by genotyping PCR and sequencing. Finally, cells were transformed with a centromeric plasmid containing the  $\phi$ 31C integrase ORF under the control of the galactose inducible promoter. KAN: *KanMX*.

The *attB/attP*  $\phi$ C31 system enables unidirectional recombination, and thus ensures that recombination only occurs once per cell (Figure 3-21a). Expression of the  $\phi$ C31 integrase, under the control of the galactose inducible promoter, showed similar kinetics to that of  $P_{GAL1}$  Cre (Figure 3-21b). Excision rates were also comparable to those observed in the *loxP*/Cre system: loop out levels reached 68% after 180 min at TER603 and 70% at TER1417 after 120 min (not shown). Figure 3-21c shows the topological analysis of loop outs excised with  $\phi$ C31 integrase. The pattern observed is similar to that previously seen in the Cre-mediated loop outs. In G2/M, two additional bands are apparent that are absent in G1, putatively corresponding to the supercoiled and open catenanes. We are currently identifying

these bands with the aforementioned *in vitro* enzymatic treatments, namely nicking enzyme and topo II.

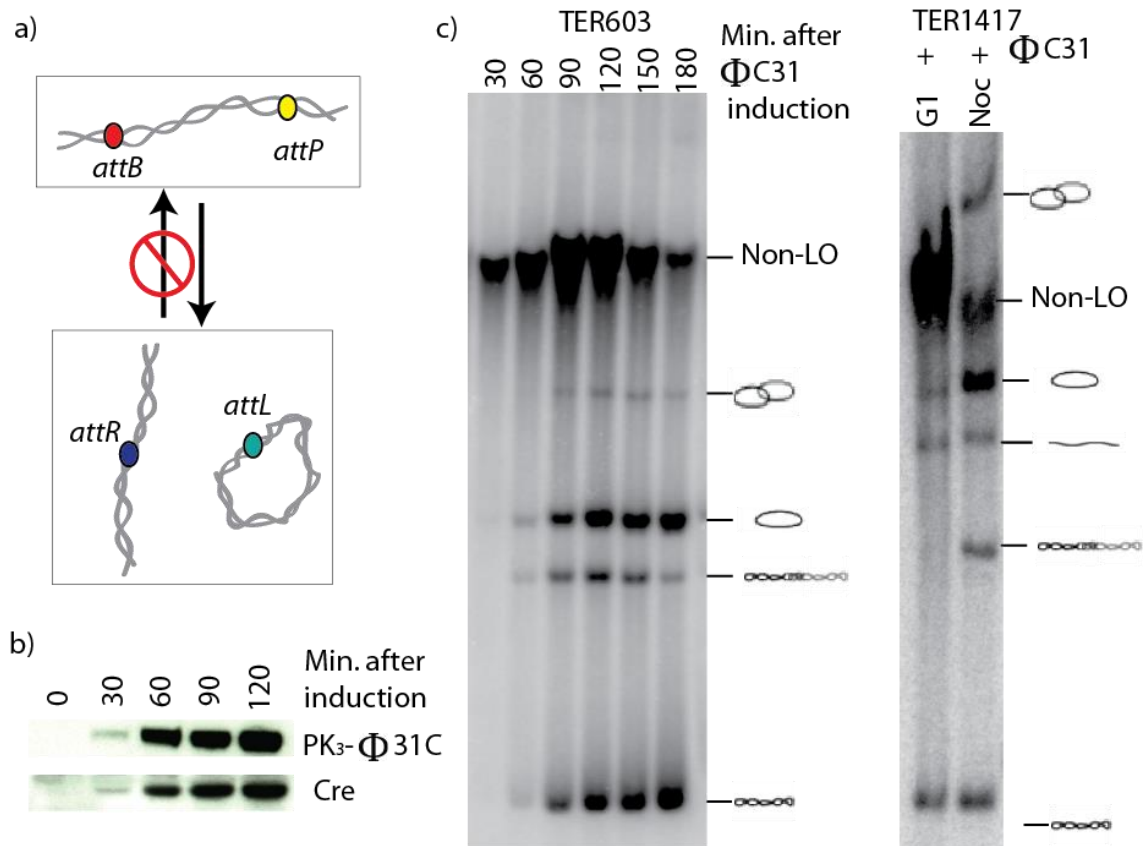


**Figure 3-21. Unidirectional site-specific recombination system to study chromosomal topology**

a) Schematic showing the basis of the  $\phi$ C31 system: recombination occurs only between *attB* and *attP* sites, and produces *attR* and *attL*. b) Western showing the induction of P<sub>GAL1</sub>- $\phi$ C31 upon galactose addition. c) Southern blots of *attB*-TER603-*attP* loop out in G2/M arrested cells (right) and of *attB*-TER1417-*attP* loop outs in G1 and G2/M.

### 3.9.2 Telomeres

The unidirectional recombinase system allowed us to study the topology of a telomeric region (construction of a similar strain with the *loxP* system was not possible because excision of the *K.I. URA3-loxP* cassette on 5-FOA plates never yielded the right sequence). Topological analysis of this chromosomal locus revealed a different pattern from other regions (Figure 3-22).

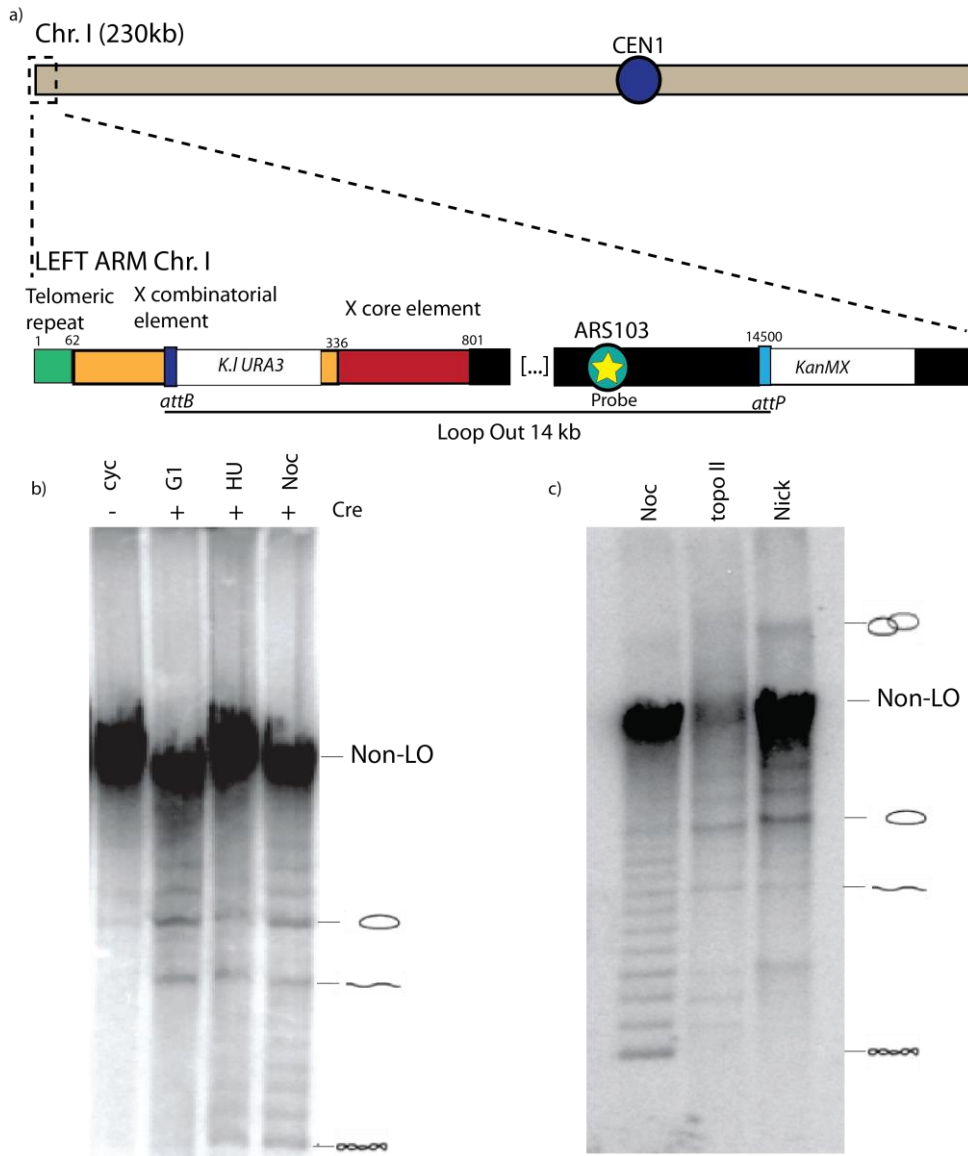


**Figure 3-22. Analysis of a telomeric loop out**

a) Schematic of the loop out region. b) Southern blot of the excised right telomeric region in Chr. I before, during or after DNA replication. c) Enzymatic treatments with topo II and nicking enzyme of a G2/M sample.

First, we did not detect catenanes after DNA replication in telomeric loop outs, or at least they did not accumulate to the levels we have observed in other genomic loci. They only become apparent following treatment with nicking enzyme (Figure 3-22c), which we cannot currently explain. Secondly, we detected a ladder of topoisomers, probably ranging from the supercoiled to the open monomer. This is present in samples obtained from cells arrested in G1, S and G2/M, suggesting that it is not specific to a given cell cycle stage. Where does this topoisomer ladder come from? A potential explanation could arise from the fact that there is some

rotation around chromosomal ends (Joshi et al., 2010). If free rotation around telomeres indeed occurs, this could allow some torsional stress, i.e. supercoils and catenanes, to dissipate through chromosomal ends. Over a period of time, the torsional stress in the region would be a tug-of-war between DNA transactions generating it (e.g. transcription), and topoisomerases and free end rotation removing it. The ladder of topoisomers could be reflecting the fact that, in our population of cells, there are different degrees of torsional stress in the telomeric region (i.e. excision is capturing a mixture of progressively less supercoiled species, with those molecules that have lost most of their supercoils running close to open monomeric species). An additional degree of variation probably arises due to the fact that site-specific recombination is not strictly synchronous, and Cre might be looping out this chromosomal segment with different timings among the cell population during the 90 min from its induction. While this needs additional work to confirm the topoisomer assignments, we consider it interesting to note the different behaviour at chromosome ends.

## **Chapter 4**

### **Mapping Active topoisomerases**

## Chapter 4. Mapping active topoisomerases

How do topoisomerases resolve all the topological stress that accumulates during DNA transactions? An approach to tackle this question is investigating the association of topoisomerases along chromosomes using chromatin immunoprecipitation (ChIP)-based methods. Budding yeast topo I and topo II associate with chromatin during S phase, and bind around active early replication origins (Bermejo et al., 2007). Both proteins are expected to localize to the rDNA locus, on account of their reported roles in transcription and condensation (Shau & Hsieh, 1998; D'Ambrosio et al., 2008b), and probably to a multitude of other sites where they resolve topological problems. However, the interpretation of ChIP-on-chip experiments could be complicated by the transient nature of the topology-remodelling reactions of topoisomerases together with their abundance in the cell: cross-linking could create false positive peaks corresponding to more accessible DNA regions (Nolivos et al., 2016) or to binding sites where the proteins are not necessarily engaged in their reactions. On the other hand, this could be overcome by selectively immunoprecipitating topoisomerase molecules that were engaged in their topoisomerization reactions. In this chapter, we propose a method to trap active topoisomerases in budding yeast, through crosslinking these enzymes with poisons that enhance the concentration of cleavage complexes.

### 4.1 Rationale

To gain a better understanding into where topoisomerases act (and where topological problems arise), it is perhaps more instructive to perform ChIP-on-chip using drugs that trap the cleavage complexes (i.e. topo covalently bound to the newly generated termini it creates on its DNA substrate). This would enable the selection of “active” topoisomerases, namely those that are engaged in their topology-remodelling reactions. Trapping an active topo-DNA complex is possible with the use of topoisomerase poisons, namely camptothecin for topo I, and etoposide for topo II, which inhibit the religation of the topoisomerase-generated breaks on DNA. Moreover, these drugs would override the need for formaldehyde crosslinking used in ChIP experiments because topo-DNA cleavage complexes are covalently attached, thus reducing non-specific background. This type of approach

involving topoisomerase poisons and ChIP-based assays has been recently reported for *E. coli* topo IV using norfloxacin (El Sayed et al., 2016) and for human topo I in the presence of camptothecin (Baranello et al., 2016).

The topo II poison etoposide, however, has very low efficacy in budding yeast because it does not accumulate at high enough intracellular levels. The pleiotropic drug resistance (PDR) genes modulate the expression of a number of transporters of the ABC family that limit the intracellular accumulation of drugs (Balzi & Goffeau, 1995). Indeed, interfering with this gene network can render cells sensitive to a number of pharmacological compounds, including etoposide (Stepanov et al., 2008). We made use of a construct that contains a fusion of the DNA-binding domain of PDR1, a transcriptional regulator that usually activates several efflux pumps, and the open reading frame of the *CYC8* repressor (Stepanov et al., 2008). When integrated at the PDR1 locus, this fusion protein represses the genes that are under the control of PDR1.

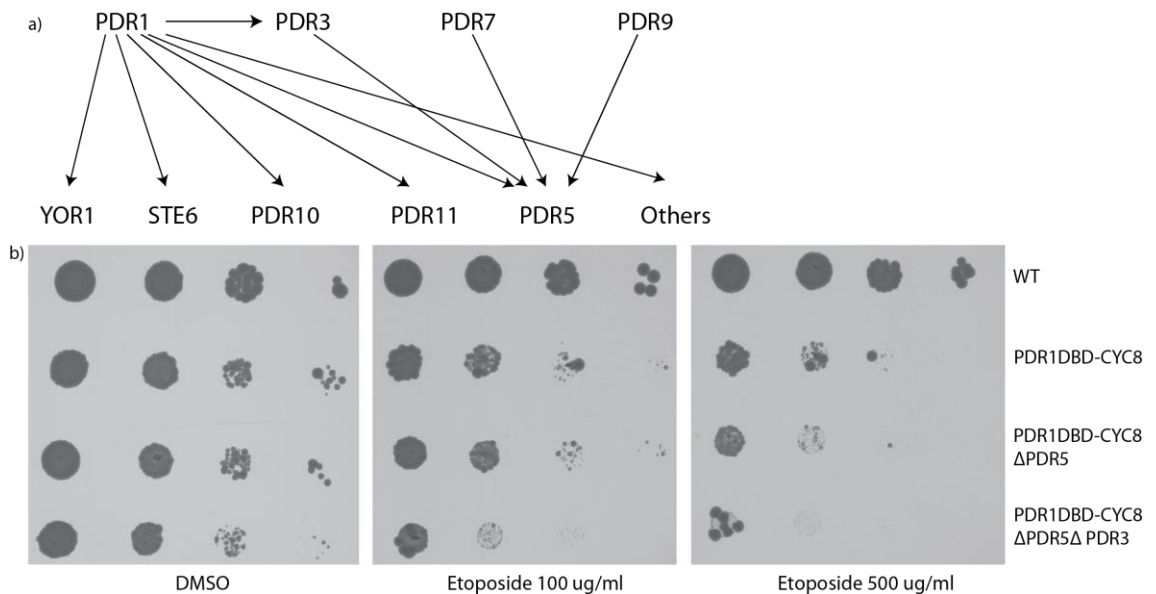


**Figure 4-1. Etoposide sensitivities of the PDR mutant strains.**

a) Simplified scheme of the PDR gene network. PDR1, 3, 7 & 9 (top line) are the transcriptional regulators that control the expression of the ABC transporters and other genes (bottom line; adapter from Balzi & Goffeau, 1995). b) Spot dilution assay of the PDR mutant strains in YPD + solvent (left), low (100 μg/ml; middle) and high (300 μg/ml; right) etoposide concentrations. PDR mutations confer sensitivity to etoposide, which is greatly enhanced by combining PDR1, PDR3 and PDR5 deletions. c) Etoposide efficiency in liquid cultures, as inferred from Rad53 phosphorylation. Cycling cells were added 500 μg/ml etoposide, TCA extracts collected 60 min later, and analysed using Western blot.

Initial trials showed that this mutation slightly increased etoposide sensitivity with respect to wildtype, but not to sufficient levels for ChIP-on-chip analyses (not shown). Thus, we additionally deleted PDR5, encoding a transporter/efflux pump, and PDR3, encoding another transcriptional regulator (Balzi & Goffeau, 1995). Together, these mutations markedly increased the sensitivity of the cells to etoposide (Figure 4-1).

## 4.2 Establishing the conditions for the ChIP

We first optimized the experimental conditions for the ChIP-on-chip assay, by testing different concentrations of etoposide and various exposure times to the drug. We reasoned that if etoposide were effectively trapping topo II-DNA cleavage complexes, DNA damage would ensue (as DNA-tracking complexes, such as the replication or transcriptional machinery, collide with the cleavage complex and trigger the formation of a permanent DSB). To monitor DNA damage, we examined Rad53 phosphorylation (Tercero et al., 2003). Rad53 is a central checkpoint kinase that, upon DNA damage, gets activated and ultimately prevents late replication origin firing as well as aids in the maintenance of replication fork stability (Tercero et al., 2003).

We first compared the levels of Rad53 phosphorylation between the different PDR mutants, and noticed that, in agreement with the spot dilution assay (Figure 4-1), the combination of PDR1, PDR3 and PDR5 mutations led to a more pronounced Rad53 phosphorylation after treatment with 300 µg/ml etoposide for 90 min (Figure 4-2a). To define when etoposide treatment started having an effect, we arrested the triple mutant in G2/M (nocodazole) and monitored the appearance of phosphorylated Rad53 (Figure 4-2b), which indicated that DNA damage was triggered 45-60 min after etoposide addition. Finally, we tested how the etoposide concentration correlated with the extent of Rad53 phosphorylation (Figure 4-2c), which suggested that higher doses of this topo II poison resulted in the most extensive phosphorylation of Rad53 (300 and 500 µg/ml).

From these experiments, we decided to perform our ChIP-on-chip experiments 60 minutes after addition of 500 µg/ml etoposide.

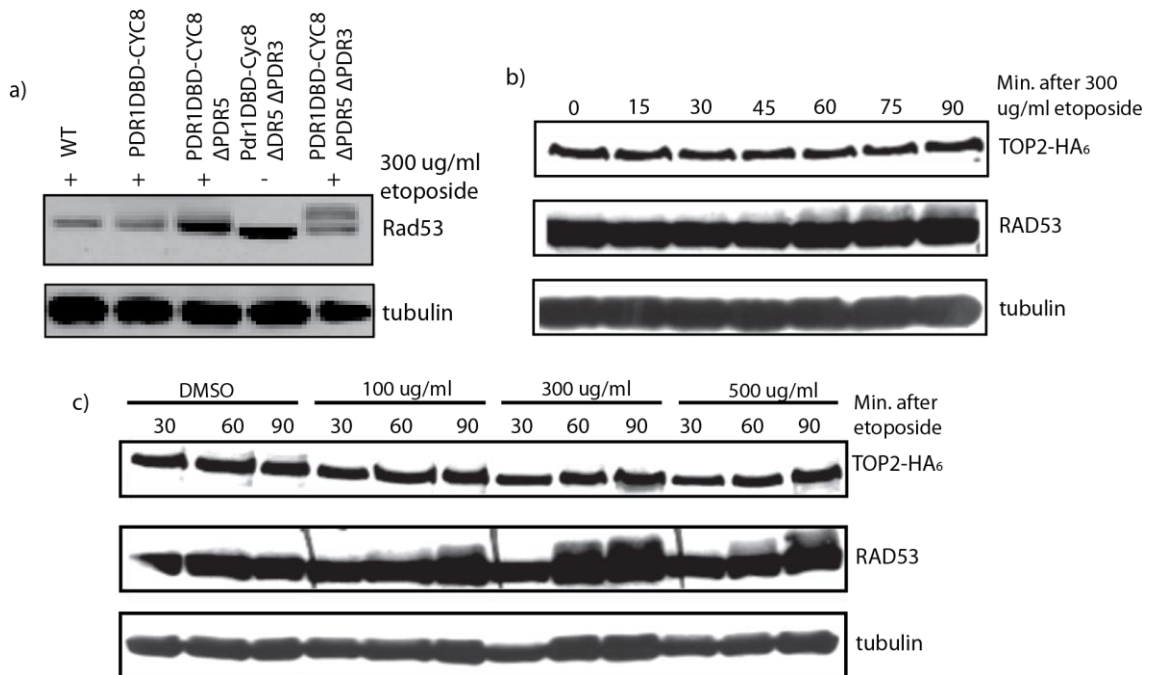


**Figure 4-2. Preliminary tests to determine the timing and concentration of etoposide**

a) Western blot showing Rad53 phosphorylation in cycling cells of the different PDR mutant backgrounds 90 min after addition of 300  $\mu\text{g/ml}$  etoposide. b) Time course showing when Rad53 phosphorylation appears following etoposide treatment during a G2/M arrest (PDR1-CYC8, PDR5 $\Delta$ , PDR3 $\Delta$  background). c) Effect of the etoposide concentration on the extent of Rad53 phosphorylation in G2/M arrested cells (PDR1-CYC8, PDR5 $\Delta$ , PDR3 $\Delta$  background)

### 4.3 Mapping active topoisomerases

#### 4.3.1 Etoposide-trapped topo II maps to replicating regions during S phase

We first decided to compare the association and the activity of topo II on budding yeast chromosomes during replication. Thus, we compared the pattern obtained by ChIP-on-chip between topo II crosslinked by formaldehyde (hereby referred to as ‘association’) and by etoposide (referred to as ‘activity’) during an HU arrest. We used the R package *Ringo* (Toedling et al., 2007) to define peaks: briefly, threshold values (above which enrichment was called a “peak”) were automatically calculated using the distribution of intensities of the smoothed data

(IP/input). Minimum and maximum peak widths were set to 40 bp and 600 bp, respectively.

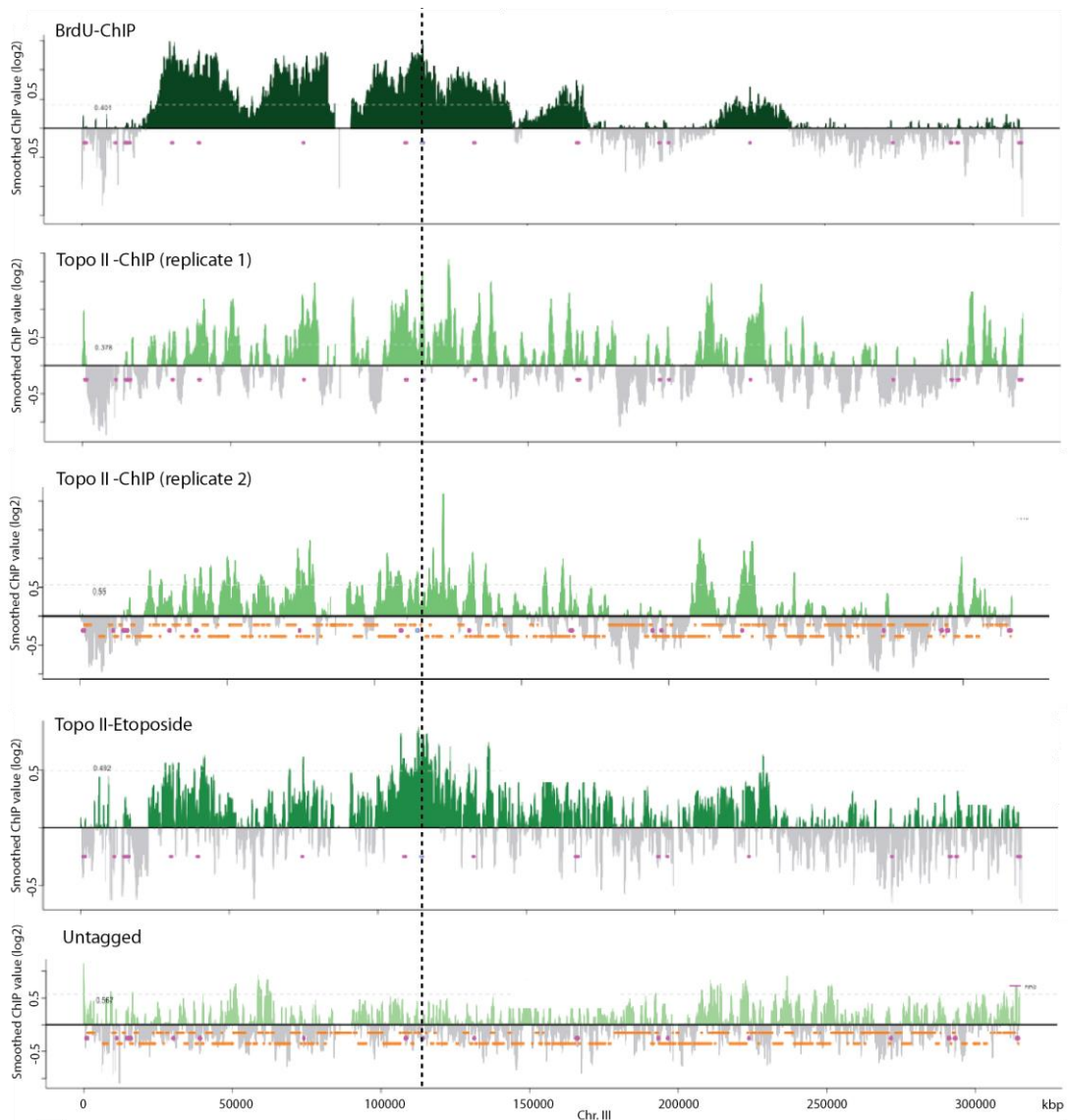


**Figure 4-3. Association and activity of topo II during S phase along Chr. III.**

Cells were released from a G1 arrest into 0.1 M HU. BrdU incorporation is shown to give an indication of replication progression at the time of sample collection. To map topo II's association with chromatin, cells were collected 90 min after G1 release and fixed with formaldehyde (second panel). The third panel shows a biological replicate of the topo II ChIP map. To analyse activity, etoposide was added to the cells 30 min into the HU arrest (final 500  $\mu\text{g}/\text{ml}$  etoposide) and cells were collected 60 min later; no formaldehyde was added (third panel). Bottom panel shows the unspecific detection of topo II using an untagged version of this enzyme (negative control). The enrichment of DNA in the IP fraction compared to a whole genome DNA sample along Chr. III is shown; centromere is marked with the dashed line, ARS with pink dots and coding DNA sequence (CDS) with orange lines.

We performed two independent repeats for each experiment. Duplicates had 92% overlapping peaks (not shown), indicating that there was a high degree of correlation between biological replicates. Overall, we detected 1556 peaks in the topo II-ChIP sample and 500 in the topo II-Etoposide sample.

While we found topo II broadly associated with replicating regions (Fig. 4-3 and in agreement with Bermejo et al., 2007), there is a clearer correlation between replication and topo II activity, etoposide-trapped topo II enrichment noticeably matching that of BrdU (Figure 4-3). This could reflect the role of topo II in dealing with replication-induced topological stress, perhaps both in relaxing the supercoils ahead of the fork, as well as the precatenanes in its wake. Moreover, we can also detect accumulation of active topo II around the centromeric region, which is not a distinctive feature in the case of formaldehyde-crosslinked topo II.

There was a high degree of correlation between genome-wide topo II-ChIP and topo II-Etoposide enrichments (Figure 4-4c & d). However, most of the overlap came from replicating regions, and there was little discernible overlap outside these regions. This is in agreement with analogous experiments that compared bacterial topo IV association and activity: topo IV cleavage sites, identified by norfloxacin treatment reportedly differed from topo IV-ChIP peaks (El Sayyed et al., 2016). These authors hypothesised that a number of topo IV-binding sites act as a reservoir, of which only a subset are activated. Nevertheless, further optimization of our topo II-Etoposide ChIP is probably required, as the relative enrichment over the input DNA was usually of lower intensity compared to topo II ChIP following formaldehyde crosslinking.

In addition to replicating regions, we found that topo II associated with centromeres, but the relative enrichment around the 16 budding yeast centromeres was only observed following etoposide treatment (Figure 4-3). *S. cerevisiae* centromeres are early-replicating loci; however, this fact alone cannot account for the accumulation of etoposide-trapped topo II, as other early-replicating regions do not see such pronounced accumulation. Other factors, including endogenous regulatory pathways that affect topo II activity (Bachant et al., 2002), unique topological characteristics of centromeres (Diaz-Ingelmo et al., 2015; Furuyama & Henikoff, 2009) and/or microtubule-generated forces (Farcas et al., 2011) might contribute to the specific localization of active topo II.

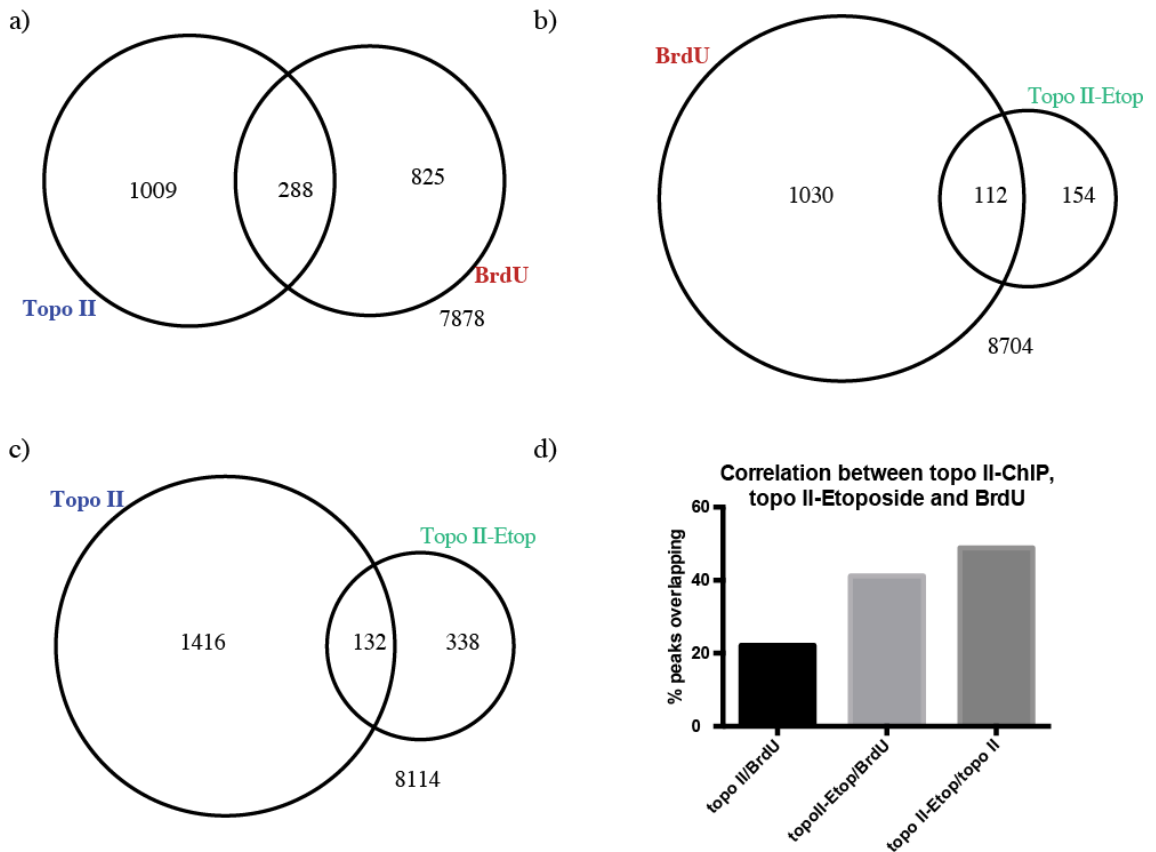


**Figure 4-4. Analysis of genome-wide topo II peaks**

a) Overlap between topo II-ChIP (association) and BrdU enrichment b) Overlap between topo II-Etoposide (activity) and BrdU peaks. c) Overlap between topo II-ChIP and topo II-Etoposide. d) Graph representation the correlations in a, b and c.

### 4.3.2 Ectopic topo II associates with replicating regions during S phase

To examine whether the pattern of topo II activity was dictated by endogenous regulatory pathways or simply by topological stress accumulation, we decided to do a similar analysis of *Paramecium bursaria chlorella virus* topo II (CV topo II; see section 5.1, Fig. 4-5) expressed in budding yeast, and presumably not subject to putative endogenous yeast topo II regulation.

Analogously to endogenous topo II, the association of CV topo II with chromatin correlates with DNA replication. Remarkably, the location of both topoisomerases is very similar, both at replicating and non-replicating regions. We do not know the precise reason that brings these topoisomerases to the latter regions; further analyses and experiments will investigate a potential correlation with transcription.

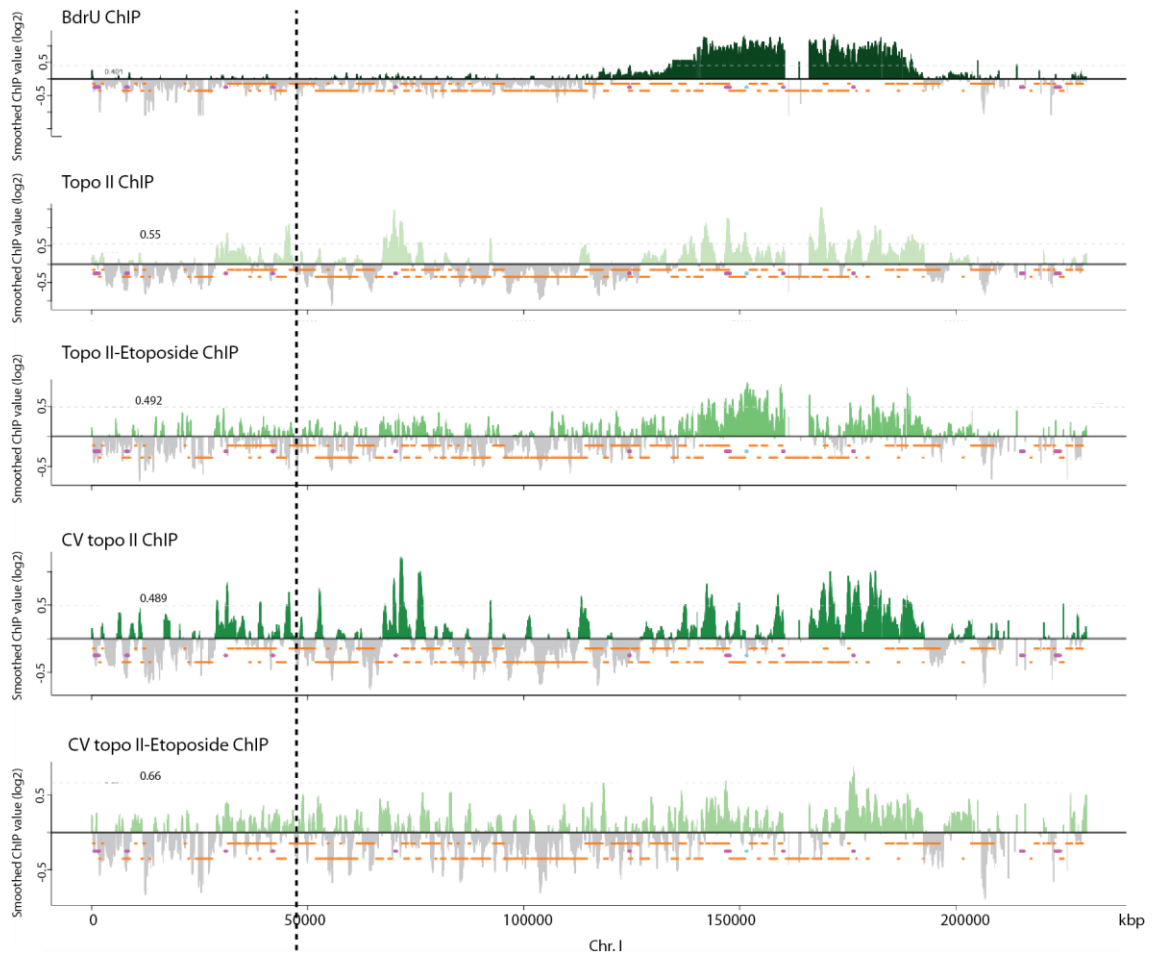


**Figure 4-5. Comparison between endogenous and ectopic topo II association and activity along budding yeast Chr. I during replication.**

Topo II association correlates with replicating regions, and also shows some additional peaks that do not overlap with topo II activity. The bottom two panels show the association and activity of the ectopic CV topo II, respectively, expressed in budding yeast after release from G1 into HU. Centromere CEN1 is marked with the dashed line, ARS with pink dots and CDS with orange lines.

The fact that the patterns of association and activity are extremely similar between the two enzymes (Figure 4-6) suggests that in most instances, it is probably topological stress (e.g. DNA crossovers) that brings topoisomerases to a given chromatin site, rather than putative regulatory factors, which would probably only affect endogenous topo II localization. The CV topo II map is slightly noisier; perhaps reflecting the fact the enzyme is overexpressed. The striking and consistent difference between the activities of the two topoisomerases lies around the centromeric regions; though both are associated with this locus, only endogenous topo II is enriched with respect to the rest of the genome (Figure 4-6c).

This opens the possibility that there is an endogenous regulatory mechanism that targets endogenous topo II to centromeres and to which CV topo II is insensitive. A potential candidate is sumoylation, which has been reported to target topo II to centromeres in mammalian (Mao et al., 2000; Yoshida et al., 2016) and yeast systems (Takahashi et al., 2006; Edgerton et al., 2016).

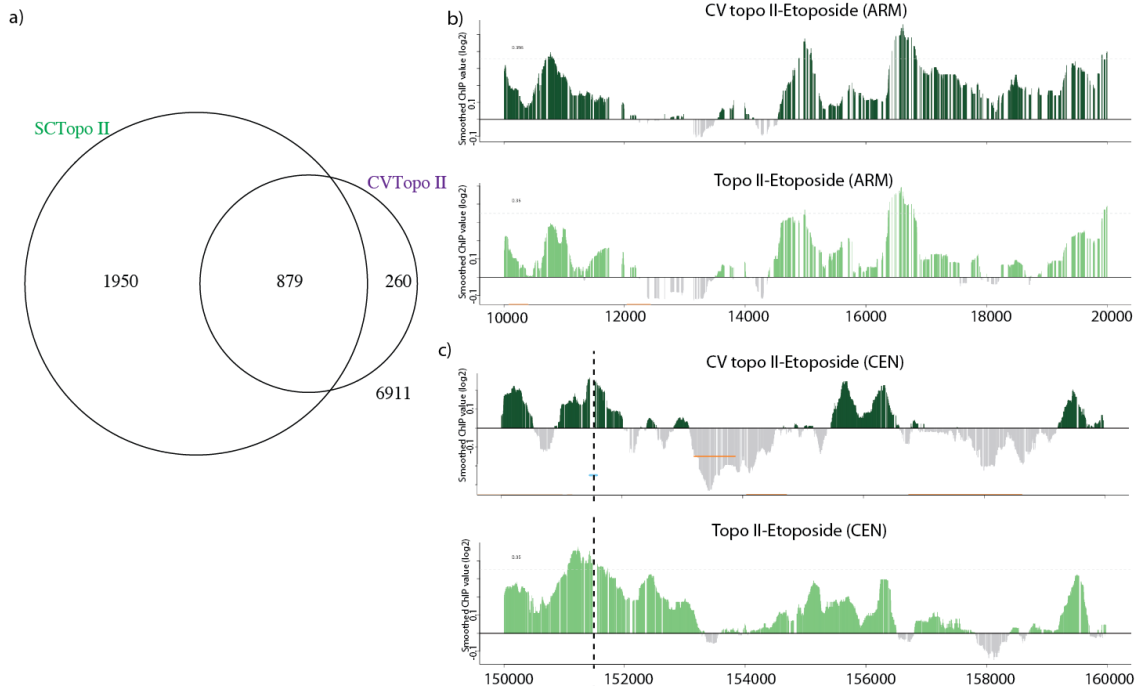


**Figure 4-6. Correlation between ectopic and endogenous topo II**

a) Peak overlap between the association of SC and CV topo II. b,c) Close-up of etoposide-trapped topo II ChIP enrichment on b) chromosome I arm and c) centromeric regions. Centromere (CEN1) is marked with the dashed line, ARS with pink dots and CDS with orange lines.

### **4.3.3 Topo I activity maps to narrow regions around early-firing origins during S phase**

We also compared the association and activity of topo I during replication, to distinguish between torsional stress coming from supercoiling and catenation, since topo I can only resolve the former. Topo I activity can be mapped by trapping the fraction of topo I molecules engaged in their topology-remodelling reaction using the drug camptothecin, which acts in an analogous manner to etoposide for topo II.

We see topo I mainly associated with replicating regions, in agreement with previous results (Bermejo et al., 2007), and with a high degree of correlation with

topo II association (41%, 754/1848 peaks overlapped with topo II peaks). Active topo I was also mostly found in chromatin regions undergoing replication. However, camptothecin trapped topo I in narrow regions surrounding early firing origins, whereas formaldehyde crosslinked topo I along broad areas of replication (Figure 4-7).

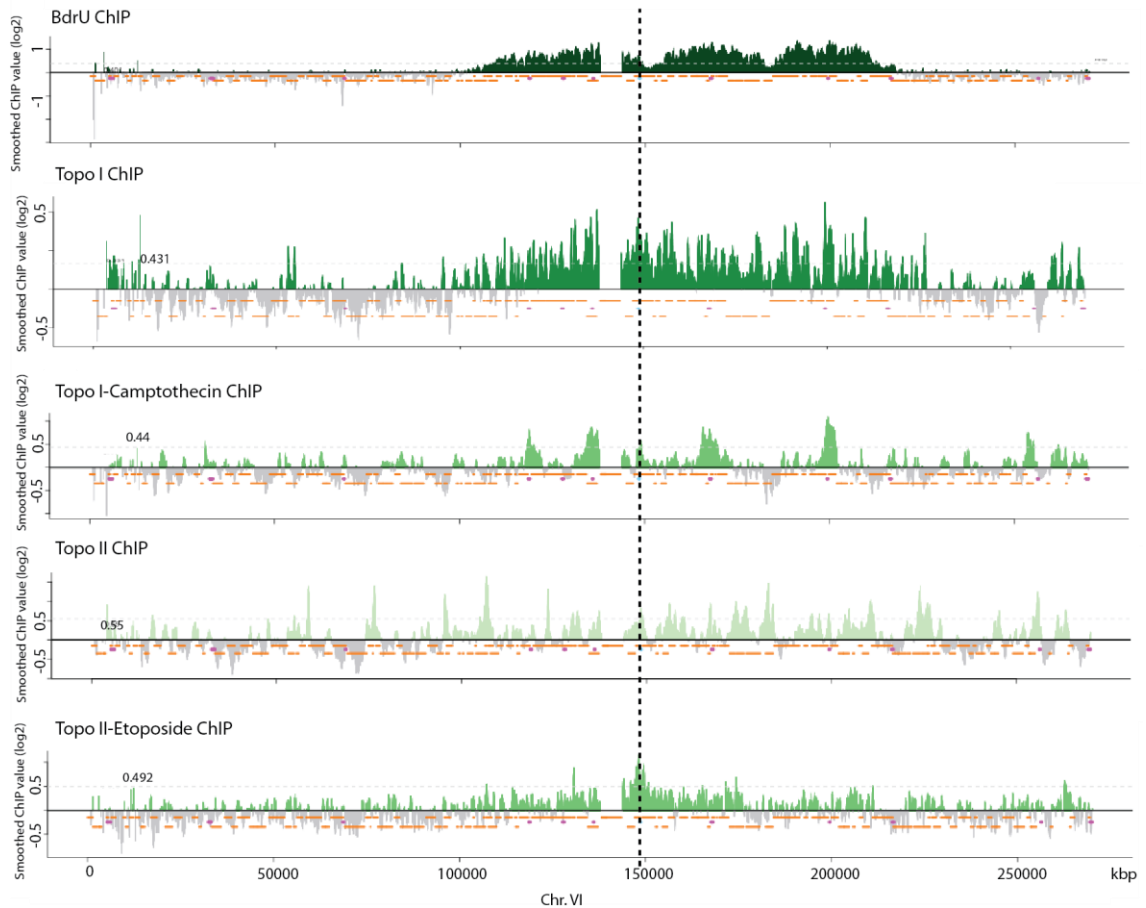


**Figure 4-7. Comparison between association and activities of topo I and topo II during DNA replication.**

Cells were released from a G1 arrest into 0.1 M HU. BrdU incorporation is shown to give an indication of replication progression at the time of sample collection. Topo I association (formaldehyde-crosslinked) and activity (crosslinked with 100  $\mu\text{g}/\text{ml}$  camptothecin) along Chr. VI are shown. For comparison, the two bottom panels show topo II-ChIP and topo II-Etoposide enrichment along the same chromosome. Centromere is marked with dashed line; ARS with pink dots and CDS with orange lines.

Etoposide trapping of topo II occurred along broad areas too. We do not know the reason behind the difference in the activity patterns of topo I and topo II. It could point to a contribution of topo I during replication initiation, for example, as the replication bubble unwinds, but less so during elongation. However, we cannot

discard potential dissimilarities in topoisomerase poison efficiencies and/or timings. Overall, these results are in line with the idea that topo I, like topo II, is required for the removal of DNA replication-induced topological stress.

#### **4.3.4 Topoisomerase association and activity are reduced during G2/M**

Finally we assessed the distribution of topoisomerase activity in G2/M by means of a nocodazole arrest. At this stage of the cell cycle, most of the replication-induced torsional stress has been removed, except for a small population of catenanes (See Chapter 3; Charbin et al., 2014; Farcas et al., 2011). Thus, comparing the activities of topoisomerases between S-phase and G2/M could indicate how the remaining catenanes are distributed along chromosomes, and what other topological challenges arise after DNA replication.

We assessed the pattern of topo II activity during G2/M (Figure 4-8) and noticed two major differences from that during S phase. Firstly, the number of peaks detected was vastly reduced, as was the height of these peaks (Nocodazole/HU: 589/1556 for topo II-ChIP and 308/500 for topo II-Etoposide ChIP). The reduction in topoisomerase enrichment could be explained by the fact that in this stage of the cell cycle there is less single-stranded DNA, that would facilitate protein binding and/or crosslinking and subsequent immunoprecipitation. This possibility needs to be further assessed.

Topo II activity appeared less well defined and more spread out along chromosomes. Its accumulation at centromeric regions was still detectable, albeit less pronounced, possibly due to the absence of spindle microtubules during the nocodazole arrest. Nevertheless, further analysis is required to compare the genome-wide patterns more in detail. A similar effect was seen for topo I activity. The number and height of topo I-camptothecin peaks was reduced (Nocodazole/HU: 995/1848 for topo I-ChIP and 329/ 695 for topo I-Camptothecin), and no longer matched the early replicating regions detected in HU. The presence of peaks at this stage of the cell cycle might correlate with actively transcribed regions, a hypothesis that we will test in our future experiments. A comparable reduction in enrichment was also observed between active CV topo II in S and G2/M phases (Nocodazole/HU: 474/1338 for CV topo II-ChIP and 439/637 for CV topo II-Etoposide).

Put together, these results make two suggestions. Firstly, it seems that in G2/M there may be a less substantial topological stress burden on chromosomes than during replication. Secondly, the lack of defined peaks after from DNA replication suggests that replication-dependent torsional stress (that forms supercoils and catenanes) may not be necessarily maintained in the chromosomal region where it originated, but perhaps is able to distribute along chromatin.

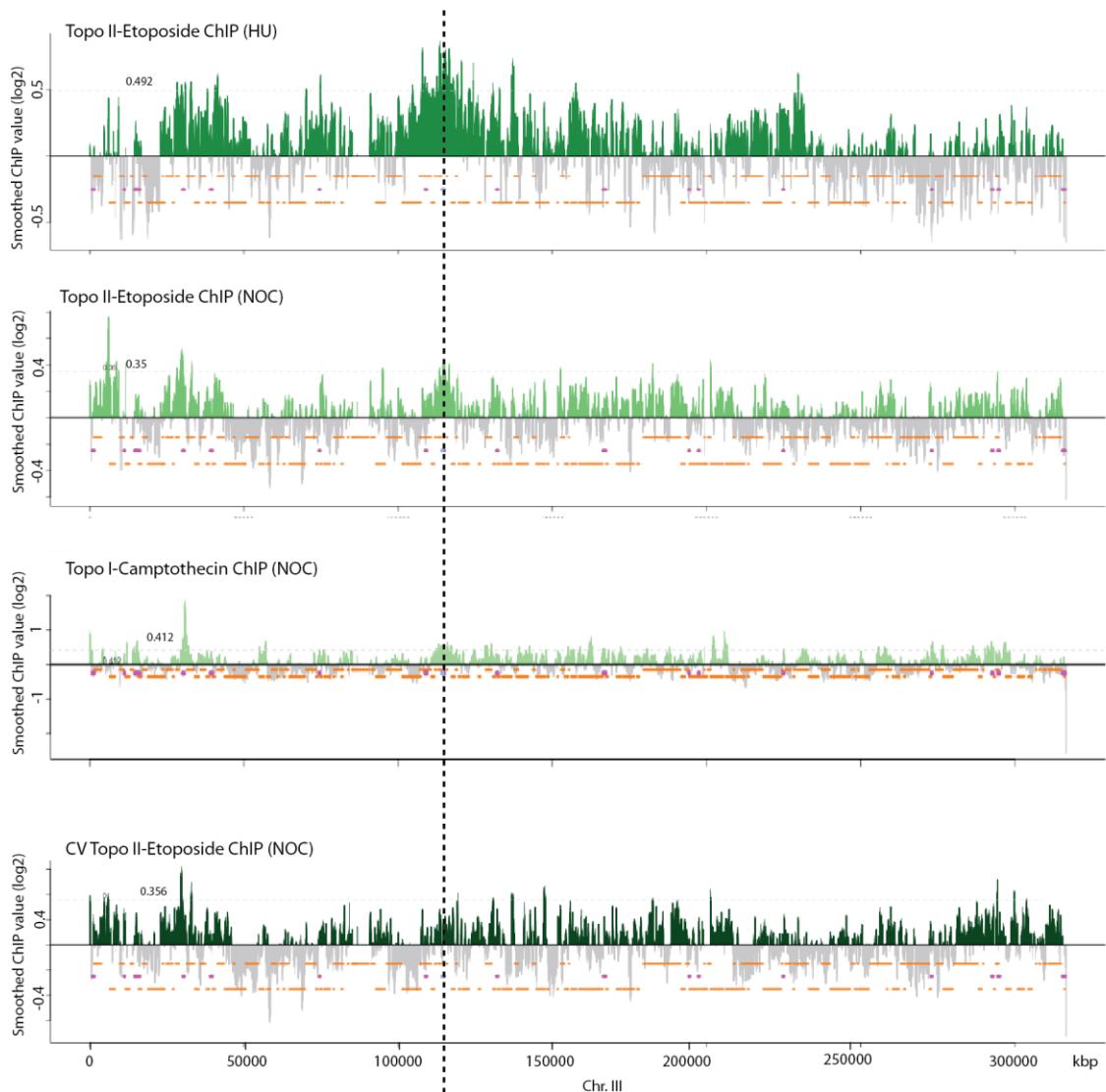


**Figure 4-8. Topoisomerase activities along Chr. III during nocodazole arrest.**

Cells were arrested in G2/M upon addition of nocodazole. Etoposide or camptothecin was added 1.5 h into the arrest, and samples were collected 60 min after drug addition. Top panel shows topo II activity during an S-phase arrest, for comparison. Centromere CEN1 is marked with dashed line, ARS with pink dots and CDS with orange lines. NOC: nocodazole.

In summary, we report in this chapter the application of a method to trap and detect active topoisomerases along budding yeast chromosomes. Similar strategies employing topoisomerase poisons have been used to compare the association and activity of topo I in human cells (Baranello et al., 2016) and topo IV in *E. coli* (El Sayyed et al., 2016), but had been inaccessible for analysis of budding yeast topo II, because the PDR gene network limited the intramolecular accumulation of etoposide. Our mutant strain (PDR1-CYC8,  $\Delta$ PDR5,  $\Delta$ PDR3) allows the analysis of etoposide-trapped type II topoisomerases for the first time.

While these results are preliminary and require further validation and analysis, they are in line with a number of observations. First, topo II and topo I are both implicated in dealing with DNA replication-induced topological stress (Bermejo et al., 2007; Figures 4-3 and 4.7). Topo II-Etoposide mapped to broad replicating regions, whereas topo I-Camptothecin was enriched in narrow regions around active replication origins, perhaps reflecting differential requirements for these topoisomerases during the different stages of replication. Secondly, the correlation between the enrichment of topo II and CV topo II (which is refractory to putative regulatory pathways that control endogenous topo II), suggests that it is probably topological stress that brings topo II to its sites of action. The observed centromeric accumulation of topo II, which was only noticeable after etoposide treatment, opens the possibility that modulation of this enzyme (e.g. sumoylation) rather than a topological property of this locus, targets topo II to the centromeres, as this early-replicating locus did not present such pronounced topo I or CV topo II enrichments. Finally, there seems to be a smaller topological burden during G2/M than in S phase, suggested by the reduction in association and activity of all three topoisomerases analysed.

## **Chapter 5**

### **Catenation and Sister Chromatid Cohesion**

## **Chapter 5. Catenation and sister chromatid cohesion**

The results from the previous two chapters suggest that chromosomal catenation persists into G2/M. This is consistent with previous observations in minichromosomes indicating that, while most catenanes are removed soon after their formation, a small population of catenanes is retained until chromosome segregation (Charbin et al., 2014; Farcas et al., 2011). Why are these catenanes resolved so late in the cell cycle, given their potential disruptive effect on chromosome segregation? One possibility is that they contribute towards sister chromatid cohesion, and that topo II is regulated to act on these specifically at the time of segregation.

### **5.1 *Paramecium Bursaria Chlorella Virus* topo II: an unregulated topo II**

To test this hypothesis, we turned to a topo II enzyme that is not subject to putative budding yeast regulatory pathways, namely *PBCV* topo II (CV topo II; D'Ambrosio et al., 2008a). CV topo II is one of the smallest topo II enzymes characterized up to date, and it lacks the regulatory C-terminal domain (CTD) of eukaryotic topoisomerases (Lavrukhin et al., 2000). We postulated that CV topo II, when introduced in budding yeast cells, would be efficient in removing those catenanes that endogenous topo II might be inhibited to resolve.

### **5.2 Sister chromatid cohesion**

A relatively simple assay to assess sister chromatid cohesion is provided by the tetO array/tetR-GFP system. An array of tet operators (tetO) is introduced at a chromosomal locus (e.g. the *URA3* locus, on the right arm of Chr. V, 35 kb away from the centromere), and can be visualized by expressing a fluorescent fusion of the tet repressor, tetR-GFP. When sister chromatid cohesion is intact, only a single GFP dot is visible; conversely, if it is compromised, two dots are detectable (Figure 5-1a).

We measured the percentage of *URA3/GFP* separation in cells overexpressing CV topo II during a G2/M arrest (nocodazole; Figure 5-1b), and noticed that 3 h after the induction of this topoisomerase, around 25% of the cells exhibited discernible sister chromatid separation. Moreover, the increase of *URA3/GFP* separation correlated with the levels of CV topo II (i.e. the higher the expression level, the higher the proportion of cells with separated GFP dots; not shown). In contrast, only 5% of the cells overexpressing endogenous topo II presented two separated *URA3/GFP* dots, similar to wildtype levels. This suggests that catenanes might contribute to sister chromatid cohesion, or at least to sister chromatid proximity.

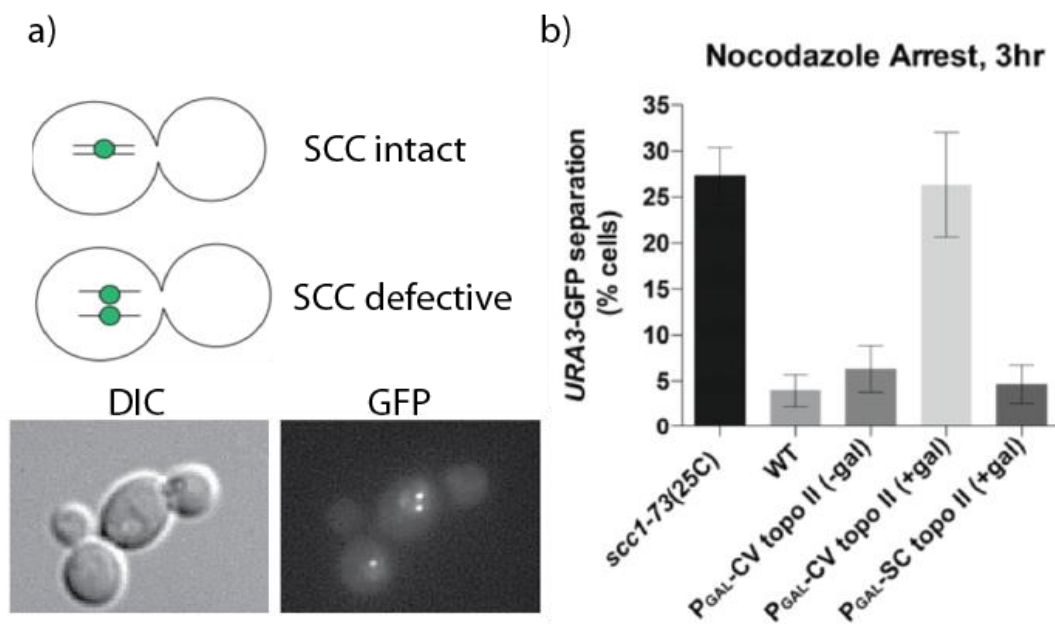


**Figure 5-1. Sister chromatid cohesion assay in the presence of an ectopic topo II**

a) Scheme of the assay (top): the tagged *URA3* locus is visible as a single GFP dot when sister chromatid cohesion is intact, but as two dots when the two sister chromatids are separated. Micrographs of the assay showing the two possible SCC scenarios (bottom; from Xu et al., 2007). b) Quantification of cells with separated GFP dots. Overexpression of CV topo II causes premature sister chromatid separation in >25% cells, similarly to the *scc1-73* allele, reported to experience cohesion defects even at permissive temperature. Conversely, only 5% of cells overexpressing endogenous topo II experience sister chromatid separation, close to levels observed in wildtype cells. SCC: sister chromatid cohesion; CV: *Paramecium Bursaria Chlorella virus 1*; SC: *Saccharomyces cerevisiae*; gal: galactose.

### 5.3 DNA damage in the presence of CV-topo II

Overexpression of CV topo II leads to low levels of Rad53 phosphorylation, indicative of DNA damage (Figure 5-2a). This could reflect the fact that CV topo II has a higher cleavage activity than budding yeast topo II (Fortune et al., 2001), and that the higher levels of cleavage complexes are more likely to be collided into by DNA tracking enzymes, ultimately resulting in permanent DSB, which are detected by DNA damage signalling pathways. Alternatively, it could indicate that CV topo II is triggering DSB formation, which could in turn disturb cohesin's topological embrace of DNA and thereby affect sister chromatid cohesion.

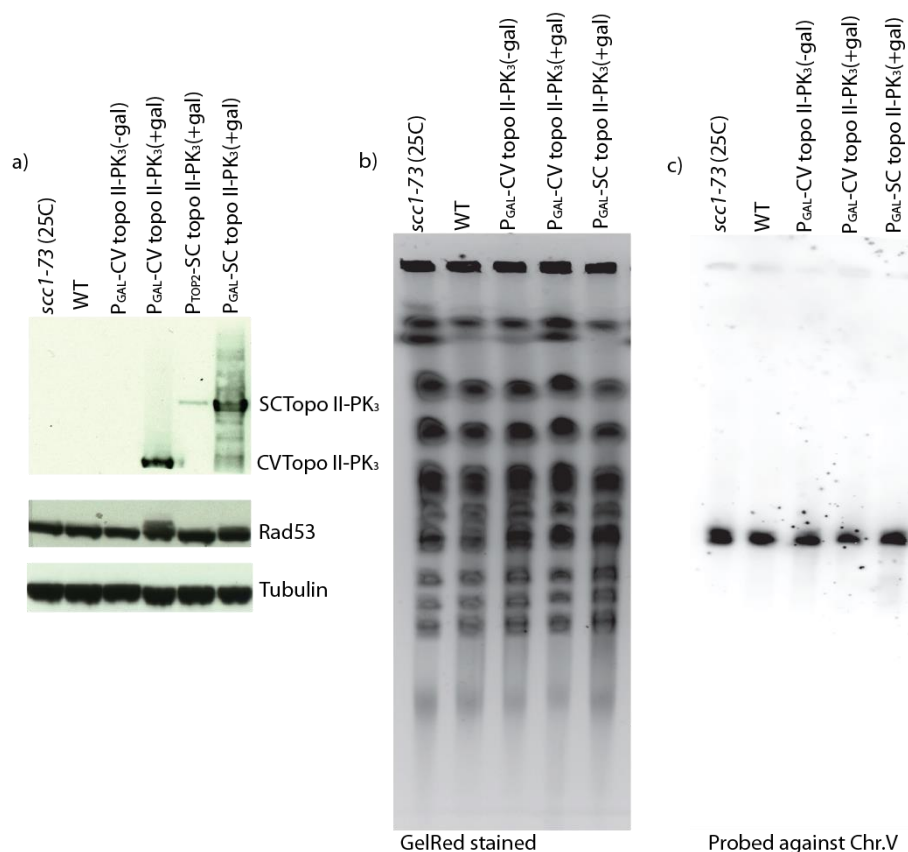


**Figure 5-2. Effect of CV topo II overexpression on genome integrity.**

a) Overexpression of CV topo II results in mild Rad53 phosphorylation. b) Chromosome integrity, observed by PFGE and GelRed<sup>TM</sup> staining, is unaffected in cells expressing CV topo II. c) Chr. V, which contains the tetO array is not detectably broken upon overexpression of CV topo II.

To distinguish between these two possibilities, we checked chromosome integrity using PFGE (Figure 5-2b). This assay showed that chromosomes were not

detectably broken by CV topo II: further analysis by Southern blotting showed that Chr. V (where the tetO array is integrated) was indistinguishable between wildtype and CV topo II-expressing cells (Figure 5-2c). This indicates that the decreased sister chromatid proximity observed in the *URA3/GFP* assay is not a result of DNA damage caused by CV topo II overexpression.

#### **5.4 Overexpression of CV topo II reduces the levels of catenated reporter plasmid in G2/M**

We further investigated whether the effect of CV topo II expression on sister chromatid cohesion is a consequence of extensive decatenation. For this purpose, we used the reporter plasmid 'prs-rDNA' (see Section 2.1.1), a centromeric minichromosome containing one 9.1 kb rDNA repeat. We arrested cells in G2/M by addition of nocodazole and overexpressed CV topo II, collecting samples at 0, 1.5 h and 3 h after the induction of the ectopic topoisomerase. As a control, we sampled wildtype cells 3 h after addition of galactose. Topological analysis of the minichromosome samples revealed that induction of CV topo II had removed substantially more catenanes than endogenous SC topo II during the arrest (Figure 5-3). This suggests that an ectopic topo II can remove catenanes that are not removed by its endogenous counterpart, which opens the possibility that endogenous topo II is in some way prevented from removing this population of catenanes in G2/M. Why endogenous topo II is unable to decatenate these intertwinings is unclear, but is in agreement with previous studies (Charbin et al., 2014; Farcas et al., 2011). Our results are in line with the hypothesis that the remaining catenanes in G2/M contribute to SCC, and thereby their removal by CV topo II leads to higher levels of sister chromatid separation. Moreover, the linear topoisomer does not markedly increase in the presence of CV topo II, again indicating that the viral topoisomerase does not cause more DSBs than its endogenous counterpart *in vivo*.

Put together, the results of this chapter indicate that post-replicative catenanes might contribute to SCC. Three lines of evidence point to this hypothesis. First, the penetrance of the phenotype of cohesin mutants is locus-specific (Figure 1-8; Antoniaci & Skibbens, 2006; Ciosk et al., 2000; Diaz-Martinez et al., 2008;

Guacci et al., 1997; Michaelis et al., 1997; Sullivan et al., 2004; Toth et al., 1999), so cohesin alone probably cannot explain genome-wide SCC. Secondly, catenanes persist into G2/M in minichromosomes (Farcas et al., 2011; Charbin et al., 2014) and authentic chromosomes (Espeli et al., 2003; Chapter 3). Finally, we have shown that expression of ectopic CV topo II removes most of the remaining G2/M catenanes in minichromosome DNA (Figure 5-3) and leads to increased *URA3/GFP* separation in nocodazole-arrested cells (Figure 5-1).

We note that CV topo II has higher cleavage levels than other type II topoisomerases. Thus, it would be important to repeat this assay in the presence of another enzyme, for example *E. coli* topo IV, to rule out the possibility that the sister chromatid separation phenotype results from DNA cleavage rather than decatenation.

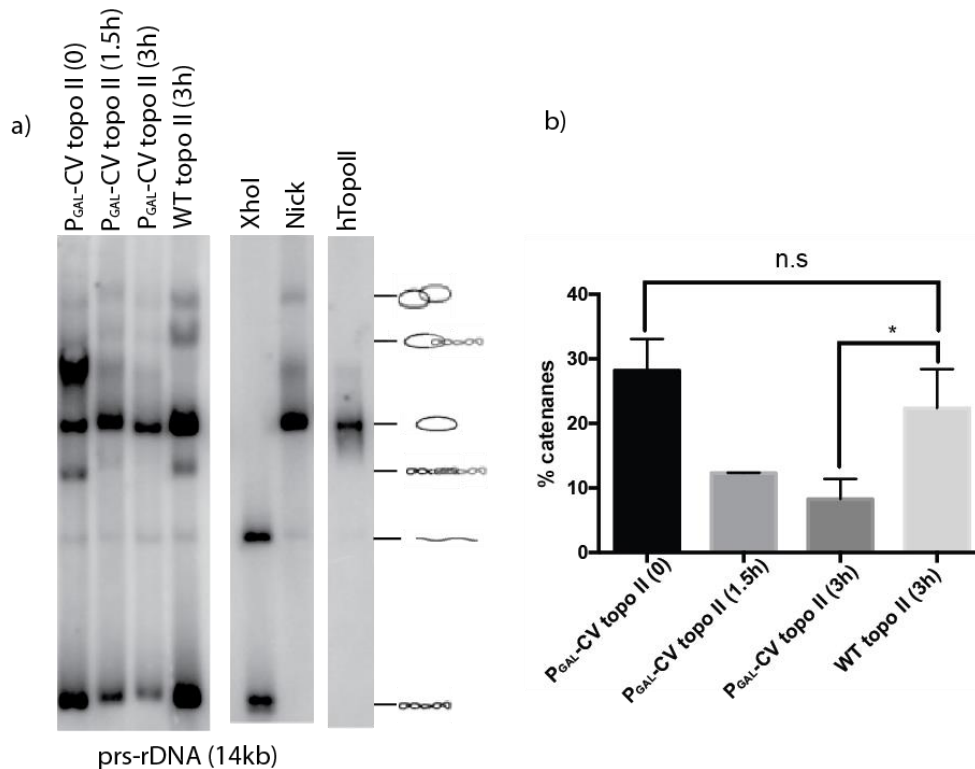


**Figure 5-3. CV topo II expression reduces minichromosome catenation in G2/M**

a) Southern blot comparing the topologies of prs-rDNA in cells the presence of ectopic CV topo II (0, 1.5 and 3 h after CV topo II induction) and wildtype cells during a G2/M arrest. b) Quantification of the catenated species. hTopo II: human topo II $\alpha$ .

## **Chapter 6**

### **Discussion**

## Chapter 6. Discussion

This project was aimed at understanding a number of aspects of chromosomal DNA topology, in particular DNA catenation. We first devised a system to study the local topologies of linear chromosomes, and used it to investigate the formation and distribution of catenanes. We then took a more protein-centric approach, and attempted to examine where active topoisomerases accumulate on chromosomes. Finally, we addressed the question of whether DNA catenation contributes towards the establishment and/or maintenance of sister chromatid cohesion. The following section will discuss the findings of this work and their significance, as well as future directions.

### 6.1 Local topologies of budding yeast chromosomes

Topological analyses have largely been performed using minichromosomes or plasmids to study the origins of chromosomal catenation and the factors that contribute to its dissolution. Using a similar initial approach, we explored how a number of chromosomal elements, including additional replication origins and the RFB sequence, might affect formation, maintenance and dissolution of intertwinings on such circular minichromosomes (not shown). We found that additional replication origins and the RFB sequence had no noticeable effects on DNA catenation. Our experiments were challenged by the technical limitations of minichromosomes, and we therefore do not discuss them in this thesis. Moreover, it still remains unclear how accurately these ectopic circular DNAs represent the behaviour and topology of endogenous chromosomes.

At the same time, investigating the topology of endogenous chromosomes is technically very challenging, which probably accounts for the very low number of published studies on the topic. Catenation along native chromosomes had been previously looked at using genome-wide analysis of budding yeast chromosome breakage by PFGE (Spell and Holm, 1994), which attributed breakage sites to intertwinings that failed to be decatenated at mitosis in a *top2-4* temperature sensitive background at restrictive temperature. This study identified very few breaks, mostly in large chromosomes. However, the relationship between

catenation and breakage is not certain. It is hardly imaginable that small chromosomes would not experience catenation events during the cell cycle when much smaller plasmid substrates exhibit a proportion of molecules catenated until G2/M even in the presence of topo II activity (Charbin et al., 2014). Moreover, the proportion of catenation events inferred from this study seems very low considering that the main cellular decatenase has been inactivated, and assuming that at least each replication termination site gives rise to intertwinings. It is therefore more likely that the sites identified in this study relate to fragile sites in the genome, rather than intertwinings between sister chromatids. DNA catenation has also been inferred from the phenotypes of topo II mutant cells, largely from anaphase bridges and lagging chromosomes (Uemura et al., 1987). The inability to directly visualize catenanes has been attributed to their transient nature (Spell & Holm, 1994; Koshland & Hartwell, 1987) and, as a consequence, little is known about their nature and distribution along chromosomes.

We used site-specific recombination to reveal unprecedented and direct information about catenation along native budding yeast chromosomes. Our loop outs reveal a pattern of topoisomers similar to that seen in minichromosome studies (Charbin et al., 2014; Farcas et al., 2011). One small difference is that the minichromosomes can be detected as three catenated species, namely open/nicked, supercoiled and mixed, whereas we only detected two species of catenated loop outs (open and supercoiled). We do not know the reason for this difference, but we suspect that the non-looped out (chromosomal) band could mask the detection of the mixed catenanes population (and possibly other topoisomers). Isolation of the loop out from the rest of the genome or removal of the unrecombined fraction (for example, by using an exonuclease) would shed some light into the source of this discrepancy.

We confirmed the identity of the different bands by determining their dependence on DNA replication and by *in vitro* enzymatic treatments. This demonstrated that post-replicative loop outs can be found as monomers as well as catenated species. Furthermore, we verified that the observed catenanes reflect the topology of chromosomes *in vivo* (as opposed to artefactually catenated monomers) by showing that catenanes are present only after DNA replication, but not in diploid cells arrested in G1 (Section 3.5.2). Nevertheless, the conformation of homologous chromosomes might differ from sister chromatids, i.e., the former may

be farther away from each other than the latter, and thus, we cannot completely rule out that the catenanes we detect may form as a result of Cre-mediated recombination. Due to the little knowledge on chromosomal intertwinings, we could not design alternative negative controls. However, the fact that the presence of the mitotic spindle could dramatically reduce the accumulation of catenanes in a centromeric loop out (Section 3.5.3) suggests that the topoisomer pattern we detect is biologically relevant. Moreover, our analyses of catenanes throughout the cell cycle (Section 3.7) show that the timing and levels of catenane accumulation correlate with measured firing timing and efficiency of replication origins. Furthermore, the fact that the catenated species in the loop outs disappear when cells return to G1 from mitosis strongly argues for their physiological relevance. A potentially insightful experiment would be to observe the configuration of our catenated loop outs in high resolution through electron microscopy. This approach will also enable the quantification of catenanes in our loop out, which has not been technically possible with 1D gel electrophoresis. We typically observe sharp bands for the two catenated species we detect (i.e. open/nicked and supercoiled catenanes), perhaps suggesting the presence of homogeneous populations of these topoisomers with similar interlinking numbers. However, we cannot rule out the possibility that these bands contain a multitude of differently catenated molecules that cannot be further resolved through 1D gel electrophoresis. We tried to address this by using 2-dimensional gel electrophoresis, but the large size of molecules did not allow the completion of this analysis. Finally, our assay probes the topologies of chromosomal regions in a large number of cells (i.e. it is a population assay). As such, we could think of two possible scenarios to explain the accumulation of catenanes G2/M: (1) the majority of the cells present low levels of catenation or (2) a small proportion of the cell population has highly catenated loop outs. Because we employ synchronized cultures of wildtype cells (and thus we would not expect large variations in topoisomerase activity between cells), and because there can only be two looped out molecules per cell, the former option is probably more likely; however, we cannot completely discard the latter possibility.

Site-specific recombination could alter the topology of chromosomes. First, Cre shares some similarities with type IB topoisomerases, and could potentially alter the supercoiling status of a given DNA substrate. However, *in vitro* studies have shown that Cre-mediated intramolecular excision does not noticeably change

Lk (Abremski et al., 1986). Furthermore, because of the reaction mechanism of Cre, we would not expect it to remove or introduce catenation events. Importantly, the relative fraction of the catenated loop out species remains fairly constant as recombination occurs (Figure 3.8), suggesting that catenation is not an indirect result of Cre-mediated excision of a given chromosomal region. Moreover, Cre, R recombinase and  $\phi$ 31C (from a different family of site-specific recombinases) produce a similar topoisomer pattern, which may indicate that, *in vivo*, topology is not discernibly affected, apart from the obvious production of a loop out. The fact that uni- and bidirectional recombination events produce a similar topoisomer pattern suggests that bidirectional systems (i.e. Cre and R) do not produce multiple recombination events (that could lead to re-integration of excised regions or fusion of monomeric loop outs) with detectable frequency. Finally, there is a third possible recombination event, namely the unequal exchange between sister chromatids (i.e. upstream *loxP/attB* and downstream *loxP/attP* on the sister chromatid). This recombination event would yield a different pattern after restriction digest than that expected from loop outs. Because we have not observed unexpected bands after treatment with restriction enzymes (Figure 3.7), we suggest that this recombination event does not occur with detectable frequencies.

One point of concern is that the recombination kinetics, which are similar between the recombination systems used in this study, may widely differ from topoisomerase reaction kinetics. This could result in loss of topological information: if a given topological domain was extensively torsionally strained, topoisomerases could alter its topology until reaching a certain equilibrium level of supercoiling and/or intertwinings. In principle, this effect could be more deleterious on catenanes, since transcription-induced torsional stress would be similar between chromosomal DNA and loop outs, as the genes in the latter are probably being transcribed after its excision from the chromosome. Thus, the catenane levels we detect could be an underestimate of those in chromosomal DNA. Further experiments addressing loop outs combined with conditional topo II depletion will help explore these possibilities.

Our experiments indicate that catenanes are distributed throughout chromosomal loci in cells arrested in G2/M (Figure 6-1). We have studied early-replicating regions, and detected catenanes in regions containing centromeres, replication origins and replication termination sites. This finding contrasts with early

minichromosome studies that found no detectable levels of catenated species (Koshland & Hartwell, 1987), but is in agreement with more recent studies that detected catenated minichromosomes before chromosome segregation (Farcas et al., 2011; Charbin et al., 2014).

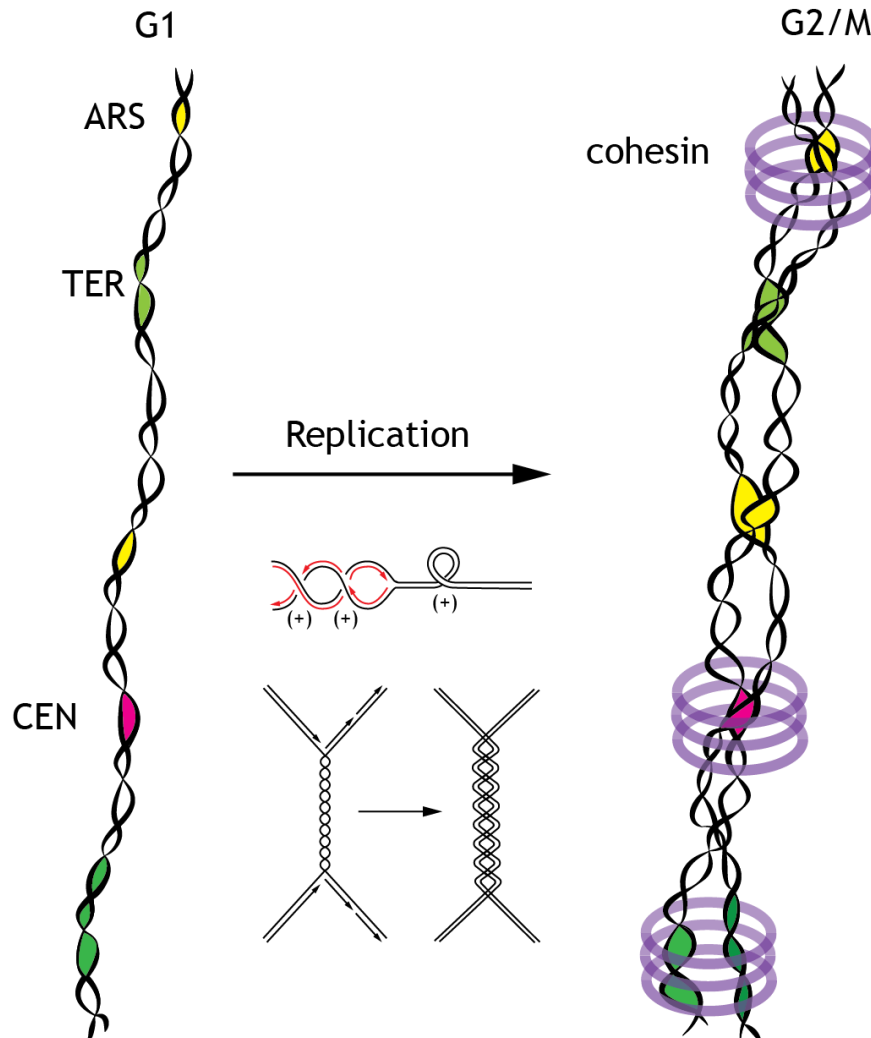


**Figure 6-1. Model for catenane formation and distribution along native budding yeast chromosomes**

Our experiments have suggested that during DNA replication, precatenanes form before termination events. Precatenanes, together with catenanes inevitably formed at replisome convergence regions are probably distributed across chromosomal regions. In G2/M a small population of catenanes is detected in replication origin, TER and centromeric regions, and is not confined to cohesin-binding sites or excluded from condensin-binding sites (not shown).

A possible explanation of this discrepancy is that the early studies used smaller minichromosomes; indeed, it seems like size positively correlates with the level of catenation of a given DNA molecule (Charbin et al., 2014). However, we

detected catenated species of our smaller loop outs (8 kb), but a similarly sized minichromosome would probably not detectably retain intertwinings. The presence of a centromere in these smaller minichromosomes (and its absence in our small loop outs) could account for this discrepancy: centromeric attachments to kinetochores and the tension exerted on them by mitotic spindles stimulate decatenation by topo II (Farcas et al., 2011; Charbin et al., 2014). Indeed, we recapitulate this effect in our centromeric loop outs, which experience a reduction in their catenated topoisomers when the mitotic spindle is present (Section 3.5.3).

### **6.1.1 SMCs and catenation**

The roles of the different SMC complexes in chromosome organization have been the focus of intensive study over the past two decades. With respect to topology, the cohesin complex has been suggested to protect catenanes from topo II-mediated disentanglement (Farcas et al., 2011). Although the molecular nature of this protection remains unclear, it has been shown that in the absence of a functional cohesin complex or when cohesion establishment factors like Eco1 or Scc2/4 are not present, the levels of centromeric minichromosomes in a G2/M arrest are reduced with respect to those found in wildtype cells (Farcas et al., 2011). We have detected catenanes in wildtype cells in chromosomal regions where cohesin is enriched during G2/M; however, regions with substantially less cohesin enrichment present no markedly different levels of catenanes. This suggests that catenanes are not restricted to regions of cohesin enrichment. It does not rule out, however, a dependence of catenanes on the presence of active cohesin complexes; future experiments will test this by looking at the topoisomer distribution of loop outs under conditions where cohesin is depleted.

In contrast, the condensin complex has been suggested to stimulate topo II-mediated decatenation. How condensin helps topo II in removing intertwinings is uncertain, with direct protein interaction and indirect modification of topo II substrate DNAs proposed as alternatives. We could not detect obvious differences in the levels of catenanes between loci with substantial condensin enrichment and loci with reduced condensin association, suggesting that intertwinings are not excluded from condensin-enriched regions. To examine the effect of condensin on chromosomal catenanes, loop outs should be carried out in the absence of

functional condensin complexes (and possibly in the presence of mitotic spindles; Baxter et al., 2011). Future experiments will also look at the relationship between DNA catenation and the Smc5/6 complex. Although, its proposed role in marking catenanes (Jeppsson et al., 2014) is not in agreement with our findings that catenanes are widely distributed along chromosomes.

Interestingly, two of our loop out regions did not present detectable levels of catenanes in a G2/M arrest, namely a telomere and the *HMR* locus. The vast reduction in catenanes at telomeres could be explained by free rotation of chromosome ends, which may allow the dissipation of torsional stress (since it does not behave like a topological domain where Lk is constant). The pattern of topoisomers we see in the loop out of this region, where we detect a ladder of topoisomers running from the most supercoiled to the open monomeric species, probably reflects the telomeric free end rotation. The second region that seems not to be catenated in G2/M is the mating locus, *HMR*. The *HMR* locus resembles closed heterochromatin regions, typical of higher eukaryotes: it assembles hypoacetylated histones, is refractory to a number of DNA modification enzymes, and is transcriptionally silent (Cheng et al., 2005). One explanation for the lack of intertwinings at the *HMR* locus is that topological stresses are strictly confined in this region, so that distribution of catenanes and supercoiling from and/or to the *HMR* locus is more restricted than elsewhere in the genome. Catenanes do form during replication at the *HMR* locus (visible in a G1 to G1 time-course experiment, Section 3.7.2); however, after their removal by topo II, catenanes from other regions might not be able to translocate to this region. We do not know whether this has a functional relevance for topology regulation, or whether it is just a consequence of the specific chromatin structure. Future experiments will look at the topology of this loop out in the absence of silent-chromatin establishment proteins, like Sir1p and Sir2p (Cheng et al., 2005), and compare the topoisomer pattern in the absence of chromatin silencing. However, we do need to confirm that the absence of detectable catenanes is not due to insufficient levels of recombination by R recombinase.

An important area that has not been addressed in this work is chromosome topology in the absence of topoisomerases. We made an initial attempt using the *top2-4* allele to look at the cell cycle topology of the ARS508 region. However, as it has been previously reported (Baxter & Diffley, 2008), this allele causes replication

problems during replication at restrictive temperature, as it specifically prevents the completion of termination events (observed in reporter plasmids, but also in native chromosomes). In our study, we detect a high molecular weight smear above the catenane band that probably corresponds to intertwined replication intermediates. The smear possibly reflects the heterogeneity in the size or replication completion of these molecules; their slow migration probably indicates that their structures are branched, which impedes migration through the agarose gel. Ideally, we would use an effective conditional allele that not just inactivates but also degrades topo II. We have tried a number of variations of the auxin-inducible degron tags to conditionally knock out this topoisomerase. However, in our hands, degradation did not occur to completion, and the low levels of topo II left are sufficient to maintain topological homeostasis (in agreement with previous observations, where leaky transcription leaky transcription of topo II driven by the repressed *GAL1* promoter complemented the lethality of the temperature sensitive allele *top2-4*; Caron et al., 1994). We cannot use degron systems that rely on galactose induction (as we have our recombinases under the control of  $P_{GAL1}$ ), or on high temperatures, which might affect the kinetics of recombination and topoisomerase action.

On the other hand, current experiments are focusing on the use of viral topoisomerases, like the CV topo II, in our loop out strains. Because (putative) yeast endogenous pathways are not expected to regulate viral topoisomerases, their expression in the cell could remove more topological stress than the endogenous enzymes. Our current focus lies on analysing the topology of our loop outs in the presence of CV topo II, to see if the catenane population is reduced.

Importantly, the fact that catenanes are present in G2/M raises some questions about the Rybenkov effect—the reported ability of topo II to simplify topology beyond the equilibrium distribution (Rybenkov et al., 1997). *In vivo*, topology simplification of chromosomal loop outs does not seem to occur to the levels seen of plasmid DNA *in vitro*, as reflected in the fact that catenanes are detected in our loop outs during prolonged metaphase arrests. Topo II treatment *in vitro* of G2/M loop outs (and minichromosomes; Charbin et al., 2014) does result in topology simplification. Thus, our observations point at additional mechanisms that control how much topoisomerases deal with torsional stress in the cell. Topo II is not sufficient to account for complete decatenation by chromosome segregation;

probably other molecules and/or chromosome movement (during mitosis) affect the activity of topo II in space and time.

### **6.1.2 Catenane formation during DNA replication**

Empirically, whether replication termination alone gives rise to catenation, or whether precatenanes form during elongation has not been decided. Understanding topological changes during replication has proven challenging, due to the fact that the topology of replication intermediates might be affected upon their isolation. Moreover, minichromosomes, due to their small size, are quickly replicated, and in unchallenged cells it is technically impossible to isolate replication intermediates without the introduction of artificial replication fork barriers. Thus, whether catenation arises from precatenanes generated during replication elongation or from replication termination is not easily distinguishable.

We have used our loop out system to probe budding yeast chromosomes for precatenane formation. We first analysed the topology of regions around a replication origin during elongation but before termination events. This indicated that intertwinings are present before termination events. In addition, we saw that introduction of the RFB sequence— which triggers a polar fork barrier and specifies a termination site— in our ARS loop out did not substantially increase the levels of intertwinings. Our results suggest that precatenanes do form during replication elongation, and that termination events probably do not create more intertwinings than elongating forks (Figures 3-17 & 3-18), which is in line with previous evidence in other model systems (Cebrian et al., 2015; Lucas et al., 2001; Peter et al., 1998). Precatenanes are formed when (+) supercoiling ahead of the replisome is transmitted to the region in its wake; a prediction of this model is that inhibiting topo I would result in an increase in precatenanes (as long as topo II cannot completely compensate for the lack of topo IB activity). Upcoming lines of research could look into this, by inhibiting topo I (e.g. using topo I inhibitors and/or poisons in the PDR mutant strain).

Although the fact that catenanes are detectable before termination (Section 3.8.1) clearly argues for the precatenane model, there are a couple of caveats. First, the use of hydroxyurea and its effects on replication fork progression could alter the topology of the replicon: topoisomerases oppose topological constraints

generated by the replisome, and both machineries have their own reaction/activity rates. Under our conditions (i.e. 0.1 M hydroxyurea), where replisomes have slowed down, topoisomerases could still be working at their original rates; thus, this would create an artificial situation where topoisomerases have removed more torsional stress than is normally generated. Moreover, in our conditions there may be some termination events (between forks coming from ARS507 and ARS508). These are probably too few to give rise to detectable catenanes; besides, analysis of replication progression between 60 and 90 min post release from G1-arrest—where most of the excision reaction occurs— suggests that the few termination events occur towards the 90 min time point. Nevertheless, future experiments will focus on looping out the region around ARS508 in a strain where ARS507 has been deleted ( $\Delta$ ARS507; Figure 6-2a).

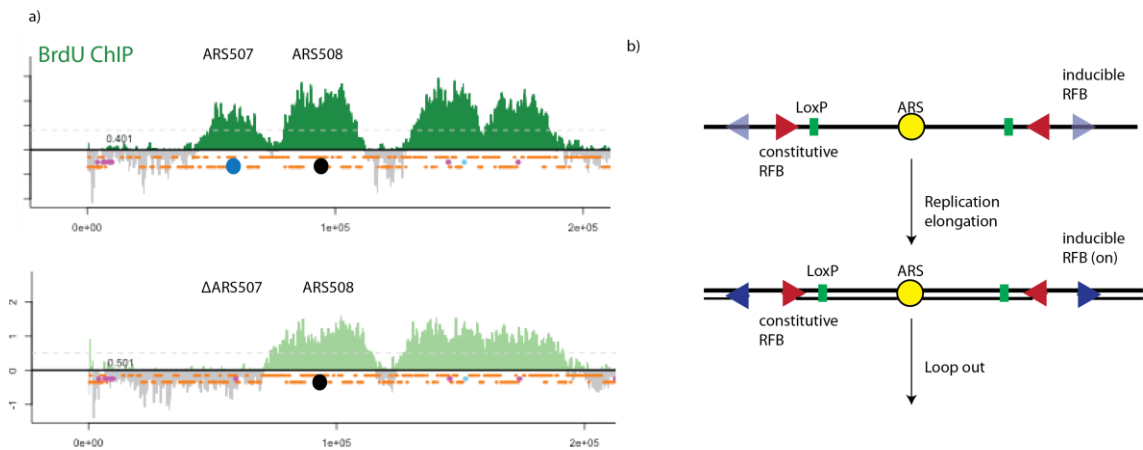


**Figure 6-2. Future experiments to study catenane formation along native chromosomes**

a) Deletion of ARS507 will provide a region completely free of termination events between the looped out ARS508 and ARS507. b) In addition, we could avoid the use of HU by constructing a system containing two constitutive RFBs (to block the outgoing forks from the ARS of interest), and inducible RFBs pausing the incoming forks from nearby replication origins.

Additionally, although it has been shown that ectopically placed RFB sequences are effective (Cebrian et al., 2014), we still need to measure the proportion of forks that stall in RFB-containing loop outs under our experimental conditions. Finally, a more conclusive experiment would be to loop out a replication origin that is farther away from neighbouring origins, if possible in the absence of HU. This would possibly require the constitutively expressed Cre-ER construct, so that recombination occurs before replication of additional origins and subsequent

termination events. Alternatively, we could make use of replication fork barriers to allow replication to progress at normal speeds, while preventing termination. For example, ARS508 could be surrounded by constitutive RFBs stopping the outgoing forks from this origin. Two inducible RFB sequences (e.g. the Tus/Ter system; Larsen et al., 2014) could be placed adjacent to the constitutive barriers, but in the opposite direction, i.e. to inducibly pause the incoming forks from ARS507 and ARS510 (Figure 6-2b).

## 6.2 Topo II activity across the genome

In eukaryotes, the division of labour between the different topoisomerase enzymes dealing with torsional stress generated during DNA transactions remains unclear. Whether topoisomerases act uniformly across the entire genome is also not completely understood, with evidence suggesting differential topoisomerase II requirements at telomeric regions (Germe et al., 2009) and mitotic centromeres, (Bachant et al., 2002; Dawlaty et al., 2008; Christensen et al., 2002). Mapping the association of these enzymes to chromatin has not particularly helped to clear these issues, as they are abundant and their association with their substrate is highly dynamic.

ChIP-based studies in higher eukaryotes have been able to specifically map the activity, rather than the association, of topoisomerases with chromatin, by trapping the cleavage complexes using topoisomerase poisons (Baranello et al., 2016; Dykhuizen et al., 2013). In yeast, similar assays have not been possible, because of the network of efflux pump/ABC transporters that interfere with the accumulation of topoisomerase poisons in the cells. In this work, we map topoisomerase activity across the budding yeast genome for the first time. We were able to do this by interfering with the PDR gene network, namely, by repressing the expression of the efflux pumps, which in turn allows the intracellular accumulation of etoposide and camptothecin. We based our strategy on a previously published construct (Stepanov et al., 2008) that targets the main PDR transcriptional regulator, in combination with two additional mutations in the PDR gene network (Section 4.1).

Chapter 4, thus, shows a new strategy to selectively target active topoisomerases in budding yeast. We generated a useful tool and optimized the

conditions of an assay that allows the previously inaccessible analysis of topoisomerases actively engaged in their topology-remodelling reactions along budding yeast chromosomes. Importantly, we show that this assay is reproducible, and although we note that further experimental work and analyses are required, our preliminary experiments provide some interesting observations.

First, we noticed potential differences between topoisomerase association and activity on chromatin. During S phase, topo II activity markedly correlates with replisome progression, underscoring the role of this topoisomerase in removing replication-induced topological stress (Section 4.3.1). Furthermore, the association and activity patterns of endogenous and ectopic topo II enzymes (i.e. *Saccharomyces cerevisiae* topo II and *Chlorella* virus topo II, respectively) highly correlate (Section 4.3.2). Although preliminary, this suggests that topological stress (supercoils and catenanes) is probably sufficient to recruit type II topoisomerases to chromatin. In contrast, at the centromeric region we mainly detect the active population of topo II. Similar observations had been made in higher eukaryotes (Porter & Farr, 2004; Rattner et al., 1996), but, again, because of the inefficacy of etoposide in yeast cells, this had not been shown in *S. cerevisiae*. Why would active topo II accumulate at this region in S phase? Perhaps it could be triggered by spindle microtubule–kinetochore attachments, which already are formed in this phase of the cell cycle. In the absence of spindles (i.e. nocodazole arrest) the accumulation is still present, but it seems less substantial (we note that this requires confirmation, e.g. through qPCR). A second possibility is that, due to the fact that the ectopic CV topo II is not as markedly enriched at this locus, there may be a regulatory basis (rather than a topological one) to account for the enhanced accumulation of endogenous topo II at centromeres. One likely scenario is that this centromeric topo II represents the sumoylated population of the enzyme (Takahashi et al., 2006). Further tests, including a G2/M arrest in the presence of mitotic spindles (i.e. depletion of Cdc20), as well as using non-sumoylatable mutants of topo II will help clarify these questions. At the last stages of mitosis, topological interlinks must be resolved to allow chromosome segregation; thus, an important future experiment will compare topo II activity in cells arrested in metaphase with cells released into anaphase.

Importantly, further experiments will focus on validating these initial results. A better time resolution during S phase could potentially help us determine

whether topo II works ahead and/or behind the fork, which would, in the latter case, provide evidence for precatenane resolution. Moreover, we will focus on replication-specific torsional stress by using transcription inhibitors (e.g. thiolutin), to remove torsional stress generated by the transcription machinery.

### **6.2.1 Organization of chromosomes**

Bacterial chromosomes are covalently closed circular molecules seemingly organized into distinct topological domains (Sinden & Pettijohn, 1981; Postow et al., 2004). Modulation of helical tension is mostly dependent on the type II topoisomerases topo IV and gyrase (Joshi et al., 2010). Eukaryotic chromosomes, however, are linear and organized into more complex chromatin fibres (Joshi et al., 2010). Whether helical tension is confined to topological domains that are demarcated by tight boundary barriers is a controversial issue (Esposito & Sinden, 1988; Freeman & Garrard, 1992; Joshi et al., 2010). Topoisomerases and DNA transactions are the main factors known to dissipate and generate, respectively, torsional stress in eukaryotic chromosomes (Salceda et al., 2006; Liu & Wang, 1987), although more extensive research to analyse the topology of these large DNA molecules will be required to determine the relative contribution of each factor towards chromosome topological homeostasis.

The notion of tight constraints holding chromosomes in budding yeast has been recently questioned. Cells lacking topo I and topo II activities and expressing the bacterial *topA*<sup>-</sup> which targets (-) sc for relaxation— present the expected reduction in transcription due to overaccumulation of (+) sc in most genes; however, transcription of genes within 100 kb from the telomere is not affected, suggesting that torsional stress is diffused through the chromosome ends, and therefore they must not be tightly held or bound (Joshi et al., 2010). Moreover, the gradual transcriptional stall (from telomeres towards internal regions of the chromosomes) indicates that helical stress dissipates slowly— as the rotation of the chromatin fibre overcomes the viscous rotational drag— and homogenously, arguing against strict barriers determining distinct topological domains (Joshi et al., 2010).

Our experiments also suggest that tight, permanent barriers separating topological domains are unlikely to be present in budding yeast. The finding that catenanes are present in most loci tested using the loop out system suggests that

intertwinings are possibly mobile and argues against strong barriers preventing their movement. Moreover, we find similar catenane densities across different chromosomal regions, indicating that their diffusion along chromosomes over time probably proceeds until reaching equilibrium. Additionally, our preliminary analysis of the topoisomer pattern of telomeric loop outs suggests that there may be some degree of rotation around chromosomal ends that allows the dissipation of torsional stress, which manifests as a ladder of differentially supercoiled monomers and the absence of catenated species. Although previous results (Joshi et al., 2010) and our data together argue against the presence of fixed, static topological domains, our detection methods cannot distinguish between the absence of barriers or the presence of dynamic barriers that allow some degree of movement and rotation. Ideally, this idea could be tested by artificially (and tightly) tethering telomeres to, for example, the nuclear membrane, and assessing the topology of the telomeric region or measuring the transcriptional effect (in *top1Δ*, *top2-4*, *topA* cells); however, such a strategy might not be technically feasible.

### 6.3 Catenation and SCC

A striking observation of this study is the fact that low levels of catenanes are present throughout most chromosomal loci tested. This is surprising because it implies that a notable amount of decatenation by topo II occurs in a short span of time (from G2/M until anaphase). The prevalence of catenanes after S-phase leads to the question of whether they have a role in chromosome organization and are actively maintained until chromosome segregation, or whether they are merely by-products of DNA replication. A parallel idea has been recently demonstrated for topo I: it is recruited to the transcriptional machinery at the time of pause release, and its activity is stimulated to remove supercoils alongside the elongating RNA polymerase (Baranello et al., 2016). In the case of topo II, it could be prevented from removing all catenanes immediately after their formation if DNA catenation contributes to maintaining SCC (Diaz-Martinez et al., 2008; Murray & Szostak, 1985). We tested this hypothesis by expressing the ectopic CV topo II that would not be modulated by putative budding yeast regulatory pathways, which indeed led to increased premature separation of sister chromatids (Section 5.2). We ascribe this effect to the ability of CV topo II to remove residual catenanes that endogenous

topo II leaves behind, rather than some impairment of chromosome integrity. However, further experiments are needed to corroborate this observation, and ensure that it is not an indirect effect, e.g. CV topo II affecting the levels and/or localization of cohesin on chromosomes, rather than catenanes.

Importantly, the fact that chromosomes are catenated in G2/M and that their intertwining might contribute towards SCC circumstantially argues against the existence of the so-called 'catenation checkpoint', at least as a sensor of intertwinings. The idea of such checkpoint came about observations that topo II inhibitors (which were originally thought not to cause DNA damage) caused cells to arrest in mitosis. The catenation checkpoint has been associated with ATM/ATR signalling (Deming et al., 2001), presents DNA damage signature features like phosphorylation of histone H2AX (Mikhailov et al., 2002) and results in a reduction in the activities of Polo-like kinase I, and Cdk1-cyclin B1 (Deming et al., 2002). Importantly, it was originally proposed that checkpoint activation was triggered upon high levels of DNA catenation. There is, however, no direct evidence suggesting that catenanes are used as signals for a pathway that results in a cell cycle arrest or delay. Indeed, it is hard to consolidate the idea of such a checkpoint with the fact that depletion of budding yeast topo II prior to DNA replication does not lead to a delay in mitotic entry, and only results in DNA damage and lagging chromosomes at mitotic exit, in manner that is dependent on the formation of the septin ring (Baxter & Diffley, 2008). Considering the observations made in this work, namely, that G2/M chromosomes are catenated, and that catenation may contribute towards complete SCC, it is unlikely that cells would sense these intertwinings to trigger a cell cycle delay.

## 6.4 Concluding remarks

We used site-specific recombination to analyse the local topology of several chromosomal regions. This enabled us to address, for the first time, questions regarding the nature of DNA intertwinings. Thus, we report here that catenanes persist along chromosomes through G2/M, both at replication origins and regions of replication termination. Moreover, their presence is not restricted to cohesin-binding sites, nor it is excluded from condensin-associated regions. Our results indicate

precatenanes form during the elongation step of DNA replication. Termination does not substantially contribute towards catenane formation, probably because catenanes form evenly during the replication process. Finally, we propose that catenanes contribute to sister chromatid cohesion, which in turn may explain why some catenanes are allowed to persist until chromosome segregation.

It has been over 60 years since the proposal of the double helix as the structure of the genetic blueprint. Since then, we have formed a “big picture” of the implications of this structure, the multitude of topological relationships that are generated during DNA transactions. We have also encountered the cellular effectors that control DNA topology, the topoisomerase family of enzymes, and have characterized their biochemical and structural properties. However, we are still far from elucidating the whole story. Indeed, their evolutionarily origin remains mysterious: why so many different topoisomerase flavours to deal with probably similar topological challenges? We need to fully understand the topologies that arise during DNA metabolism, the kind of substrates that topos have to work on in the cell (which can probably not be deciphered using *in vitro* experiments with plasmids). Studies similar to the work presented here are required to comprehend how topoisomerization is carried out in authentic eukaryotic chromosomes. Finally, future lines of research need to follow up on putative regulatory mechanisms that direct topoisomerase activity to ensure that chromosome topology is adequate for a given DNA transaction at the right time in the cell cycle.

## **Appendix**

## Chapter 7. Appendix

### 7.1 Distribution and biochemistry of topoisomerases

**Table 8. Classification of the major types of topoisomerases**

Type	Subclass	Name	Organism	ATP	Mg <sup>2+</sup>	Y-Link	Mechanism
I	IA	Topo I	B, A, P	-	+	5'	SP
		Topo III Reverse	B, A, E	-	+	5'	SP
	IB	gyrase	B, A	+	+	5'	SP
	IC	Topo I	E, V	-	-	3'	R
		Topo V	A	-	-	3'	R
II	IIA	Topo II	E,	+	+	5'	SP
		Gyrase	B, A, P	+	+	5'	SP
		Topo IV	E	+	+	5'	SP
	IIB	Topo VI	A, P	+	+	5'	SP

B: bacteria; A: Archaea; P: Plants; E; eukaryotes; SP: strand passage; R: rotation.

(Adapted from Sissi & Palumbo, 2009)

### 7.2 SMC complexes

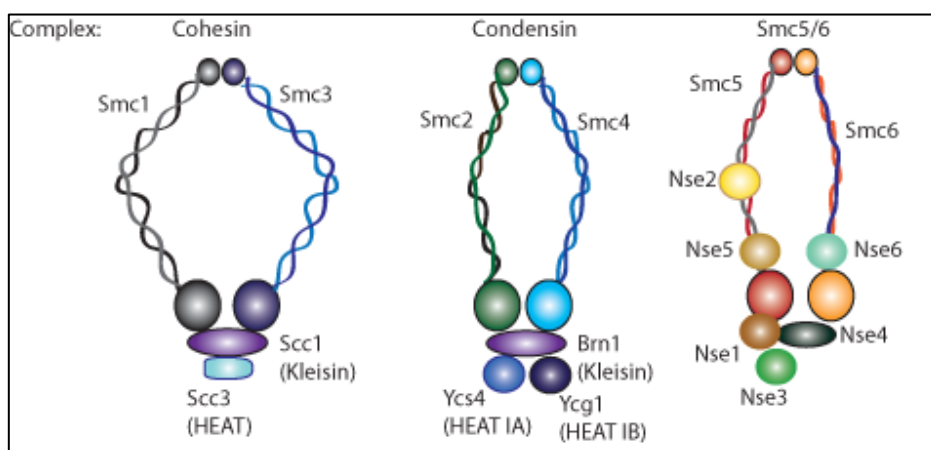


**Figure 7-1. Eukaryal SMC complexes**

Schematic representation of the three SMC complexes found in eukaryotes: cohesin (left), condensin (middle) and the SMC5/6 complex (right).

## 7.3 Construction of *loxP* /Cre loop out strains

### 7.3.1 Introduction of *loxP* sites across the genome

**Table 9. Primers for the construction of the *loxP*/Cre strains**

Locus	Upstream (FWD, REV)/ Downstream (FWD/REV)
ARS 508	Gggtaaatacgcaccaactcgcctagcaactgagtgatgaatggtttgccgttgagtcactgtcga/ ctacacgattcaaaaacgccaagatctgtagtagagacagcaagcattgccatacttctcggacat Tatatactataaaaaagttttgcttccactagtgacagcgtaatagccgttgagtcactgtcga/ aggttattcaatgaagatatgacatatatcataaccactaacaaaacagcaccatacttctcggacat
TER 501	Gatttgtcagcacatatacaacaagaagtattggttgcgttgaagaaaaaccgttgagtcactgtcga/ ctgttccctatttttttacacacggcccaaatgttattactattctccatacttctcggacat Ttcgagtcctgcagttgctgtatttttctttttcaattccctccgttgagtcactgtcga/ accatttaggaaaagtaattgttcttaccgcctcgatctgacgaaccatacttctcggacat
TER 301	Ttggatagtgattagagtgtatagcccggtaggtatcaggagcgggtaccgttgagtcactgtcga/ gaaattctacataaggccaagtttaggcttaaaactgtgggtccgctcgccatacttctcggacat Gtgaagcaccacaaaatacggaccctgcattgtcaaccaatftaacataatcgtagcattggcgatttga gaatcactgtcgaataactcgtataa/ Tcacagtacgatcgttcttgtgacggttacgaagaagccctgaaatgtccaaccaatatgcaccagaac attgttctcggacattgataactcg
TER 301b	Aaactccaccttatataacgtaagcaaagtttatgtaacaaaaaacgttgagtcactgtcga/ cagtcgaagtttacctgaaagtgaaagaaggttgattagttctttttccatacttctcggacat Gtgaagcaccacaaaatacggaccctgcattgtcaaccaatftaacataatcgtagcattggcgatttga gaatcactgtcgaataactcgtataa/ Tcacagtacgatcgttcttgtgacggttacgaagaagccctgaaatgtccaaccaatatgcaccagaac attgttctcggacattgataactcg
TER 404	Gagttcctacatttatacgaaggtaaaattgtaaaaaacatgaatgcggcccgttgagtcactgtcga/ caccacgtgatttttttaatatataggaacaatttcgagccggatagccatacttctcggacat Ggattttctatctcgtctcgtcaatatgctgcttaggattataatcttcaaggatattatctttcccactgtc gaataactcgtataa/ Gggctagctttggctgttatacgtataaccacacacctggttctgtacgaacgttgaagaaagcaagcaa ggttctcggacattgataactcg
TER	ggctttgaccttgccgtaccgatcgggaaattgtgccctgaaagattccgtt ccgttgagtcactgtcga/ tctattgacaggagcaaagcctgcccaagagggtgacagaagcgcgta ccatacttctcggacat

603	aagggccaacaacaaaaactatttcgaatagcaaggtagctccatcctgtacatgcaagaccgtcacaca gc cactgtcgaataacttcgtataa/ taccagtggaggacgaccggacatgtgagccatctggaaggatagatgcatggggttctccgatga catttctcggacattgataacttcg
TER 701	ttgggtcgtgtataatgatacatattaacaactggggagtcaaaagtgcctt ccggtgagtcactgtcga/ accaacctaattacaataacttcgaagtactatcataagtttccttatctagcg ccatacttctcggacat ccattaatcttatgttagttacattatactgtcattttagttgcagtaagtatactttttatctagctttttctg cactgtcgaataacttcgtataa/ gttcacatagcatagaattgtataatacagaaataacaatatattagagtttagtagaattctgagctttttca aaaaaaagggttctcggacattgataacttcg
TER 1004	agacctctgtcgcagttcacacaaaaatagcatatctttactattgtcccgttgagtcactgtcga / gacctagggatttcggttgctggttagctcgtttcgcaatggtagc ccatacttctcggacat Ctttgaattttgcatttccactttccactcgcaacggaatccgggtggcaaaaaagggaagcattgaaat gcaactgtcgaataacttcgtataa/ ctgtgtgactttgaagtagcaattctatcgttaattgtacaccgtctcgcaactgtttaaaatactgttaaagatt gttctcggacattgataacttcg
TER 1004b	agacctctgtcgcagttcacacaaaaatagcatatctttactattgtcccgttgagtcactgtcga / gacctagggatttcggttgctggttagctcgtttcgcaatggtagc ccatacttctcggacat Gaatataataaataaaatattgtgtgtgtgtagttctaaagaaaaatttacagtgaaaaggtaacaccg gggagcactgtcgaataacttcgtataa/ attgggactcaatgggtctgctcaggcatttgcgtctcggaatcagttatacagaatacgttaagtctacgtaat ga ttctcggacattgataacttcg

Primers for the construction of loop out strains (*loxP/Cre* system); primers were ordered from Sigma Aldrich, 0.05  $\mu$ M HPLC purified. For each strain, the primer pair for introducing the *loxP* upstream is shown in grey, and for the downstream *loxP* in black.

### 7.3.2 Checking the *loxP* strains

**Table 10. Primers for genotyping and sequencing of the *loxP/Cre* strains**

	Upstream sequencing	Downstream Sequencing
ARS508	gcaacgttcagcgatact cgggctcatctggttagtt	taccaccaacgatgcttctg ctgagaaaagcatgcgaaat
TER501	ctggcatgattgtcagcac aacctcccctaggtcacia	tgacctatgtgggaaacaga gaaatctgcgcactctgtca

TER301	ggaaagtcagcaatcctt atgtggacacttgcttac	ggcagtgataaacttttg ttggtgtaactgagcg
TER 301b	tccggtcattccacggtaat cttcctgttgactgctt	ggcagtgataaacttttg ttggtgtaactgagcg
TER404	cacatattactgataaggatggac acattgcatcttatcaacttatt	cttcttaccggcgaagt aacaccacctcctgaaaga
TER603	ggtccaggaacccatag cacatgtgattatagttctctcc	gtctcgctcgaaggcaa gttcggtctgataaggtagc
TER 701	ccaaggattgagcagctt ttgcgctcgattgac	ggcaatgaccacatggaataaa gaagtggcctaggtcac
TER1004	cagtaaagacagctgggaa ctatctgtgttctgttctcc	caaacgattgatgtccacttg caagctctcaacaccgatc
TER1004b	cagtaaagacagctgggaa ctatctgtgttctgttctcc	tgggattgagatatagtgaacctc gcgaaaatagcgatagatcgag

Primer pairs for genotyping and sequencing for each *loxP* strain are shown. Introduction of the *loxP-K.I.URA3-loxP* was checked by a genotyping PCR. Excision of the cassette (leaving a single *loxP* in the chromosome) was further confirmed by sequencing.

## 7.4 Construction of *attB/φ31C*

### 7.4.1 Introduction of *attB* and *attP* sites across the genome

**Table 11. List of primers for the construction of the *attB/φ31C* strains**

Locus	Upstream (FWD, REV)/ Downstream (FWD/REV) primers
Telo1A	Cactgccacttaccctaccattaccctaccatccaccatgacactactcaccatactggaattccggtgag tcactgtcg/ gtagggtaagcacgtgtgttatttacgatcattgttagcgtttcaatatggtgggtagaagaagaggc ctccaatgcagggtg gaactagctgaactagttcgctctcagaagaaccagagggtggaactactggttgaatgacggatgt acgctgcaggctgacggatc/ tcatttctcccctgtcatttcttacaacaacctccacttctatatctctgaatcatttaaatatggcggcgtt agtatcgaatc

TER1004	Acattcaaaacggaacatcttggattctctgtccttaaaactactaaacaaaagaattccggtgagtc ctgtcg/ caatcattcctagacattctcgtggctcttcttgcacaatcaatggcatagtttgaggcctccaatgca ggtagg
	ggcatacttacttacttaaaattcatttacattagctctgtacttctgattacgctgcaggctgcacggatc/ tggaataattctacacgaaaatagtattacgcaatggttttcattatggcggcgtagtatcgaatc
TER1417	acagatcatggttgaaaggctcggcgctcacaaccgaaatgtgtgcagagtcGAATTCGGT TGAGTCACTGTCTG ttgtgtactaaaattacgcatttatagaatagtatcataactgttggtagaGaggcctCCAATGCA GGTGG acttttctgtactgcctgcaatctctattctcattcatcacacatctattTACGCTGCAGGTCTGA CGGATC gtaaaattggatacacgacgacgctttacttataggctaacaaaaaatttaacgcATGGCGG CGTTAGTATCGAATC
TER603	Ggctttgaccttgcctgaccgatcgggaaattgtgccctgaaagattccggtgaattccggtgagtcact gtcg/ tctattgacaggagcaaagctgcccagaagaggtgcacagaagcgccttagaggcctccaatgca ggtagg
	aaactattcgaatagcaaggtagcttccatcctgtacatgcaagaccgtcacacagctacgctgcag gtcgcaggatc/ taccagtggaggacgaccggacatgtgagccatctggaaggatagatgcatggatggcggcggt agtatcgaatc

Primers for the construction of loop out strains (*attB/φ31C* system); primers were ordered from Sigma Aldrich, 0.05 μM HPLC purified. For each strain, the primer pair for introducing the *attB* site is shown in grey, and for the *attP* site in black.

#### 7.4.2 Checking the *attB/φ31C* strains

**Table 12. List of primers used for genotyping and sequencing the *attB/φ31C* strains**

	Upstream	Downstream
Telo1A	Ctgccacttaccctaccattac acaatattgggaccgccgaatgagatataga	atctctgtgtagaaatagggcaccatgtgg cccattctatcctagcaatggaacttc
TER1004	ggaagaatcaaagggaatttgatattaaagaa ccttatgatgcagagcaataaattcagt	tagtgcgtgtgtccacattagg ccagtacagaaaaggcgg
TER603	ggtccaggaacctatagg cacatgtgatttatagttctctcc	gtctgcctcgaaggcaa gttcggctggataaggtagc

TER1004	ggaagaatcaaaggaattgatattaaagaa ccttatgatgcagagcaataaattcagt	tagtgctggtgtccacattagg ccagtacagaaaaggcgg
---------	--	--

Primer pairs for genotyping and sequencing for each *loxP* strain are shown. Introduction of the *attB-K.I URA3* and the *attP-KanMX* cassettes was confirmed by genotyping and sequencing PCRs.

## 7.5 Detection of loop outs

**Table 13. List of probes used in this study**

Locus	Primers	Length (bp)	Tm (C)
ARS508 TER501	ctgtagctggacgctgagg tgcggtatgtgcggtgc	189	85.87
TER404	atgctcgtttcaatatctttcttacc gcttgagaaagggttatcgctg	479	78.81
TER603	Gagattgacgttacgtacatatgt Catacactcacctcatgacagatc	441	80.18
TER702	Ctggctgacaccaccaaattggc Aaaattgtgtggctcttcttac	220	81.39
HMR	gttttcgggctcattctttc cagaagaagaagttgaattaaggg	511	78.29
TER1004	ccagaattgtctcctaaatg cttatgatgcagagcaataaattcag	570	77.96
TER1417	ccacagcatatatttgtaaccg cctggagttattaagagagatt	448	78.64
Telo1A	gcagaacgacgcaccatttcat gattacctgaacaagctcccattaac	213	81.36
Chr. IV PFGE	tgttgacatcaaccaatttatcg tcttttctgtcttactagaggtgga	1440	77.17
Amp <sup>R</sup>	Cgtgtagataactacgat Gagcaactcggtcgccgc	525	79.27

$$T_m = 81.5 + 16.6(\log_{10}[Na^+]) + 0.41(\%G + C) - (600/N)$$

## 7.6 Prs-rDNA sequencing primers

AMPR034	ggaaagaagaccctgttga
AMPR035	ttcgtgccttgttga
AMPR036	tcacattgcgtcaacat
AMPR037	cgtgaagaatccatatccag
AMPR038	ctctgctccttgtggtag
AMPR039	acccaaacactcgcataga
AMPR040	aaagttgccctctccaaat
AMPR041	gatgcgagaaccaagagat
AMPR042	ggatcgaagatgatcaga
AMPR043	tctggacctggtgagttc
AMPR044	atctggtgatcctgccag
AMPR045	cttcaaagggctcgaga
AMPR046	acggaatggtacgttga
AMPR047	ggcagtattgagaccatga
AMPR048	caccacactcctaccaat
AMPR049	ggtatgcgagttgtaag

## **Reference List**

## Reference List

- ABDURASHIDOVA, G., RADULESCU, S., SANDOVAL, O., ZAHARIEV, S., DANAILOV, M.B., DEMIDOVICH, A., SANTAMARIA, L., BIAMONTI, G., RIVA, S., FALASCHI, A. (2007). Functional interactions of DNA topoisomerases with a human replication origin. *EMBO J.* **26**, 998-1009.
- ABREMSKI, K., FROMMER, B., HOESS, R.H. (1986). Linking-number changes in the DNA substrate during cre-mediated *loxP* site-specific recombination. *J. Mol. Biol.* **192**, 17-26.
- ACKERMAN, P., GLOVER, C.V., OSHEROFF, N. (1988). Phosphorylation of DNA topoisomerase II in vivo and in total homogenates of Drosophila Kc cells. The role of casein kinase II. *J. Biol. Chem.* **263**, 12653-12660.
- ADACHI, N., MIYAIKE, M., IKEDA, H., KIKUCHI, A. (1992). Characterization of cDNA encoding the mouse DNA topoisomerase II that can complement the budding yeast top2 mutation. *Nucleic Acids Res.* **20**, 5297-5303.
- ADRIAN, M., TEN HEGGELER-BORDIER, B., WAHLI, W., STASIAK, A.Z., STASIAK, A. DUBOCHET, J. (1990). Direct visualization of supercoiled DNA molecules in solution. *The EMBO J.* **9**, 4551.
- AGOSTINHO, M., RINO, J., BRAGA, J., FERREIRA, F., STEFFENSEN, S., FERREIRA, J. (2004). Human topoisomerase II alpha: targeting to subchromosomal sites of activity during interphase and mitosis. *Mol. Biol. Cell* **15**, 2388-2400.
- ALMAGRO, S., RIVELINE, D., HIRANO, T., HOUCHMANDZADEH, B., DIMITROV, S. (2004). The mitotic chromosome is an assembly of rigid elastic axes organized by structural maintenance of chromosomes (SMC) proteins and surrounded by a soft chromatin envelope. *J. Biol. Chem.* **279**, 5118-5126.
- ALONSO-SARDUY, L., RODUIT, C., DIETLER, G., KASAS, S. (2011). Human topoisomerase II-DNA interaction study using atomic force microscopy. *FEBS Letter* **385**, 3139-3145.
- ALSNER, J., SVEJSTRUP, J.Q., KJELDSSEN, E., SORENSEN, B.S., WESTERGAARD, O. (1992). Identification of an N-terminal domain of eukaryotic DNA topoisomerase I dispensable for catalytic activity but essential for in vivo function. *J. Biol. Chem.* **267**, 12408-12411.
- ALTSCHUL, S.F., GISH, W., MILLER, W., MYERS, E.W. & LIPMAN, D.J. (1990). Basic local alignment search tool. *J. Mol. Biol.* **215**, 403-410.
- ANDERSEN, C.L., WANDALL, A., KJELDSSEN, E., MIELKE, C., KOCH, J. (2002). Active, but not inactive, human centromeres display topoisomerase II activity *in vivo*. *Chromosome Res.* **10**, 305-312.
- ANDREWS, C.A., VAS, A.C., MEIER, B., GIMENEZ-ABIAN, J.F., DIAZ-MARTINEZ, L.A., GREEN, J., ERICKSON, S.L., VARDERWALL, K.E., HSU, W.S., CLARKE, D.J. (2006). A mitotic topoisomerase II checkpoint in budding yeast is required for genome stability but acts independently of Pds1/securin. *Genes Dev.* **20**, 1162-1174.

- ANTONIACCI, L.M. & SKIBBENS, R.Y. (2006). Sister-chromatid telomere cohesion is nonredundant and resists both spindle forces and telomere motility. **Curr. Biol.** **16**, 902-906
- AZARO, M.A. & LANDY, A. (2002).  $\lambda$  integrase and the  $\lambda$  Int family. In *Mobile DNA genetic elements II*. ASM Press, Washington, DC, pp 118-148.
- AZUMA, Y., ARNAOUTOV, A., DASSO, M. (2003). SUMO-2/3 regulates topoisomerase II in mitosis. **J. Cell Biol.** **163**, 477-487.
- BAASE, W.A. & WANG, J.C. (1974) I protein from *Drosophila melanogaster*. **Biochemistry** **13**, 4299-4303.
- BACHANT, J., ALCASABAS, A., BLAT, Y., KLECKNER, N., ELLEDGE, S. J. (2002). The SUMO-1 isopeptidase Smt4 is linked to centromeric cohesion through SUMO-1 modification of DNA topoisomerase II. **Mol. Cell.** **9**, 1169-1182.
- BACHRATI, C.Z. & HICKSON, I.D. (2003). RecQ helicases: suppressors of tumorigenesis and premature aging. **Biochem. J.** **374**, 577-606.
- BALDWIN, E.L. & OSHEROFF, N. (2005). Etoposide, topoisomerase II and cancer. **Curr. Med. Chem. Anticancer Agents** **5**, 363-372.
- BALZI, E. & GOFFEAU, A. (1995). Yeast multidrug resistance: the PDR network. **J. Bioenerg. Biomembr.** **27**, 71-76.
- BARANELLO, L., WOJTOWICZ, D., CUI, K., DEVAIAH, B.N., CHUNG, H.J., CHAN-SALIS, K.Y., GUHA, R., WILSON, K., ZHANG, X., ZHANG, H., PIOTROWSKI, J., THOMAS, C.J., SINGER, D.S., PUGH, B.F., POMMIER, Y., PRZYTYCKA, T.M., KOUZINE, F., LEWIS, B.A., ZHAO, K., LEVENS, D. (2016). RNA polymerase II regulates topoisomerase 1 activity to favor efficient transcription. **Cell** **165**, 357-371.
- BATES, A.D., O'DEA, M.H., GELLERT, M. (1996). Energy coupling in *Escherichia coli* DNA gyrase: the relationship between nucleotide binding, strand passage and DNA supercoiling. **Biochemistry** **35**, 1409-1416.
- BATES, A.D. & MAXWELL, A. (2005). DNA topology. **New York: Oxford University Press**.
- BATES, A.D. & MAXWELL, A. (2007). Energy coupling in type II topoisomerases: why do they hydrolyze ATP? **Biochem.** **46**, 7929-7941.
- BAUER, W.R., RESSNER, E.C., KATES, J., PATZKE, J.V. (1977). A DNA nicking-closing enzyme encapsidated in vaccinia virus: partial purification and properties. **Proc. Natl. Acad. Sci. USA** **74**, 1841-1845.
- BAUER PI, BUKI KG, COMSTOCK JA, KUN E (2000) Activation of topoisomerase I by poly [ADP-ribose] polymerase. **Int. J. Mol. Med.** **5**, 533-540.
- BAXTER, J. & ARAGON, L. (2012). A model for chromosome condensation based on the interplay between condensin and topoisomerase II. **Trends Genet** **28**, 110-117.
- BAXTER, J., SEN, N., MARTINEZ, V.L., DE CARANDINI, M.E., SCHVARTZMAN, J.B., DIFFLEY, J.F., ARAGON, L. (2011). Positive supercoiling of mitotic DNA drives decatenation by topoisomerase II in eukaryotes. **Science** **331**, 1328-1332.

- BAXTER, J. & DIFFLEY, J.F. (2008). Topoisomerase II inactivation prevents the completion of DNA replication in budding yeast. *Mol. Cell* **30**, 790-802.
- BELTEKI, G., GERTSENSTEIN, M., OW, D.W., NAGY, A. (2003). Site-specific cassette exchange and germline transmission with mouse ES cells expressing  $\phi$ C31 integrase. *Nature Biotech.* **21**, 321-324.
- BENSIMON, D., SIMON, A., CROQUETTE, V., BENSIMON, A. (1995). Stretching DNA with a receding meniscus: experiments and models. *Phys. Res. Lett.* **74**, 4754-4757.
- BERGERAT, A., DE MASSY, B., GADELLE, D., VAROUTAS, P.C., NICOLAS, A., FORTERRE, P. (1997). An atypical topoisomerase II from Archaea with implications for meiotic recombination. *Nature* **386**, 414-417.
- BERMEJO, R., BRANZEI, D., FOIANI, M. (2008). Cohesion by topology: sister chromatids interlocked by DNA. *Genes Dev.* **22**, 2297-2301.
- BERMEJO, R., DOKSANI, Y., CAPRA, T., KATOU, Y.M., TANAKA, H., SHIRAHIGE, K., FOIANI, M. (2007). Top1- and Top2-mediated topological transitions at replication forks ensure fork progression and stability and prevent DNA damage checkpoint activation. *Genes Dev.* **21**, 1921-1936.
- BERMUDEZ, I., GARCIA-MARTINEZ, J., PEREZ-ORTIN, J.E., ROCA, J. (2010). A method for genome-wide analysis of DNA helical tension by means of psoralen-DNA photobinding. *Nucleic Acid Res.* **38**, e182
- BERMUDEZ-LOPEZ, M., CESCHIA, A., DEPICCOLI, G., COLOMINA, N., PASERO, P., ARAGON, L., TORRES-ROSELL, J. (2010). The Smc5/6 complex is required for dissolution of DNA-mediated sister chromatid linkages. *Nucleic Acids Res.* **38**, 6502-6512.
- BHALLA, N., BIGGINS, S., MURRAY, A.W. (2002). Mutation of *YCS4*, a budding yeast condensin subunit, affects mitotic and nonmitotic chromosome behaviour. *Mol. Biol. Cell* **13**, 632-645.
- BHAT, M.A., PHILIP, A.V., GLOVER, D.M., BELLEN, H.J. (1996) Chromatid segregation at anaphase requires the *barren* product, a novel chromosome-associated protein that interacts with topoisomerase II. *Cell* **87**, 1103-1114.
- BHRIAN, N.N. & DORMAN, C.J. (1993). Isolation and characterization of a *topA* mutant of *Shigella flexneri*. *Mol. Microbiol.* **7**, 351-358.
- BI, X. & BROACH, J.R. (1997). DNA in transcriptionally silent chromatin assumes a distinct topology that is sensitive to cell cycle progression. *Mol. Cell. Biol.* **17**, 7077-7087
- BLOOM, K.S. & CARBON, J. (1982). Yeast centromere DNA is in a unique and highly ordered structure in chromosomes and small circular minichromosomes. *Cell* **29**, 305-317.
- BLOOM, K. (2008). Beyond the code: the mechanical properties of DNA as they relate to mitosis. *Chromosoma* **117**, 103-110.
- BOCQUET, N., BIZARD, A.H., ABDULRAHMAN, W., LARSEN, N.B., FATY, M., CAVADINI, S., BUNKER, R.D., KOWALCZYKOWSKI, S.C., CEJKA, P., HICKSON, I.D., THOMAI, N.H. (2014).

- Structural and mechanistic insight into Holliday-junction dissolution by Topoisomerase III $\alpha$  and RMI1. **Nature Struct. Mol. Biol.** **21**, 261-268.
- BOTCHAN, P., WANG, J.C., ECHOLS, H. (1973). Effect of circularity and superhelicity on transcription from bacteriophage  $\lambda$  DNA. **Proc. Natl. Acad. Sci. USA** **70**, 3077-3081.
- BRANZEI, D. & FOIANI, M. (2008). Regulation of DNA repair throughout the cell cycle. **Nature Rev. Mol. Cell Biol.** **9**, 297-308.
- BREIER, A.M., WEIER, H.U., COZZARELLI, N.R. (2005). Independence of replisomes in *Escherichia coli* chromosomal replication. **Proc. Natl. Acad. Sci.** **102**, 3942-3947.
- BRILL, S.J., DINARDO, S., VOELKEL-MEIMAN, K., STERNGLANZ, R. (1987). Need for DNA topoisomerase activity as a swivel for DNA replication for transcription of ribosomal RNA. **Nature** **326**, 414-416.
- BROWN, P.O. & COZZARELLI, N.R. (1981). Catenation and knotting of duplex DNA by type 1 topoisomerases: a mechanistic parallel with type 2 topoisomerases. **Proc. Natl. Acad. Sci. USA** **31**, 843-847.
- BUCK, D. (2009). DNA topology. Applications of knot theory (Proc. Sympos. Appl. Math., 66, Amer. Math. Soc., 2009), pp.47-79.
- BUCK, G.R. & ZECHIEDRICH, E.L. (2004). DNA disentangling by type-2 topoisomerases. **J. Mol. Biol.** **340**, 933-939
- BURGESS, S.M. & KLECKNER, N. (1999). Collisions between yeast chromosomal loci in vivo are governed by three layers of organization. **Genes Dev.** **13**, 1871-1883.
- BURNIER, Y., DORIER, J., STASIAK, A. (2008). DNA supercoiling inhibits DNA knotting. **Nucleic Acids Res.** **36**, 4956-4963.
- CARDENAS, M.E., DANG, Q., GLOVER, C.V. & GASSER, S.M. (1992). Casein kinase II phosphorylates the eukaryote-specific C-terminal domain of topoisomerase II in vivo. **EMBO J.** **11**, 1785.
- CARON, P.R., WATT, P. & WANG, J.C. (1994). The C-terminal domain of *Saccharomyces cerevisiae* DNA topoisomerase II. **Mol. Cell Biol.** **14**, 3197-3207.
- CAPRANICO, G. & BINASCHI, M. (1998). DNA sequence selectivity of topoisomerases and topoisomerase poisons. **Biochim. Biophys. Acta** **1400**, 185-194.
- CEBRIAN, J., CASTAN, A., MARTINEZ, V., KADOMATSU-HERMOSA, M.J., PARRA, C., FERNANDEZ-NESTOSA, M.J., SCHAEERER, C., HERNANDEZ, P., KRIMER, D.B., SCHVARTZMAN, J.B. (2015). Direct evidence for the formation of precatenanes during DNA replication. **J. Biol. Chem.** **290**, 13725-13735.
- CEBRIAN, J., MONTURUS, E., MARTINEZ-ROBLES, M.L., HERNANDEZ, P., KRIMER, D.B., SCHVARTZMAN, J.B. (2014). Topoisomerase 2 is dispensable for the replication and segregation of small yeast artificial chromosomes (YACs). **PLoS one** **9**, e104995.
- CEJKA, P., PLANK, J. L., DOMBROWSKI, C. C., KOWALCZYKOWSKI, S. C. (2012). Decatenation of DNA by the *S. cerevisiae* Sgs1–Top3–Rmi1 and RPA complex: A mechanism for disentangling chromosomes. **Molecular Cell** **47**, 886–896.

- CERRITELLI, S.M., CHON, H., CROUCH, R.J. (2011). A new twist for topoisomerase. **Science** **332**, 1510-1511.
- CHAMPOUX, J.J. (2001). DNA topoisomerases: structure, function, and mechanism. **Annu. Rev. Biochem.** **70**, 369-413.
- CHAMPOUX, J.J. & BEEN, M. (1980). Mechanistic studies of DNA replication and genetic recombination. In **ICN-UCLA symposia on molecular and cellular biology (ed. B. Alberts)**, pp. 909-815. Academic, New York.
- CHAMPOUX, J.J. & DULBECCO, R. (1972). An activity from mammalian cells that untwists superhelical DNA- a possible swivel for DNA replication. **Proc. Natl. Acad. Sci. USA** **74**, 1841-1845.
- CHAN, K.L., NORTH, P.S., HICKSON, I.D. (2007). BLM is required for faithful chromosome segregation and its localization defines a class of ultrafine anaphase bridges. **EMBO J.** **26**, 3397-3409.
- CHANG, C.R., WU, C.S., HOM, Y., GARTENBERG, M.R. (2005). Targeting of cohesin by transcriptionally silent chromatin. **Genes Dev.** **19**, 3031-3042.
- CHARBIN, A., BOUCHOUX, C., UHLMANN, F. (2014). Condensin aids sister chromatid decatenation by topoisomerase II. **Nucleic Acids Res.** **42**, 340-348.
- CHARVIN, G., BENSIMON, D., CROQUETTE, V. (2003). Single-molecule study of DNA unlinking by eukaryotic and prokaryotic type-II topoisomerases. **Proc. Natl. Acad. Sci. USA** **100**, 9820-9825.
- CHARVIN, G., STRICK, T.R., BENSIMON, D., CROQUETTE, V. (2005). Tracking topoisomerase activity at the single-molecule level. **Annu. Rev. Biophys. Biomol. Struct.** **34**, 201-219.
- CHEN, Y.T., WU, J., MODRICH, P., HSIEH, T.S. (2016). The C-terminal 20 amino acids of drosophila topoisomerase 2 are required for binding to a BRCA1 C Terminus (BRCT) domain-containing protein, Mus101, and fidelity of DNA segregation. **JBC** **291**, 13216-13228.
- CHENG, C., KUSSIE, P., PAVLETICH, N., SHUMAN, S. (1998). Conservation of structure and mechanism between eukaryotic topoisomerase I and site-specific recombinases. **Cell** **92**, 841-850.
- CHUNG, H.M., SHEA, C., FIELDS, S., TAUB, R.N., VAN DER PLOEG, L.H.T., TSE, D.B. (1990). Architectural organization in the interphase nucleus of the protozoan *Trypanosoma brucei*: location of telomeres and mini-chromosomes. **EMBO J.** **9**, 2611-2619.
- CHRISTENSEN, M. O., LARSEN, M.K., BARTHELMES, H.U., HOCK, R., ANDERSEN, C.L., KJELDEN, F., KNUDSEN, B.R., WESTERNGAARD, O., BOEGE, F., MIELKE, C. (2002). Dynamics of human DNA topoisomerases II $\alpha$  and II $\beta$  in living cells. **J. Cell Biol.** **157**, 31-44.
- CHRISTENSEN, M.O., KROKOWSKI, R.M., BARTHELMES, H.U., HOCK, R., BOEGE, F., MIELKE, C. (2004) Distinct effects of topoisomerase I and RNA polymerase I inhibitors suggest a dual mechanism of nucleolar/ nucleoplasmic partitioning of topoisomerase I. **J. Biol. Chem.** **279**, 21873–21882.

- CIOSK, R., SHIRAYAMA, M., SHEVCHENKO, A., TANAKA, T., TOTH, A., SHEVCHENKO, A. & NASMYTH, K. (2000). Cohesin's binding to chromosomes depends on a separate complex consisting of Scc2 and Scc4 proteins. *Mol. Cell* **5**, 243-254.
- CLARKE, D.J. (ed.) (2009). DNA topoisomerases. *Methods in Mol. Biol.* **582**, DOI 10.1007/978-1-60761-340-4\_1 ©Humana Press.
- CLARKE, L. & CARBON, J. (1980). Isolation of a yeast centromere and construction of functional small circular chromosomes. *Nature* **287**, 504-509.
- COEHLO, P.A., QUEIROZ-MACHADO, J., SUNKEL, C.E. (2003). Condensin-dependent localisation of topoisomerase II to an axial chromosomal structure is required for sister chromatid resolution during mitosis. *J. Cell Sci.* **116**, 4763-4776.
- COOK, P.R. (1991). The nucleoskeleton and the topology of replication. *Cell* **66**, 627-635
- CORBETT, K.D., SCHOEFFLER, A.J., THOMSEN, N.D., BERGER, J.M. (2005). The structural basis for substrate specificity in DNA topoisomerase IV. *J. Mol. Biol.* **351**, 545-561.
- CRISONA, N.J., STRICK, T.R., BENSIMON, D., CROQUETTE, V. & COZZARELLI, N.R. (2000) Preferential relaxation of positively supercoiled DNA by E. coli topoisomerase IV in single-molecule and ensemble measurements. *Genes Dev.*, **14**, 2881–2892.
- CRISONA, N.J. & COZZARELLI, N.R. (2006). Alteration of *Escherichia coli* topoisomerase IV conformation upon enzyme binding to positively supercoiled DNA. *J. Biol. Chem.* **281**, 18927-18932.
- CUVIER, O. AND HIRANO, T. (2003). A role of topoisomerase II in linking DNA replication to chromosome condensation. *J. Cell Biol.* **160**, 645-655.
- D'AMBROSIO, C., KELLY, G., SHIRAHIGE, K., UHLMANN, F. (2008a). Condensin-dependent rDNA decatenation introduces a temporal pattern to chromosome segregation. *Current Biol.* **18**, 1084-1088.
- D'AMBROSIO, C., SCHMIDT, C.K., KATOU, Y., KELLY, G., ITOH, T., SHIRAHIGE, K., UHLMANN, F. (2008b). Identification of *cis*-acting sites for condensin loading onto budding yeast chromosomes. *Genes & Dev.* **22**, 2215-2227.
- D'AMOURS, D., STEGMEIER, F., AMON, A. (2004). Cdc14 and condensin control the dissolution of cohesion-independent linkages at repeated DNA. *Cell* **117**, 455-469.
- D'ARPA, P., BEARDMORE, C., LIU, L.F. (1990). Involvement of nucleic acid synthesis in cell killing mechanisms of topoisomerase poisons. *Cancer Res.* **50**, 6916-6924.
- DASSO, M. (2008). Emerging roles of the SUMO pathway in mitosis. *Cell Div.* **2**, 5.
- DAVEY, C.A., SARGENT, D.F., LUGER, K., MAEDER, A.W., RICHMOND, T.J. (2002). Solvent mediated interactions in the structure of the nucleosome core particle at 1.9 Å resolution. *J. Mol. Biol.* **319**, 1097-1113.
- DAWLATY, M.M., MALUREANU, I., JEGANATHAN, K.B., KAO, F., SUSTMANN, C., TAHK, S., SHUAI, K., GORSSCHEDL, R., VAN DEURSEN, J.M. (2008). Resolution of sister centromeres requires RanBP2-mediated SUMOylation of topoisomerase II $\alpha$ . *Cell* **133**, 103-115.

- DEEHAN KENNEY, R. & HEALD, R. (2006). Essential roles for cohesion in kinetochore and spindle function in *Xenopus* egg extracts. **J. Cell Sci.** **119**, 5057-5066
- DEIBLER, R.W., MANN, J.K., DE SUMMERS, W.L., ZECHIEDRICH, L. (2007). Hin-mediated DNA knotting and recombining promote replicon dysfunction and mutation. **BMC Mol. Biol.** **8**, 44.
- DELBRÜCK M. (1954). On the replication of deoxyribonucleic acid (DNA). **Proc. Natl. Acad. Sci. USA** **40**, 783–788
- DELIUS, H. & WORCEL, A. (1974). Electron microscopic visualization of the folded chromosome of *Escherichia coli*. **J. Mol. Biol.** **82**, 107IN1109-108IN2.
- DEMING, P.B., CISTULLI, C.A., ZHAO, H., GRAVES, P.R., PIWNICA-WORMS, H., PAULES, R.S., DOWNES, C.S., KAUFMANN, W.K. (2001). The human decatenation checkpoint. **Proc. Natl. Acad. Sci. USA** **98**, 12044-12049.
- DEMING, P.B., FLORES, K.G., DOWNES, C.S., PAULES, R.S., KAUFMANN, W.K. (2002). ATR enforces the topoisomerase II-dependent G2 checkpoint through inhibition of Plk1 kinase. **J. Biol. Chem.** **277**, 36832-36838.
- DE PICCOLI, G., CORTES-LEDESMA, F., IRA, G., TORRES-ROSELL, J., UHLE, S., FARMER, S., HWANG, J.Y., MACHIN, F., CESCHIA, A., MCALEENAN, A., CORDON-PRECIADO, V., CLEMENTE-BLANCO, A., VILELLA-MITJANA, F., ULLAL, P., JARMUZ, A., LEITAO, B., BRESSAN, D., DOTIWALA, F., PAPUSHA, A., ZHAO, X., MYUNG, K., HABER, J.E., AGUILERA, A. & ARAGON, L. (2006). Smc5–Smc6 mediate DNA double-strand-break repair by promoting sister-chromatid recombination. **Nature Cell Biol.** **8**, 1032-1034.
- DEVORE, R.F., CORBETT, A.H. AND OSHEROFF, N. (1992). Phosphorylation of Topoisomerase II by Casein Kinase II and Protein Kinase C: Effects on Enzyme-mediated DNA Cleavage/Religation and Sensitivity to the Antineoplastic Drugs Etoposide and 4'-(1-Acridinylamino) methane-sulfon-m-anisidide. **Cancer Res.** **52**, 2156-2161.
- DEWAR, J.M., BUDZOWSKA, M., WALTER, J.C. (2015). The mechanism of DNA replication termination in vertebrates. **Nature** **525**, 345-350.
- DEWAR, H., TANAKA, K., NASMYTH, K., TANAKA, T.U. (2004). Tension between two kinetochores suffices for their bi-orientation on the mitotic spindle. **Nature** **428**, 93-98.
- DEWEESE, J.E., OSHEROFF, M.A., OSHEROFF, N. (2009). DNA topology and topoisomerases: teaching a “knotty” subject. **Biochem. Mol. Biol. Educ.** **37**, 2-10.
- DEWEESE, J.E. & OSHEROFF, N. (2009). The DNA cleavage reaction of topoisomerase II: wolf in sheep’s clothing. **Nucleic Acids Res.** **37**, 738-748.
- DIAZ-INGELMO, O., MARTINEZ-GARCIA, B., SEGURA, J., VALDES, A., ROCA, J. (2015). DNA topology and global architecture of point centromeres. **Cell Reps.** **13**, 667-677.
- DIAZ-MARTINEZ, L.A., GIMENEZ-ALBIAN, J.F., AZUMA, Y., GUACCI, V., GIMENEZ-MARTINEZ, G., LANIER, L.M., CLARKE, D.J. (2006). PIAS $\gamma$  is required for faithful chromosome segregation in human cells. **PLoS ONE** **1**, e53. Doi: 10.1371/journal.pone.0000053.

- DIAZ-MARTINEZ, L.A., GIMENEZ-ALBIAN, J.F., CLARKE, D.J. (2008). Chromosome cohesion- rings knots and fellowship. **J. Cell. Sci.** **121**, 2107-2114.
- DINARDO, S., VOELKEL, K., STERNGLANZ, R. (1984). DNA topoisomerase II mutant of *Saccharomyces cerevisiae*: Topoisomerase II is required for segregation of daughter molecules at the termination of DNA replication. **Proc. Natl. Acad. Sci. USA** **81**, 2616-2620.
- DINGMAN, C.W. (1974). Bidirectional chromosome replication: some topological considerations. **J. Theor. Biol.** **43**, 187-195.
- DONG, K.C. & BERGER, J.M. (2007). Structural basis for gate-DNA recognition and bending by type IIA topoisomerases. **Nature** **450**, 1201-1205.
- DOWNES, C.S., CLARKE, D.J., MULLINGER, A.M., GIMENEZ-ABIAN, J.F., CREIGHTON, A.M., JOHNSON, R.T. (1994). A topoisomerase II-dependent G2 cycle checkpoint in mammalian cells. **Nature** **372**, 467-470.
- DROLET, M. (2006). Growth inhibition mediated by excess negative supercoiling: the interplay between transcription elongation, R-loop formation and DNA topology. **Mol. Microbiol.** **59**, 723-730.
- DROLET, M., PHOENIX, P., MENZEL, R., MASSÉ, E., LIU, L.F. & CROUCH, R.J. (1995). Overexpression of RNase H partially complements the growth defect of an Escherichia coli delta topA mutant: R-loop formation is a major problem in the absence of DNA topoisomerase I. **Proc. Natl. Acad. Sci. USA**, **92**, 3526-3530.
- DUGUET, M. (1997). When helicase and topoisomerase meet! **J. Cell Sci.** **110**, 1345-1350.
- DYKHUIZEN, E.C., HARGREAVES, D.C., MILLER, E.L., CUI, K., KORSHUNOV, A., KOOL, M., PFISTER, S., CHO, Y.J., ZHAO, K., CRABTREE, G.R. (2013). BAF complexes facilitate decatenation of DNA by topoisomerase II $\alpha$ . **Nature** **497**, 624-627.
- EDGERTON, H., JOHANSSON, M., KEIFENHEIM, D., MUKHERJEE, S., CHACON, J.M., BACHANT, J., GARDNER, M., CLARKE, D.J. (2016). A noncatalytic function of the topoisomerase II CTD in Aurora B recruitment to inner centromeres during mitosis. **J. Cell Biol.** **213**, 651-664.
- EL SAYYED, H., LE CHAT, L., LEBAILLY, E., VICKRIDGE, E., PAGES, C., CORNET, F., LAGOMARSINO, M.C., ESPELI, O. (2016). Mapping Topoisomerase IV binding and activity sites on the *E. coli* genome. **PLoS Genet.** **12**, e1006025.
- EMBLETON, M.L., VOLOGODSKII, A.V., HALFORD, S.E. (2004). Dynamics of DNA loop capture by the SfiI restriction endonuclease on supercoiled and relaxed DNA. **J. Mol. Biol.** **339**, 53-66.
- ESPELI, O., LEVINE, C., HASSING, H., MARIANS, K.J. (2003). Temporal regulation of topoisomerase IV activity in E-coli. **Mol. Cell** **11**, 189-201
- ESPOSITO, F. & SINDEN, R.R. (1988). DNA supercoiling and eukaryotic gene expression. **Oxf. Surv. Eukaryot. Genes** **5**, 1-50.
- FACHINETTI, D., BERMEJO, R., COCITO, A., MINARDI, S., KATOU, Y., KANO, Y., SHIRAHIGE, K., AZVOLINSKY, A., ZAKIAN, V.A., FOIANI, M. (2010). Replication termination

- at eukaryotic chromosomes is mediated by topo II and occurs at genomic loci containing pausing elements. *Mol. Cell.* **39**,595-605.
- FALASCHI, A. (2000). Eukaryotic DNA replication: a model for a fixed double replisome. *Trends Genet.* **16**, 88-92.
- FARCAS, A.M., ULUOCAK, P. HELMHART, W., NASMYTH, K. (2011). Cohesin's concatenation of sister DNAs maintains their intertwining. *Mol. Cell* **44**, 97-107
- FARNSHAW, W.C., HALLIGAN, B., COOKE, C.A., HECK, M.M., LIU, L.F. (1985). Topoisomerase II is a structural component of mitotic chromosome scaffolds. *J. Cell Biol.* **100**, 1706-1715.
- FERGUSON, M. & WARD, D.C. (1992). Cell cycle dependent chromosomal movement in pre-mitotic human T-lymphocyte nuclei. *Chromosoma* **101**, 557-565.
- FIELD-BERRY, S.C. & DEPAMPHILIS, M.L (1989). Sequences that promote formation of catenated intertwines during termination of DNA replication. *Nucleic Acids Res*, **17**, 3261-3273.
- FLORIDIA, G., ZATTERALE, A., ZUFFARDI, O., TYLER-SMITH, C. (2000). Mapping of a human centromere onto the DNA by topoisomerase II cleavage. *EMBO Rep.* **1**, 489-493.
- FORTERRE, P. & GADELLE, D. (2009). Phylogenomics of DNA topoisomerases: their origin and putative roles in the emergence of modern organisms. *Nucleic Acids Res.* **37**, 679-692.
- FORTERRE, P. GRIBALDO, S., GADELLE, D. SERRE, M.C. (2007). Origin and evolution of DNA topoisomerases. *Biochimie* **89**, 427-446.
- FORTUNE, J.M., LAVRUKHIN, O.V., GURNON, J.R., VAN ETTEN, J.L., LLOYD, S., OSHEROFF, N. (2001). Topoisomerase II from *Chlorella* virus PBCV-1 has an exceptionally high DNA cleavage activity. *J. Biol. Chem.* **276**, 24401-24408.
- FORTUNE, J.M., & OSHEROFF, N. (2000). Topoisomerase II as a target for anticancer drugs: when enzymes stop being nice. *Prog. Nucl. Acid. Res. Mol. Biol.* **64**, 221-253.
- FRANKLIN, R. & GOSLING, R.G. (1953). Molecular configuration in sodium thymonucleate. *Nature* **171**, 740-741.
- FREEMAN, L.A. & GARRARD, W.T. (1992). DNA supercoiling in chromatin structure and gene expression. *Crit. Rev. Eukaryot. Gene Expr.* **2**, 165-209.
- FRIEDMAN, K. & BREWER, B. (1995) Analysis of replication intermediates by two-dimensional agarose gel electrophoresis. *Meth. Enzymol.* **262**, 613-627.
- FURUYAMA, T. & HENIKOFF, S. (2009). Centromeric nucleosomes induce positive DNA supercoils. *Cell* **138**, 104-113.
- GALANDE, S. & MUNIYAPPA, K. (1997). Effects of nucleosomes and antitumor drugs on the catalytic activity of type II topoisomerase from rat testis. *Biochem. Pharmacol.* **53**, 1229-1238
- GALLEGO-PAEZ, L.M., TANAKA, H., BANDO, M., TAKAHASHI, M., NOZAKI, N., NAKATO, R., SHIRAHIGE, K., HIROTA, T. (2014). Smc5/6-mediated regulation of replication progression contributes to chromosome assembly during mitosis in human cells. *Mol. Biol. Cell.* **25**, 302-317.

- GARTENBERG, M.R., & WANG, J.C. (1992) Positive supercoiling of DNA greatly diminishes mRNA synthesis in yeast. *Proc. Natl. Acad. Sci. USA* **89**, 11461-11465.
- GARTENBERG, M.R. & WANG, J.C. (1993). Identification of barriers to rotation of DNA segments in yeast from the topology of DNA rings excised by an inducible site-specific recombinase. *Proc. Natl. Acad. Sci. USA* **90**, 10514-10518.
- GELLERT, M., MIZUUCHI, K., O'DEA, M.H., NASH, H.A. (1976a). DNA gyrase: an enzyme that introduces superhelical turns into DNA. *Proc. Natl. Acad. Sci. USA* **73**, 3872-3876.
- GELLERT, M., O'DEA, M.H., ITOH, T., TOMIZAWA, J.I. (1976b). Novobiocin and coumermycin inhibit DNA supercoiling catalysed by DNA gyrase. *Proc. Natl. Acad. Sci. USA* **74**, 4474-4478.
- GERLICH, D., BEAUDOUIN, J., KALBFUSS, B., DAIGLE, N., EILS, R., ELLENBERG, J. (2003). Global chromosome positions are transmitted through mitosis in mammalian cells. *Cell* **112**, 751-764.
- GERME, T., MILLER, K. & COOPER, J.P. (2009). A non-canonical function of topoisomerase II in disentangling dysfunctional telomeres. *EMBO J.* **28**, 2803-2811.
- GERMOND, J.E., ROUVIERE-YANIV, J., YANIV, M., BRUTLAG, D. (1979). Nicking-closing enzyme assembles nucleosome-like structures in vitro. *Proc. Natl. Acad. Sci. USA* **76**, 3770-3783.
- GOBERT, C., BRACCO, L., ROSSI, F., OLIVIER, M., TAZI, J., LAVELLE, F., LARSEN, A.K., RIOU, J.F. (1996). Modulation of DNA topoisomerase I activity by p53. *Biochemistry* **35**, 5778-5786.
- GOODWIN, A., WANG, S.W., TODA, T., NORBURY, C., HICKSON, I.D. (1999). Topoisomerase III is essential for accurate nuclear division in *Schizosaccharomyces pombe*. *Nucleic Acids Res.* **27**, 4050-4058.
- GORBSKY, G.J. (1994). Cell cycle progression and chromosome segregation in mammalian cells cultured in the presence of the topoisomerase II inhibitors ICRF-187 [(+)-1,2-bis(3,5-dioxopiperazinyl-1-yl)propane; ADR-529] and ICRF-159 (Razoxane). *Cancer Res.* **54**, 1042-1048.
- GOTO, T. & WANG, J.C. (1982). Yeast topoisomerase II. *J. Biol. Chem.* **257**, 5866-5872.
- GOTO, T., & WANG, J.C. (1984). Yeast DNA topoisomerase II is encoded by a single-copy, essential gene. *Cell* **36**, 1073-1080.
- GRAINGE, I. & JAYARAM, M. (1999). The integrase family of recombinases: organization and function of the active site. *Mol. Microbiol.* **33**, 449-456.
- GROTH, A.C., OLIVARES, E.C., THYGARAJAN, B., CALOS, M.P. (2000). A phage integrase directs efficient site-specific integration in human cells. *Proc. Natl. Acad. Sci. USA* **97**, 5995-6000.
- GROTH, A.C., FISH, M., NUSSE, R., CALOS, M.P. (2004). Construction of transgenic Drosophila by using the site-specific integrase from phage  $\phi$ C31. *Genetics* **166**, 1775-1782.
- GUACCI, V., HOGAN, E., KOSHLAND, D. (1994). Chromosome condensation and sister chromatid pairing in budding yeast. *J. Cell Biol.* **125**, 517-530.

- HABER, J.E., THORBURN, P.C., ROGERS, D. (1984). Meiotic and mitotic behavior of dicentric chromosomes in *Saccharomyces cerevisiae*. **Genetics** **106**, 185-205.
- HAERING, C., FARCAS, A.M., ARUMUGAM, O., METSON, J. NASMYTH, K. (2008). The cohesin ring concatenates sister DNA molecules. **Nature** **454**, 297-301.
- HALMER, L., VESTNER, B., GRUSS, C. (1998). Involvement of topoisomerases in the initiation of simian virus 40 minichromosome replication. **J. Biol. Chem.** **273**, 34792-34798.
- HANDE, K.R. (1998) Etoposide: four decades of development of a topoisomerase II inhibitor. **Eur. J. Cancer** **34**, 1514–1521.
- HARMON, F.G., DIGATE, R.J., KOWALCZYKOWSKI, S.C. (1999). ReqQ helicase and topoisomerase III comprise a novel DNA strand passage function: a conserved mechanism for control of DNA recombination. **Mol. Cell.** **3**, 611-620.
- HAYAMA, R. & MARIANS, K.Y. (2010). Physical and functional interaction between the condensin MukB and the decatenase topoisomerase IV in *Escherichia coli*. **Proc. Natl. Acad. Sci. USA** **107**, 18826-18831.
- HEDIGER, F., NEUMANN, F.R., VAN HOUWE, G., DUBRANA, K., GASSER, S.M. (2002). Live imaging of telomeres, ku and sir proteins define redundant telomere-anchoring pathways in yeast. **Curr. Biol.** **12**, 2076-2089.
- HERSHEY, A.D., BURGI, E., INGRAHAM, L. (1963). Cohesion of DNA molecules isolated from phage lambda. **Proc. Natl. Acad. Sci. USA** **49**, 748-755.
- HIASA H. & MARIANS, K.J. (1994) Topoisomerase III, but not topoisomerase I, can support nascent chain elongation during theta-type DNA replication. **J. Biol. Chem.** **269**, 32655-32659.
- HIRANO, T. (2000). Chromosome cohesion, condensation, and separation. **Annu. Rev. Biochem.** **69**, 115-144.
- HIRANO, T. (2010). How to separate entangled sisters: interplay between condensin and decatenase. **Proc. Natl. Acad. Sci. USA** **107**, 18749-18750.
- HIRANO, T., FUNAHASHI, S.I., UEMUERA, T., YANAGIDA, M. (1986). Isolation and characterization of *Schizosaccharomyces pombe* cut mutants that block nuclear division but not cytokinesis. **EMBO J.** **5**, 2973-2979.
- HOLM, C., GOTO, T., WANG, J.C., BOTSTEIN, D. (1985). DNA topoisomerase II is required at the time of mitosis in yeast. **Cell** **41**, 553-563.
- HOLM, C.O., STEARNS, T., BOTSTEIN, D. (1989). DNA topoisomerase II must act at mitosis to prevent nondisjunction and chromosome breakage. **Mol. Cell Biol.** **9**, 159-168.
- HOLM, C. (1994). Coming undone: how to untangle a chromosome. **Cell** **77**, 955-957.
- HOLMES, V.F. & COZZARELLI, N.R. (2000). Closing the ring: links between SMC proteins and the partitioning, condensation and supercoiling of chromosomes. **Proc. Natl. Acad. Sci. USA** **97**, 1322-1324.
- HOUCHMANDZADEH, B., MARKO, J.F., CHATENAY, D., LIBCHABER, A. (1997). Elasticity and structure of eukaryote chromosome studied by micromanipulation and micropipette aspiration. **J. Cell Biol.** **139**, 1-12.

- HSIANG, Y.H. & LIU, L.F. (1985). Identification of mammalian DNA topoisomerase I as an intracellular target of the anticancer drug camptothecin. **Cancer Res.** **48**, 1722-1726.
- HU, Y., CLOWER, R.V., MELENDY, T. (2006). Cellular topoisomerase I modulates origin binding by bovine papilloma virus type 1 E1. **J. Virol.** **80**, 4363-4371.
- HUERTAS, P. & AGUILERA, A. (2003). Cotranscriptionally formed DNA: RNA hybrids mediate transcription elongation impairment and transcription-associated recombination. **Mol. Cell** **12**, 711-721.
- IROBALIEVA, R.N., FOGG, J.M., CATANESE, D.J., SUTTHIBUTPONG, T., CHEN, M., BARKER, A.K., LUDTKE, S.J., HARRIS, S.A., SCHMID, M.F., CHIU, W. AND ZECHIEDRICH, L. (2015). Structural diversity of supercoiled DNA. **Nature Comms.** **6**.
- ISHIDA, R., TAKASHIMA, R., KOUJIN, T., SHIBATA, M., NOZAKI, N., SETO, M., MORI, H., HARAGUCHI, T. AND HIRAOKA, Y. (2001). Mitotic specific phosphorylation of serine-1212 in human DNA topoisomerase II alpha. **Cell Struct. Funct.** **26**, 215-226.
- IVANOV, D., & NASMYTH, K. (2008). A physical assay for sister chromatid cohesion in vitro. **Mol. Cell** **27**, 300-310.
- JACOB, F., BRENNER, S., CUZIN, F. (1963). On the regulation of DNA replication in bacteria. **Cold Spring Harbor Symp. Quant. Biol.** **28**, 329-347.
- JACKSON, D.A. & COOK, P.R. (1986). Replication occurs at the nucleoskeleton. **EMBO J.** **5**, 1403-1410.
- JENSEN, S., ANDERSEN, A.H., KJELDSEN, E., BIRSACK, H., OLSEN, E.H., ANDERSEN, T.B., WESTERGAARD, O., JAKOBSEN, B.K (1996). Analysis of functional domain organization in DNA topoisomerase II from humans and *Saccharomyces cerevisiae*. **Mol. Cell. Biol.** **16**, 3866-3877.
- JENSEN, L.H., DEJLIGBJERG, M., HANSEN, L.T., GRAUSLIND, M., JENSEN, P.B., SEHESTED, M. (2004). Characterisation of cytotoxicity and DNA damage induced by the topoisomerase II-directed bisdioxopiperazine anti-cancer agent ICRF-187 (dexrazoxane) in yeast and mammalian cells. **BMC Pharmacol.** **4**, 31.
- JEPPSSON, K., CARLBORG, K.K., NAKATO, R., BERTA, D.G., LILIENTHAL, I., KANNO, T., LINDQVIST, A., BRINK, M.C., DANTUMA, N.P., KATOU, Y., SHIRAHIGE, K., SJÖGREN, C. (2014). The chromosomal association of the Smc5/6 complex depends on cohesion and predicts the level of sister chromatid entanglement. **PLoS Genet.** **10**, e1004680.
- JOSHI, R.S., PIÑA, B., ROCA, J. (2010). Positional dependence of transcriptional inhibition by DNA torsional stress in yeast chromosomes. **EMBO J.** **29**, 740-748.
- JOSHI, R.S., PIÑA, B., ROCA, J. (2012). Topoisomerase II is required for the production of long Pol II gene transcripts in yeast. **Nucleic Acids Res.** **40**, 7907-7915.
- KAMPRANIS, S.C. & MAXWELL, A. (1996). Conversion of DNA gyrase into a conventional type II topoisomerase. **Proc. Natl. Acad. Sci. USA** **93**, 14416-14421.
- KAMPRANIS, S.C., BATES, A.D., MAXWELL, A. (1999). A model for the mechanism of strand passage by DNA gyrase. **Proc. Natl. Acad. Sci. USA** **96**, 8414-8419.

- KARAYAN, L., RIOU, J.F., SEITE, P., MIGEON, J., CANTEREAU, A., LARSEN, C.J. (2001). Human ARF protein interacts with topoisomerase I and stimulates its activity. ***Oncogene* 20**, 836–848.
- KAS, E. & LAEMMLI, U.K. (2001). *In vivo* topoisomerase II cleavage of the *Drosophila* histone and satellite III repeats: DNA sequence and structural characteristics. ***EMBO J.* 11**, 705-716.
- KAUFMANN, S.H. (1998). Cell death induced by topoisomerase-targeted drugs: more questions than answers. ***Biochim. Biophys. Acta Gene Struct. Expr.* 1400**, 195-211.
- KAWAMURA, R., POPE, L.H., CHRISTENSEN, M.O., SUN, M., TEREKHOVA, K., BOEGE, F., MIELKE, C., ANDERSEN, A.H., MARKO, J.F. (2010). Mitotic chromosomes are constrained by topoisomerase II-sensitive DNA entanglements. ***J. Cell Biol.* 188**, 653-663.
- KAWANISHI, M. (1993). Topoisomerase I and II activities are required for Epstein-Barr virus replication. ***J. Gen. Virol.* 74**, 2263-2268.
- KEENEY, S., GIROUX, C.N. & KLECKNER, N. (1997) Meiosis-specific DNA double-strand breaks are catalyzed by Spo11, a member of a widely conserved protein family. ***Cell*, 88**, 375–384.
- KEGEL, A., BETTS-LINDROOS, H., KANNO, T., JEPSSON, K., STROM, L., KATOU, Y., ITOH, T., SHIRAHIGE, K., SJOGREN, C. (2011). Chromosome length influences replication-induced topological stress. ***Nature* 471**, 392-396.
- KIKUCHI, Y. & NASH, H.A. (1979). Nicking-closing activity associated with bacteriophage lambda int gene product. ***Proc. Natl. Acad. Sci. USA* 76**, 3760-3764.
- KIM, N., HUANG, S.N., WILLIAMS, J., LI, Y.C., CLARK, A.B., CHO, J.E., KUNKEL, T.A., POMMIER, Y., JINKS-ROBERTSON, S. (2011). Mutagenic processing of ribonucleotides in DNA by yeast topoisomerase I. ***Science* 332**, 1561-1564.
- KIM, R.A. & WANG, J.C. (1989a). Function of DNA topoisomerases as replication swivels in *Saccharomyces cerevisiae*. ***J. Mol. Biol.* 208**, 257-267.
- KIM, R.A. & WANG, J.C. (1989b). A subthreshold level of DNA topoisomerases leads to the excision of yeast rDNA as extrachromosomal rings. ***Cell* 57**, 975-985.
- KIM, R.A. & WANG, J.C. (1992). Identification of the yeast TOP3 gene product as a single strand-specific DNA topoisomerase. ***J. Biol. Chem.* 267**, 17178-17185.
- KIMURA, K. & HIRANO, T. (1997). ATP-dependent positive supercoiling of DNA by 13S condensin: a biochemical implication for chromosome condensation. ***Cell* 90**, 625-634.
- KIRKEGAARD, K. & WANG, J.C. (1981). Mapping the topography of DNA wrapped around gyrase by nucleolytic and chemical probing of complexes of unique DNA sequences. ***Cell* 23**, 721-729.
- KOBAYASHI, T., NOMURA, M., HORIUCHI, T. (2001). Identification of DNA *cis* elements essential for expansion of ribosomal DNA repeats in *Saccharomyces cerevisiae*. ***Mol. Cell. Biol.* 21**, 136-147.
- KORNBERG, A. (1984). Enzyme studies on the replication of the *Escherichia coli* chromosome. ***Adv. Exp. Med. Biol.* 179**, 3-16.

- KOSHLAND, D., & HARTWELL, L.H. (1987). The structure of sister minichromosome DNA before anaphase in *Saccharomyces cerevisiae*. **Science** **238**, 1713-1716
- KOSTER, D.A., CROQUETTE, V., DEKKER, C., SHUMAN, S., DEKKER, N.H. (2005) Friction and torque govern the relaxation of DNA supercoils by eukaryotic topoisomerase I $\beta$ . **Nature** **343**, 671-674.
- KRAMLINGER, V.M. & HIASA, H. (2006). The “GyrA-box” is required for the ability of DNA gyrase to wrap DNA and catalyze the supercoiling reaction. **J. Biol. Chem.**, **281**, 3738–3742.
- KRETZSCHMAR, M., MEISTERERNST, M., ROEDER, R.G. (1993). Identification of human DNA topoisomerase I as a cofactor for activator-dependent transcription by RNA polymerase II. **Proc. Natl. Acad. Sci. USA** **90**, 11508–11512
- KREUZER, K.N. & COZZARELLI, N.R. (1980). Formation and resolution of DNA catenanes by DNA gyrase. **Cell** **20**, 245-254.
- KROGH, B.O. & SHUMAN, S. (2000). Catalytic mechanism of DNA topoisomerase IB. **Mol. Cell** **5**, 1035-1041.
- KROGH, B.O. & SHUMAN, S. (2002). A poxvirus-like type IB topoisomerase family in bacteria. **Proc. Natl. Acad. Sci. USA**, **99**, 1853–1858.
- KWAN, K.Y. & WANG, J.C. (2001). Mice lacking DNA topoisomerase III $\beta$  develop to maturity but show a reduced mean lifespan. **Proc. Natl. Acad. Sci. USA** **98**, 5717-5727.
- LAINE, J.P., OPRESKO, P.L., INDIG, F.E., HARRIGAN, J.A., VON KOBBE, C., BOHR, V.A. (2003) Werner protein stimulates topoisomerase I DNA relaxation activity. **Cancer Res** **63**, 7136–7146.
- LANE, A.B., GIMENEZ-ABIAN, J.F., CLARKE, D.J. (2013). A novel chromatin tether domain controls topoisomerase I $\alpha$  dynamics and mitotic chromosome formation. **J. Cell Biol.** **200**, 471-486.
- LAPONOGOV, I., VESELKOV, D.A., CREVEL, I.M.T., PAN, X.S., FISHER, L.M. & SANDERSON, M.R. (2013). Structure of an ‘open’ clamp type II topoisomerase-DNA complex provides a mechanism for DNA capture and transport. **Nucleic acids research** **41**, 9911-9923.
- LARSEN, N.B., SASS, E., SUSKI, C., MANKOURI, H.W, HICKSON, I.D. (2014). The Escherichia coli Tus–Ter replication fork barrier causes site-specific DNA replication perturbation in yeast. **Nature Comms.** **5**.
- LAVOIE, B.D, HOGAN, E., KOSHLAND, D. (2002). In vivo dissection of the chromosome condensation machinery: reversibility of condensation distinguishes contributions of condensin and cohesin. **J. Cell Biol.** **156**, 805-815.
- LAVRUKHIN, O.V., FORTUNE, J.M., WOOD, T.G., BURBANK, D.E., VAN ETTEN, J.L. & LLOYD, R.S. (2000). Topoisomerase II from Chlorella virus PBCV-1: Characterization of the smallest known type II topoisomerase. **J. Biol. Chem.** **275**. 6915-6921.
- LEBEL, M., SPILLARE, E.A., HARRIS, C.C., LEDER, P. (1999). The Werner syndrome gene product co-purifies with the DNA replication complex and interacts with PCNA and topoisomerase I. **J. Biol. Chem.** **274**,37795–37799.

- LEPPARD, J.B., CHAMPOUX, J.J. (2005). Human DNA topoisomerase I: relaxation, roles, and damage control. **Chromosoma** **114**, 75-85.
- LEVINE, C. & MARIANS, K.J. (1998). Identification of dnaX as a high-copy suppressor of the conditional lethal and partition phenotypes of the parE10 allele. **J. Bacteriol.** **180**, 1232-1240.
- LEVINE, C., HIASA, H. AND MARIANS, K. (1998). DNA gyrase and topoisomerase IV: biochemical activities, physiological roles during chromosome replication, and drug sensitivities. **BBA Gene Struct. Express.** **1400**, 29-43.
- LI, X. & MANLEY J.L. (2006). Cotranscriptional processes and their influence on genome stability. **Genes Dev.** **20**, 1838-1847.
- LI, Y., STEWART, N.K., BERGER, A.J., VOS, S., SCHOEFFLER, A.J., BERGER, J.M., CHAIT, B.T. & OAKLEY, M.G. (2010). Escherichia coli condensin MukB stimulates topoisomerase IV activity by a direct physical interaction. **Proc. Natl. Acad. Sci. USA** **107**, 18832-18837.
- LI, W. & WANG, J.C. (1998). Mammalian DNA topoisomerase III $\alpha$  is essential in early embryogenesis. **Proc. Natl. Acad. Sci. USA** **95**, 1010-1013.
- LINKA, R.M., PORTER, A.C., VOLKOV, A., MIELKE, C., BOEGE, F. & CHRISTENSEN, M.O. (2007). C-terminal regions of topoisomerase II $\alpha$  and II $\beta$  determine isoform-specific functioning of the enzymes in vivo. **Nucleic Acids Res.** **35**, 3810-3822.
- LIPPERT, M.J., KIM, N., CHO, J.E., LARSON, R.P., SCHOENLY, N.E., O'SHEA, S.H. AND JINKS-ROBERTSON, S. (2011). Role for topoisomerase 1 in transcription-associated mutagenesis in yeast. **Proc. Natl. Acad. Sci. USA** **108**, 698-703.
- LISTER, J.A. (2010). Transgene excision in zebrafish using the phiC31 integrase. **Genesis** **48**, 137-143.
- LIU, Z., DEIBLER, R.W., CHAN, H.S., ZECHIEDRICH, L. (2009). The why and how of DNA unlinking. **Nucleic Acids Res.** **37**, 661-671.
- LIU, L.F., LIU, C.C., ALBERTS, B.M. (1980). Type II DNA topoisomerases: enzymes that can unknot a topologically knotted DNA molecule via a reversible double strand break. **Cell** **19**, 697-707.
- LIU, L.F., PERKOCHA, L., CALENDAR, R., WANG, J.C. (1981). Knotted DNA from bacteriophage capsids. **Proc. Natl. Acad. Sci. USA** **78**, 5498-5502.
- LIU, L.F., ROWE, T.C., YANG, L., TEWEY, K.M., CHEN, G.L. (1983) Cleavage of DNA by mammalian DNA topoisomerase II. **J. Biol. Chem.**, **258**, 15365–15370. 67.
- LIU, L.F. & WANG, J.C. (1978). *Micrococcus luteus* DNA gyrase: active components and a model for its supercoiling of DNA. **Proc. Acad. Sci. USA** **75**, 2098-2102.
- LIU, L.F. & WANG, J.C. (1981). DNA-DNA gyrase complex: the wrapping of the DNA duplex outside the enzyme. **Cell** **15**, 979-984.
- LIU, L.F. & WANG, J.C. (1987). Supercoiling of the DNA template during transcription. **Proc. Natl. Acad. Sci. USA** **84**, 7024-7027.

- LOPEZ, C.R., YANG, S., DEIBLER, R.W., RAY, S.A., PENNINGTON, J.M., DIGATE, R.J., HASTINGS, P.J., ROSENBERG, S.M., ZECHIEDRICH, E.L. (2005). A role for topoisomerase III in a recombination pathway alternative to RuvABC. *Mol. Microbiol.* **58**, 80-101.
- LOU, Z., MINTER-DYKHOUSE, K., CHEN, J. (2005). BRCA1 participates in DNA decatenation. *Nature Struct. Mol. Biol.* **12**, 589-593.
- LUCAS, I., GERME, T., CHEVRIER-MILLER, M., HYRIEN, O. (2001). Topoisomerase II can unlink replicating DNA by precatenane removal. *EMBO J.* **20**, 6509-6519.
- LYNN, R., GIAEVER, G., SWANBERG, S.L., WANG, J.C. (1986). Tandem regions of yeast DNA topoisomerase II share homology with different subunits of bacterial gyrase. *Science* **233**, 647-649.
- MACHÍN, F., TORRES-ROSELL, J., JARMUZ, A. & ARAGÓN, L. (2005). Spindle-independent condensation-mediated segregation of yeast ribosomal DNA in late anaphase. *J. Cell Biol.* **168**, 209-219.
- MANICHANH, C., ROCA, J. (2013). Topoisomerase II minimizes DNA entanglements by proofreading DNA topology after DNA strand passage *Nucleic Acid Res.* gkt1037.
- MAO, Y., DESAI, S.D., LIU, L.F. (2000). SUMO-1 conjugation to human DNA topoisomerase II isozymes. *J. Biol. Chem.* **275**, 26066-26073.
- MARCHETTI, F., BISHOP, J.B., LOWE, X., GENEROSO, W.M., HOZIER, J., WYROBEK, A.J. (2001). Etoposide induces heritable chromosomal aberrations and aneuploidy during male meiosis in the mouse. *Proc. Natl. Acad. Sci. USA* **98**, 3952-3957.
- MARKO, J.F. (2008). Micromechanical studies of mitotic chromosomes. *Chromosome Res.* **16**, 469-497.
- MARKO, J.F. & SIGGIA, E.D. (1997). Polymer models of meiotic and mitotic chromosomes. *Mol. Biol. Cell*, **8**, 2217-2231.
- MARTINCIC, D. & HANDE, K.R. (2005) Topoisomerase II inhibitors. *Cancer Chemother. Biol. Response Modif.* **22**, 101–121.
- MARTINEZ-GARCIA, B., FERNANDEZ, X., DIAZ-INGELMO, O., RODRIGUEZ-CAMPOS, A., MATERA, A.G. (1999). Nuclear bodies: multifaceted subdomains of the interchromatin space. *Trends Cell Biol.* **9**, 302-309.
- MCCLENDON, A.K. & OSHEROFF, N. (2007). DNA topoisomerase II, genotoxicity, and cancer. *Mutat. Res.-Fund. Mol. M.* **623**, 83-97.
- MCCLENDON, A.K., RODRIGUEZ, A.C. & OSHEROFF, N. (2005) Human topoisomerase II $\alpha$  rapidly relaxes positively supercoiled DNA: implications for enzyme action ahead of replication forks. *J. Biol. Chem.* **280**, 39337–39345.
- MCDONALD, W.H., PAVLOVA, Y., YATES, J.R. 3<sup>RD</sup>, BODDY, M.N. (2003). Novel essential DNA repair proteins Nse1 and Nse2 are subunits of the fission yeast Smc5-Smc6 complex. *J. Biol. Chem.* **278**, 45460-45467.
- MCGUFFEE, S.R., SMITH, D.J., WHITEHOUSE, I. (2013). Quantitative, genome-wide analysis of eukaryotic replication initiation and termination. *Mol. Cell* **50**, 123-135.

- MEGEE, P.C. AND KOSHLAND, D. (1999). A functional assay for centromere-associated sister chromatid cohesion. **Science** **285**, 254-257.
- MICHAELIS, C., CISOK, R., NASMYTH, K. (1997). Cohesins: chromosomal proteins that prevent premature separation of sister chromatids. **Cell** **91**, 35-45.
- MIKHAILOV, A., COLE, R.W., RIEDER, C.L. (2002). DNA damage during mitosis in human cells delays the metaphase/anaphase transition via the spindle-assembly checkpoint. **Curr. Biol.** **12**, 1797-1806.
- MIRKIN, S.M. (2001). DNA topology: fundamentals. **Encyclopedia of Life Sciences**, DOI: 10.1038/npg.els.0001038.
- MIRKIN, E.V. & MIRKIN, S.M. (2005). Mechanisms of transcription-replication collisions in bacteria. **Mol. Cell. Biol.** **25**, 888-895.
- MISTELI, T. (2001). Protein dynamics: implications for nuclear architecture and gene expression. **Science** **291**, 843-847.
- MITCHELL, J.S. & HARRIS, S.A. (2013). Thermodynamics of writhe in DNA minicircles from molecular dynamics simulations. **Phys. Rev. Lett.** **110**, 148105.
- MITCHELL, J.S., LAUGHTON, C.A., HARRIS, S.A. (2011). Atomistic simulations reveal bubbles, kinks and wrinkles in supercoiled DNA. **Nucleic Acids Res.** **39**, 2928-3938.
- MITKOVA, A.V., BISWAS-FISS, E.E., BISWAS, S.B. (2005). Modulation of synthesis in *Saccharomyces cerevisiae* nuclear extract by DNA polymerases and the origin recognition complex. **J. Biol. Chem.** **280**, 6285-6292.
- MO, Y.Y., WANG, C., BECK, W.T. (2000). A novel nuclear localization signal in human DNA topoisomerase I. **J. Biol. Chem.** **275**, 41107-41113.
- MONDAL, N. & PARVIN, J.D. (2001). DNA topoisomerase II $\alpha$  is required for RNA polymerase II transcription on chromatin templates. **Nature** **413**, 435-438.
- MORHAM, S.G., KLUCKMAN, K.D., VOULOMANOS, N., SMITHIES, O. (1996). Targeted disruption of the mouse topoisomerase I gene by camptothecin selection. **Mol. Cell Biol.** **16**, 6804-6809.
- MORRISON, C., HENZING, A.J., JENSEN, O.N., OSHEROFF, N., DODSON, H., KANDELS-LEWIS, S.E., ADAMS, R.R. AND EARNSHAW, W.C. (2002). Proteomic analysis of human metaphase chromosomes reveals topoisomerase II alpha as an Aurora B substrate. **Nucleic Acids Res.** **26**, 5318-5327.
- MURAKAMI, S., YANAGIDA, M., NIWA, O. (1995). A large circular minichromosome of *Schizosaccharomyces pombe* requires a high dose of type II DNA topoisomerase for its stabilization. **Mol. Gen. Genet.** **246**, 671-679.
- MURRAY, A.W. & SZOSTAK, J.W. (1983). Construction of artificial chromosomes in yeast. **Nature** **305**, 189-193.
- MURRAY, A.W. & SZOSTAK, J.W. (1985) Chromosome segregation in mitosis and meiosis. **Annu. Rev. Cell Biol.** **1**, 289-315.

- NAKAMURA, H., MORITA, T., SATO, C. (1986). Structural organisation of replicon domains during DNA synthetic phase in the mammalian nucleus. *Exp. Cell Res.* **165**, 291-297.
- NASMYTH, K. (2005). How might cohesin hold sister chromatids together? *Philos. Trans. R. Soc. Lond. B. Biol. Sci.* **360**, 483-496.
- NEUMAN, K.C., CHARVIN, G., BENSIMON, D., CROQUETTE, V. (2009). Mechanisms of chiral discrimination by topoisomerase IV. *Proc. Natl. Acad. Sci. USA* **106**, 6986-6991.
- NICOLAS, E., UPTON, A.L., UPHOFF, S., HENRY, O. BADRINARAYANAN, A., SHERRATT, D. (2014). The SMC complex MukBEF recruits topoisomerase IV to the origin of replication region in live *Escherichia coli*. *mBio* **5**, e01001-e01003.
- NITISS, J.L. (1998). Investigating the biological functions of DNA topoisomerases in eukaryotic cells. *Biochim. Biophys. Acta* **1400**, 63-81.
- NOLIVOS, S., UPTON, A.L., BADRINARAYANAN, A., MULLER, J., ZAWADZKA, K., WIKTOR, J., GILL, A., ARCISZEWSKA, L., NICOLAS, E., SHERRATT, D. (2016). MatP regulates the coordinated action of topoisomerase IV and MukBEF in chromosome segregation. *Nat. Comms.* **7**, 10466. DOI: 10.1038/ncomms10466.
- NORDEN, C., MENDOZA, M., DOBBELAERE, J., KOTWALIWALE, C.V., BIGGINS, S., BARRAL, Y. (2006). The NoCut pathway links completion of cytokinesis to spindle midzone function to prevent chromosome breakage. *Cell* **125**, 85-98.
- OCAMPO-HAFALLA, M.T., KATOU, Y., SHIRAHIGE, K. AND UHLMANN, F., (2007). Displacement and re-accumulation of centromeric cohesin during transient pre-anaphase centromere splitting. *Chromosoma* **116**, 531-544.
- OLAVARRIETA, L., HERNANDEZ, P., KRIMER, D.B., SCHVARTZMAN, J.B. (2002). DNA Knotting caused by head-on collision of transcription and replication. *J. Mol. Biol.* **322**, 1-6.
- O'REILLY, N., CHARBIN, A., LOPEZ-SERRA, L., UHLMANN, F. (2012). Facile synthesis of budding yeast a-factor and its use to synchronize cells of a mating type. *Yeast* **29**, 233-240.
- PAULSON, J.R. & LAEMMLI, U.K. (1977). The structure of histone-depleted metaphase chromosomes. *Cell*, **12**, 817-828.
- PENG, H. & MARIANS, K.J. (1993). Decatenation activity of topoisomerase IV during oriC and pBR322 DNA replication *in vitro*. *Proc. Natl. Acad. Sci. USA* **90**, 8571-8675.
- PETER, B.J., ULLSPERGER, C., HIASA, H., MARIANS, K.J., COZZARELLI, N.R. (1998). The structure of supercoiled intermediates in DNA replication. *Cell* **276**, 819-827.
- POIRIER, M.G. & MARKO, J.F. (2002). Mitotic chromosomes are chromatin networks without a mechanically contiguous protein scaffold. *Proc. Natl. Acad. Sci. USA* **99**, 15393-15397.
- POMMIER, Y., POURQUIER, P., FAN, Y., STRUMBERG, D. (1998). Mechanism of action of eukaryotic DNA topoisomerase I and drugs targeted to the enzyme. *Biochim. Biophys. Acta* **1400**, 83-105.
- POPE, L.H., XIONG, C., MARKO, J.F. (2006). Proteolysis of mitotic chromosomes induces gradual and anisotropic decondensation correlated with a reduction of elastic modulus and structural sensitivity to rarely cutting restriction enzymes. *Mol. Biol. Cell.* **17**, 104-113.

- PORTER, A.C.G., & FARR, C.J. (2004). Topoisomerase II untangling its contribution at the centromere. **Chromosome Res.** *12*, 569-583.
- POSTOW, L., PETER, B.J., COZZARELLI, N.R. (1999). Knot what we thought before: the twisted story of replication. **BioEssays** *21*, 805-808.
- POSTOW, L., ULLSPERGER, C., KELLER, R.W., BUSTAMANTE, C., VOLOGODSKII, A.V., COZZARELLI, N.R. (2001). Positive torsional strain causes the formation of a four-way junction at replication forks. **J. Biol. Chem.** *276*, 2790-2796.
- POSTOW, L., HARDY, C.D., ARSUAGA, J., COZZARELLI, N.R. (2004). Topological domain structure of the *Escherichia coli* chromosome. **Genes Dev.** *18* 1766-1779.
- RACKO, D., BENEDETTI, F., DORIER, J., BURNIER, Y., STASIAK, A. (2015). Generation of supercoils in nicked and gapped DNA drives DNA unknotting and postreplicative decatenation. **Nucleic Acids Res.** *43*, 7229-7236.
- RAGHURAMAN, M.K., BREWER, B.J., FANGMAN, W.L. (1997). Cell cycle-dependent establishment of a late replication program. **Science** *276*, 806-809.
- RAMSPERGER, U. & STAHL, H. (1995). Unwinding of chromatin by the SV40 large T antigen DNA helicase. **EMBO J.** *14*, 3215-3225.
- RATTNER, J.B., HENDZEL, M.J., FURBEE, C.S., MULLER, M.T., BAZETT-JONES, D.P. (1996). Topoisomerase II alpha is associated with the mammalian centromere in a cell cycle- and species-specific manner and is required for proper centromere/kinetochore structure. **J. Cell Biol.** *134*, 1097-1007.
- REDINBO, M.R., CHAMPOUX, J.J., HOL, W.G. (2000) Novel insights into catalytic mechanism from a crystal structure of human topoisomerase I in complex with DNA. **Biochemistry** *39*, 6832-6840.
- REMUS, D., BEALL, F.L., BOTCHAN, M.R. (2004). DNA topology, not DNA sequence, is a critical determinant for *Drosophila* ORC-DNA binding. **EMBO J.** *23*, 897-907.
- RENSHAW, M.J., WARD, J.J., KANEMAKI, M., NATSUME, K., NEDELEC, F.J., TANAKA, T. (2010). Condensins promote chromosome recoiling during early anaphase to complete sister chromatid separation. **Dev. Cell** *19*, 232-244.
- REYES-LAMOTHE, R., POSSOZ, C., DANILOVA, O., SHERRATT, D.L. (2008). Independent positioning and action of *Escherichia coli* replisomes in live cells. **Cell** *133*, 90-102
- ROCA, J. & WANG, J.C. (1994). DNA transport by a type II DNA topoisomerase: evidence in favour of a two-gate mechanism. **Cell** *77*, 609-616.
- ROCA, J., BERGER, J.M., HARRISON, S.C., WANG, J.C. (1996). DNA transport by a type II topoisomerase: direct evidence for a two-gate mechanism. **Proc. Natl. Acad. Sci. USA** *93*, 4057-4062.
- ROCA, J., BERGER, J.M., WANG, J.C. (1993). On the simultaneous binding of eukaryotic DNA topoisomerase II to a pair of double-stranded DNA helices. **J. Biol. Chem.** *268*, 14250-14255.

- ROGAKOU, E.P., PILCH, D.R., ORR, A.H., IVANOVA, V.S., BONNER, W.R. (1998). DNA double-stranded breaks induce histone H2AX phosphorylation on serine 139. *J. Biol. Chem.* **273**, 5858-5868.
- ROGAKOU, E.P., BOON, C., REDON, C., BONNER, W.M. (1999). Megabase chromatin domains involved in DNA double-strand breaks in vivo. *J. Cell Biol.* **146**, 905-916.
- ROSE, D., THOMAS, W., HOLM, C. (1990). Segregation of recombined chromosomes in meiosis I requires DNA topoisomerase II. *Cell* **60**, 1009-1017.
- ROTTMANN, M., SCHRÖDER, H.C., GRAMZOW, M., RENNEISEN, K., KURELEC, B., DORN, A., FRIESE, U., MUELLER, W.E. (1987). Specific phosphorylation of proteins in pore complex-laminae from the sponge *Geodia cydonium* by the homologous aggregation factor and phorbol ester. Role of protein kinase C in the phosphorylation of DNA topoisomerase II. *EMBO J.* **6**, 3939.
- RYBENKOV, V.V., ULLSPERGER, C., VOLOGODSKII, A.V., COZZARELLI, N.R. (1997). Simplification of DNA topology below equilibrium values by type II topoisomerases. *Science* **277**, 690-693.
- SAKA, Y., SUTANI, T., YAMASHITA, Y., SAITOH, S., TAKEUCHI, M., NAKASEKO, Y., YANAGIDA, M. (1994). Fission yeast cut3 and cut14, members of a ubiquitous protein family, are required for chromosome condensation and segregation in mitosis. *EMBO J.* **13**, 4938-4952.
- SALCEDA, J., FERNANDEZ, X., ROCA, J. (2006). Topoisomerase II, not topoisomerase I, is the proficient relaxase of nucleosomal DNA. *EMBO J.* **25**, 2575-2583.
- SANDER, M. & HSIEH, T. (1983) Double strand DNA cleavage by type II DNA topoisomerase from *Drosophila melanogaster*. *J. Biol. Chem.*, **258**, 8421-8428.
- SAUCIER, J.M. & WANG, J.C. (1972). Angular alteration of the DNA helix by *E. coli* RNA polymerase. *Nat. New Biol.* **239**, 167-170.
- SAHYOUN, N., WOLF, M., BESTERMAN, J., HSIEH, T.S., SANDER, M., LEVINE, H., CHANG, K.J., CUATRECASAS, P. (1986). Protein kinase C phosphorylates topoisomerase II: topoisomerase activation and its possible role in phorbol ester-induced differentiation of HL-60 cells. *Proc. Natl. Acad. Sci.* **83**, 1603-1607.
- SCHALBETTER, S.A., MANSOUBI, S., CHAMBERS, A.L., DOWNS, J.A., BAXTER, J. (2015). Fork rotation and DNA precatenation are restricted during DNA replication to prevent chromosomal instability. *Proc. Natl. Acad. Sci. USA* **112**, e4565.  
Doi:10.1073/pnas.1505356112.
- SCHOEFFLER, A.J. & BERGER, J.M. (2008). DNA topoisomerases: harnessing and constraining energy to govern chromosome topology. *Q. Rev. Biophys.* **41**, 41-101.
- SCHULTZ, M.C., BRILL, S.J., JU, Q., STERNGLANZ, R., REEDER, R.H. (1992). Topoisomerases and yeast rRNA transcription: negative supercoiling stimulates initiation and topoisomerase activity is required for elongation. *Genes Dev.* **6**, 1332-1341.
- SCHVARTZMAN, J.B. & STASIAK, A. (2004). A topological view of the replicon. *EMBO Rep.* **5**, 256-261.

- SCLIMENTI, C.R., THYAGARAJAN, B., CALOS, M.P. (2001). Directed evolution of a recombinase for improved genomic integration at a native human sequence. ***Nucleic Acids Res.* 29**, 5044-5051.
- SHAIU, W.L. & HSIEH, T.S. (1998). Targeting to transcriptionally active loci by the hydrophilic N-terminal domain of *Drosophila* topoisomerase I. ***Mol. Cell. Biol.* 18**, 4358-4367.
- SHAPIRO, P.S., WHALEN, A.M., TOLWINSKI, N.S., WILSBACHER, J., FROELICH-AMMON, S.J., GARCIA, M., OSHEROFF, N., AHN, N.G. (1999). Extracellular signal-regulated kinase activates topoisomerase II $\alpha$  through a mechanism independent of phosphorylation. ***Mol. Cell. Biol.* 19**, 3551-3560.
- SHARMA, S., DOHERTY, K.M., BROSH, R. M. Jr. (2006). Mechanisms of RecQ helicases: guardian angels of the DNA replication fork. ***Chromosoma* 117**, 219-33
- SHERRATT, D.J. & WIGLEY, D.B. (1998). Conserved themes but novel activities in recombinases and topoisomerases. ***Cell* 93**, 149-152.
- SIMMONS, D.T., MELENDY, T., USHER, D., STILLMAN, B. (1996). Simian virus 40 large T antigen binds to topoisomerase I. ***Virology* 222**, 365-374.
- SINDEN, R.R. & PETTIJOHN, D.E. (1981). Chromosomes in living *Escherichia coli* cells are segregated into domains of supercoiling. ***Proc. Natl. Acad. Sci. USA* 78**, 228-228.
- SISSI, C. & PALUMBO, M. (2009). Effects of magnesium and related divalent metal ions in topoisomerase structure and function. ***Nucleic Acids Res.* 37**, 702-711.
- SISSI, C. & PALUMBO, M. (2010). In front of and behind the replication fork: bacterial type IIA topoisomerases. ***Cell. Mol. Life Sci.* 67**, 2001-2004.
- SKOUFIAS, D.A., LACROIX, F.B., ANDREASSEN, P.R., WILSON, L., MARGOLIS, R.L. (2004). Inhibition of DNA decatenation, but not DNA damage, arrests cells at metaphase. ***Mol. Cell* 15**, 977-990.
- SMILEY, R.D., COLLINS, T.R.L., HAMMES, G.G., HSIEH, T.S. (2007). Single-molecule measurements of the opening and closing of the DNA gate by eukaryotic topoisomerase II. ***Proc. Natl. Acad. Sci. USA* 104**, 4840-4845.
- SPELL, R.M. & HOLM, C. (1994). Nature and distribution of chromosomal intertwinings in *Saccharomyces cerevisiae*. ***Mol. Cell Biol.* 14**, 1465-1476.
- SPENCE, J.M., CRITCHER, R., EBERSOLE, T.A., VALDIVIA, M.M., EARNSHAW, W.C., FUKAGAWA, T. & FARR, C.J. (2002). Co-localization of centromere activity proteins and topoisomerase II within a subdomain of the major human X alpha-satellite array. ***EMBO J* 21**, 5269-5280.
- SOGO, J.M., STASIAK, A., MARTINEZ-ROBLES, M.L., KRIMER, D.B., HERNANDEZ, P., SCHVARTZMAN, J.B. (1999). Formation of knots in partially replicated DNA molecules. ***J. Mol. Biol.* 286**, 637-643.
- STEWART, L., IRETON, G.C., CHAMPOUX, J.J. (1997). Reconstitution of human topoisomerase I by fragment complementation. ***J. Mol. Biol.* 269**, 355-372.

- STEWART, L., IRETON, G.C., CHAMPOUX, J.J. (1999). A functional linker in human topoisomerase I is required for maximum sensitivity to camptothecin in a DNA relaxation assay. **J. Biol. Chem.** **274**, 32950–32960.
- STINCHCOMB, D.T., MANN, C., DAVIS, R.W. (1982). Centromeric DNA from *Saccharomyces cerevisiae*. **J. Mol. Biol.** **158**, 157-179.
- STRAY, J.E. & LINDSLEY, J.E. (2003). Biochemical analysis of the yeast condensin Smc2/4 complex: an ATPase that promotes knotting of circular DNA. **J. Biol. Chem.** **278**, 26238-26248.
- STRAY, J.E., CRISONA, N.J., BELOTSERKOVSKII, B.P., LINDSLEY, J.E., COZZARELLI, N.R. (2005). The *Saccharomyces cerevisiae* Smc2/4 condensin compacts DNA into (+) chiral structures without net supercoiling. **J. Biol. Chem.** **280**, 34723-34734.
- STRICK, T.R., CROQUETTE, V. BENSIMON, D. (2000). Single-molecule analysis of DNA uncoiling by a type II topoisomerase. **Nature** **404**, 901-904.
- STROS, M., BACIKOVA, A., POLANSKA, E., STOKROVA, J., STRAUSS, F. (2007). HMGB1 interacts with human topoisomerase  $\text{I}\alpha$  and stimulates its catalytic activity **Nucleic Ac. Res.** **35**, 5001-5013.
- STRUHL, K., STINCHCOMB, D.T., SCHERER, S., DAVIS, R. (1979). High frequency transformation of yeast: autonomous replication of hybrid DNA molecules. **Proc. Natl. Acad. Sci. USA** **76**, 1035-1039.
- STRUNNIKOV, A.V., HOGAN, E., KOSHLAND, D. (1995). SMC2, a *Saccharomyces cerevisiae* gene essential for chromosome segregation and condensation, defines a subgroup within the SMC family. **Genes Dev.** **9**, 587-599.
- STUCHINSKAYA, T., MITCHENALL, L.A., SCHOEFLER, A.J., CORBETT, K.D., BERGER, J.M., BATES, A.D., MAXWELL, A. (2009). How do type II topoisomerases use ATP hydrolysis to simplify DNA topology beyond equilibrium? Investigating the relaxation reaction of nonsupercoiling type II topoisomerases. **J. Mol. Biol.** **385**, 1397-1408.
- SUGIMOTO-SHIRASU, K., STACEY, N.J., CORSAR, J., ROBERTS, K. & MCCANN, M.C. (2002) DNA topoisomerase VI is essential for endoreduplication in Arabidopsis. **Curr. Biol.**, **12**, 1782–1786.
- SULLIVAN, M., HIGUCHI, T., KATIS, V.L., UHLMANN, F. (2004). Cdc14 phosphatase induces rDNA condensation and resolves cohesin-independent cohesion during budding yeast anaphase. **Cell** **117**, 471-482.
- SUNDIN, O. & VARSHAVSKY, A. (1980). Terminal stages of SV40 DNA replication proceed via multiply intertwined catenated dimers. **Cell** **21**, 115-125.
- SUNDIN, O. & VARSHAVSKY, A. (1981). Arrest of segregation leads to accumulation of highly intertwined catenated dimers: dissection of the final stages of SV40 DNA replication. **Cell** **25**, 659-669.
- SUSKI, C. & MARIANS, K.J. (2008) Resolution of converging replication forks by RecQ and topoisomerase III. **Mol. Cell**, **30**, 779–789.

- SZOSTAK, J.W. & BLACKBURN, E.H. (1982). Cloning yeast telomeres on linear plasmid vectors. *Cell* **29**, 245-255.
- SZOSTAK, J.W. (1982). Structural requirements for telomere resolution. *Cold Spring Harbor Symp. Quant. Biol.* **47**, 1187-1194.
- TACK, L.C., & DEPAMPHILIS, M.L. (1983). Analysis of simian virus 40 chromosome-T-antigen complexes: T-antigen is preferentially associated with early replication DNA intermediates. *J. Virol.* **48**, 281-295.
- TAKAHASHI, Y., YONG-GONZALEZ, V., KIKUCHI, Y., STRUNNIKOV, A. (2006). SIZ1/SIZ2 control of chromosome transmission fidelity is mediated by the sumoylation of topoisomerase II. *Genetics* **172**, 783-794.
- TAKAHASHI, Y., & STRUNNIKOV, A. (2008). In vivo modelling of polysumoylation uncovers targeting of topoisomerase II to the nucleolus via optimal level of SUMO modification. *Chromosoma* **117**, 189-198.
- TAMAICHI, H., SATO, M., PORTER, A.C.G., SHIMIZU, T., MIZUTANI, S., TAKAGI, M. (2013). Ataxia telangiectasia mutated-dependent regulation of topoisomerase alpha expression and sensitivity to topoisomerase II inhibitor. *Cancer Sci.* **104**, 178-184.
- TANAKA, T., COSMA, M.P., WIRTH, K. & NASMYTH, K. (1999). Cohesin ensures bipolar attachment of microtubules to sister centromeres and resists their precocious separation. *Nat. Cell. Biol.* **2**, 492-499.
- TAVORMINA, P.A., COME, M.G., HUDSON, J.R. (2002). Rapid exchange of mammalian topoisomerase II alpha at kinetochores and chromosome arms in mitosis. *J. Cell Biol.* **158**, 23-29.
- TERCERO, J.A., LONGHESE, M.P., DIFFLEY, J.F.X. A central role for DNA replication forks in checkpoint activation and response. *Mol. Cell* **11**, 1323-1336.
- TEWEY, K.M., CHEN, G.L., NELSON, E.M., LIU, L.F. (1984) Intercalative antitumor drugs interfere with the breakage-reunion reaction of mammalian DNA topoisomerase II. *J. Biol. Chem.* **259**, 13560-13566.
- THADANI, R., UHLMANN, F., HEEGER, S. (2012). Condensin, chromatin crossbarring and chromosome condensation. *Curr. Biol.* **22**, pR1012-R1021.
- THORPE, H.M., WILSON, S.E., SMITH, M.C.M. (2000). Control of directionality in the site-specific recombination system of the *Streptomyces* phage  $\phi$ C31. *Mol. Microbiol.* **38**, 232-241.
- THYAGARAJAN, B., OLIVARES, E.C., HOLLIS, R.P., GINSBURG, D.S., CALOS, M.P. (2001). Site-specific genomic integration in mammalian cells mediated by phage  $\phi$ C31 integrase. *Mol. Cell. Biol.* **21**, 3926-3934.
- TIMSIT, Y. (2011). Local sensing of global DNA topology: from crossover geometry to type II topoisomerase processivity. *Nucleic Acids Res.* **39**, 8665-8676.
- TRIGUEROS, S., SALCEDA, J., BERMUDEZ, I., FERNANDEZ, X., ROCA, J. (2004). Asymmetric removal of supercoils suggests how topoisomerase II simplifies DNA topology. *J. Mol. Biol.* **335**, 723-731.

- TOEDLING, J., SKLYAR, O. & HUBER, W. (2007). Ringo—an R/Bioconductor package for analyzing ChIP-chip readouts. *BMC bioinformatics* **8**, p.1.
- TOMSON, B.N., D'AMOURS, D., ADAMSON, B.S., ARAGON, L., AMON, A. (2006). Ribosomal DNA transcription-dependent processes interfere with chromosome segregation. *Mol. Cell. Biol.* **26**, 6239-6247.
- TORRES-ROSELL, J., SUNJEVARIC, I., DEPICCOLI, G., SACHER, M., ECKERT-BOULET, N., REID, R., JENTSCH, S., ROTHSTEIN, R., ARAGON, L., LISBY, M. (2007). The Smc5-Smc6 complex and SUMO modification of Rad52 regulates recombinatorial repair at the ribosomal gene locus. *Nat. Cell Biol.* **9**, 923-931.
- TOYODA, Y. & YANAGIDA, M. (2006). Coordinated requirements of human topo II and cohesion for metaphase centromere alignment under Mad2-dependent spindle checkpoint surveillance. *Mol. Biol. Cell.* **17**, 2287-2302.
- TSCHUMPER, G. & CARBON, J. (1983). Copy number control by a yeast centromere. *Gene* **23**, 221-232.
- TSE, Y. & WANG, J.C. (1980). *E. coli* and *M. luteus* DNA topoisomerase I can catalyze catenation or decatenation of double-stranded DNA rings. *Cell* **22**, 269-276.
- TUDURI, S., CRABBÉ, L., CONTI, C., TOURRIERE, H., HOLTGREVE-GREZ, H., JAUCH, A., PANTESCO, V., DE VOS, J., THOMAS, A., THEILLET, C., POMMIER, Y. (2009). Topoisomerase I suppresses genomic instability by preventing interference between replication and transcription. *Nature Cell Biol.* **11**, 1315-1324.
- UEMURA, T. & YANAGIDA, M. (1986). Mitotic spindle pulls but fails to separate chromosomes in type II DNA topoisomerase mutants: uncoordinated mitosis. *EMBO J* **5**, 1003.
- UEMURA, T., OHKURA, H., ADACHI, Y., MORINO, K., SHIOZAKI, K. AND YANAGIDA, M. (1987). DNA topoisomerase II is required for condensation and separation of mitotic chromosomes in *S. pombe*. *Cell* **50**, 917-925.
- UHLMANN, F., LOTTSPEICH, F., NASMYTH, K. (1999). Sister-chromatid separation at anaphase onset is promoted by cleavage of the cohesin subunit Scc1. *Nature* **400**, 37-42.
- UHLMANN, F., WERNIC, D., POUPART, M.A., KOONIN, E.V., NASMYTH, K. (2000). Cleavage of cohesin by the CD clan protease separin triggers anaphase in yeast. *Cell* **103**, 375-386.
- VAGNARELLI, P., MORRISON, C., DODSON, H., SONODA, E., TAKEDA, S., EARNSHAW, W.C. (2004). Analysis of Scc1-deficient cells defines a key metaphase role of vertebrate cohesin in linking sister kinetochores. *EMBO Rep.* **5**, 167-171.
- VAN DUYNE, G.D. (2015). Cre Recombinase. *Microbiol. Spectrum* **3**.
- VELEZ-CRUZ, R., RIGGINS, J.N., DANIELS, J.S., CAI, H., GUENGERICH, F.P., MARNETT, L.J., OSHEROFF, N. (2005). Exocyclic DNA lesions stimulate DNA cleavage mediated by human topoisomerase II $\alpha$  in vitro and in cultured cells. *Biochemistry* **44**, 3972-2981.
- VERZIJLBERGEN, K.F., MENENDEZ-BENITO, V., VAN WELSEME, T., VAN DEVENTER, S.J., LINDSTROM, D.L., OVAA, H., NEEFJES, J., GOTTSCHLING, D.E., VAN LEEUWEN, F.,

- (2010). Recombination-induced tag exchange to track old and new proteins. *Proc. Natl. Acad. Sci.* **107**, 64-68.
- VINOGRAD, J. LEBOWITZ, J., RADLOFF, R., WATSON, R., LAIPIS, P. (1965). The twisted circular form of polyoma viral DNA. *Proc. Natl. Acad. Sci. USA* **53**, 1104-1111.
- VISINTIN, R., H, WANG, E.S., AMON, A. (1999). Cfi1 prevents premature exit from mitosis by anchoring Cdc14 phosphatase in the nucleolus. *Nature* **398**, 818-823.
- VOLOGODSKII, A. (2009). Theoretical models of DNA topology simplification by type IIA DNA topoisomerases. *Nucleic Acids Res.* **37**, 5126-5137.
- VOLOGODSKII, A. & COZZARELLI, N.R. (1996). Effect of supercoiling on the juxtaposition and relative orientation of DNA sites. *Biophys. J.* **70**, 2548-2556.
- VOLOGODSKII, A.V., ZHANG, W., RYBENKOV, V.V., PODTELEZHNIKOV, A.A., SUBRAMANIAN, D., GRIFFITH, J.D., COZZARELLI, N.R. (2001). Mechanism of topology simplification by type II DNA topoisomerases. *Proc. Natl. Acad. Sci.* **98**, 3045-3049.
- VOS, S.M., TRETTER, E.M., SCHMIDT, B.H., BERGER, J.M. (2011). All tangled up: how cells direct, manage and exploit topoisomerase function. *Nature Rev. Mol. Cell Biol.*, **12**, 827-841.
- WALLIS, J.W., CHREBET, G., BRODSKY, G., ROLFE, M., ROTHSTEIN, R. (1989). A hyper-recombination mutation in *S. cerevisiae* identifies a novel eukaryotic topoisomerase. *Cell* **58**, 409-419.
- WAN, L.H., MAYER, B., STEMMANN, O., NIGG, E.A. (2009). Centromere DNA decatenation depends on cohesin removal and is required for mammalian cell division. *J. Cell Sci.* **123**, 806-813.
- WANG, J.C. (1969). Variation of the average rotational angle of the DNA helix and the superhelical turns of covalently closed cyclic  $\lambda$  DNA. *J. Mol. Biol.* **43**, 25-39.
- WANG, J.C. (1971). Interaction between DNA and an *Escherichia coli* protein  $\omega$ . *J. Mol. Biol.* **55**, 523-533.
- WANG, J.C. (1973). *In DNA Synthesis in Vitro, R.D. Wells and R.B. Inman, eds* (Baltimore: University Park Press) pp 163-174.
- WANG, J.C. (1974a). The degree of unwinding of the DNA helix by ethidium: I. Titration of twisted PM2 DNA molecules in alkaline cesium chloride density gradients. *J. Mol. Biol.* **89**, 783-801.
- WANG, J.C. (1974b). Interactions between twisted DNAs and enzymes: the effects of superhelical turns. *J. Mol. Biol.* **87**, 797-816.
- WANG, J.C. (1979). Helical repeat of DNA in solution. *Proc. Natl. Acad. Sci. USA* **76**, 200-203.
- WANG, J.C. (1996). DNA topoisomerases. *Annu. Rev. Biochem.* **65**, 635-692.
- WANG, J.C. (1998). Moving one DNA double helix through another by a type II DNA topoisomerase: the story of a simple molecular machine. *Q. Rev. Biophys.* **31**, 107-144.
- WANG, J.C. (2002). Cellular roles of DNA topoisomerases: a molecular perspective. *Nat. Rev. Mol. Cell Biol.* **3**, 430-440.

- WANG, J.C. (2009). A journey in the world of DNA rings and beyond. *Annu. Rev. Biochem.* **78**, 31-54.
- WANG, J.C., CARON, P.R., KIM, R.A. (1990). The role of DNA topoisomerases in recombination and genome stability: a double-edged sword? *Cell* **62**, 403-406.
- WANG, X., REYES-LAMOTHE, R., SHERRATT, D.J. (2008). Modulation of *Escherichia coli* sister chromosome cohesion by topoisomerase IV. *Genes & Dev* **22**, 2426-2433.
- WASSERMAN, R.A., AUSTIN, C.A., FISHER, L.M., WANG, J.C. (1993). Use of yeast in the study of anticancer drugs targeting DNA topoisomerases: expression of a functional recombinant human DNA topoisomerase II $\alpha$  in yeast. *Cancer Res.*, **53**, 3591-3596.
- WASSERMAN, S.A., DUNGAN, J.M., COZZARELLI, N.R. (1985). Discovery of a predicted DNA knot substantiates a model for site-specific recombination. *Science* **229**, 171-174.
- WATSON, J.D. & CRICK, F.H.C. (1953a). A structure for deoxyribose nucleic acid. *Nature* **171**, 737-738.
- WATSON, J.D. & CRICK, F.H.C. (1953b). Genetical implications of the structure of deoxyribonucleic acid. *Nature* **171**, 964-967.
- WATT, P.M., & HICKSON, I.D. (1994). Structure and function of type II topoisomerases. *Biochem. J.* **303**, 681-695.
- WILKINS, M.H.F., STOKES, A.R., WILSON, H.R. (1953). Molecular structure of deoxyribose nucleic acids. *Nature* **171**, 738-740.
- WORLAND, S.T. & WANG, J.C. (1989). Inducible overexpression, purification, and active site mapping of DNA topoisomerase II from the yeast *Saccharomyces cerevisiae*. *J. Biol. Chem.* **264**, 4412-4416.
- WU, J. & LIU, L.F. (1997). Processing of topoisomerase I cleavable complexes into DNA by transcription. *Nucleic Acids Res.* **25**, 4181-4186.
- WYCKOFF, E. & HSIEH, T.S. (1988). Functional expression of a Drosophila gene in yeast: genetic complementation of DNA topoisomerase II. *Proc. Natl. Acad. Sci. USA*, **85**, 6272-6276.
- XU, H., BOONE, C., BROWN, G.W. (2007). Genetic dissection of parallel sister-chromatid cohesion pathways. *Genetics* **176**, 1417-1429.
- XU, Z. & BROWN, W.R. (2016). Comparison and optimization of ten phage encoded serine integrases for genome engineering in *Saccharomyces cerevisiae*. *BMC biotechnology* **16**, 1.
- YAN, J., MAGNASCO, M.O., MARKO, J.F. (1999). A kinetic proofreading mechanism for disentanglement of DNA by topoisomerases. *Nature* **401**, 932-935.
- YAN, J., MAGNASCO, M.O., MARKO, J.F. (2001). Kinetic proofreading can explain the suppression of supercoiling of circular DNA molecules by type-II topoisomerases. *Proc. Natl. Acad. Sci. USA* **71**, 4135-4139.
- YANAGIDA, M. (2009). Clearing the way for mitosis: is cohesion a target? *Nature Rev. Mol. Cell. Biol.* **10**, 489-496.
- YANG, X., LI, W., PRESCOTT, E.D., BURDEN, S.J. & WANG, J.C. (2000) DNA topoisomerase II $\beta$  and neural development. *Science* **287**, 131-134.

- YOGO, K., OGAWA, T., HAYASHI, M., HARADA, Y., NISHIZAKA, T., KINOSITA, K. (2012). Direct observation of strand passage by DNA-Topoisomerase and its limited processivity. ***PLoS ONE* 7**, e34920. Doi:10.1371/journal.pone.0034920.
- YOSHIDA, M.M., TING, L., GYGI, S.P., AZUMA, Y. (2016). Sumoylation of DNA topoisomerase II $\alpha$  regulates histone H3 kinase Haspin and H3 phosphorylation in mitosis. ***J. Cell Biol.* 213**, 665-678.
- ZECHIEDRICH, E.L., CHRISTIANSEN, K., ANDERSEN, A.H., WESTERGAARD, O., OSHEROFF, N. (1989) Double-stranded DNA cleavage/religation reaction of eukaryotic topoisomerase II: evidence for a nicked DNA intermediate. ***Biochemistry*, 28**, 6229–6236.
- ZECHIEDRICH, E.L., KHODURSKY, A.B., & COZZARELLI, N.R. (1997). Topoisomerase IV, not gyrase, decatenates products of site-specific recombination in *Escherichia coli*. ***Genes & Dev.* 11**, 2580-2592.
- ZECHIEDRICH, E.L. & OSHEROFF, N. (1990). Eukaryotic topoisomerases recognize nucleic acid topology by preferentially interacting with DNA crossovers. ***EMBO J.* 9**, 4555-4562.